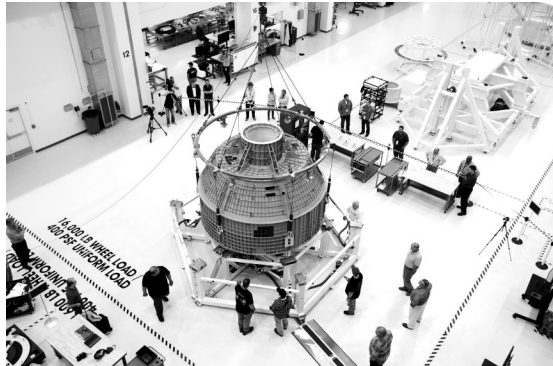


1

Introduction to Materials Science and Engineering



(Source: NASA)



(Source: Daniel Casper/NASA)

One of the most exciting proposed NASA missions is the human journey to Mars by the 2030s. The scientific questions that can be answered by actual human presence on Mars are too numerous and very exciting. A convoy of three NASA orbiters and two active rovers are already functioning on and around Mars to gather more information about the Red Planet in order to pave the way for future manned explorations. NASA engineers, together with U.S. aerospace companies such as Lockheed Martin, are putting together the Space Launch System (SLS) rocket that will take the Orion spacecraft on its manned Mars mission. Consider the technologies and the engineering knowledge needed to build the Orion spacecraft and complete such a mission. Following are some of the engineering and materials-related issues considered by NASA and Lockheed Martin in manufacturing the spacecraft.

Pressure testing: The Orion capsule, called the “birdcage,” has an underlying welded metallic structure that must contain the atmosphere for the crew during launch, space travel, reentry, and landing. The capsule will provide living space for the astronauts and must withstand the loads sustained during launch and landing. It is crucial that the structure be able to withstand the maximum internal pressurization needed for the journey. What metal would be suitable for the underlying structure? What properties should it have?

Tile bonding: During reentry, the Orion spacecraft will enter Earth’s atmosphere at speeds of 25,000 miles per hour and will be exposed to very high temperatures exceeding 5000°F. The “birdcage” of Orion, discussed above, cannot function at such high temperatures and requires a thermal protection system. NASA will use about 1300 ceramic tiles to protect the capsule in addition to a heat shield. Why use ceramic

LEARNING OBJECTIVES

By the end of this chapter, students will be able to

1. Describe the subject of materials science and engineering as a scientific discipline.
2. Cite the primary classification of materials.
3. Give distinctive features and characteristics of each group of materials.
4. Name various material from each group. Give some applications of different types of materials.

5. Evaluate how much you know and how much you do not know about materials.
6. Establish the importance of materials science and engineering in the selection of materials for various applications.

tiles? What properties do they possess that makes them attractive as a thermal protection system? What is the heat shield made of? What characteristics should it have?

Flight systems and subsystems: For Orion to function and communicate, it needs its avionics. This includes electrical power storage and distribution, thermal control systems, cabin pressure monitoring, communication command, data handling, guidance, navigation and controls, propulsion, and computers. The slew of sensors and actuators needed for these operations require the use of advanced electronics materials. What are the applications of electronics materials in space travel? Why are such materials crucial to the success of the mission?

Vibration tests: The Orion spacecraft will encounter vibrations due to interaction with Earth's atmosphere. It is crucial that the spacecraft be able to withstand such vibrations, and all systems, structural or electronic, must function under extreme conditions. NASA tested the Orion capsule using two electromagnetic shakers and exposed it to vibration frequencies ranging from 5 Mhz to 500 Mhz. What strategies for vibration dampening could be used? What materials would be beneficial for dampening vibration?

These are only some of the questions, tests, and considerations that NASA and Lockheed Martin engineers make in manufacturing of this complex system. Can you think of other issues that need be considered? What is the role of materials science and engineering in answering those questions? ■

1.1 MATERIALS AND ENGINEERING

Humankind, **materials**, and engineering have evolved over the passage of time and are continuing to do so. All of us live in a world of dynamic change, and materials are no exception. The advancement of civilization has historically depended on the improvement of materials to work with. Prehistoric humans were restricted to naturally accessible materials such as stone, wood, bones, and fur. Over time, they moved

from the materials Stone Age into the newer Copper (Bronze) and Iron ages. Note that this advance did not take place uniformly everywhere—we shall see that this is true in nature even down to the microscopic scale. Even today we are restricted to the materials we can obtain from Earth's crust and atmosphere (Table 1.1). According to Webster's dictionary, materials may be defined as substances of which something is composed or made. Although this definition is broad, from an engineering application point of view, it covers almost all relevant situations.

The production and processing of materials into finished goods constitutes a large part of our present economy. Engineers design most manufactured products and the processing systems required for their production. Since products require materials, engineers should be knowledgeable about the internal structure and properties of materials, as well as methods to manufacture components from those materials, so that they can choose the most suitable material for each application and develop the best processing methods.

Research and development engineers create new materials or modify the properties of existing ones. Design engineers use existing, modified, or new materials to design and create new products and systems. Sometimes design engineers have a problem in their design that requires a new material to be created by research scientists and engineers.

For example, NASA engineers designing the supersonic passenger planes (X-planes) (Fig. 1.1) will have to use high-temperature materials that withstand temperatures in excess of 1800°C in the engine environment in order to achieve supersonic airspeeds as high as Mach 12 to 25 (12 to 25 times the speed of sound in air). In addition, these planes must meet the demands of today's society by flying greener (less damaging to the environment and more renewable), safer, and quieter.

Another area that demands the most from materials scientists and engineers is space exploration. The design and construction of the *International Space Station*

Table 1.1 The most common elements in planet Earth's crust and atmosphere by weight percentage and volume

Element	Weight Percentage of the Earth's Crust
Oxygen (O)	46.60
Silicon (Si)	27.72
Aluminum (Al)	8.13
Iron (Fe)	5.00
Calcium (Ca)	3.63
Sodium (Na)	2.83
Potassium (K)	2.70
Magnesium (Mg)	2.09
Total	98.70
Gas	Percent of Dry Air by Volume
Nitrogen (N ₂)	78.08
Oxygen (O ₂)	20.95
Argon (Ar)	0.93
Carbon dioxide (CO ₂)	0.03

**Figure 1.1**

Nasa's X-plane is in the preliminary design stage and is expected to be built based on Quiet Supersonic Technology (QueSST). The major goals for the new designs are to burn half the fuel, generate 75% less pollution, and be quieter than conventional jets even during supersonic flight.

(Source: NASA)

(ISS) and the *Mars Exploration Rover* (MER) missions are examples of space research and exploration activities that require the absolute best from our materials scientists and engineers. The construction of ISS, a large research laboratory moving at a speed of 27,000 km/h through space, required the selection of materials that would function in an environment far different than ours on Earth (Fig. 1.2). The materials had to be lightweight to minimize payload weight during liftoff. The outer shell had to protect against the impact of tiny meteoroids and human-made debris. The internal air pressure of roughly 15 psi is constantly stressing the modules. Additionally, the modules must withstand the massive stresses at launch. Materials selection for MERs is also a challenge, especially considering that they must survive an environment in which night temperatures could be as low as -96°C . These and other constraints push the limits of material selection in the design of complex systems.

We must remember that materials usage and engineering designs are constantly changing. This change continues to accelerate. No one can accurately predict the long-term advances in material design and usage. In 1943 the prediction was made that successful people in the United States would own their own autogyros (auto-airplanes). How wrong that prediction was! At the same time, the transistor, the integrated circuit, and television (color and high-definition included) were neglected. Thirty years ago, many

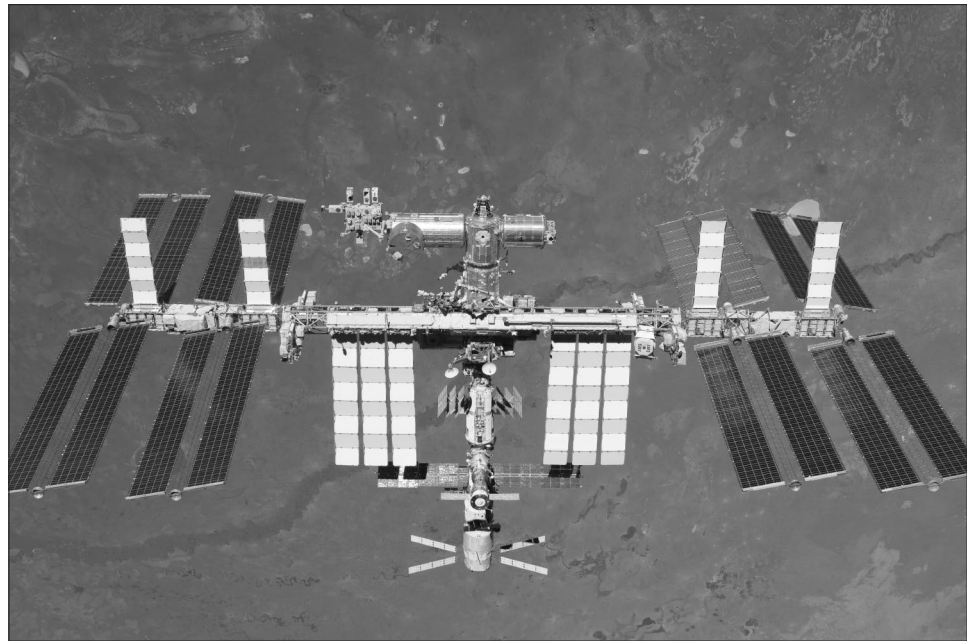


Figure 1.2

The International Space Station.

(Source: NASA)

people would not have believed that someday computers would become a common household item similar to a telephone or a refrigerator. And today, we still find it hard to believe that someday space travel will be commercialized, and we may even colonize Mars. Nevertheless, science and engineering push and transform our most unachievable dreams to reality.

The search for new advanced materials goes on continuously. The industries that benefit heavily from new advances in materials science and engineering and require a tremendous number of materials experts in their daily operations are aerospace, automotive, biomaterials, chemical, electronics, energy, metals, and telecommunications. The focus on certain materials differs significantly between industries. For instance, in aerospace and automobile industries, the focus is mainly structural and is on air-frame and engine materials. In biomaterials industries, the focus is on materials that are biocompatible (can survive in the human body) and also on synthesizing biological materials and components. In the chemical industries, the focus is on traditional chemicals, polymers, and advanced ceramics. In the electronics industries, material used in computers and commercial electronics takes center stage. In the energy industry, materials used in extraction of both fossil-based and renewable energy are the focus. Each industry also seeks different characteristics in their materials. These characteristics and the needs in the respective industries are presented in Table 1.2.

Table 1.2 Use of advanced materials in selected industries and their desired characteristics.

Desired Characteristics	Industry							
	Aerospace	Automotive	Biomaterials	Chemical	Electrical	Energy	Metals	Telecommunication
Light and strong	✓	✓	✓				✓	
High temperature resistance	✓			✓		✓	✓	
Corrosion resistance	✓	✓	✓	✓		✓	✓	
Rapid switching					✓	✓		✓
Efficient processing	✓	✓	✓	✓	✓	✓	✓	✓
Near net shape forming	✓	✓	✓	✓	✓	✓	✓	✓
Recycling		✓		✓			✓	
Prediction of service life	✓	✓	✓	✓	✓	✓		✓
Prediction of physical properties	✓	✓	✓	✓	✓	✓	✓	✓
Materials data base	✓	✓	✓	✓	✓	✓	✓	✓

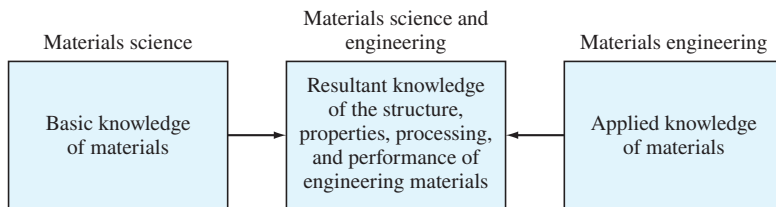
Source: National Academy of Sciences.

More recently, the field of nanomaterials has attracted a great deal of attention from scientists and engineers all over the world. Novel structural, chemical, and mechanical properties of nanomaterials have opened new and exciting possibilities in the application of these materials to a variety of engineering and medical problems. These are only a few examples of the search by engineers and scientists for new and improved materials and processes for a multitude of applications. In many cases, what was impossible yesterday is a reality today!

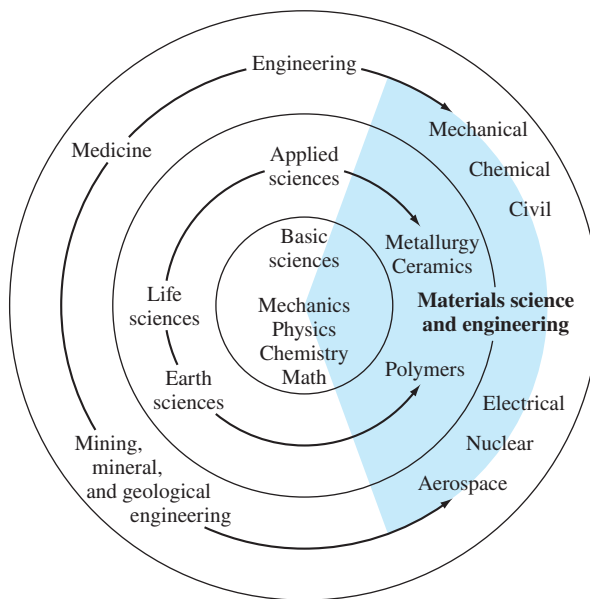
Engineers in all disciplines should have some basic and applied knowledge of engineering materials so that they will be able to do their work more effectively when using them. The purpose of this book is to serve as an introduction to the internal structure, properties, processing, and applications of engineering materials. Because of the enormous amount of information available about engineering materials and due to the limitations of this book, the presentation has had to be selective.

1.2 MATERIALS SCIENCE AND ENGINEERING

Materials science is primarily concerned with the search for basic knowledge about the internal structure, properties, and processing of materials. **Materials engineering** is mainly concerned with the use of fundamental and applied knowledge of materials so that the materials can be converted into products needed or desired by society. The term *materials science and engineering* combines both materials science and materials engineering and is the subject of this book. Materials science is at the basic knowledge end of the materials knowledge spectrum, and materials engineering is at the applied knowledge end, and there is no demarcation line between the two (Fig. 1.3).

**Figure 1.3**

Materials knowledge spectrum. Using the combined knowledge of materials from materials science and materials engineering enables engineers to convert materials into the products needed by society.

**Figure 1.4**

This diagram illustrates how materials science and engineering forms a bridge of knowledge from the basic sciences to the engineering disciplines.

(Source: National Academy of Sciences.)

Figure 1.4 shows a three-ringed diagram that indicates the relationship among the basic sciences (and mathematics), materials science and engineering, and the other engineering disciplines. The basic sciences are located within the inner ring or core of the diagram, while the various engineering disciplines (mechanical, electrical, civil, chemical, etc.) are located in the outermost third ring. The applied sciences, metallurgy, ceramics, and polymer science are located in the middle ring. Materials science

and engineering is shown to form a bridge of materials knowledge from the basic sciences (and mathematics) to the engineering disciplines.

1.3 TYPES OF MATERIALS

For convenience most engineering materials are divided into *three* main or fundamental classes: **metallic materials**, **polymeric materials**, and **ceramic materials**. In this chapter we shall distinguish among them on the basis of some of their important mechanical, electrical, and physical properties. In subsequent chapters, we shall study the internal structural differences among these types of materials. In addition to the three main classes of materials, we shall consider two processing or applicational classes, **composite materials** and **electronic materials**, because of their great engineering importance.

1.3.1 Metallic Materials

These materials are inorganic substances that are composed of one or more metallic elements and may also contain some nonmetallic elements. Examples of metallic elements are iron, copper, aluminum, nickel, and titanium. Nonmetallic elements such as carbon, nitrogen, and oxygen may also be contained in metallic materials. Metals have a crystalline structure in which the atoms are arranged in an orderly manner. Metals in general are good thermal and electrical conductors. Many metals are relatively strong and ductile at room temperature, and many maintain good strength even at high temperatures.

Metals and alloys¹ are commonly divided into two classes: **ferrous metals and alloys** that contain a large percentage of iron such as the steels and cast irons and **nonferrous metals and alloys** that do not contain iron or contain only a relatively small amount of iron. Examples of nonferrous metals are aluminum, copper, zinc, titanium, and nickel. The distinction between ferrous and nonferrous alloys is made because of the significantly higher usage and production of steels and cast irons when compared to other alloys.

Metals in their alloyed and pure forms are used in many industries, including aerospace, biomedical, semiconductor, electronic, energy, civil structural, and transport. The U.S. production of basic metals such as aluminum, copper, zinc, and magnesium is expected to follow the U.S. economy fairly closely. For instance, in the United States alone, the primary metal product manufacturing industry distributed approximately \$280 billion worth of products in 2014. The production of iron and steel (41% of the total primary metal distributed) has been steady considering global competition and the always-important economic reasons.

Materials scientists and engineers are constantly trying to improve the properties of existing alloys and to design and produce new alloys with improved strength, high-temperature strength, creep (see Sec. 7.4), and fatigue (see Sec. 7.2) properties. The existing alloys may be improved by better chemistry, composition control, and

¹ A metal alloy is a combination of two or more metals or a metal (metals) and a nonmetal (nonmetals).

processing techniques. For example, by 1961, new and improved nickel-base, iron-nickel-cobalt-base **superalloys** were available for use in high-pressure turbine airfoils in aircraft gas turbines. The term *superalloy* was used because of their improved performance at elevated temperatures of approximately 540°C (1000°F) and high stress levels. Figure 1.5 shows a PW-4000 gas turbine engine that is made primarily of metal alloys and superalloys. Figures 1.6a and 1.6b show the fan blades and the compressor bales for gas turbines similar to the PW-4000. The metals used in the fan blades and the compressor blades must be able to withstand high temperatures and pressures generated during operation. By 1980, casting techniques were improved to produce directionally solidified columnar grain (see Sec. 4.2) and single crystal casting nickel-base alloys for the compressor blades and titanium alloys for the fan blades. By the 1990s, single crystal directionally solidified cast alloys were standard in many aircraft gas turbine applications. The better performance of superalloys at elevated operating temperatures significantly improved the efficiency of the aircraft engines.

To show the diversity of applications, many of the metal alloys discussed above such as titanium alloys, stainless steel, and cobalt-base alloys are also used in

PW4000 112-INCH FAN ENGINE

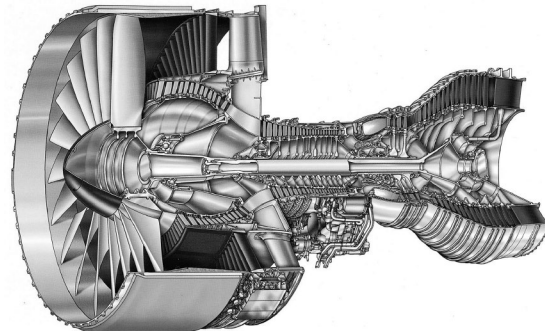


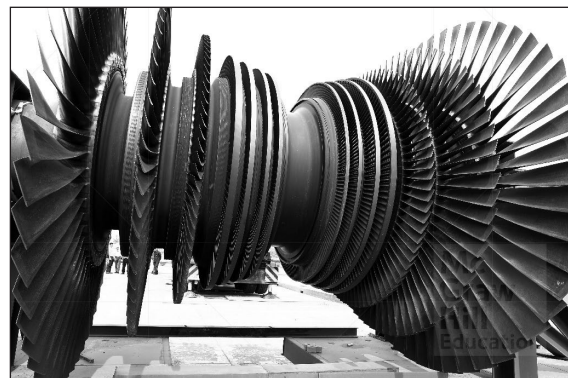
Figure 1.5

The aircraft turbine engine (PW 4000-112") shown is made principally of metal alloys. The latest high-temperature, heat-resistant, high-strength nickel-base alloys are used in this engine. This engine has many advanced, service-proven technologies to enhance operational performance and durability. These include second-generation single-crystal turbine blade materials, powder metal disks, and an improved full authority digital electronic control.

(©United Technologies Corporation - Pratt & Whitney Division)



(a)



(b)

Figure 1.6

(a) Gas turbine fan blades and (b) Gas turbine compressor blades similar to those used in PW-4000.

((a) ©SteveMann/123RF; (b) ©MISS KANITHAR AIUMLA-OR/Shutterstock)

biomedical applications, including orthopedic implants, heart valves, fixation devices, and bone screws. These materials offer high strength, stiffness, and biocompatibility. Biocompatibility is important because the environment inside the human body is extremely corrosive, and therefore materials used for such applications must be effectively impervious to this environment.

In addition to better chemistry and composition control, researchers and engineers also concentrate on improving new processing techniques for these materials. Processes such as hot isostatic pressing (see Sec. 11.4) and isothermal forging have led to improved fatigue life of many alloys. Also, powder metallurgy techniques (see Sec. 11.4) will continue to be important since improved properties can be obtained for some alloys with lower finished product cost.

1.3.2 Polymeric Materials

Most polymeric materials consist of long molecular chains or networks that are usually based on organics (carbon-containing precursors). Structurally, most polymeric materials are noncrystalline, but some consist of mixtures of crystalline and non-crystalline regions. In general, polymeric materials have low densities and relatively low softening or decomposition temperatures. The strength and ductility of polymeric materials vary greatly from low strength, high deformability (rubber band) to high strength, low deformability, and high durability (vulcanized rubber used in tires). Because of the nature of their internal structure, most polymeric materials are poor conductors of electricity. Some of these materials are good insulators and are used for electrical insulative applications. Some of the often-noted applications of polymeric materials are *digital video disks* (DVDs) (Fig. 1.7a), automobile tires, and shoe soles (Fig. 1.7b). These applications show the diverse utility and importance of polymers in our everyday lives.

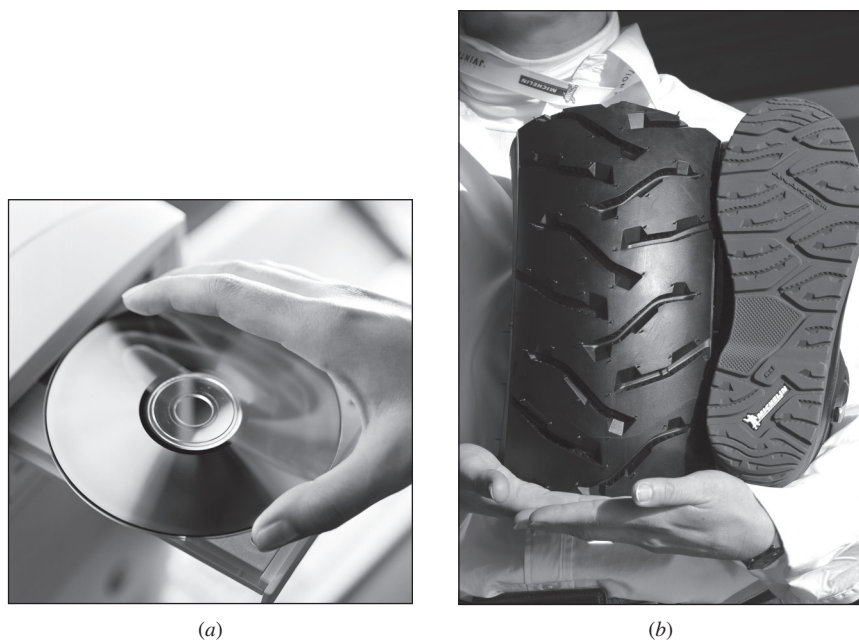


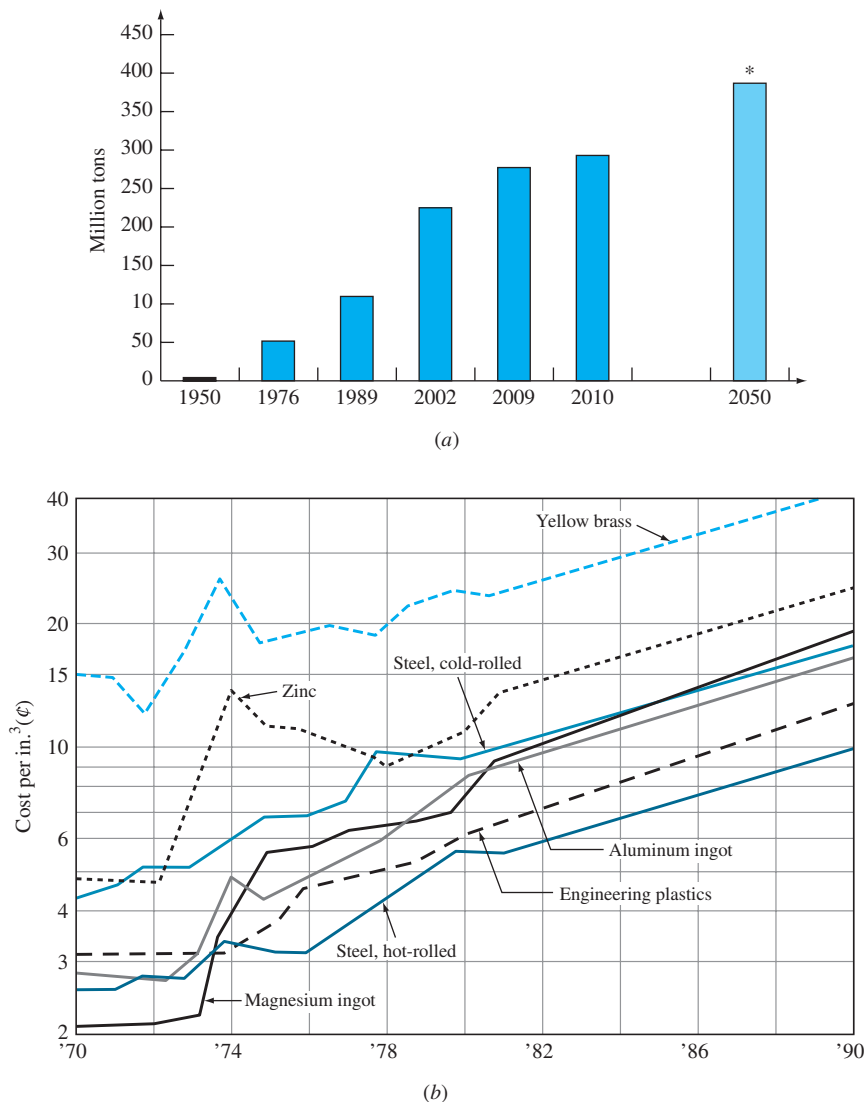
Figure 1.7

(a) Plastic resin producers are developing ultrapure, high-flow grades of polycarbonate plastic for DVDs. (b) Synthetic rubber is often used in the structure of tires because of its strength, durability, and thermal stability.

(a) ©PhotoDisc/Getty Images; (b) ©THIERRY ZOCCOLAN/AFP/Getty Images)

Historically, in terms of use, plastic materials have been the fastest-growing basic material in the United States and the world, with an overall growth of approximately 500 percent on a weight basis from 1976 to 2010 (Fig. 1.8a). Plastics continue to substitute for metals, glass, and paper in most of the main volume markets, such as automobile, packaging, and construction, for which plastics are suitable. From 1970 to 1990, engineering plastics such as nylon remained competitive with metals, according to some predictions, in terms of cost (Fig. 1.8b).

The polymer-supplying industries are increasingly focusing on the development of polymer-polymer mixtures, also known as *alloys* or **blends**, to fit specific applications for which no other single polymer is suitable. Because blends are produced based on existing polymers with well-known properties, their development is less costly and more reliable than synthesizing a new single polymer for a specific application. For example, elastomers (a highly deformable type of polymer) are often blended with other plastics to improve the impact strength of the material. Such blends have important applications in automotive bumpers, power tool housings, sporting goods, and the synthetic components used in many indoor track facilities, which are generally made

**Figure 1.8**

(a) Figure showing annual world production of plastics. The figure shows an increase from approximately 50 million Tons in 1977 to just under 300 million Tons in 2010. The projected production of plastics exceeds 350 million Tons by 2060. (b) Historical and expected competitive costs of engineering plastic resins versus some common metals from 1970 to 1990. Engineering plastics are expected to remain competitive with cold-rolled steel and other metals.

((a) Source: Algalita; (b) Source: *Modern Plastics*, August 1982, p. 12, and new data, 1998.)

of a combination of rubber and polyurethane. Acrylic coatings blended with various fibers and fillers and with brilliant colors are used as coating material for tennis courts and playgrounds. Still other polymer-coating materials are being used for protection against corrosion, aggressive chemical environments, thermal shock, impact, wear, and abrasion. The search for new polymers and blends continues because of their low cost and suitable properties for many applications.

1.3.3 Ceramic Materials

Ceramic materials are inorganic materials that consist of metallic and nonmetallic elements chemically bonded together. Ceramic materials can be crystalline, non-crystalline, or mixtures of both. Most ceramic materials have high hardness and high-temperature strength but tend to be brittle (little or no deformation prior to fracture). Ceramic materials may be classified into 1) traditional ceramics, which includes glass, clay products, and refractories, used mostly for construction and smelting applications, or 2) advanced engineering ceramics, which includes silicon carbide and alumina used for advanced applications in manufacturing and auto industries. Advantages of ceramic materials for engineering applications include light weight, high strength and hardness, good heat and wear resistance, reduced friction, and insulative properties. The insulative properties, along with the high heat and wear resistance of many conventional ceramics, make them useful for furnace linings for heat treatment and melting of metals such as steel. Advanced ceramic components are finding their way into applications that have been normally dedicated to metals, such as in automobile engines, jet engines, (Fig. 1.9) and high-performance bearings (Fig. 1.10).

The historic rate of growth for traditional ceramic materials, such as tiles and bricks, has been driven mainly by the construction sector in the United States and the world. For instance, just for ceramic tiles alone the production in the world increased from 8.6 billion square meters in 2009 to 11.9 billion square meters in 2013, a growth of approximately 40%. The worldwide growth in sales of glass and advanced ceramics reached \$17.6 billion in 2010 thanks to applications in electronics (largest percentage of sales), optical, healthcare, and aerospace industries. The trend in the use of ceramics in these markets is expected to continue at a rate of 5% to 7%.

In the past few decades, an entirely new family of ceramics of oxides, nitrides, and carbides, with improved properties, have been produced. The new generation of ceramic materials, called *engineering ceramics*, *structural ceramics*, or **advanced ceramics** has higher strength, better wear and corrosion resistance (even at higher temperatures), and enhanced resistance to thermal shock (due to sudden exposure to very high or very low temperatures). Among the established advanced ceramic materials are alumina (oxide), silicon nitride (nitride), and silicon carbide (carbide).

An important aerospace application for advanced ceramics is the use of ceramic tiles for the Space Shuttle. The ceramic tiles are made of silicon carbide because of its ability to act as a heat shield and to quickly return to normal temperatures upon removal of the heat source. These ceramic materials thermally protect the aluminum



(a)



(b)

Figure 1.9

(a) Examples of a newly developed generation of engineered ceramic materials for advanced engine applications. The black items include engine valves, valve seat inserts, and piston pins made of silicon nitride. The white item is a port-manifold liner made of an alumina ceramic material. (b) GE Aviation's next generation Adaptive Engine Technology uses advanced engineering ceramics to demonstrate their effectiveness in high-stress, high-temperature jet engine environments.

((a) Courtesy of Kyocera Industrial Ceramics Corp.; (b) Courtesy of GE Aviation)

internal substructure of the Space Shuttle during ascent and reentry into the Earth's atmosphere (see Figs. 11.39 and 11.40). Another application for advanced ceramics that points to the versatility, importance, and future growth of this class of materials is its use as a cutting tool material. For instance, silicon nitride with a high thermal shock resistance and fracture toughness is an excellent cutting tool material.

The applications for ceramic materials are truly unlimited as they can be applied to aerospace, metal manufacturing, biomedical, automobile, and numerous other industries. The two main drawbacks for this class of materials are that they are (1) difficult to process into finished products and are therefore expensive and (2) brittle and have low fracture toughness compared to metals. If techniques for developing high-toughness ceramics are developed further, there could be a tremendous upsurge in engineering applications for these materials.

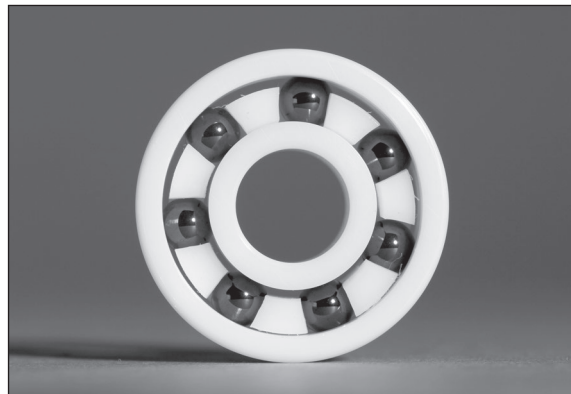


Figure 1.10

High-performance ceramic ball bearings and races are made from titanium and carbon nitride feedstocks through powder metal technology.

(©Editorial Image, LLC/Alamy)

1.3.4 Composite Materials

A composite material may be defined as two or more materials (phases or constituents) integrated to form a new one. The constituents keep their properties, and the overall composite will have properties different than each of them. Most composite materials consist of a selected filler or reinforcing material and a compatible resin binder to produce the characteristics and properties desired. Usually, the components do not dissolve in each other, and they can be physically identified by an interface between them. Composites can be of many types. Some of the predominant types are fibrous (composed of fibers in a matrix) and particulate (composed of particles in a matrix). Many different combinations of reinforcements and matrix materials are used to produce composite materials. For example, the matrix material may be a metal such as aluminum, a ceramic such as alumina, or a polymer such as epoxy. Depending on the type of matrix used, the composite may be classified as a *metal matrix composite* (MMC), a *ceramic matrix composite* (CMC), or a *polymer matrix composite* (PMC). The fiber or particulate materials may also be selected from any of the three main classes of materials with examples such as carbon, glass, aramid, silicon carbide, and others. The combinations of materials used in the design of composites depend mainly on the type of application and the environment in which the material will be used.

Composite materials have replaced many metallic components, especially in aerospace, avionics, automobile, civil structural, and sports equipment industries. An average annual gain of about 5% is predicted for the future use of these materials. One reason for this gain is their high strength and stiffness-to-weight ratio. Some advanced composites have stiffness and strength similar to some structural metal alloys but with significantly lower density, and therefore lower overall component weight. These characteristics make advanced composites extremely attractive in situations where component weight is critical. Generally speaking, similar to ceramic materials, the

main disadvantage of most composite materials is their brittleness and low fracture toughness. Some of these shortcomings may be improved, in certain situations, by the proper selection of the matrix material.

One of the main users of the lightweight advanced composite materials is the aerospace industry (Fig. 1.11a). For instance, the use of composite materials in the commercial aerospace sector was close to 6% in the 1990s and more than 50% in 2014 in advanced aircraft such as Boeing 787 and Airbus 350. Two outstanding types of *modern composite materials* used for aerospace applications are fiberglass-reinforcing material in a polyester or epoxy matrix and carbon fibers in an epoxy matrix. Figure 1.11b shows schematically where carbon-fiber-epoxy composite material was

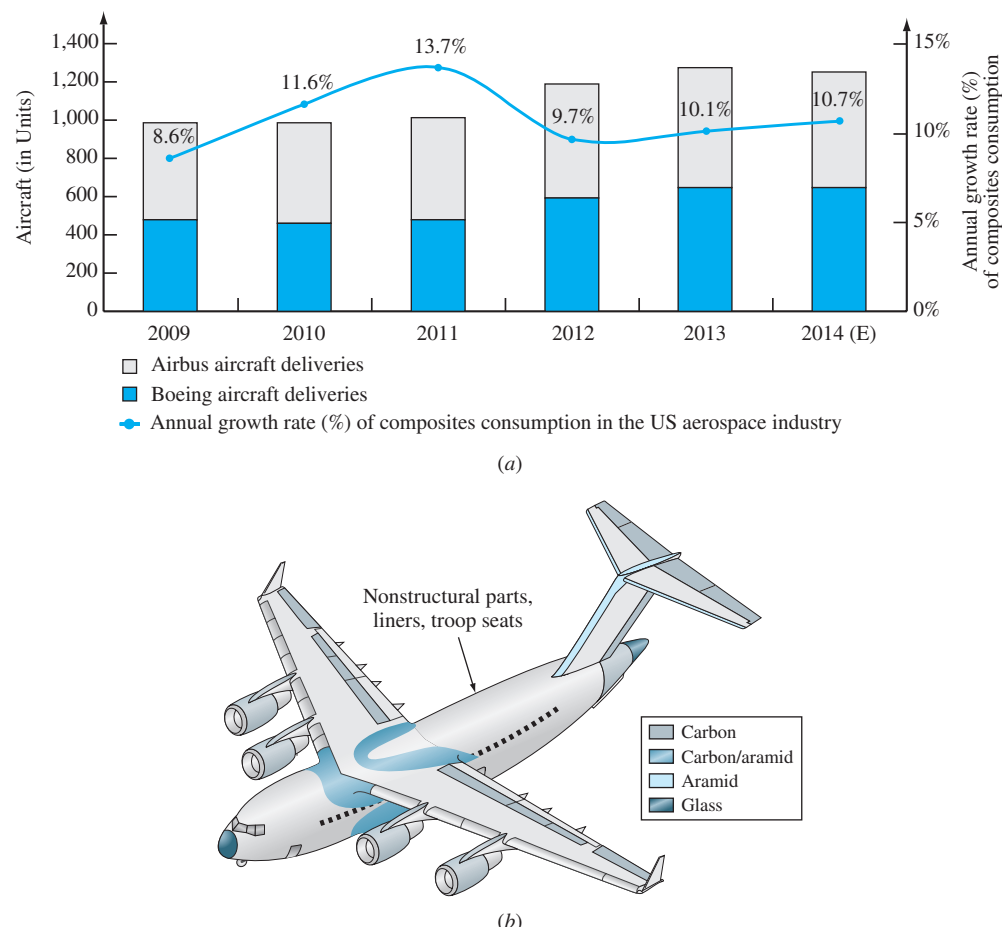


Figure 1.11

(a) Annual growth rate in consumption of composite materials in Airbus and Boeing aircraft.

(b) Overview of the wide variety of composite parts used in the Air Force's C-17 transport.

This airplane has a wingspan of 165 ft and uses 15,000 lb of advanced composites.

((a) Source: *Composite Manufacturing Magazine*, 2015; (b) Source: *Advanced Composites*, May/June 1988, p. 53.)

used for the wings and engines of the C-17 transport plane. Since these airplanes have been constructed, new cost-saving procedures and modifications have been introduced (see *Aviation Week & Space Technology*, June 9, 1997, p. 30).

1.3.5 Electronic Materials

Electronic materials are not a major type of material by production volume (tonnage) but are an extremely important type of material for advanced engineering technology. The applications of electronic materials in the semiconductor industry, specifically for mobile phones, electronic chips, integrated circuits, flat panel displays, and photolithographic printing, will continue to drive the market for such materials. The most important electronic material is pure silicon that is modified in various ways to change its electrical characteristics. A multitude of complex electronic circuits can be miniaturized on a silicon chip that is about 3/4 in. square (1.90 cm square) (Fig. 1.12). Microelectronic devices have made possible such new products as communication satellites, advanced computers, handheld calculators, digital watches, and robots.

The use of silicon and other semiconductor materials in solid-state and microelectronics has shown a tremendous growth in the past decades, and this growth pattern is expected to continue. The market size for electronic materials and the associated chemicals was reported at \$47.7 billion in 2015 (Fig. 1.13); the growth is expected to continue to a projected level of \$70 billion in 2024. The figure shows the importance of silicon as the primary material and chemicals as processing materials in the semiconductor industry. The impact of computers and other industrial types of equipment using integrated circuits made from silicon chips has been spectacular. The full effect of computerized robots in modern manufacturing is yet to be determined. Electronic

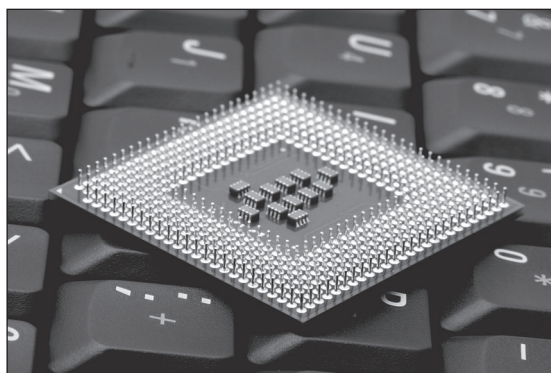
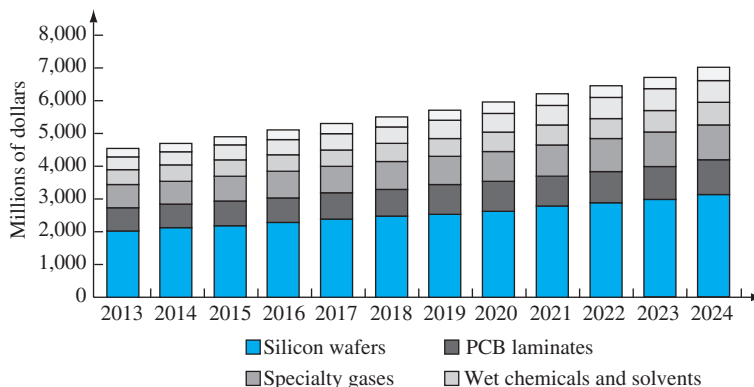


Figure 1.12

Modern microprocessors have a multitude of outlets, as indicated on this picture of Intel's Pentium II microprocessor.

(©IMP/Alamy RF)

**Figure 1.13**

The revenue history of the electronic materials and chemicals industry by application including silicon wafer, printed circuit board (PCB) laminates, and the associated gases, chemicals, and solvents.

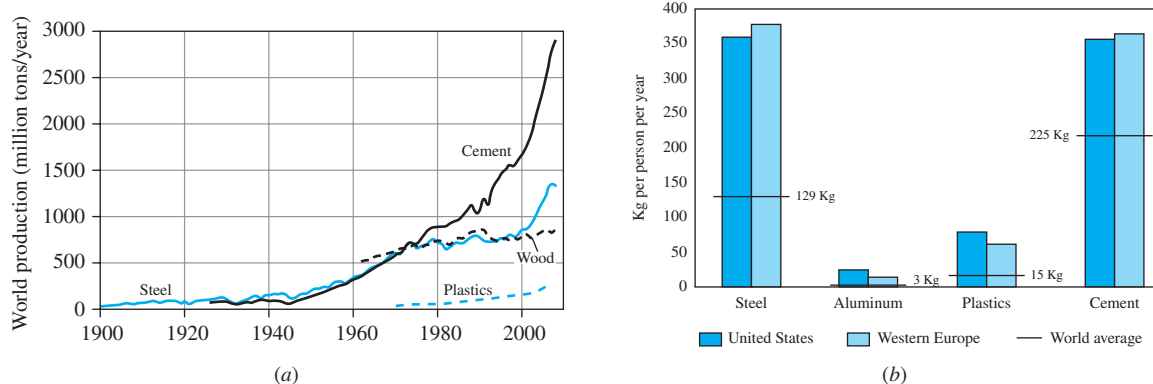
(Source: Grand View Research.)

materials will undoubtedly play a vital role in the “factories of the future” in which almost all manufacturing may be done by robots assisted by computer-controlled machine tools.

Over the years, integrated circuits have been made with greater and greater densities of transistors on a single silicon chip, with a corresponding decrease in transistor width. For example, in 2005 the point-to-point resolution for the smallest measurement on a silicon chip was $0.1 \mu\text{m}$. For a chip size of 520 mm^2 , the total number of printed transistors reached 200 million. With advances in nanotechnology, it is expected that smaller integrated circuits (ICs) with significantly larger numbers of printed devices will be manufactured, resulting in faster and more powerful computers.

1.4 COMPETITION AMONG MATERIALS

With the growth of world population and the rapid economic growth in emerging markets such as China, Korea, and India, outpacing the population growth, the per capita consumption of all materials is projected to rise. In this environment of growth and consumption, materials compete with each other for existing and new markets. Over a period of time, many factors arise that make it possible for one material to replace another for certain applications. Certainly cost is a factor. If a breakthrough is made in the processing of a certain type of material so that its cost is decreased substantially, this material may replace another for some applications. Another factor that causes material replacement changes is the development of a new material with special properties for some applications. As a result, over a period of time, the usage of different materials changes at different rates. For instance, from 1961 to 2012, the worldwide consumption of steel increased by 426%, aluminum by 945%, cement (a ceramic construction material) by 1100%, wood by 160%, polymers and plastics by 4800%. These

**Figure 1.14**

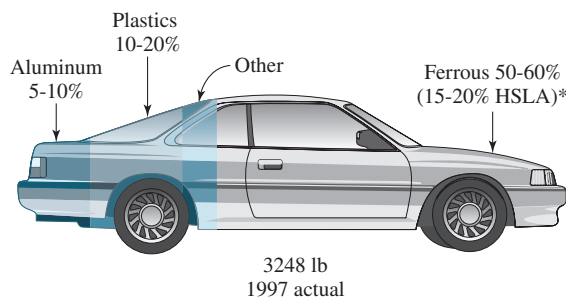
(a) Competition of four major materials produced in the United States on a weight (millions of tons) basis. The rapid rise in the production of cement and polymers (plastics) is evident. (b) Average per-person use of selected materials in the United States and western Europe.

((a) Source: J.P. Birat et al. *Revue de Metallurgie* 110, 95-129 (2013); (b) Source: Grida.)

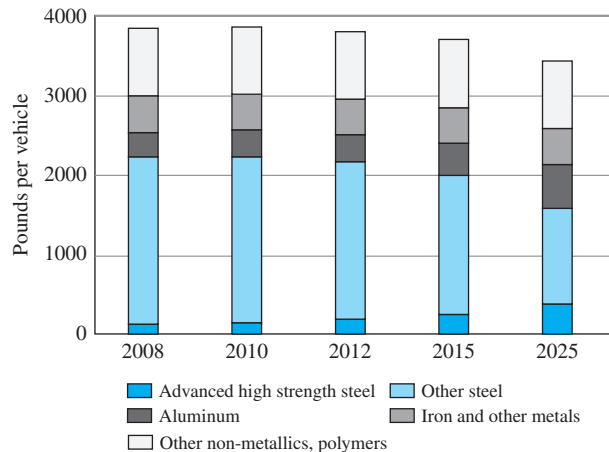
diversely different growth numbers show the steep competition in material usage in all industries (metal springs replaced by plastic springs; metal aircraft and automobile body parts replaced by plastics and composites; cast iron engines replaced by aluminum alloy engines; wooden tennis rackets replaced by aluminum or polymer composite rackets, etc.).

Figure 1.14a shows graphically the historical growth of raw materials production during the 20th and early 21st centuries. The figure shows that cement and steel grew at roughly the same pace until the 1970s, but the need for construction accelerated the need for cement at a much more rapid pace than steel. Wood and polymers/plastics show an outstanding increase in production since 1960. On a volume basis, the production increases for polymers are even more dramatic since these are light materials. The average per-person consumption of some selected materials including steel, aluminum, plastics, and cement in the United States and western Europe is shown in Figure 1.14b.

The competition among materials is evident in the composition of the U.S. auto. In 1970, the average U.S. auto weighed 1100 kg and consisted of about 79% cast iron, steel, and other metals, 8% plastics and rubber, and 14% other materials (composites and ceramics). For comparison, in 2010, the average vehicle weight is 1400 kg (larger cars) and consists of about 61% metals, 22% plastic and rubber, and 20% other materials. Thus, in the period 1970–2010 the percentage of metals used in a car declined, that of polymers increased, and that of other materials increased slightly. Additionally, in 1997 the domestic U.S. auto weighed an average of 3248 lb (1476 kg), and plastics comprised about 7.4% of it (Fig. 1.15). The trend in the usage of materials appears to be more aluminum, more advanced high-strength steel, less conventional steel and cast iron, and a lot more polymers and plastics, (Fig. 1.16).

**Figure 1.15**

Breakdown of weight percentages of major materials used in the average 1997 U.S. automobile.

**Figure 1.16**

Predictions and use of materials in U.S. automobile.
(Source: AG Metal Miner, 2013.)

For some applications only certain materials can meet the engineering requirements for a design, and these materials may be relatively expensive. For example, the modern jet engine (Fig. 1.5) requires high-temperature nickel-base superalloys to function. These materials are expensive, and no cheap substitute has been found to replace them. Thus, although cost is an important factor in engineering design, the materials used must also meet performance specifications. Replacement of one material by another will continue in the future since new materials are being discovered and new processes are being developed.

1.5 RECENT ADVANCES IN MATERIALS SCIENCE AND TECHNOLOGY AND FUTURE TRENDS

In recent decades, a number of exciting initiatives in materials science have been undertaken that could potentially revolutionize the future of the field. Smart materials (devices at micrometer-size scale) and nanomaterials are two categories of materials that will critically affect all major industries.

1.5.1 Smart Materials

Some smart materials have been around for years but are finding more applications. They have the ability to sense external environmental stimuli (temperature, stress, light, humidity, and electric and magnetic fields) and respond to them by changing their properties (mechanical, electrical, or appearance), structure, or functions. These materials are generically called **smart materials**. Smart materials or systems that use smart materials consist of sensors and actuators. The sensory component detects a change in the environment, and the actuator component performs a specific function or

a response. For instance, some smart materials change or produce color when exposed to changes in temperature, light intensity, or an electric current.

Some of the more technologically important smart materials that can function as actuators are **shape-memory alloys** and **piezoelectric ceramics**. Shape-memory alloys are metal alloys that, once strained, revert back to their original shape upon an increase in temperature above a critical transformation temperature. The change in shape back to the original is due to a change in the crystal structure above the transformation temperature. One biomedical application of a shape-memory alloys is as a stent for supporting weakened artery walls or for expanding narrowed arteries (Fig. 1.17). The deformed stent is first delivered in the appropriate position in the artery using a probe (Fig. 1.17a). The stent expands to its original shape and size after increasing its temperature to body temperature (Fig. 1.17b). For comparison, the conventional method of expanding or supporting an artery is through the use of a stainless steel tube that is expanded using a balloon. Examples of shape-memory alloys are nickel-titanium and copper-zinc-aluminum alloys.

Actuators may also be made of piezoelectric materials. The materials produce an electric field when exposed to a mechanical force. Conversely, a change in an external electric field will produce a mechanical response in the same material. Such materials may be used to sense and reduce undesirable vibrations of a component through their actuator response. Once a vibration is detected, a current is applied to produce a mechanical response that counters the effect of the vibration.

Now let us consider the design and development of systems at micrometer-size scale that use smart materials and devices to sense, communicate, and actuate: such is the world of **microelectromechanical systems** (MEMs). Originally, MEMs were

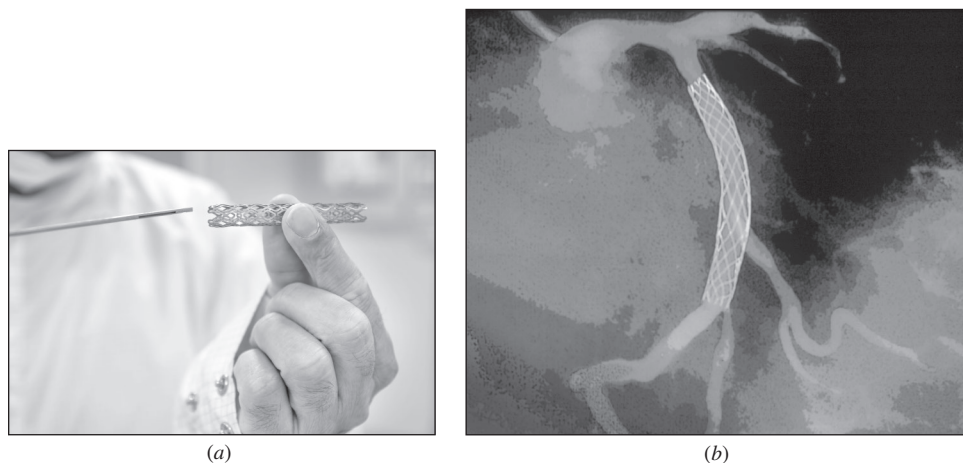


Figure 1.17

Shape-memory alloys used as a stent to expand narrowed arteries or support weakened ones: (a) stent on a probe and (b) stent positioned in a damaged artery for support.

((a) ©Czgur/Getty Images; (b) ©GJLP, CNRI/Science Source)

devices that integrated technology, electronic materials, and smart materials on a semiconductor chip to produce what were commonly known as **micromachines**. The original MEMs device had the microscopic mechanical elements fabricated on silicon chips using integrated circuits technology; MEMs were used as sensors or actuators. But today the term “MEMs” is extended to any miniaturized device. The applications of MEMs are also numerous, including but not limited to micropumps, locking systems, motors, mirrors, and sensors. For instance, MEMs are used in automobile air bags to sense both the deceleration and the size of the person sitting in the car and to deploy the air bag at a proper speed.

1.5.2 Nanomaterials

Nanomaterials are generally defined as those materials that have a characteristic length scale (that is, particle diameter, grain size, layer thickness, etc.) smaller than 100 nm ($1 \text{ nm} = 10^{-9} \text{ m}$). Nanomaterials can be metallic, polymeric, ceramic, electronic, or composite. In this respect, ceramic powder aggregates of less than 100 nm in size, bulk metals with grain size less than 100 nm, thin polymeric films with thickness less than 100 nm, and electronic wires with diameter less than 100 nm are all considered nanomaterials or nanostructured materials. A few examples of materials with micro- and nano-scale features are presented in Figure 1.18.

At the nanoscale, the properties of the material are neither that of the molecular or atomic level nor that of the bulk material. Although a tremendous amount of research and development activity has been devoted to this topic in the past decade, early research on nanomaterials dates back to the 1960s when chemical flame furnaces were used to produce particles smaller than one micron ($1 \text{ micron} = 10^{-6} \text{ m} = 10^3 \text{ nm}$) in size. The early applications of nanomaterials were as chemical catalysts and pigments. Metallurgists have always been aware that by refining the grain structure of a metal to ultrafine (submicron) levels, its strength and hardness increase significantly in comparison to the coarse-grained (micron-size) bulk metal. For example, nanostructured pure copper has a yield strength six times that of coarse-grained copper.

The reasons for the recent extraordinary attention to these materials may be due to the development of (1) new tools that make the observation and characterization of these materials possible and (2) new methods of processing and synthesizing nanostructured materials that enable researchers to produce these materials more easily and at a higher yield rate.

The future applications of nanomaterials are limited only by the imagination, and one of the major obstacles in fulfilling this potential is the ability to efficiently and inexpensively produce these materials. Consider the manufacturing of orthopedic and dental implants from nanomaterials with better biocompatibility characteristics, better strength, and better wear characteristics than metals. One such material is nanocrystalline zirconia (zirconium oxide), a hard and wear-resistant ceramic that is chemically stable and biocompatible. This material can be processed in a porous form, and when it is used as implant material, it allows for bone to grow into its pores, resulting in a more stable fixation. The metal alloys that are currently used for this application do not allow for such interaction and often loosen over time, requiring

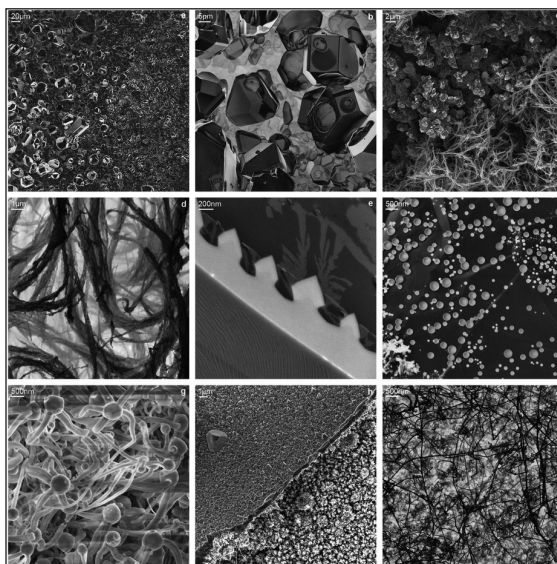


Figure 1.18

Various micro and nano features in materials. (a) Transition from large microcrystals (left side) to nanocrystals (right side); (b) high-magnification view of microcrystals and various faces; (c) nanodendrites, bottom right; (d) nanodendrites, magnified view (e) nanoscale graphite grown in SiC substrate; (f) spherical quantum dots; (g) nano-octopus structure; (h) pyramidal quantum dots; (i) nanowires.

(Source: Nature.com)

further surgery. Nanomaterials may also be used in producing paint or coating materials that are significantly more resistant to scratching and environmental damage. Also, electronic devices such as transistors, diodes, and even lasers may be developed on a nanowire. Such materials science advancements will have both technological and economical impact on all areas of engineering and industries.

Welcome to the fascinating and exceedingly interesting world of materials science and engineering!

1.6 DESIGN AND SELECTION

Material engineers should be knowledgeable about various classes of materials, their properties, structure, manufacturing processes involved, environmental issues, economic issues, and more. As the complexity of the component under consideration increases, the complexity of the analysis and the factors involved in the materials selection process also increase. Consider the materials selection issues for the frame and forks of a bicycle. The selected material must be strong enough to support the load

without yielding (permanent deformation) or fracture. The chosen material must be stiff to resist excessive elastic deformation and fatigue failure (due to repeated loading). The corrosion resistance of the material may be a consideration over the life of the bicycle. Also, the weight of the frame is important if the bicycle is used for racing: it must be lightweight. What materials will satisfy all of these requirements? A proper materials selection process must consider the issues of strength, stiffness, weight, and shape of the component (shape factor) and utilize materials selection charts in order to determine the most suitable material for the application. The detailed selection process is outside the scope of this textbook, but we use this example as an exercise in identifying various material candidates for this application. It turns out that a number of materials may satisfy the strength, stiffness, and weight considerations, including some aluminum alloys, titanium alloys, magnesium alloys, steel, carbon fiber reinforced plastic (CFRP), and even wood. Wood has excellent properties for our application, but it cannot be easily shaped to form a frame and the forks. Further analysis shows CFRP is the best choice; it offers a strong, stiff, and lightweight frame that is both fatigue and corrosion resistant. However, the fabrication process is costly, and as a result these bicycles are mostly used for competitive races; the bicycle in Figure 1.19 was designed for the U.S. athletes in the Rio Olympics.

Therefore, if cost is an issue, advanced composite materials may not be the most suitable choice. The remaining materials, all metal alloys, are all suitable and comparatively easy to manufacture into the desired shape. If cost is a major issue, steel emerges as the most suitable choice. On the other hand, if lower bicycle weight is important, the aluminum alloys emerge as the most suitable material. Titanium and magnesium alloys are more expensive than both aluminum and steel alloys and are lighter than steel; however, they do not offer significant advantages over aluminum.



Figure 1.19

Track Aero bicycle made of carbon composites designed for low weight, high stiffness, and maximal aerodynamic efficiency.

(©EnVogue_Photo/Alamy)

1.7 SUMMARY

Materials science and materials engineering (collectively, materials science and engineering) form a bridge of materials knowledge between the basic sciences (and mathematics) and the engineering disciplines. Materials science is concerned primarily with the search for basic knowledge about materials, whereas materials engineering is concerned mainly with using applied knowledge about materials.

The three main types of materials are metallic, polymeric, and ceramic materials. Two other types of materials that are very important for modern engineering technology are composite and electronic materials. All these types of materials will be dealt with in this book. Smart materials and devices in micrometer-size scale and nanomaterials are presented as new classes of materials with novel and important applications in many industries.

Materials compete with each other for existing and new markets, and so the replacement of one material by another for some applications occurs. The availability of raw materials, cost of manufacturing, and the development of new materials and processes for products are major factors that cause changes in materials usage.

1.8 DEFINITIONS

Sec. 1.1

Materials: substances of which something is composed or made. The term *engineering materials* is sometimes used to refer specifically to materials used to produce technical products. However, there is no clear demarcation line between the two terms, and they are used interchangeably.

Sec. 1.2

Materials science: a scientific discipline that is primarily concerned with the search for basic knowledge about the internal structure, properties, and processing of materials.

Materials engineering: an engineering discipline that is primarily concerned with the use of fundamental and applied knowledge of materials so that they can be converted into products needed or desired by society.

Sec. 1.3

Metallic materials (metals and metal alloys): inorganic materials that are characterized by high thermal and electrical conductivities. Examples are iron, steel, aluminum, and copper.

Polymeric materials: materials consisting of long molecular chains or networks of low-weight elements such as carbon, hydrogen, oxygen, and nitrogen. Most polymeric materials have low electrical conductivities. Examples are polyethylene and *polyvinyl chloride* (PVC).

Ceramic materials: materials consisting of compounds of metals and nonmetals. Ceramic materials are usually hard and brittle. Examples are clay products, glass, and pure aluminum oxide that has been compacted and densified.

Composite materials: materials that are mixtures of two or more materials. Examples are fiberglass-reinforcing material in a polyester or epoxy matrix.

Electronic materials: materials used in electronics, especially microelectronics. Examples are silicon and gallium arsenide.

Ferrous metals and alloys: metals and alloys that contain a large percentage of iron such as steels and cast irons.

Nonferrous metals and alloys: metals and alloys that do not contain iron, or if they do contain iron, it is only in a relatively small percentage. Examples of nonferrous metals are aluminum, copper, zinc, titanium, and nickel.

Superalloys: metal alloys with improved performance at elevated temperatures and high stress levels.

Blends: mixture of two or more polymers, also called polymer alloys.

Advanced ceramics: new generation of ceramics with improved strength, corrosion resistance, and thermal shock properties; also called engineering or structural ceramics.

Sec. 1.5

Smart materials: materials with the ability to sense and respond to external stimuli.

Shape-memory alloys: materials that can be deformed but return to their original shape upon an increase in temperature.

Piezoelectric ceramics: materials that produce an electric field when subjected to mechanical force (and vice versa).

Microelectromechanical systems (MEMs): any miniaturized device that performs a sensing and/or actuating function.

Micromachine: MEMs that perform a specific function or task.

Nanomaterials: materials with a characteristic length scale smaller than 100 nm.

1.9 PROBLEMS

Knowledge and Comprehension Problems

- 1.1 What are materials? List eight commonly encountered engineering materials.
- 1.2 What are the main classes of engineering materials?
- 1.3 What are some of the important properties of each of the five main classes of engineering materials?
- 1.4 Define a composite material. Give an example of a composite material.
- 1.5 Provide a list of characteristics for structural materials to be used in space applications.
- 1.6 Define smart materials. Give an example of such material and an application for it.
- 1.7 What are MEMs? Give an application for MEMs.
- 1.8 What are nanomaterials? What are some proposed advantages of using nanomaterials over their conventional counterparts?
- 1.9 Nickel-base superalloys are used in the structure of aircraft turbine engines. What are the major properties of this metal that make it suitable for this application?
- 1.10 Make a list of items that you find in your kitchen (at least 15 items). In each item, determine the class of materials (identify the specific material if you can) used in the structure of the item.
- 1.11 Make a list of all the major components of your school's basketball court. For each major component, determine the class of materials used in its structure (identify the specific materials if you can).
- 1.12 Make a list of major components in your automobile (at least 15 components). For each component, determine the class of materials used in its structure (identify the specific material if you can).

- 1.13 Make a list of major components in your computer (at least 10 components). For each component, determine the class of materials used in its structure (identify the specific material if you can).
- 1.14 Make a list of major components in your classroom including the constructional elements (at least 10 components). For each component, determine the class of materials used in its structure (identify the specific material if you can).
- 1.15 Perform a search on the history of “automobiles” and report how the usage of various types of materials in the structure of an automobile has changed in this field over the years.
- 1.16 Perform a search on the history of “wheels” and report on how the materials usage in this component has changed.
- 1.17 Perform a search on the history of “recording media” and report on how the usage of materials has changed in this field over the years.
- 1.18 Perform a search on the history of “sport track materials” and report on how the usage of materials has changed in this field over the years.

Application and Analysis Problems

- 1.19 List some materials usage changes that you have observed over a period of time in some manufactured products. What reasons can you give for the changes that have occurred?
- 1.20 (a) What kind of material is OFHC copper? (b) What are the desirable properties of OFHC copper? (c) What are the applications of OFHC copper in the power industry?
- 1.21 (a) To which class of materials does PTFE belong? (b) What are its desirable properties? (c) What are its applications in cookware manufacturing industries?
- 1.22 Why should civil engineers be knowledgeable about composition, properties, and processing of materials?
- 1.23 Why should mechanical engineers be knowledgeable about composition, properties, and processing of materials?
- 1.24 Why should chemical engineers be knowledgeable about composition, properties, and processing of materials?
- 1.25 Why should ocean engineers be knowledgeable about composition, properties, and processing of materials?
- 1.26 Why should petroleum engineers be knowledgeable about composition, properties, and processing of materials?
- 1.27 Why should electrical engineers be knowledgeable about composition, properties, and processing of materials?
- 1.28 Why should biomedical engineers be knowledgeable about composition, properties, and processing of materials?
- 1.29 (a) To which class of materials does **kevlar** belong? (b) What are its desirable properties? (c) What are its applications in space industries?
- 1.30 (a) To which class of materials does **silicon** belong? (b) What are its desirable properties? (c) What are its applications in chip manufacturing industries?
- 1.31 (a) To what class of materials does **zirconium oxide** belong? (b) What are its desirable properties? (c) What are its applications in manufacturing industries?

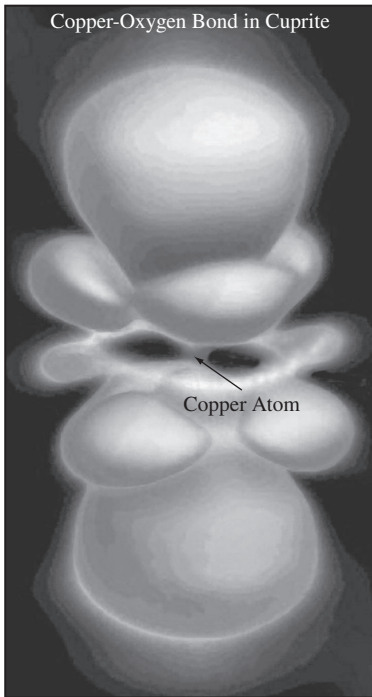
Synthesis and Evaluation Problems

- 1.32 What factors might cause materials usage predictions to be incorrect?
- 1.33 Consider the common household component in a lightbulb: (a) identify various critical components of this item, (b) determine the material selected for each critical component, and (c) design a process that would be used to assemble the lightbulb.
- 1.34 (a) Name the important factors in selecting materials for the frame of a mountain bike. (b) Steel, aluminum, and titanium alloys have all been used as the primary metals in the structure of a bicycle; determine the major weaknesses and strengths of each. (c) The more-modern bikes are made of advanced composites. Explain why, and name a specific composite used in the structure of a bike.
- 1.35 (a) Name the important criteria for selecting materials to use in a protective sports helmet. (b) Identify materials that would satisfy these criteria. (c) Why would a solid metal helmet not be a good choice?
- 1.36 Why is it important or helpful to classify materials into different groups as we have done in this chapter?
- 1.37 A certain application requires a material that must be very hard and corrosion resistant at room temperature and atmosphere. It would be beneficial, but not necessary, if the material were also impact resistant. (a) If you only consider the major requirements, which classes of materials would you search for this selection? (b) If you consider both major and minor requirements, which classes would you search? (c) Suggest a material.
- 1.38 Give as many examples as you can on how materials science and engineering is important to the topic in the cover image.
- 1.39 When selecting materials to be used inside the human body, what are some major factors that must be considered?
- 1.40 In the sport of tennis, for optimal performance, the racket face and handle must be made of a material that is very stiff (resistant to elastic deformation). Why is this important?

2

CHAPTER

Atomic Structure and Bonding



(©Tom Pantages)

Atomic orbitals represent the statistical likelihood that electrons will occupy various points in space. Except for the innermost electrons of the atoms, the shapes of the orbitals are nonspherical. Until recently, we have only been able to imagine the existence and shape of these orbitals because no experimental verifications were available. Recently, scientists have been able to create a three-dimensional image of these orbitals using a combination of X-ray diffraction and electron microscopy techniques. The chapter-opening image shows the orbital of “d” state electrons of the copper-oxygen bond in Cu₂O. Through an understanding of the bonding in copper oxides, using the techniques just described, researchers edge closer to explaining the nature of high-temperature superconductivity in copper oxides.¹ ■

¹ www.aip.org/physnews/graphics/html/orbital.html

LEARNING OBJECTIVES

By the end of this chapter, students will be able to

1. Describe the nature and structure of an atom as well as its electronic structure.
2. Describe various types of primary bonds including ionic, covalent, and metallic.
3. Describe covalent bonding by carbon.
4. Describe various types of secondary bonds and differentiate between these and primary bonds.
5. Describe the effect of bond type and strength on the mechanical and electrical performance of various classes of materials.
6. Describe mixed bonding in materials.

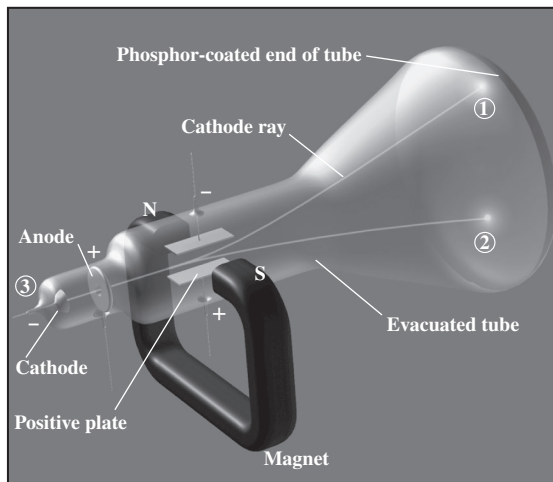
2.1 ATOMIC STRUCTURE AND SUBATOMIC PARTICLES

In the fifth century BC, the Greek philosopher Democritus² postulated that matter ultimately consists of small, indivisible particles which he called *atomos* (or *atoms*), meaning uncuttable or indivisible. This idea was lost on the scientific community until the seventeenth century when Robert Boyle³ asserted that elements are made up of “simple bodies” that themselves are not made up of any other bodies, a description of the atom very similar to that of Democritus some 2200 years prior. In the early nineteenth century, atomism was reborn as John Dalton⁴ hypothesized the most precise definition of the building blocks of matter by stating that matter is made up of small particles called *atoms* and that all atoms in a pure substance are identical, having the same size, shape, mass, and chemical properties. Furthermore, he hypothesized that the atoms of one pure substance are different from the atoms of other pure substances and when combined, in specific simple fractions, form different compounds—the **law of multiple proportions**. Finally, he proposed that a chemical reaction is explained by separation, combination, or rearrangement of atoms and that a chemical reaction does not lead to the creation or destruction of matter—the **law of mass conservation**. Dalton’s and Boyle’s assertions ignited a revolution in the field of chemistry.

² Democritus (460 BC–370 BC). Greek materialist philosopher with contributions to the fields of mathematics, minerals and plants, astronomy, epistemology, and ethics.

³ Robert Boyle (1627–1691). Irish philosopher, chemist, physicist, and inventor best known for the formulation of Boyle’s law (studied in physics and thermodynamics).

⁴ John Dalton (1766–1844). English chemist, meteorologist, and physicist.

**Figure 2.1**

A cathode ray tube, consisting of a glass tube, cathode, anode, deflecting plates, and a fluorescence screen.

In the late nineteenth century, Henri Becquerel⁵ and Marie⁶ and Pierre Curie⁷ in France introduced the concept of radioactivity. They suggested that atoms of newly found elements such as polonium and radium spontaneously emit rays, and they named this phenomenon *radioactivity*. The radiation was shown to consist of α (alpha), β (beta), and γ (gamma) rays. It was also shown that α and β particles have both charge and mass, while γ particles have no detectable mass or charge. The major conclusion from these findings was that atoms must be made up of smaller constituents or subatomic particles.

Cathode ray experiments were instrumental in identifying one of the constituents or subatomic particles of the atom (Fig. 2.1). A cathode ray consists of a glass tube with air extracted from it. At one end of this tube, two metal plates are connected to a high-voltage source. The negatively charged plate (cathode) emits an invisible ray that is attracted by the positively charged plate (anode). The invisible ray is called a *cathode ray*; it consists of negatively charged particles and comes directly from the atoms in the cathode. A hole at the center of the anode allows passage to the invisible ray that continues to travel to the end of the tube, where it strikes a specially coated plate (fluorescence screen) and produces tiny flashes, (Fig. 2.1). In a series of such experiments, Joseph J. Thompson⁸ concluded that

⁵ Henri Becquerel (1852–1908). French physicist and Nobel laureate (1903).

⁶ Marie Curie (1867–1934). Polish (French citizenship) physicist and chemist and Nobel laureate (1903).

⁷ Pierre Curie (1859–1906). French physicist and Nobel laureate (1903); shared with Marie Curie and Henri Becquerel.

⁸ Joseph J. Thompson (1856–1940). British physicist and Nobel laureate.

atoms in all matters are made of smaller particles that are negatively charged, called *electrons*. He also calculated the ratio of mass to charge of these electrons to be 5.60×10^{-19} g/C where *Coulomb*, C, is the unit of electrical charge. Later, Robert Millikan,⁹ in his oil-drop experiments, determined the fundamental quantity of charge or the charge of an electron (regardless of the source) to be 1.60×10^{-19} C. For an electron, this quantity of charge is represented by -1 . Using the ratio of mass to charge of the electron measured by Thompson and the charge of the electron measured by Millikan, the mass of an electron was determined to be 8.96×10^{-28} g. Based on this evidence of the existence of negatively charged electrons, it was deducted that the atom must also contain an equal number of positively charged subatomic particles to maintain its electrical neutrality.

In 1910, Ernest Rutherford,¹⁰ Thompson's student, bombarded a very thin foil of gold with positively charged α particles. He noticed that many of the α particles passed through the foil without deflection, some were slightly deflected, and a few were either largely deflected or completely bounced back. He concluded that (1) most of the atom must be made up of empty space (thus, most particles pass through without deflection) and (2) a small neighborhood at the center of the atom, the nucleus, houses positively charged particles of its own. He suggested that those α particles that deflected intensely or bounced back must have interacted closely with the positively charged nucleus of the atom. The positively charged particles in the nucleus were called *protons*. It was later determined that the proton carries the same quantity of charge as an electron but opposite in sign and that it has a mass of 1.672×10^{-24} g (1840 times the mass of the electron). For a proton this quantity of charge is represented by $+1$.

Finally, since atoms are electrically neutral, they must have an equal number of electrons and protons. However, neutral atoms have a mass that is larger than the mass of protons alone. In 1932, James Chadwick¹¹ provided the first evidence of an isolated neutron outside the atom. These particles with no electrical charge and with a mass of 1.674×10^{-24} g (slightly larger than a proton) were called *neutrons*. The mass, charge, and charge unit of the electrons, protons, and neutrons are presented in Table 2.1.

Table 2.1 Mass, charge, and charge unit of protons, neutrons, and electrons

Particle	Mass (g)	Charge	
		Coulomb (C)	Charge Unit
Electron	9.10939×10^{-28}	-1.60022×10^{-19}	-1
Proton	1.67262×10^{-24}	$+1.60022 \times 10^{-19}$	$+1$
Neutron	1.67493×10^{-24}	0	0

⁹ Robert Millikan (1868–1953). American physicist (first PhD in physics from Columbia University) and Nobel laureate (1923).

¹⁰ Ernest Rutherford (1871–1937). Physicist from New Zealand and Nobel laureate (1908).

¹¹ James Chadwick (1891–1974). English physicist and Nobel laureate (1935).

According to an atomic model, a typical atomic radius was about 100 *picometers* (1 picometer = 1×10^{-12} m) with a much smaller nucleus of 5×10^{-3} picometer. If one enlarges an atom to the size of a football stadium, the corresponding nucleus would be the size of a marble. The electrons were thought to be dispersed at some distance from the nucleus in what was called the *charge cloud*. This atomic model and the corresponding dimensions are schematically presented in Figure 2.2.

When studying the interaction of atoms (similar or different atoms), the electron configuration of each atom is of critical importance. The electrons (especially the ones with the highest energy) determine the extent of reactivity or the tendency of an atom to bond with another.

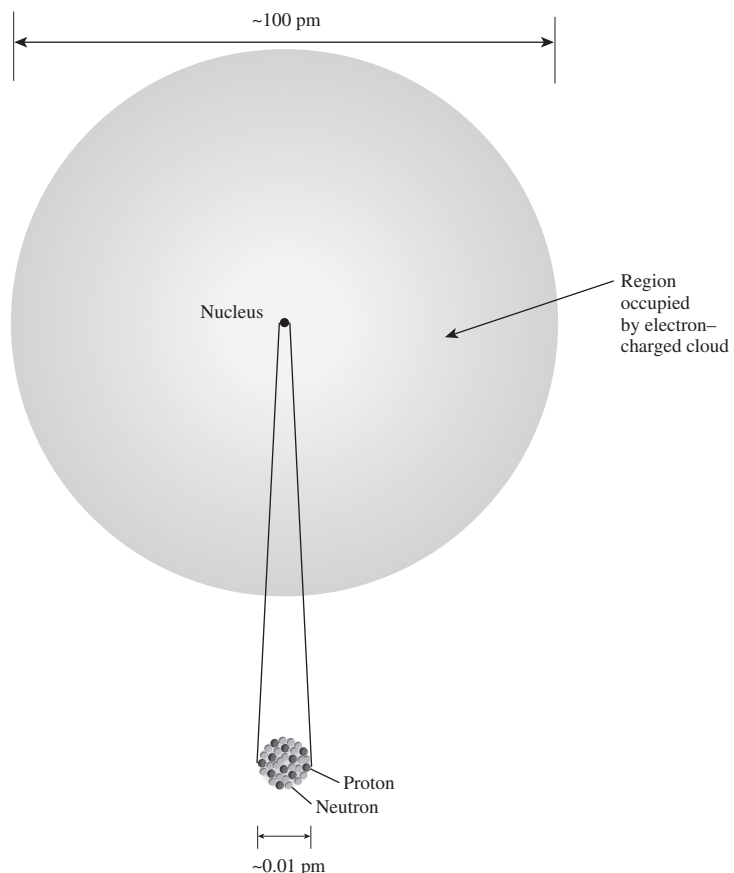


Figure 2.2

The relative size of an atom and its nucleus that is made up of protons and neutrons. Note that contrary to the schematic, the atom boundaries are not well defined.

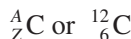
2.2 ATOMIC NUMBERS, MASS NUMBERS, AND ATOMIC MASSES

2.2.1 Atomic Numbers and Mass Numbers

In the early twentieth century, it was discovered that each atom has a specific number of protons in its nucleus; this number was named the **atomic number** (Z). Each element has its own characteristic atomic number that defines that element. For instance, any atom with 6 protons is by definition a carbon atom. In a neutral atom, the atomic number or the number of protons is also equal to the number of electrons in its charge cloud.

The mass of an atom, *atomic mass*, is expressed in **atomic mass units** (amu). One amu is defined as exactly 1/12th the mass of a carbon atom with 6 protons and 6 neutrons. This also indicates that the mass of one neutron or one proton is very close to 1 amu. Thus, a carbon-12 atom itself has an atomic mass of 12 amu.

The **mass number** (A) is the sum of protons and neutrons in a nucleus of an atom. Except for hydrogen, which does not have a neutron in its most common form, all nuclei contain both protons and neutrons. For instance the carbon atom has a mass number of 12 (6 protons + 6 neutrons). The proper way of expressing both the mass number and the atomic number of an atom, exemplified here with a carbon atom, is



The Z number is redundant; by definition we know the number of protons from the identity of the atom, so often the presentation ${}^{12}\text{C}$ (or carbon-12) is considered sufficient. For example, if we want to find the number of neutrons in iodine-131 (${}^{131}\text{I}$), we see from the periodic table that I is the fifty-third element (53 protons). We can easily determine the number of neutrons to be 78 ($131 - 53$). Not all atoms of the same element necessarily have the same number of neutrons, although they all have the same number of protons. These variations (the same atomic number but different mass numbers) are called **isotopes**. As an example, the hydrogen atom has three isotopes: ${}_1^1\text{H}$ (hydrogen), ${}_1^2\text{H}$ (deuterium), and ${}_1^3\text{H}$ (tritium).

Based on previous discussion, it is known that an amu provides us with a relative measure of the mass of an atom with respect to the carbon atom. But how do we find the mass of one atom in grams? Well, it was experimentally determined that the number of atoms in 12 grams of ${}^{12}\text{C}$ is 6.02×10^{23} (called *Avogadro's number* in honor of the Italian scientist¹²). To appreciate the magnitude of this number, consider that if you could distribute 6.022×10^{23} pennies equally among the population of the Earth (~6 billion), each person would receive over 1.0 trillion dollars! One **mole** or **gram-mole** (mol) of any element is then defined as the amount of substance that contains 6.02×10^{23} atoms. Avogadro's number corresponds to the number of atoms needed to create a mass in units of grams numerically equal to the atomic mass in amu of the substance under consideration. For instance, one atom of ${}^{12}\text{C}$ has an atomic

¹² Amedeo Avogadro (1776–1856). Italian scientist and professor of physics at the University of Turin.

mass of 12 amu, while one mole of ^{12}C has a mass of 12 grams and contains 6.02×10^{23} atoms; this mass is called the *relative atomic mass*, *molar mass*, or *atomic weight*. It is important to note that the relative atomic mass of each element reported in most textbooks (including this one) represents the *average relative atomic mass* of that element for all its naturally occurring isotopes weighed by their isotopic abundance. For instance, the relative atomic mass for carbon is reported as 12.01 grams instead of 12 grams. This is due to some C isotopes such as ^{13}C (1.07% abundant) being more massive than ^{12}C (98.93% abundant).

**EXAMPLE
PROBLEM 2.1**

The most abundant isotopes of iron, Fe, are:

^{56}Fe (91.754%), with an atomic mass of 55.934 amu

^{54}Fe (5.845%), with an atomic mass of 53.939 amu

^{57}Fe (2.119%), with an atomic mass of 56.935 amu

^{58}Fe (0.282%), with an atomic mass of 57.933 amu

Solution

- a. Find the average atomic mass of Fe.

$$[(91.754 \times 55.934) + (5.845 \times 53.939) + (2.119 \times 56.935) + (0.282 \times 57.933)]/100 = 55.8 \text{ amu} \text{ (mass of one Fe atom in amu)}$$

- b. What is the relative atomic mass of iron?

As discussed previously, the relative atomic mass will have numerically the same value as the average atomic mass but with units of grams, 55.849 grams. Compare this value to that reported in the periodic table, Figure 2.3.

- c. How many atoms are there in 55.849 grams of Fe?

$$6.02 \times 10^{23} \text{ atoms}$$

- d. How many atoms are there in one gram of Fe?

$$\begin{aligned} 1 \text{ g Fe} &\times (1 \text{ mol Fe}/55.849 \text{ g Fe}) \times (6.02 \times 10^{23} \text{ atoms Fe}/1 \text{ mol Fe}) \\ &= 1.078 \times 10^{22} \text{ atoms of Fe} \end{aligned}$$

- e. What is the mass in grams of one atom of Fe?

$$55.849 \text{ g}/6.02 \times 10^{23} \text{ atoms} = 9.277 \times 10^{-23} \text{ gram/atom.}$$

- f. Based on the answer in part e, what is the mass in grams of one amu? The average atomic mass of Fe is found to be 55.846 amu in part a. In part e, the corresponding mass in grams is found to be 9.277×10^{-23} gram. The mass in grams of one amu is therefore $9.277 \times 10^{-23}/55.846 = 1.661 \times 10^{-24}$ g.

MAIN-GROUP ELEMENTS		Periodic Table of the Elements																		MAIN-GROUP ELEMENTS															
		IA (1)		TRANSITION ELEMENTS																VIIIA (18)															
Period	1	H 1.008	IIA (2)																	2	He 4.003														
	2	3 Li 6.941	4 Be 9.012																	5 B 10.81	6 C 12.01	7 N 14.01	8 O 16.00	9 F 19.00	10 Ne 20.18										
	3	11 Na 22.99	12 Mg 24.31																	13 Al 26.98	14 Si 28.09	15 P 30.97	16 S 32.07	17 Cl 35.45	18 Ar 39.95										
	4	19 K 39.10	20 Ca 40.08	21 Sc 44.96	22 Ti 47.88	23 V 50.94	24 Cr 52.00	25 Mn 54.94	26 Fe 55.85	27 Co 58.93	28 Ni 58.69	29 Cu 63.55	30 Zn 65.39	31 Ga 69.72	32 Ge 72.61	33 As 74.92	34 Se 78.96	35 Br 79.90	36 Kr 83.80																
	5	37 Rb 85.47	38 Sr 87.62	39 Y 88.91	40 Zr 91.22	41 Nb 92.91	42 Mo 95.94	43 Tc (98)	44 Ru 101.1	45 Rh 102.9	46 Pd 106.4	47 Ag 107.9	48 Cd 112.4	49 In 114.8	50 Sn 118.7	51 Sb 121.8	52 Te 127.6	53 I 126.9	54 Xe 131.3																
	6	55 Cs 132.9	56 Ba 137.3	57 La 138.9	72 Hf 178.5	73 Ta 180.9	74 W 183.9	75 Re 186.2	76 Os 190.2	77 Ir 192.2	78 Pt 195.1	79 Au 197.0	80 Hg 200.6	81 Tl 204.4	82 Pb 207.2	83 Bi 209.0	84 Po (209)	85 At (210)	86 Rn (222)																
	7	87 Fr (223)	88 Ra (226)	89 Ac (227)	104 Rf (261)	105 Db (262)	106 Sg (266)	107 Bh (262)	108 Hs (265)	109 Mt (266)	110 Uun (269)	111 Uuu (272)	112 Uub (277)	113 Uug (285)	114 Uuh (289)	115 Uuo (289)	116 Uuh (289)	117 Uuo (289)	118 Uuo (289)																
INNER TRANSITION ELEMENTS																																			
6 Lanthanides																																			
6																																			
6 Ce 140.1																																			
6 Pr 140.9																																			
6 Nd 144.2																																			
6 Pm (145)																																			
6 Sm 150.4																																			
6 Eu 152.0																																			
6 Gd 157.3																																			
6 Tb 158.9																																			
6 Dy 162.5																																			
6 Ho 164.9																																			
6 Er 167.3																																			
6 Tm 168.9																																			
6 Yb 173.0																																			
6 Lu 175.0																																			
7 Actinides																																			
7 90 Th 232.0																																			
7 91 Pa (231)																																			
7 92 U 238.0																																			
7 93 Np (237)																																			
7 94 Pu (242)																																			
7 95 Am (243)																																			
7 96 Cm (247)																																			
7 97 Bk (247)																																			
7 98 Cf (251)																																			
7 99 Es (252)																																			
7 100 Fm (257)																																			
7 101 Md (258)																																			
7 102 No (259)																																			
7 103 Lr (260)																																			

Figure 2.3

The updated periodic table showing seven periods, eight main group elements, transition elements, and inner transition elements. Note that the majority of the elements are classified as metals or metalloids.

Dmitri Mendeleev¹³ first organized the elements in a table that has evolved to what we now call the *periodic table*. He ordered the elements in a horizontal row according to their relative atomic mass. He then started a new row when he found an element that had similar chemical properties to one of the elements in the

¹³ Dmitri I. Mendeleev (1834–1907). Russian chemist and inventor.

**EXAMPLE
PROBLEM 2.2**

An intermetallic compound has the chemical formula Ni_xAl_y , where x and y are simple integers, and consists of 42.04 wt% nickel and 57.96 wt% aluminum. What is the simplest formula of this nickel aluminide?

■ Solution

We first determine the mole fraction of nickel and aluminum in this compound. Using a basis of 100 g of the compound, we have 42.04 g of Ni and 57.96 g of Al. Thus,

$$\text{No. of moles of Ni} = 42.04 \text{ g Ni} \times (1 \text{ mol Ni}/58.71 \text{ g Ni}) = 0.7160 \text{ mol}$$

$$\text{No. of moles of Al} = 57.96 \text{ g Al} \times (1 \text{ mol Al}/26.98 \text{ g Al}) = 2.148 \text{ mol}$$

$$\text{Total} = 2.864 \text{ mol}$$

Thus,

$$\text{mole fraction of Ni} = 0.1760/2.864 = 0.25$$

$$\text{mole fraction of Al} = 2.148/2.864 = 0.75$$

The simplest formula in terms of gram-mole fraction becomes $\text{Ni}_{0.25}\text{Al}_{0.75}$. To express this in integer form we multiply both fractions by 4, resulting in NiAl_3 .

previous row. After completing his table, he noticed that the elements in the same column had similar chemical characteristics. He also noticed that some columns contained empty spots that he attributed to elements not being found yet (e.g., gallium and germanium). These elements were later found and had properties close to what Mendeleev had suggested.

Later, scientists observed that arranging the elements based on increasing atomic number instead of relative atomic mass reveals a periodic behavior. This behavior is referred to as the **law of chemical periodicity**, which states that the properties of elements are functions of their atomic number in a periodic manner. A new periodic table based on this number (z) was developed by H.G.J. Moseley.¹⁴ An updated version of this table is presented in Figure 2.3. Note that each horizontal row of elements is called a *period* (i.e., first period, second period, . . . seventh period), and each vertical column of the elements is called a *group* (i.e., group 1A, 2A, . . . 8A). The transition and the inner transition elements (heavy metals) are also shown. Each element is presented by its chemical symbol above which the atomic number is presented. Below the symbol, the atomic mass, in amu, or the relative molar mass, in grams, is presented (recall they are the same number). As an example, based on the information in the periodic table, aluminum has 13 protons ($Z = 13$); one mole of aluminum has a mass of 26.98 grams (or 26.98 grams/mol) and contains 6.02×10^{23} atoms. Thus far, 109 elements have been discovered and named, ranging from hydrogen with an atomic number of 1 to meitnerium with an atomic number of 109 (six others have been discovered but are yet to be named).

¹⁴ Henry G.J. Moseley (1887–1915). English physicist.

2.3 THE ELECTRONIC STRUCTURE OF ATOMS

2.3.1 Planck's Quantum Theory and Electromagnetic Radiation

In the early 1900s, Max Planck,¹⁵ a German scientist, discovered that atoms and molecules emit energy only in certain discrete quantities, called **quanta**. Prior to that, scientists believed that energy in any amount (continuous) could be emitted from an atom. Max Planck's *quantum theory* altered the direction of science. To understand his discovery, we must first understand the nature of waves.

There are many different types of waves such as water waves, sound waves, and light waves. In 1873, James Clerk Maxwell¹⁶ proposed that the nature of visible light is in the form of electromagnetic radiation. In **electromagnetic radiation**, energy is released and transmitted in the form electromagnetic waves. Electromagnetic waves travel at the speed of light, c , 3.00×10^8 meters per second (186,000 miles/s) in vacuum.

Just like any other wave, the important characteristics that define the electromagnetic waves are wavelength (often given in nm or 10^{-9} m), frequency (s^{-1} or Hz), and speed (m/s). The speed of the wave, c , is related to its frequency, ν , and wavelength, λ , as follows:

$$\nu = \frac{c}{\lambda} \quad (2.1)$$

A variety of electromagnetic waves including radio, microwave, infrared, visible, ultraviolet, X-ray, and gamma ray waves are presented in Figure 2.4. These waves differ from each other according to their wavelengths and frequencies. For instance, a radio antenna produces large wavelengths (10^{12} nm \sim 1 km) and low frequencies (10^6 Hz); a microwave oven produces microwaves with wavelengths of around 10^7 nm (significantly shorter than radio waves) and frequencies of 10^{11} Hz (significantly higher than radio waves). As the wavelength decreases and frequency increases, we reach the infrared range of 10^3 nm wavelength and 10^{14} Hz frequency (heat lamps operate in this range). When the wavelength is in the range of 700 nm (red light) to 400 nm (violet), the resulting radiation is visible (visible range). The ultraviolet rays (10 nm), X-rays (0.1 nm), and gamma rays (0.001 nm) are again in the invisible range.

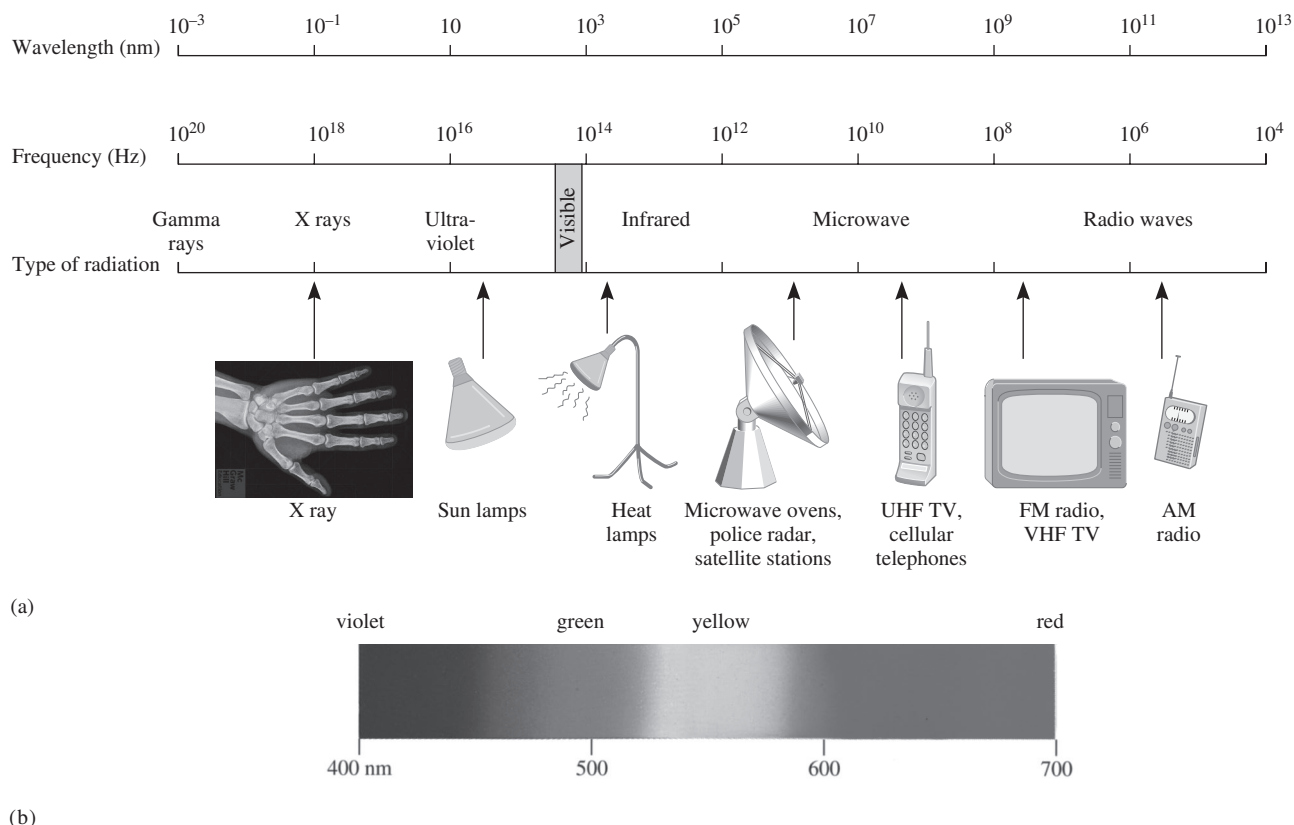
When, for example, a tungsten filament is heated, its atoms emit energy in the form of electromagnetic radiation that appears as visible white light to us. Planck suggested that energy emitted from the atoms associated with this radiation is emitted in a quantum form. The energy of a single quantum of energy is given by the following equation, where h is the Planck's constant (6.63×10^{-34} J·s, where J is Joule) and ν is the frequency of radiation (Hz).

$$E = h\nu \quad (2.2)$$

More specifically, according to Planck, energy is always released in integer multiples of $h\nu$ ($1h\nu, 2h\nu, 3h\nu, \dots$) and never in noninteger multiples, such as $1.34 h\nu$. Eq. 2.2 also implies that as the frequency of radiation increases, its energy will also

¹⁵ Max Karl Ernst Ludwig Planck (1858–1947). German physicist and Nobel laureate (1918). Three of his doctoral students received Nobel prizes.

¹⁶ James Clerk Maxwell (1831–1879). Scottish mathematician and physicist.

**Figure 2.4**

Electromagnetic spectrum extending from low-wavelength, high-frequency gamma rays to large-wavelength, low-frequency radio waves. (a) The full spectrum. (b) Visible spectrum.

(©kravka/Shutterstock)

increase. Thus, when referring to the electromagnetic spectrum, gamma rays produce higher energies than X-rays, X-rays higher than ultraviolet rays, and so on.

Inserting Eq. 2.1 into Eq. 2.2, the energy associated with a form of radiation can also be calculated in terms of the wavelength of the radiation:

$$E = \frac{hc}{\lambda} \quad (2.3)$$

2.3.2 Bohr's Theory of the Hydrogen Atom

In 1913, Neils Bohr¹⁷ used Max Planck's quantum theory to explain how the excited hydrogen atom absorbs and emits only certain wavelengths of light, a phenomenon

¹⁷ Neils Henrik Davis Bohr (1885–1962). Danish physicist and Nobel laureate (1922).

that had yet to be explained. He suggested that electrons travel in circular paths around the nucleus with discrete angular momenta (a product of velocity and radius). Furthermore, he suggested that the energy of the electron is restricted to a specific energy level that places the electron at that fixed circular distance from the nucleus. He called this the *orbit* of the electron. If the electron loses or gains a specific amount of energy, it will then change its orbit to another circular orbit at a fixed distance from its nucleus (Fig. 2.5). In his model, the value of the orbit, the principal quantum number n , can range from 1 to infinity. The energy of the electron and the size of its orbit increases as n increases. The $n = 1$ orbit represents the lowest energy state and is therefore closest to the nucleus. The normal state of the hydrogen electron is at $n = 1$ and is called the *ground state*. For an electron to move from a lower orbit, for instance, the ground state, $n = 1$, to a higher excited state, $n = 2$, a specific amount of energy must be absorbed (Fig. 2.5). In contrast, when the electron drops from the excited state, $n = 2$, to the ground state, $n = 1$, the same amount of energy must be released. As discussed previously, this quantum of energy emitted or released will be in the form of electromagnetic radiation, called a **photon**, with a specific wavelength and frequency.

Bohr developed a model for the determination of the allowed energy of the hydrogen electron depending on its quantum state, n (Fig. 2.6). Only energy levels according to this equation were allowed.

$$E = -2\pi^2 me^4/n^2 h^2 = \frac{-13.6}{n^2} \quad (2.4)$$

where m and e are the mass and the charge of the electron, respectively, and $eV = 1.60 \times 10^{-19}$ J. The negative sign was used because Bohr assigned zero to the energy of a completely separated electron with no kinetic energy at $n = \infty$. Thus, the energy of any electron at a lower orbit would be negative. According to Bohr's

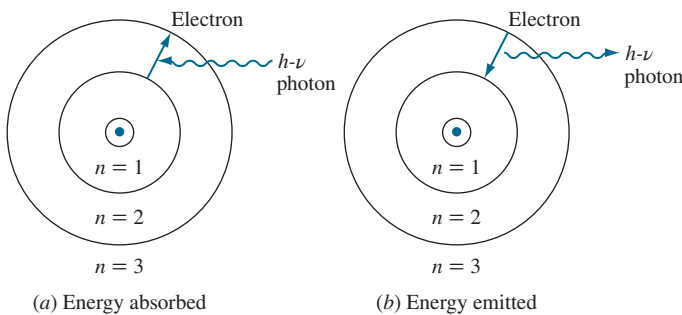
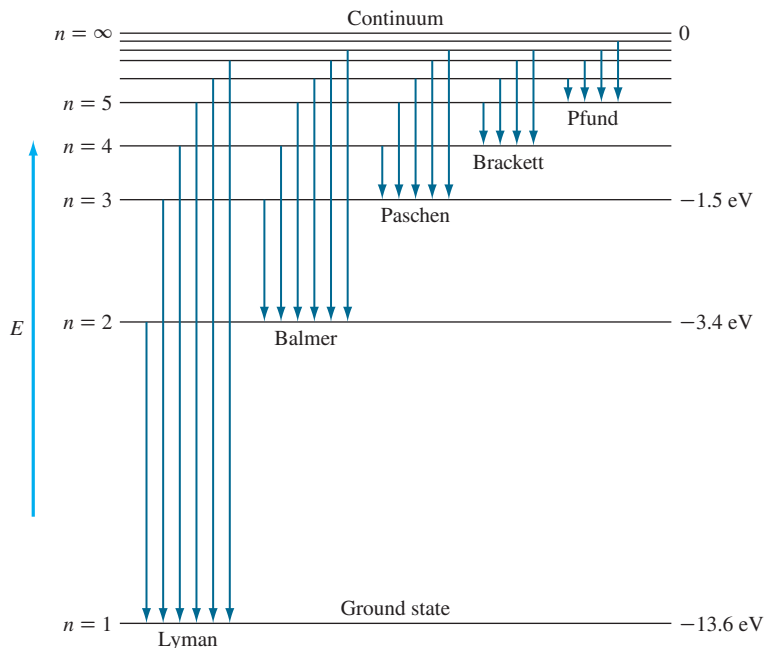


Figure 2.5

- (a) The hydrogen electron being excited into a higher orbit.
- (b) An electron in a higher energy orbit dropping to a lower orbit, resulting in the emission of a photon of energy $h\nu$.

(This figure is only acceptable for Bohr's model.)

**Figure 2.6**

Energy-level diagram for the line spectrum of hydrogen.

(Source: F.M. Miller, *Chemistry: Structure and Dynamics*, McGraw-Hill, 1984, p. 141.)

equation, the energy of the electron in the ground state, $n = 1$, is -13.6 eV . In order to separate that electron from its nucleus, energy must be absorbed by the electron. The minimum energy required to accomplish this is called the **ionization energy**. As n increases, the energy associated with the electron in that orbit also increases (becomes less negative). For instance when $n = 2$, the corresponding energy level for the electron is $-13.6/2^2$ or -3.4 eV .

Bohr explained the quantity of energy released or absorbed by the electron as it changed orbits based on the difference in the energy of the electron between the final and initial orbits ($\Delta E > 0$ when energy is released and $\Delta E < 0$ when energy is absorbed):

$$\Delta E = E_f - E_i = -13.6 \left(\frac{1}{n_f^2} - \frac{1}{n_i^2} \right) \quad (2.5)$$

where f and i represent the final and the initial states of the electron, respectively. For instance, the energy associated with a transition from $n = 2$ to $n = 1$ would result in a $\Delta E = E_2 - E_1 = -13.6 \left(\frac{1}{2^2} - \frac{1}{1^2} \right) = 13.6 \times 0.75 = 10.2 \text{ eV}$. The electron emits a photon of 10.2 eV as it drops to $n = 1$ (energy is released). The wavelength of this photon is determined according to $\lambda = hc/E = (6.63 \times 10^{-34} \text{ J s}) (3.00 \times 10^8 \text{ m/s}) / 10.2 \text{ eV} = (1.6 \times 10^{-19} \text{ J/eV}) 1.2 \times 10^{-7} \text{ m or } 120 \text{ nm}$. From Figure 2.4, this wavelength corresponds to the ultraviolet range.

Various possible transitions of the hydrogen electron or the emission spectrum of hydrogen are presented in Figure 2.6. In this figure, each horizontal line represents an acceptable energy level or orbit, according to principal quantum number n , for the hydrogen electron. The visible emissions all fall under the Balmer series. The Lyman series corresponds to the ultraviolet emissions, while the Paschen and the Brackett series correspond to infrared emissions.

**EXAMPLE
PROBLEM 2.3**

A hydrogen atom exists with its electron in the $n = 3$ state. The electron undergoes a transition to the $n = 2$ state. Calculate (a) the energy of the corresponding photon, (b) its frequency, and (c) its wavelength. (d) Is the energy absorbed or emitted, and (e) which series does it belong to and what specific type of emission does it represent?

■ Solution

- a. Energy of the photon emitted is

$$\begin{aligned} E &= \frac{-13.6 \text{ eV}}{n^2} \\ \Delta E &= E_3 - E_2 \\ &= \frac{-13.6}{3^2} - \frac{-13.6}{2^2} = 1.89 \text{ eV} \blacktriangleleft \\ &= 1.89 \text{ eV} \times \frac{1.60 \times 10^{-19} \text{ J}}{\text{eV}} = 3.02 \times 10^{-19} \text{ J} \blacktriangleleft \end{aligned} \quad (2.3)$$

- b. The frequency of the photon is

$$\begin{aligned} \Delta E &= h\nu \\ \nu &= \frac{\Delta E}{h} = \frac{3.02 \times 10^{-19} \text{ J}}{6.63 \times 10^{-34} \text{ J} \cdot \text{s}} \\ &= 4.55 \times 10^{14} \text{ s}^{-1} = 4.55 \times 10^{14} \text{ Hz} \blacktriangleleft \end{aligned}$$

- c. The wavelength of the photon is

$$\begin{aligned} \Delta E &= \frac{hc}{\lambda} \\ \text{or } \lambda &= \frac{hc}{\Delta E} = \frac{(6.63 \times 10^{-34} \text{ J} \cdot \text{s})(3.00 \times 10^8 \text{ m/s})}{3.02 \times 10^{-19} \text{ J}} \\ &= 6.59 \times 10^{-7} \text{ m} \\ &= 6.59 \times 10^{-7} \text{ m} \times \frac{1 \text{ nm}}{10^{-9} \text{ m}} = 659 \text{ nm} \blacktriangleleft \end{aligned}$$

- d. Energy is released as its quantity is positive, and the electron is transitioning from a higher orbit to a lower orbit.
- e. The emission belongs to the Balmer series (Fig. 2.6) and corresponds to visible red light (Fig. 2.4).

2.3.3 The Uncertainty Principle and Schrödinger's Wave Functions

Although Bohr's model worked very well for a simple atom such as hydrogen, it did not explain the behavior of more complex (multielectron) atoms, and it left many unanswered questions. Two new discoveries helped scientists explain the true behavior of the atom. The first was the proposal by Louis de Broglie¹⁸ that particles of matter such as electrons could be treated in terms of both particles and waves (similar to light). He proposed that the wavelength of an electron (or any other particle) can be determined by determining the product of its mass and its speed (its momentum) using Eq. 2.6.

$$\lambda = \frac{h}{mv} \quad (2.6)$$

Later, Werner Heisenberg¹⁹ proposed the **uncertainty principle** stating that it is impossible to simultaneously determine the exact position and the exact momentum of a body, for instance an electron. The uncertainty principle is mathematically expressed by Eq. 2.7, where h is the Planck's constant, Δx is the uncertainty in the position, and Δu is the uncertainty in speed.

$$\Delta x \cdot m\Delta u \geq \frac{h}{4\pi} \quad (2.7)$$

Heisenberg's reasoning was that any attempt at measurement would alter the velocity and position of the electron. Heisenberg also rejected Bohr's concept of an "orbit" of fixed radius for an electron; he asserted that the best we can do is to provide the probability of finding an electron with a given energy within a given space.

EXAMPLE PROBLEM 2.4

If, according to de Broglie, all particles could be viewed in terms of both wave and particle properties, then compare the wavelength of an electron moving at 16.67% of the speed of light with that of a baseball with a mass of 0.142 kg traveling at 96.00 mi/hr (42.91 m/s). What is your conclusion?

■ **Solution**

According to Eq. 2.6, we need the mass and speed of the particle to determine the particle's wavelength. Accordingly,

$$\begin{aligned}\lambda_{\text{electron}} &= \frac{h}{mv} = \frac{6.62 \times 10^{-34} \text{ kg} \cdot \text{m}^2/\text{s}}{(9.11 \times 10^{-31} \text{ kg})(0.1667 \times 3.0 \times 10^8 \text{ m/s})} \\ &= 1.5 \times 10^{-10} \text{ m} = 0.15 \text{ nm}\end{aligned}$$

(note the diameter of the atom is about 0.1 nm)

¹⁸ Louis Victor Pierre Raymond de Broglie (1892–1987). French physicist and Nobel laureate (1929).

¹⁹ Werner Karl Heisenberg (1901–1976). German physicist and Nobel laureate (1932).

$$\lambda_{\text{baseball}} = \frac{6.62 \times 10^{-34} \text{ kg} \cdot \text{m}^2/\text{s}}{(0.142 \text{ kg})(42.91 \text{ m/s})} = 1.08 \times 10^{-34} \text{ m}$$

$$= 1.08 \times 10^{-25} \text{ nm}$$

The wavelength of a baseball is 10^{24} times smaller (much too short to observe) than that of an electron. In general, particles with ordinary size will have immeasurably small wavelengths, and we cannot determine their wave properties.

**EXAMPLE
PROBLEM 2.5**

For the Example Problem 2.4, if the uncertainty associated with the measurement of the speed of the baseball is (a) 1 percent, and (b) 2 percent, what are the corresponding uncertainties in knowing the position of the baseball? What is your conclusion?

■ Solution

According to Eq. 2.7, we will first calculate the uncertainty in the measurement of the speed to be $(0.01 \times 42.91 \text{ m/s}) 0.43$ for part (a) and $(0.02 \times 42.91) = 0.86 \text{ m/s}$ for part (b).

a. Rewriting Eq. 2.7 gives:

$$\Delta x \geq \frac{h}{4\pi m \Delta u} \geq \frac{6.62 \times 10^{-34} \text{ kg} \cdot \text{m}^2/\text{s}}{4\pi(0.142 \text{ kg})(0.43 \text{ m/s})} \geq 8.62 \times 10^{-34} \text{ m}$$

b. Rewriting Eq. 2.7 gives:

$$\Delta x \geq \frac{h}{4\pi m \Delta u} \geq \frac{6.62 \times 10^{-34} \text{ kg} \cdot \text{m}^2/\text{s}}{4\pi(0.142 \text{ kg})(0.86)} \geq 4.31 \times 10^{-34} \text{ m}$$

As the uncertainty with measurement of speed increases, the uncertainty in measurement of position decreases.

The understanding was nearly completed when Erwin Schrödinger²⁰ used the *wave equation* to explain the behavior of electrons. Solution of the wave equation is in terms of a wave function, ψ (psi). The square of the wave function, ψ^2 , presents the probability of finding an electron of a given energy level in a given region of space. The probability is called **electron density** and can be graphically expressed by an array of dots (called the *electron cloud*), each dot expressing a possible position of the electron with a specific energy level. For instance, the electron density distribution in Figure 2.7a is for the ground-state hydrogen atom. Although the general shape is spherical (as Bohr suggested), it is clear according to this model that the electron can exist at any given position relative to the nucleus. Also, the highest probability of finding an electron, in the ground state, is very close to the nucleus (where the density of dots is the highest). Moving away from the nucleus, the probability of finding an electron decreases.

²⁰ Erwin Rudolf Josef Alexander Schrödinger (1887–1961). Austrian physicist and Nobel laureate (1933).

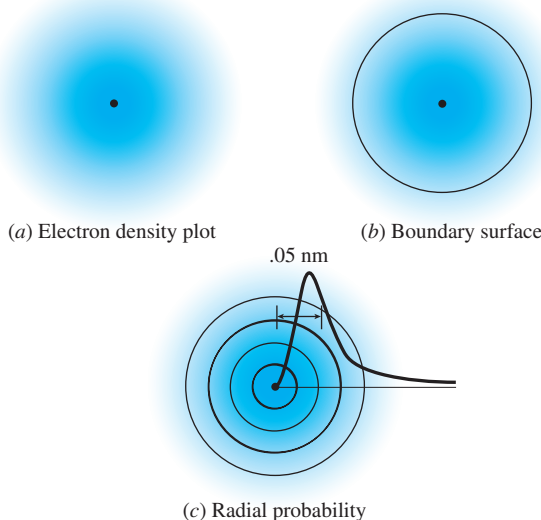


Figure 2.7

(a) The electron density plot for the hydrogen electron in the ground state, (b) the 90% boundary surface diagram, and (c) successive spherical shells and radial probability distribution (dark line).

If one solves the wave equation, different wave functions and thus electron density graphs will be generated. These wave functions are called the **orbitals**. We would like to immediately differentiate between the term *orbital* used here and the term *orbit* used by Bohr as being two distinct concepts (these terms must not be used interchangeably). An orbital has a characteristic energy level as well as a characteristic distribution of electron density.

Another way to probabilistically represent the location of an electron with a given energy level is by drawing the boundary inside which we have a 90% chance of finding that electron. For the ground-state electron, there is a 90% probability of finding an electron within a sphere of radius 100 pm. The sphere in Figure 2.7b is an alternative to the electron density diagram and is called the **boundary surface** representation. Note that a boundary surface of 100% probability for the same electron would have infinite dimensions. As discussed previously, the highest probability of finding an electron in Figure 2.7a is very close to its nucleus; however, if we divide the sphere into equally spaced concentric segments, Figure 2.7c, the *total probability* of finding an electron will be highest not at the nucleus but slightly farther away from it. Total probability, also called the *radial probability*, considers the probability of the electron being at a spherical layer with respect to the volume of that layer. Near the nucleus, for instance in the first layer, the probability is high but the volume is small; in the second layer, the probability of finding an electron is less than

the first layer but the volume of the second layer is much larger (increase in volume is more than decrease in probability) and thus the total probability of observing an electron is higher in the second layer. This second layer is located near the nucleus at a distance of 0.05 nm or 50 pm as shown in Figure 2.7c. This effect diminishes as the distance from the nucleus increases because the probability levels drop much faster than the volume of the layer increases.

Boundary surface diagrams for electrons of higher energy levels become more complicated and are not necessarily spherical. This will be discussed in more detail in the future sections.

2.3.4 Quantum Numbers, Energy Levels, and Atomic Orbitals

The modern quantum mechanics proposed by Schrödinger and others requires a set of four integers called the *quantum numbers* to identify the energy and the shape of the boundary space, or the electron cloud, and the spin for any electron in any atom. We are no longer limited to the hydrogen atom. The first quantum numbers are n , ℓ , m_ℓ , and m_s .

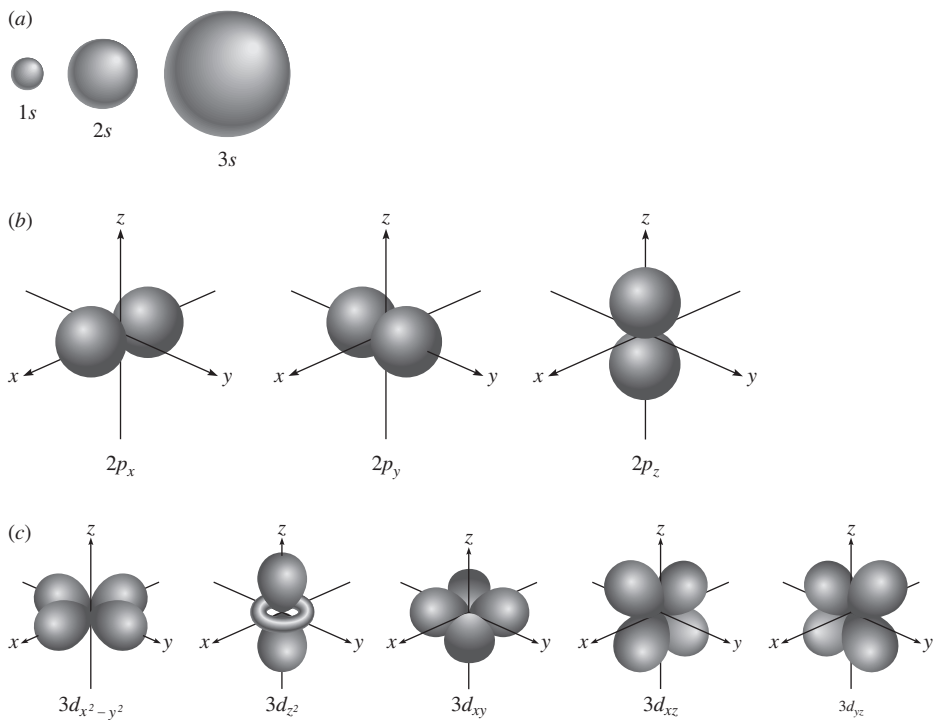
The Principal Quantum Number, n : Principal Energy Levels or Shells The **principal quantum number**, n , is the most important in determining the energy level of the electron under consideration. It only takes on integer values of one or greater than one, that is, $n = 1, 2, 3, \dots$. Each principal energy level is also known as a *shell* representing a collection of subshells and orbitals with the same principal number, n . As n increases, so does the energy of the electron under consideration, indicating that the electron is less tightly bonded to the nucleus (easier to ionize). Finally, as n increases, the probability of finding the electron farther from the nucleus also increases.

The Subsidiary or Orbital Quantum Number, ℓ : Subshells Within each principal shell, n , there exist subshells. When $n = 1$, there is only one kind of subshell possible, one similar to that presented in Figure 2.7. When $n = 2$, however, two different subshells are possible, and three different subshells when $n = 3$, and so on. The subshells are represented by the **orbital quantum number**, ℓ . The shape of the electron cloud or the boundary space of the orbital is determined by this number. The quantum number ℓ may be represented by an integer ranging from 0 to $n - 1$, or by letters.

Number designation	$\ell = 0, 1, 2, 3, \dots, n - 1$
Letter designation	$\ell = s, p, d, f, \dots$

Thus for $n = 1$, $\ell = s$; for $n = 2$, $\ell = s$ or p ; for $n = 3$, $\ell = s, p$, or d ; and so on. Therefore, the representation 3s represents a principal energy level, n , of 3 and the subshell, ℓ , of s.

The s subshell ($\ell = 0$), regardless of n , always looks spherical (Fig. 2.8a). However, as n becomes larger, the size of the sphere increases, indicating that the electrons can travel farther from the nucleus.

**Figure 2.8**

Schematic diagram of (a) s, (b) p, and (c) d orbitals.

The p subshells ($\ell = 1$) are not spherical. In fact they are dumbbell shaped with two electron density lobes on either side of the nucleus (Fig. 2.8a). There are three p orbitals within a given subshell, and they are different in their orientation in space. The three orbitals are mutually perpendicular. The d subshells are significantly more complicated in shape, Figure 2.8c, and they play an important role in the chemistry of transition metal ions.

The Magnetic Quantum Number, m_ℓ : Orbitals and Their Orientations The **magnetic quantum number**, m_ℓ , represents the orientation of the orbitals within each subshell. The quantum number m_ℓ will take on values ranging from $+\ell$ to $-\ell$. For instance, when $\ell = 0$ or s, the corresponding m_ℓ is 0; when $\ell = 1$ or p, the corresponding m_ℓ is $-1, 0$, and $+1$; when $\ell = 2$ or d, the corresponding m_ℓ is $-2, -1, 0, +1, +2$, and so on. Thus, for every subshell, ℓ , there are $2\ell + 1$ orbitals within the subshell. In terms of s, p, d, and f, there is a maximum of one s, three p, five d, and seven f orbitals in each subenergy level. The total number of orbitals in a principal shell (including all available subshells) can be expressed as n^2 ; for instance, one orbital in $n = 1$, four orbitals in $n = 2$, and nine orbitals in $n = 3$. Orbitals with the same subshell have the same energy level. The boundary space diagrams of s, p, and d orbitals are shown in

Figure 2.8. It is important to note that the size of boundary spaces becomes larger as n increases, indicating the higher probability of finding an electron with that energy level farther from the nucleus of the atom.

The Spin Quantum Number, m_s : Electron Spin In the helium atom ($Z = 2$), both electrons are occupying the first principal shell ($n = 1$), the same subshell ($\ell = 0$ or s), and the same magnetic quantum number ($m_\ell = 0$). Do these two electrons have identical quantum numbers? To completely describe any electron in an atom, in addition to n , ℓ , and m_ℓ , we must also identify its **spin quantum number**, m_s . The spin quantum number can take on either $+\frac{1}{2}$ or $-\frac{1}{2}$. The electron can have only the two directions of spin, and no other position is allowed. In addition, according to **Pauli's exclusion principle**, no more than two electrons can occupy the same orbital of an atom, and the two electrons must have opposite spins. In other words, no two electrons can have the same set of four quantum numbers. For instance, in the atom of He, what makes its two electrons distinct from a quantum mechanics point of view is the spin quantum number; $m_s = \frac{1}{2}$ for one and $m_s = -\frac{1}{2}$ for the other. A summary of the allowed values of the quantum numbers is presented in Table 2.2.

Since only two electrons can occupy a single orbital, and since each principal energy level or shell, n , allows n^2 orbitals, a general rule may be stated that each principal energy level can accommodate a maximum number of $2n^2$ electrons (Table 2.3). For instance, the $n = 2$ principal energy level can accommodate a maximum of $2(2)^2 = 8$ electrons; two in its s subshell and six in its p subshell, which itself contains three orbitals.

Table 2.2 Allowed values for the quantum numbers of electrons

n	Principal quantum number	$n = 1, 2, 3, 4, \dots$	All positive integers
ℓ	Subsidiary quantum number	$\ell = 0, 1, 2, 3, \dots, n - 1$	n allowed values of ℓ
m_ℓ	Magnetic quantum number	Integral values from $-\ell$ to $+\ell$ including zero	$2\ell + 1$
m_s	Spin quantum number	$+\frac{1}{2}, -\frac{1}{2}$	2

Table 2.3 Maximum number of electrons for each principal atomic shell

Shell Number, n (Principal Quantum Number)	Maximum Number of Electrons in Each Shell ($2n^2$)	Maximum Number of Electrons in Orbitals
1	$2(1^2) = 2$	s^2
2	$2(2^2) = 8$	s^2p^6
3	$2(3^2) = 18$	$s^2p^6d^{10}$
4	$2(4^2) = 32$	$s^2p^6d^{10}f^{14}$
5	$2(5^2) = 50$	$s^2p^6d^{10}f^{14} \dots$
6	$2(6^2) = 72$	$s^2p^6 \dots$
7	$2(7^2) = 98$	$s^2 \dots$

2.3.5 The Energy State of Multielectron Atoms

Thus far, the majority of the discussion has focused on the single electron atom of hydrogen. The single electron in this atom can be energized to various principal energy levels and regardless of the subsidiary quantum number (subshell), its energy level will be that of the principal shell in which it exists. However, when more than one electron exists, electrostatic attraction effects between the electron and the nucleus as well as repulsion effects between the electrons will lead to more complex energy states or splitting of energy levels. Thus, the energy of an orbital in a multielectron atom depends not only on its n value (size) but also on its ℓ value (shape).

For instance, consider the single electron in an H atom and the single electron in the ionized He atom (He^+). Both electrons are in the 1s orbital. However, recall that the nucleus of the He atom has two protons versus the one proton in the H nucleus. The orbital energies are -1311 kJ/mol for the H electron and -5250 kJ/mol for the He^+ electron. It is more difficult to remove the He^+ electron because it has a stronger attraction to its nucleus of two protons. In other words, the higher the charge of the nucleus, the higher is the attraction force on an electron and the lower the energy of the electron (a more stable system); this is called the **nucleus charge effect**.

Let us now compare the He atom to the He ion. Both have the same nucleus charge but differ in the number of electrons. The orbital energy of the 1s He electron is -2372 kJ/mol while that of He^+ is -5250 kJ/mol . It is significantly less difficult to remove one of the two electrons in the He atom than it is to remove the single He^+ electron. This is mainly due to the fact that the two electrons in the He atom repel each other and this counteracts the attraction force of the nucleus. It is almost as if the electrons shield each other from the full force of the nucleus; this is called the **shielding effect**.

Next, let us compare the Li atom ($Z = 3$) in its ground state and the first excited state of the Li^{2+} ion. Note that both have a nucleus charge of +3; Li has two 1s electrons and one 2s electron, while Li^{2+} has one electron that is excited to its 2s level (first excited state). The orbital energy of the 2s Li electron is -520 kJ/mol while that of Li^{2+} is -2954 kJ/mol . It is easier to remove the 2s electron in the Li atom because the pair of 1s electrons in the inner shell shield the 2s electron from the nucleus (a majority of the time). The 2s electron in the Li^{2+} does not have the 1s pair and is therefore attracted strongly to its nucleus. Thus, the inner electrons shield the outer electrons and do so more effectively than electrons in the same sublevel (compare the orbital energy levels with those in the previous paragraph).

Finally, we will compare the Li atom in its ground state with the Li atom excited to its first level. The ground state Li atom has its outer electron in the 2s orbital while the excited Li atom has its outer electron in the 2p orbital. The orbital energy of the 2s electron is -520 kJ/mol while that of the 2p electron is -341 kJ/mol . Thus, the 2p orbital has a higher state of energy than the 2s orbital. This is because the 2s electron spends part of its time penetrating closer to the nucleus (much more than the 2p electron), thus having stronger attraction to the nucleus, less energy, and a

more stable state. We can further generalize that for multielectron atoms, in a given principal shell, n , the lower the value of ℓ , the lower will be the energy of the subshell. (i.e., s < p < d < f.)

The preceding exercise shows that due to various electrostatic effects, the principal energy levels, n , split into several subenergy levels, ℓ , as shown in Figure 2.9. This

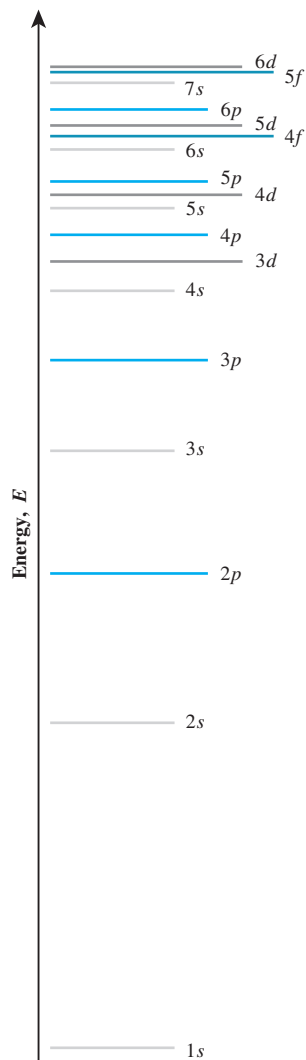


Figure 2.9

The energy level for all subenergy levels up to $n = 7$. The orbitals will fill in the same exact order.

figure shows the order in which the various principal and subenergy levels exist relative to each other. For instance, the electrons within 3p subshells have a higher energy than 3s and a lower energy than 3d. Note in this figure that the 4s subshell has a lower energy than the 3d subshell.

2.3.6 The Quantum-Mechanical Model and the Periodic Table

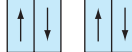
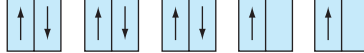
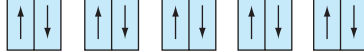
In the periodic table, the elements are classified according to their ground-state electron configuration. As a result, atoms of a particular element (say Li with three electrons) contain one more electron than the element preceding it (He with two electrons). These electrons are found in principal energy shells, subshells, and orbitals. But how do we know the particular order in which the electrons fill the orbitals? The electrons fill the first available principal energy levels first. The maximum number of electrons in each principal energy level is given in Table 2.3. Next, within each principal energy level, they fill the lowest energy subshells first, that is, s, followed by p, d, and finally f. The s, p, d, and f subenergy levels will allow a maximum of 2, 6, 10, and 14 electrons, respectively. Each subshell level will have its own energy level, and the order in which each subenergy level is filled is given by Fig. 2.9.

There are two different forms of expressing the *orbital occupancy*: (1) electron configuration and (2) orbital box diagram.

The electron configuration notation consists of the value of the principal shell, n , followed with the letter designation of the subshell, ℓ , and finally the number of electrons in that sublevel presented as a superscript. For instance, the electron configuration of oxygen, O, with eight electrons is $1s^22s^22p^4$. For oxygen, after filling the 1s orbital with two electrons, six electrons remain. According to Figure 2.9, two of the six electrons fill the 2s orbital ($2s^2$) and the remaining four will occupy the p orbital ($2p^4$). The next element, fluoride, F, will have one more electron with a configuration of $1s^22s^22p^5$ while the element immediately before, nitrogen, N, will have one less electron with a configuration of $1s^22s^22p^3$. To understand this more clearly, the electronic structures of the first 10 elements in the periodic table are given in Table 2.4.

Let us now consider the element scandium (Sc) with 21 electrons. The first five energy levels in increasing order of energy are (Fig. 2.9) $1s^2$, $2s^2$, $2p^6$, $3s^2$, $3p^6$. This will account for 18 electrons. Three electrons remain to complete the electronic structure of Sc. Chronologically, one would assume that the next three electrons would fill the 3d orbital, thus completing the configuration with $3d^3$. However, according to Figure 2.9, the next orbital to be filled is 4s and not 3d. This is because the 4s energy level is lower than 3d (due to shielding and penetration effects), and as we discussed previously, the lowest energy levels are always occupied first. Therefore, the next two electrons (nineteenth and twentieth) will fill the 4s orbitals and the last electron (twenty-first) will then occupy the 3d orbital. The final configuration for Sc, in the order that the orbitals were filled, is $1s^22s^22p^63s^23p^64s^23d^1$; however, it is also acceptable to show the configuration according to the principal energy level, $1s^22s^22p^63s^23p^63d^14s^2$. Note that the inner core electrons, $1s^22s^22p^63s^23p^6$, represent

Table 2.4 Allowed values for the quantum numbers and electrons

	Electron Configuration	Orbital Box Diagram		
		1s	2s	2p
H	1s ¹			
He	1s ²			
Li	1s ² 2s			
Be	1s ² 2s ¹			
B	1s ² 2s ² 2p ¹			
C	1s ² 2s ² 2p ²			
N	1s ² 2s ² 2p ³			
O	1s ² 2s ² 2p ⁴			
F	1s ² 2s ² 2p ⁵			
Ne	1s ² 2s ² 2p ⁶			

the electronic structure of the noble gas argon. Thus, one can represent the electronic configuration for Sc as [Ar]4s²3d¹.

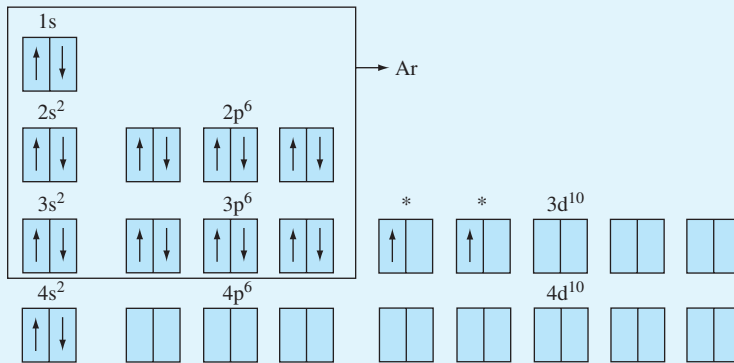
One can also show the orbital occupancy using the orbital box diagram. The advantage of the orbital box diagram is that unlike the electron configuration notation, it also shows the paired spins (opposite spin) of electrons in an orbital. The orbital box diagrams for the first 10 elements in the periodic table are presented in Table 2.4. For oxygen, O, with seven electrons, the first two electrons will occupy the 1s orbital (the lowest energy orbital) with paired spins, followed by the next two electrons occupying the 2s orbital (the next lowest energy orbital) with paired spins. The next three electrons, however, will fill the three p orbitals randomly (all p orbitals have the same energy level) with the same spin. Although the p orbital selection process is random, for convenience, we show filling up from left to right. The last electron then pairs the spin of one of the three electrons in the p orbital randomly (note the spin direction

**EXAMPLE
PROBLEM 2.6**

Show the electronic structure of the atom titanium (Ti) using the orbital box diagram.

■ Solution

Ti has 22 electrons. Therefore, the inner core electrons will have the structure of the noble gas argon, $1s^2 2s^2 2p^6 3s^2 3p^6$, accounting for 18 of the 22 electrons. Four electrons remain. After the 3p orbital is filled, according to Figure 2.9, the next orbital to be filled is not 3d and is instead 4s. As explained previously, this is because the energy level of the 4s orbital is lower than the 3d orbital. The next two electrons (nineteenth and twentieth) occupy 4s¹ and 4s². Finally, the last two electrons (*twenty-first and *twenty-second) will then fill the available slots in the d orbital as shown in the figure, [Ar]4s²3d².



of the last electron is opposite to the other three in the p orbital). In other words, the electrons will not occupy the three p orbitals pair by pair. For element F, with one more electron than O, the next p orbital will be paired, and finally for Ne, with two more electrons than O, all three p orbitals are paired. This is also the case with the five d orbitals in the third principal shell: after each of the five d orbitals is filled with one electron of the same spin, any remaining electrons will pair the d orbitals one by one and with opposite spin.

It is important to note that some irregularities exist in the orbital occupancy of elements, and not all elements follow exactly the stated rules. For instance, one would expect that copper with 29 electrons (8 more than Sc) has an electronic structure of [Ar]3d⁹4s²; however, it has the [Ar]3d¹⁰4s¹ electronic structure. The reasons for these irregularities are not completely known, but one explanation is that the energy level of the corresponding 3d and 4s orbitals are extremely close for copper. Chromium, Cr, is another element that does not follow the stated rules with an electronic structure of [Ar]3d⁵4s¹. The partial ground-state configuration of all elements in the periodic table is given in Figure 2.10 in which some of the irregularities may be observed.

Main-Group Elements (s block)										Main-Group Elements (p block)											
Period number : highest occupied energy level	1A (1)																	8A (18)			
	ns ¹																	ns ² np ⁶			
	1 H 1s ¹	2A (2) ns ²																2 He 1s ²			
	3 Li 2s ¹	4 Be 2s ²	Transition Elements (d block)										3A (13) ns ² np ¹	4A (14) ns ² np ²	5A (15) ns ² np ³	6A (16) ns ² np ⁴	7A (17) ns ² np ⁵				
	11 Na 3s ¹	12 Mg 3s ²	3B (3)	4B (4)	5B (5)	6B (6)	7B (7)	(8)	8B (9)	(10)	1B (11)	2B (12)	2s ² p ¹	6 C 2s ² p ²	7 N 2s ² p ³	8 O 2s ² p ⁴	9 F 2s ² p ⁵	10 Ne 2s ² p ⁶			
	19 K 4s ¹	20 Ca 4s ²	21 Sc 4s ² 3d ¹	22 Ti 4s ² 3d ²	23 V 4s ² 3d ³	24 Cr 4s ¹ 3d ⁵	25 Mn 4s ² 3d ⁵	26 Fe 4s ² 3d ⁶	27 Co 4s ² 3d ⁷	28 Ni 4s ² 3d ⁸	29 Cu 4s ¹ 3d ¹⁰	30 Zn 4s ² 3d ¹⁰	31 Al 3s ² 3p ¹	13 Si 3s ² 3p ²	14 P 3s ² 3p ³	15 S 3s ² 3p ⁴	16 Cl 3s ² 3p ⁵	17 Ar 3s ² 3p ⁶			
	37 Rb 5s ¹	38 Sr 5s ²	39 Y 5s ² 4d ¹	40 Zr 5s ² 4d ²	41 Nb 5s ¹ 4d ⁴	42 Mo 5s ¹ 4d ⁵	43 Tc 5s ² 4d ⁵	44 Ru 5s ¹ 4d ⁷	45 Rh 5s ¹ 4d ⁸	46 Pd 4d ¹⁰	47 Ag 5s ¹ 4d ¹⁰	48 Cd 5s ² 4d ¹⁰	49 In 5s ² 5p ¹	50 Sn 5s ² 5p ²	51 Sb 5s ² 5p ³	52 Te 5s ² 5p ⁴	53 I 5s ² 5p ⁵	54 Xe 5s ² 5p ⁶			
	55 Cs 6s ¹	56 Ba 6s ²	57 La* 6s ² 5d ¹	72 Hf 6s ² 5d ²	73 Ta 6s ² 5d ³	74 W 6s ² 5d ⁴	75 Re 6s ² 5d ⁵	76 Os 6s ² 5d ⁶	77 Ir 6s ² 5d ⁷	78 Pt 6s ¹ 5d ⁹	79 Au 6s ¹ 5d ¹⁰	80 Hg 6s ² 6p ¹	81 Tl 6s ² 6p ²	82 Pb 6s ² 6p ³	83 Bi 6s ² 6p ⁴	84 Po 6s ² 6p ⁵	85 At 6s ² 6p ⁶	86 Rn			
	87 Fr 7s ¹	88 Ra 7s ²	89 Ac** 7s ² 6d ¹	104 Rf 7s ² 6d ²	105 Db 7s ² 6d ³	106 Sg 7s ² 6d ⁴	107 Bh 7s ² 6d ⁵	108 Hs 7s ² 6d ⁶	109 Mt 7s ² 6d ⁷	110 Ds 7s ² 6d ⁸	111 Rg 7s ² 6d ⁹	112 7s ² 6d ¹⁰	113 7s ² 7p ¹	114 7s ² 7p ²	115 7s ² 7p ³	116 7s ² 7p ⁴					
Inner Transition Elements (f block)																					
6	*Lanthanides		58 Ce 6s ² 4f ¹ 5d ¹	59 Pr 6s ² 4f ³	60 Nd 6s ² 4f ⁴	61 Pm 6s ² 4f ⁵	62 Sm 6s ² 4f ⁶	63 Eu 6s ² 4f ⁷	64 Gd 6s ² 4f ⁷ 5d ¹	65 Tb 6s ² 4f ⁹	66 Dy 6s ² 4f ¹⁰	67 Ho 6s ² 4f ¹¹	68 Er 6s ² 4f ¹²	69 Tm 6s ² 4f ¹³	70 Yb 6s ² 4f ¹⁴	71 Lu 6s ² 4f ¹⁴ 6d ¹					
7	**Actinides		90 Th 7s ² 6d ²	91 Pa 7s ² 5f ² 6d ¹	92 U 7s ² 5f ³ 6d ¹	93 Np 7s ² 5f ⁴ 6d ¹	94 Pu 7s ² 5f ⁶	95 Am 7s ² 5f ⁷	96 Cm 7s ² 5f ⁷ 6d ¹	97 Bk 7s ² 5f ⁹	98 Cf 7s ² 5f ¹⁰	99 Es 7s ² 5f ¹¹	100 Fm 7s ² 5f ¹²	101 Md 7s ² 5f ¹³	102 No 7s ² 5f ¹⁴	103 Lr 7s ² 5f ¹⁴ 6d ¹					

Figure 2.10

The partial ground-state configuration of all elements in the periodic table.

2.4 PERIODIC VARIATIONS IN ATOMIC SIZE, IONIZATION ENERGY, AND ELECTRON AFFINITY

2.4.1 Trends in Atomic Size

In the previous sections, we learned that some electrons can occasionally lie far from the nucleus, and this makes establishing an absolute shape for the atom difficult. To remedy this, we represented an atom as a sphere with a definite radius in which the

electrons spend 90 percent of their time. In practice, however, the atomic size is determined as half the distance between the nuclei of two adjacent atoms in a solid sample of an element. This distance is also called the **metallic radius**, and we use this definition for the metallic elements in the periodic table. For other elements that commonly form covalent molecules (such as Cl, O, N, etc.), we define the atomic size as half the distance between the nuclei of the identical atoms within the molecule, called **covalent radius**. Thus, the size of an atom will depend on its immediate neighbors, and it varies slightly from substance to substance.

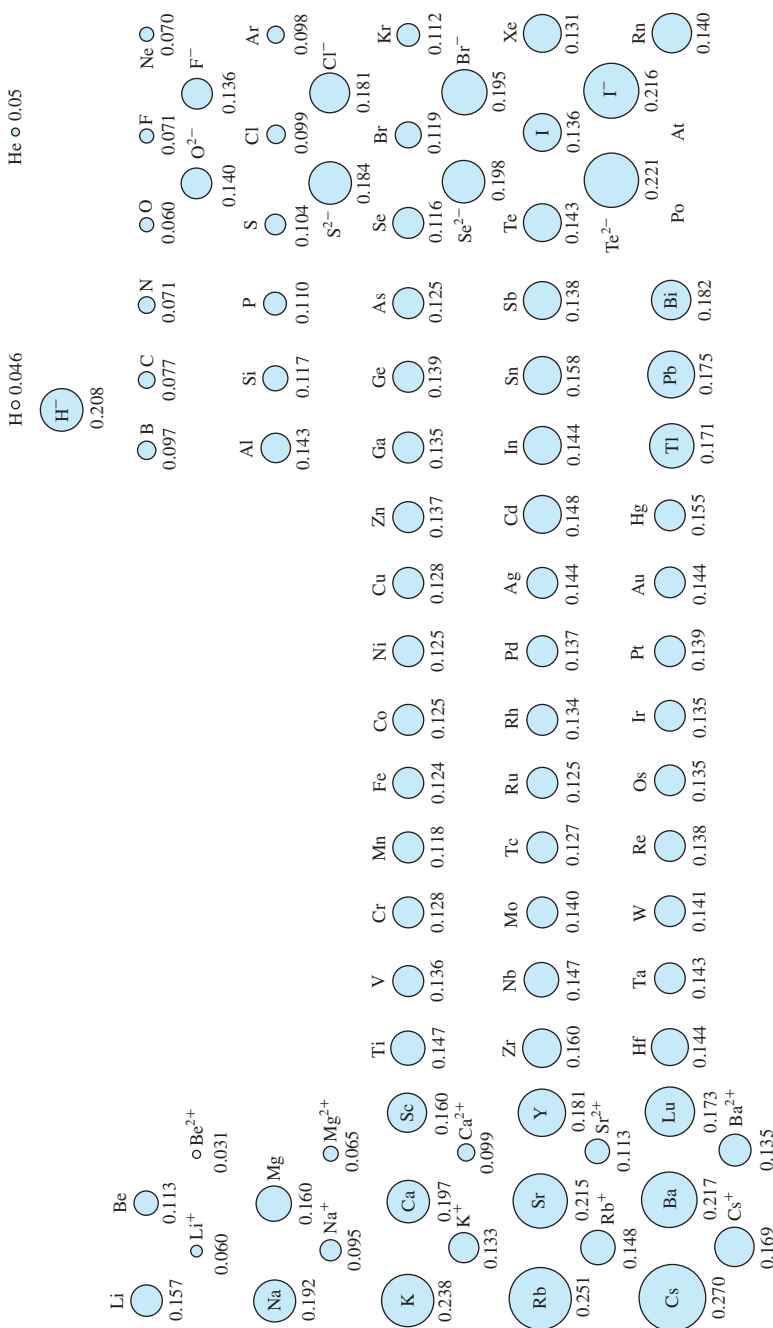
Atomic size is directly influenced by electron configuration; it therefore varies with both a period and a group. In general there are two opposing forces at work: as the principal quantum number, n , increases (moving from one period to the next in table), the electrons occupy positions farther from the nucleus and the atoms become larger. Thus, as one moves from top to bottom in a group, the size of the atom, generally, increases. On the other hand, as the charge of the nucleus increases, as we move across a period (more protons), electrons are attracted more strongly to the nuclei, and this tends to shrink the size of the atom. The size of an atom is therefore governed by the net effect of the two forces. This is important because atomic size influences other atomic and material properties. The general trends hold rather well for the main group elements, 1A through 8A, with some exceptions, but the trends are less predictable for transition elements (Fig. 2.11).

2.4.2 Trends in Ionization Energy

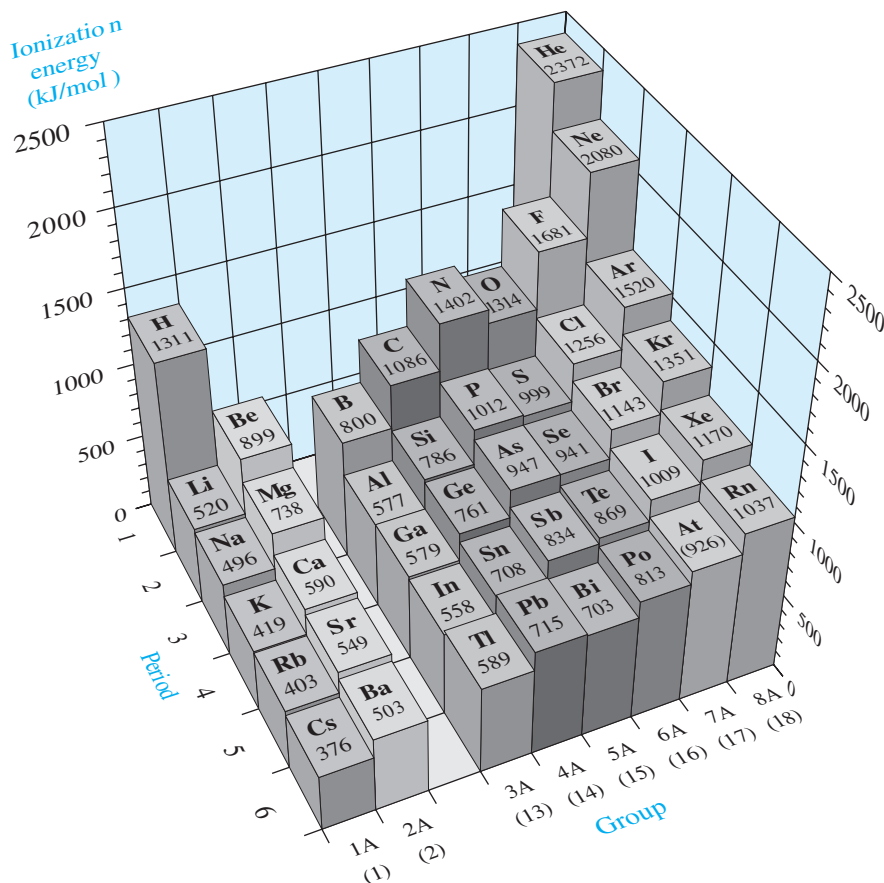
The energy required to remove an electron from its atom is called the *ionization energy* (IE). The ionization energy is always positive because to remove an electron from an atom, energy must be supplied to the system. Atoms with many electrons can lose more than one electron; however, it is the energy required for the removal of the outermost electron, the **first ionization energy** (IE₁), that plays the key role in the chemical reactivity of the specific atom.

Trends in first ionization energy of atoms show approximately an inverse relationship to atomic size (Fig. 2.12). In comparing Figures 2.11 and 2.12, unlike atomic size, as we move to the right across a period, the ionization energy increases, and as we move down in a group, the ionization energy drops. In other words, as the atomic size decreases, it takes more energy to remove an electron from its atom. The decrease in atomic size across a period increases the attraction between the nucleus and its electrons; thus, it is harder to remove those electrons, and the ionization energy increases. We can therefore generalize that group 1A and 2A elements are highly susceptible to ionization. Conversely, as the atomic size increases, moving down in a group, the distance between the nucleus and the outermost electrons increases, resulting in lower attraction forces between them; this will lower the energy required for the removal of electrons and thus the ionization energy.

For many electron atoms, as the first outer core electron is removed, it takes more energy to remove a second outer core electron; this indicates that the **second ionization energy**, IE₂, will be higher. The increase in energy for successive electron removal will be exceptionally large when the outer core electrons are completely removed and what

**Figure 2.11**

The atomic and ionic size variations in the periodic table.

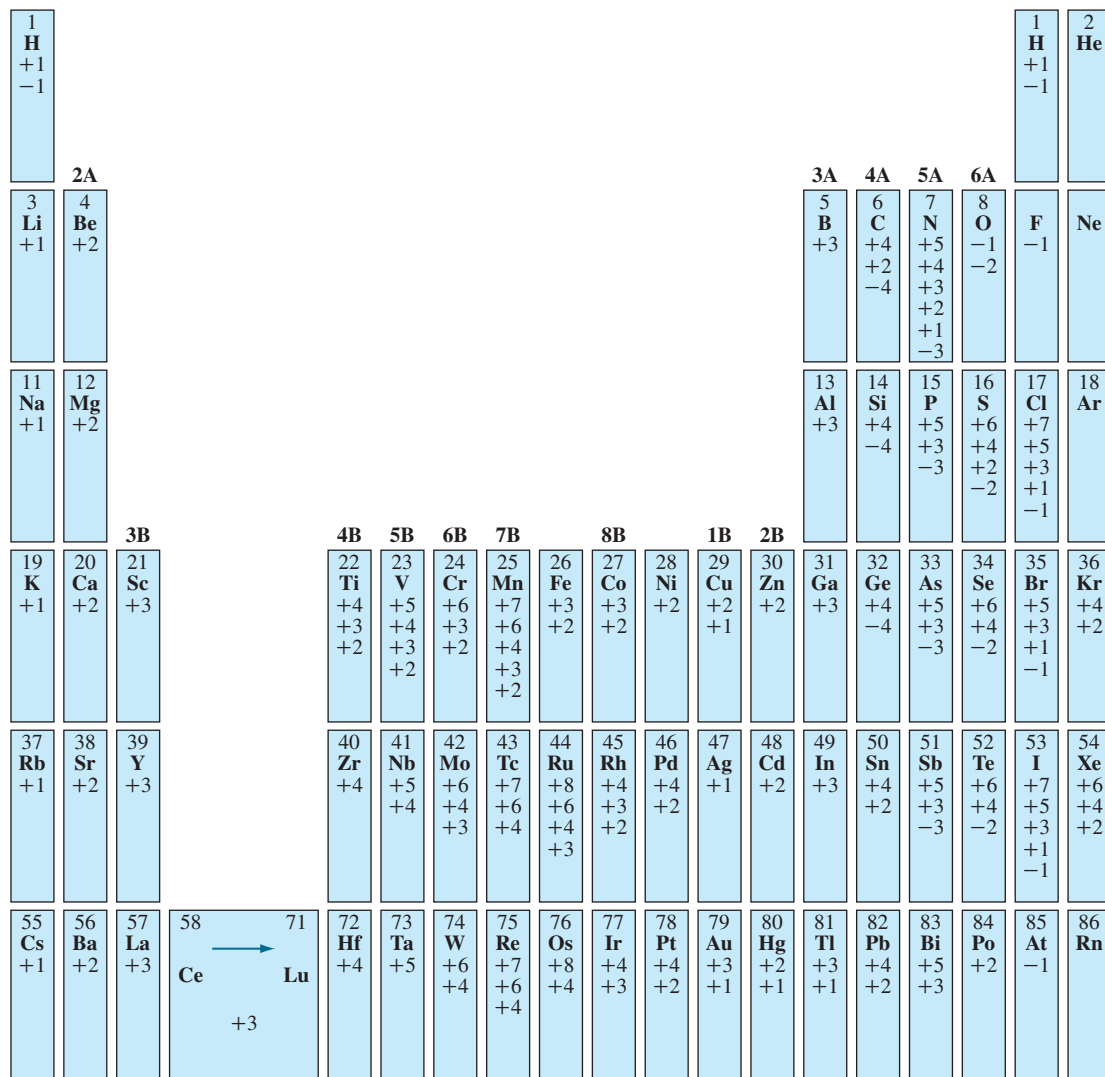
**Figure 2.12**

The ionization energy variations in the periodic table.

remain are the inner core electrons. For instance, the Li atom has one outer core electron, $2s^1$, and two inner core electrons, $1s^1$ and $1s^2$. When successively removing electrons, it takes 0.52 MJ/mole to remove the $2s^1$ electron, 7.30 MJ/mole for the $1s^2$ electron, and 11.81 MJ/mole for the $1s^1$ electron. Because of the higher levels of energy required to remove the inner core electrons, they are rarely involved in chemical reactions. The number of outer electrons that an atom can give up through the ionization process is called the **positive oxidation number** and is shown for each element in Figure 2.13. Note that some elements have more than one positive oxidation number.

2.4.3 Trends in Electron Affinity

Contrary to those atoms in group 1A and 2A with low IE₁ that have a tendency to easily lose their outermost electrons, some atoms have a tendency to accept one or more electrons and release energy in the process. This property is named the **electron affinity**.

**Figure 2.13**

The oxidation number variations in the periodic table.

(Source: R.E. Davis, K.D. Gailey, and K.W. Whitten, *Principles of Chemistry*, Saunders College Publishing, 1984, p. 299.)

(EA). As with ionization energy, there is a *first electron affinity*, EA1. The change in energy when an atom accepts the first electron, EA1, is opposite to that of an atom losing an electron, that is, here energy is released. Similar to ionization energy, electron affinity increases (more energy is released after accepting an electron) as we move to the right across a period and decreases as we move down in a group. Thus, groups 6A and 7A have in general the highest electron affinities. The number of electrons that an atom can gain is called the **negative oxidation number** and is shown for each element in Figure 2.13. Note that some elements have both positive and negative oxidation numbers.

2.4.4 Metals, Metalloids, and Nonmetals

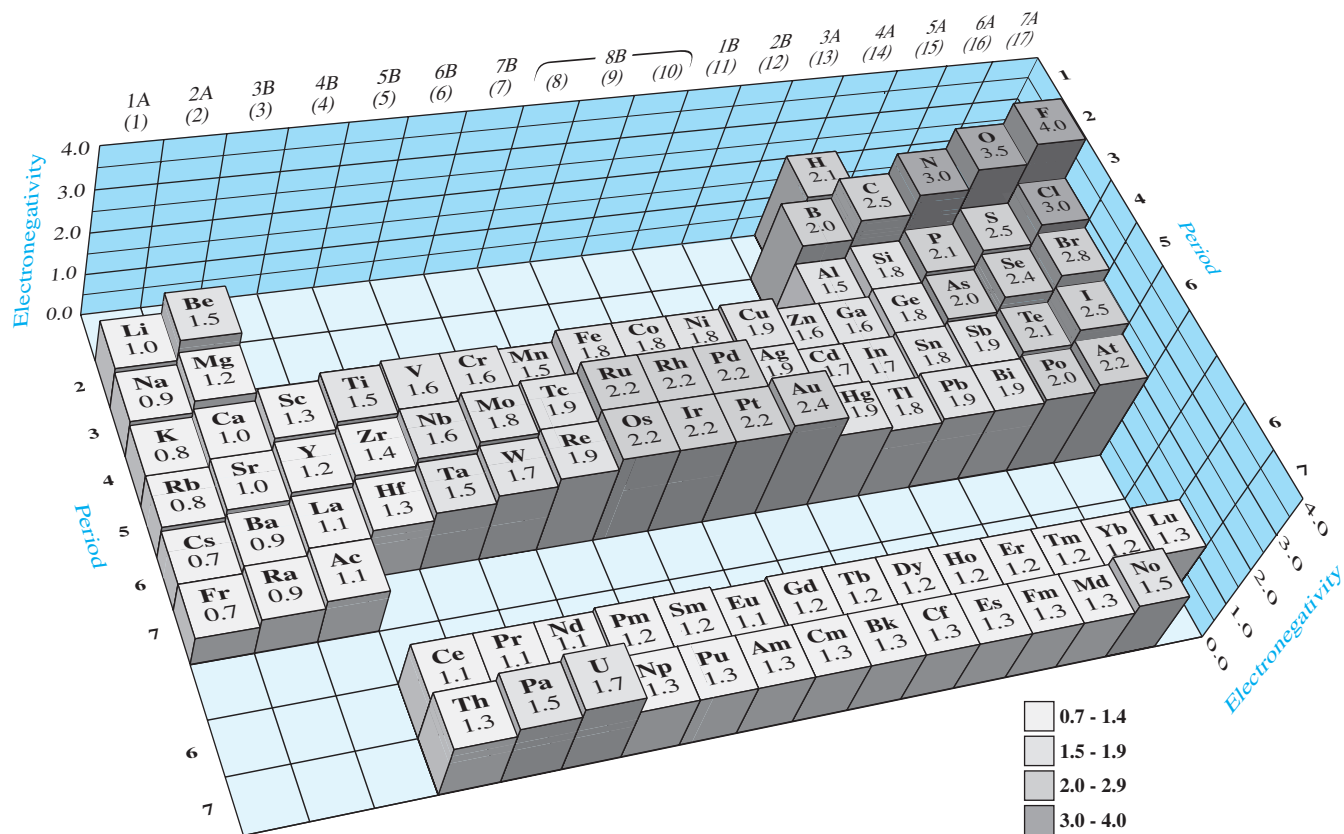
Notwithstanding the exceptions, in general, group 1A and 2A atoms have low ionization energies and little to no electron affinity. These elements, called **reactive metals** (or simply metals), are electropositive, meaning that they have the natural tendency of losing electrons and in the process form cations (a positively charged ion forming as a result of losing an electron with its negative charge). The group 6A and 7A elements have a high ionization energy and very high electron affinity. These elements, called **reactive nonmetals** (or simply nonmetals), are electronegative, meaning that they have the natural tendency of accepting electrons and in the process form anions (a negatively charged ion forming as a result of accepting an electron with its negative charge).

In group 3A, the first element, boron, can behave either in a metallic or a nonmetallic manner. Such elements are called **metalloids**. The remaining members are all metals. In group 4A the first member, carbon, and the next two members, silicon and germanium, are metalloids, while the remaining elements, tin and lead, are metals. In group 5A, nitrogen and phosphorous are nonmetals, arsenic and antimony are metalloids, and finally bismuth is a metal. Thus, elements in groups 3A through 5A can behave in a variety of manners, but it is clear that as we move down in a group, the metallic behavior dominates; as we move right in a period, the nonmetallic behavior dominates. These various characteristics are well represented by the **electronegativity** of atoms indicating the degree by which they attract electrons to themselves (Fig. 2.14). In this figure, the electronegativity of each atom is presented in a range of 0.8 to 4.0. As expected, nonmetals are more electronegative than metals, while metalloids have intermediate electronegativities.

The atoms in group 8A are noble gases. They have very high ionization energy and no electron affinity. These elements are very stable and are the least reactive of all elements. With the exception of He, all remaining elements in this group (Ne, Ar, Kr, Xe, and Rn) have the s^2p^6 outer core electronic structure.

2.5 PRIMARY BONDS

The driving force behind the formation of bonds between atoms is that each atom seeks to be in the most stable state. Through bonding with other atoms, the potential energy of each bonding atom is lowered, resulting in a more stable state. These bonds are called **primary bonds** and possess large interatomic forces.

**Figure 2.14**

The electronegativity variations in the periodic table.

We have already established that the behavior and characteristics of an atom, for instance, atomic size, ionization energy, and electron affinity, depend on its electronic structure and the attractive force between the nucleus and its electrons as well as the repulsive forces between electrons. Similarly, the behavior and properties of a material are directly dependent on the type and the strength of the bonds among its atoms. In the following sections, we will discuss the nature and characteristics of the existing primary and secondary bonds.

Recall that the elements in the periodic table can be classified into metals and nonmetals. The metalloids can behave either as metals or as nonmetals. There are three possible primary bonding combinations between the two types of atoms: (1) metal-nonmetal, (2) nonmetal-nonmetal, and (3) metal-metal.

2.5.1 Ionic Bonds

Electronic and Size Considerations Metals and nonmetals bond through electron transfer and **ionic bonding**. Ionic bonding is typically observed between atoms with large differences in their electronegativities (see Fig. 2.14); for instance, atoms of group 1A or 2A (reactive metals) with atoms of group 6A or 7A (reactive nonmetals). As an example, let us consider the ionic bonding between the metal Li with an electronegativity of 1.0 and the nonmetal F with an electronegativity of 4.0. In short, the Li atom loses an electron and forms a cation, Li^+ . In this process, the radius decreases from $r = 0.157 \text{ nm}$ for the Li^+ atom to $r = 0.060 \text{ nm}$ for the Li^+ cation. This reduction in size occurs because (1) after the ionization, the frontier electron is no longer in $n = 2$ but rather in $n = 1$ state and (2) the balance between the positive nucleus and the negative electron cloud is lost, and the nucleus can exert a stronger force on the electrons, thus pulling them closer. Conversely, the F atom gains the electron lost by Li and forms an anion, F^- . In this case, the radius increases from $r = 0.071 \text{ nm}$ for the F atom to $r = 0.136 \text{ nm}$ for the F^- . It can be generalized that when a metal forms a cation, its radius reduces, and when a nonmetal forms an anion, its radius increases. The ionic sizes for various elements are given in Figure 2.11. After the electron transfer process is completed, Li will have completed its outer electronic structure and takes on the structure of the noble gas He. Similarly, F will have completed its outer electronic structure and takes on the electronic structure of the noble gas Ne. The electrostatic attraction forces between the two ions will then hold the ions together to form an ionic bond. The ionic bonding process between Li and F is presented in electron configuration, orbital diagram, and electron dot formats in Figure 2.15.

Force Considerations From a force balance point of view, the positive nucleus of one ion will attract the negative charge cloud of the other ion and vice versa. As a result, the *interionic distance*, a , decreases, and they become closer. As the ions

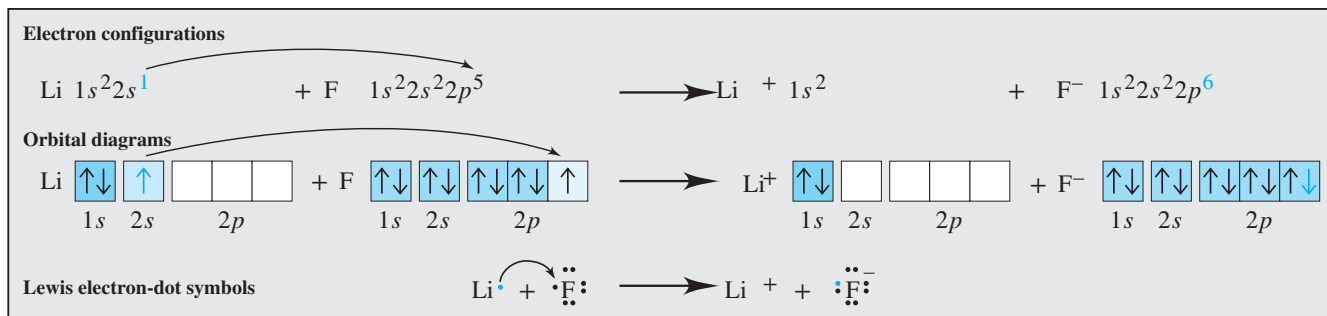


Figure 2.15

The ionic bonding process between Li and F. (a) Electron configuration presentation, (b) orbital diagram presentation, and (c) electron-dot symbol representation.

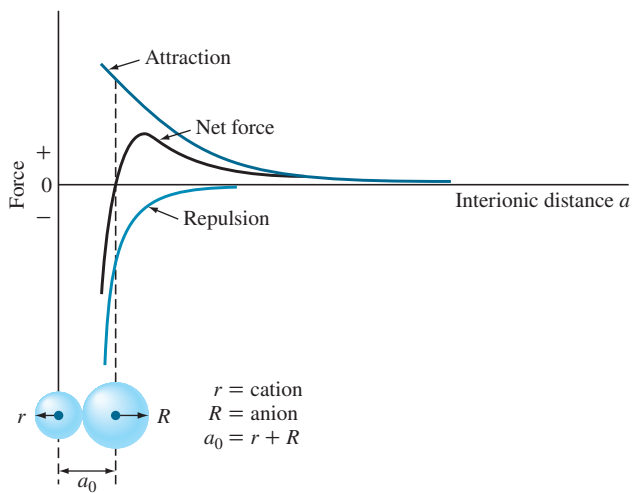


Figure 2.16
The attraction repulsion forces developed during ionic bonding. Note that net force is zero when the bond is formed.

come closer, the negative electron charge clouds will interact, and a repulsion force is developed. These two opposing forces will eventually balance each other to a net force of zero, and that is when the **equilibrium interionic distance**, a_0 , is reached and a bond is formed (Fig. 2.16).

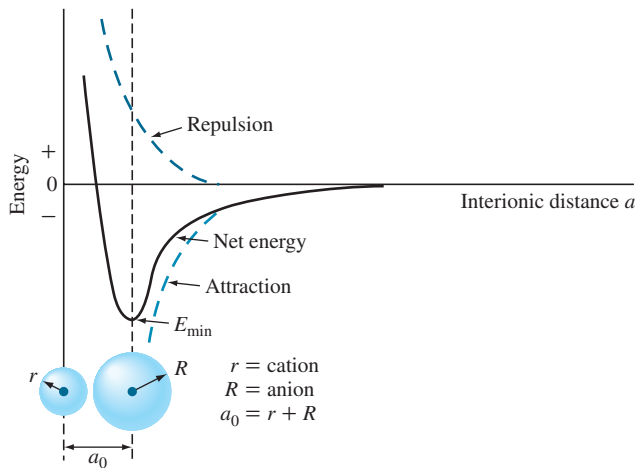
The net force at any interionic distance may be calculated from the following equation, Eq. 2.8,

$$F_{\text{net}} = \left[\frac{z_1 z_2 e^2}{4\pi\epsilon_0 a^2} \right] - \left[\frac{nb}{a^{n+1}} \right] \quad (2.8)$$

↑ Attraction energy
↓ Repulsion energy

in which z_1 and z_2 are the number of electrons removed from and added to each atom (they must have opposite signs), b and n are constants, e is the electron charge, a is the interionic distance, and ϵ_0 is the permittivity of space, $8.85 \times 10^{-12} \text{ C}^2/\text{N} \cdot \text{m}^2$.

E_{net} may be determined using Eq. 2.9. While the net force at equilibrium, when the bond is formed, is zero, the potential energy of the bond is at its lowest, E_{min} . The minimum energy, E_{min} , may be determined by substituting a_0 into Eq. 2.9. E_{min} is negative as shown in (Fig. 2.17), which indicates that if one wanted to break the bond, an amount of energy equal to E_{min} must be expended.

**Figure 2.17**

The energy variations during ionic bonding. Note that the net energy is minimum when the bond is formed.

$$E_{\min} = \left[\frac{z_1 z_2 e^2}{4\pi\epsilon_0 a} \right] + \left[\frac{b}{a^n} \right] \quad (2.9)$$

↑ Attraction energy
↓ Repulsion energy

**EXAMPLE
PROBLEM 2.7**

If the attractive force between Mg^{2+} and S^{2-} ions at equilibrium is 1.49×10^{-9} N, calculate (a) the corresponding interionic distance. If S^{2-} ion has a radius of 0.184 nm, calculate (b) the ionic radius for Mg^{2+} and (c) the repulsion force between the two ions at this position.

Solution

The value of a_0 , the sum of the Mg^{2+} and S^{2-} ionic radii, can be calculated from a rearranged form of Coulomb's law, Eq. 2.10.

$$\text{a. } a_0 = \sqrt{\frac{-Z_1 Z_2 e^2}{4\pi \epsilon_0 F_{\text{attraction}}}} \quad (2.10)$$

$$Z_1 = +2 \text{ for } \text{Mg}^{2+} \quad Z_2 = -2 \text{ for } \text{S}^{2-}$$

$$|e| = 1.60 \times 10^{-19} \text{ C} \quad \epsilon_0 = 8.85 \times 10^{-12} \text{ C}^2/(\text{N} \cdot \text{m}^2)$$

$$F_{\text{attractive}} = 1.49 \times 10^{-9} \text{ N}$$

Thus,

$$a_0 = \sqrt{\frac{-(2)(-2)(1.60 \times 10^{-19} \text{C})^2}{4\pi[8.85 \times 10^{-12} \text{C}^2/(\text{N} \cdot \text{m}^2)](1.49 \times 10^{-8} \text{N})}} \\ = 2.49 \times 10^{-10} \text{ m} = 0.249 \text{ nm}$$

b.

$$a_0 = r_{\text{Mg}^{2+}} + r_{\text{s}^{2-}}$$

$$0.249 \text{ nm} = r_{\text{Mg}^{2+}} + 0.184 \text{ nm}$$

or

$$r_{\text{Mg}^{2+}} = 0.065 \text{ nm} \blacktriangleleft$$

The repulsion force between Na^+ ($r = 0.095 \text{ nm}$) and Cl^- ($r = 0.181 \text{ nm}$) ions at equilibrium is $-3.02 \times 10^{-9} \text{ N}$. Calculate (a) the value of constant b using the repulsive force section of Eq. 2.8, and (b) the bonding energy, E_{\min} . Assume $n = 9$.

**EXAMPLE
PROBLEM 2.8**

■ **Solution**

- a. To determine the b value for an NaCl ion pair,

$$F = -\frac{nb}{a^{n+1}}$$

The repulsive force between an Na^+Cl^- ion pair is $-3.02 \times 10^{-9} \text{ N}$. Thus,

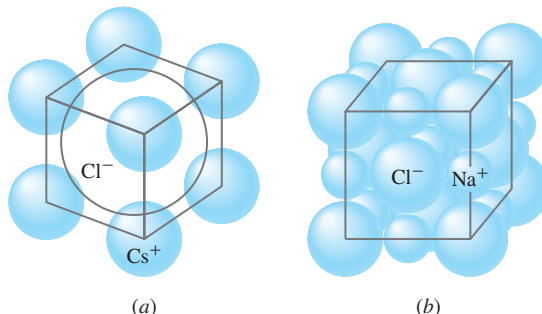
$$-3.20 \times 10^{-9} \text{ N} = \frac{-9b}{(2.76 \times 10^{-10} \text{ m})^{10}} \\ b = 8.59 \times 10^{-106} \text{ N} \cdot \text{m}^{10} \blacktriangleleft$$

- b. To calculate the potential energy of the Na^+Cl^- ion pair, use Eq. 2.9.

$$E_{\text{Na}^+\text{Cl}^-} = \frac{+Z_1 Z_2 e^2}{4\pi\epsilon_0 a} + \frac{b}{a^n} \\ = \frac{(+)(-)(1.60 \times 10^{-19} \text{C})^2}{4\pi[8.85 \times 10^{-12} \text{C}^2/(\text{N} \cdot \text{m}^2)](2.76 \times 10^{-10} \text{m})} + \frac{8.59 \times 10^{-106} \text{ N} \cdot \text{m}^{10}}{(2.76 \times 10^{-10} \text{m})^9} \\ = -8.34 \times 10^{-19} \text{ J}^* + 0.92 \times 10^{-19} \text{ J}^* \\ = -7.42 \times 10^{-19} \text{ J} \blacktriangleleft$$

*1 J = 1 N·m

Ion Arrangement in Ionic Solids Although in the previous discussions, we focused on a pair of ions, an anion attracts cations from all directions and bonds with as many of these cations as possible. Alternatively, a cation attracts anions from all directions and bonds with as many of them as possible. This, in part, determines the ionic packing arrangement, and it is how the three-dimensional structure of the ionic solid is formed. Thus, when ions pack, they do so in a 3-D manner, with no preferred

**Figure 2.18**

The ionic arrangement in two ionic solids: (a) CsCl and (b) NaCl.

(Source: C.R. Barrett, W.D. Nix, and A.S. Tetelman, *The Principles of Engineering Materials*, Prentice-Hall, 1973, p. 27.)

orientation (no separate single molecules exist), and as a result, the bonds are called *nondirectional* bonds.

The number of cations that can pack around an anion (packing efficiency) is determined by two factors: (1) their relative sizes and (2) charge neutrality. Consider CsCl and NaCl ionic solids. In the case of CsCl, eight Cl⁻ anions ($r = 0.181$ nm) pack around a central Cs⁺ cation ($r = 0.169$ nm) as shown in Figure 2.18a. Conversely, in the case of NaCl, only six Cl⁻ anions, pack around a central Na⁺ cation ($r = 0.095$ nm) as shown in Figure 2.18b. In CsCl, the ratio of the radius of cation to anion $r_{\text{Cs}^+}/r_{\text{Cl}^-} = 0.169/0.181 = 0.93$. The same ratio for NaCl is $0.095/0.181 = 0.525$. Thus, as the ratio of cation to anion radii decreases, fewer anions can surround a cation.

Electrical neutrality is the second contributing factor. For instance, in an NaCl ionic solid, for every one Na⁺ ion there must be one Cl⁻ ion in the overall solid. However, in CaF₂, for every Ca²⁺ cation, there must be two F⁻ anions.

Energy Considerations in Ionic Solids To understand the energy considerations in ionic solid formation, consider the LiF ionic solid. Production of LiF ionic solid will result in the release of about 617 kJ/mol, or in other words, the *heat of formation* for LiF is $\Delta H^\circ = -617$ kJ/mol. However, the bonding process from the ionization stage to formation of an ionic solid can be divided into five steps, and some of these steps will require expending energy.

- Step 1 Converting solid Li to gaseous Li (1s²2s¹): This step is called *atomization* and requires approximately 161 kJ/mol of energy, $\Delta H^1 = +161$ kJ/mol.
- Step 2 Converting the F₂ molecule to F atoms (1s²2s¹2p⁵): This step requires 79.5 kJ/mol, $\Delta H^2 = +79.5$ kJ/mol.
- Step 3 Removing the 2s¹ electron of Li to form a cation, Li⁺: The energy required for this stage is 520 kJ/mol, $\Delta H^3 = +520$ kJ/mol.

- Step 4 Transferring or adding an electron to the F atom to form an anion, F^- : This process actually releases energy. Therefore, the change in energy is designated as negative and is approximately -328 kJ/mol , $\Delta H^4 = -328 \text{ kJ/mol}$.
- Step 5 Formation of an ionic solid from gaseous ions. The electrostatic attraction forces between cations and anions will produce ionic bonds between gaseous ions to form a three-dimensional solid. The energy associated with this process is called the **lattice energy** and is unknown, $\Delta H^5 = ? \text{ kJ/mol}$.

According to the **Hess law**, the total heat of formation of LiF should be equal to the sum of the heats of formation required in each step. In other words, as presented in Eq. 2.11,

$$\Delta H^0 = \Delta H^1 + \Delta H^2 + \Delta H^3 + \Delta H^4 + \Delta H^5 \quad (2.11)$$

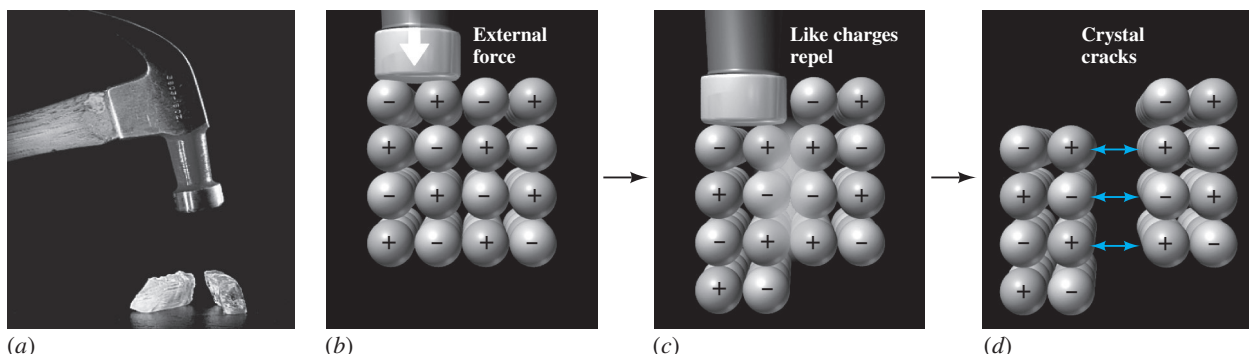
From this relationship, we can determine the magnitude of the lattice energy, $\Delta H^5 = \Delta H^0 - [\Delta H^1 + \Delta H^2 + \Delta H^3 + \Delta H^4] = -617 \text{ kJ} - [161 \text{ kJ} + 79.5 \text{ kJ} + 520 \text{ kJ} - 328 \text{ kJ}] = -1050 \text{ kJ}$. This means that although energy is expended in steps 1, 2, and 3, a greater amount of lattice energy is produced during the ionic solid formation phase (1050 kJ). In other words, the energy expended for steps 1, 2, and 3 is supplied and exceeded by the lattice energy produced in step 5 when ions are attracted to form a solid. This verifies the concept that atoms form bonds to lower their potential energies. The lattice energies associated with various ionic solids are given in Table 2.5. Examination of the table shows that (1) lattice energies decrease as we move down in groups or as the size of the ion increases and (2) lattice energies significantly increase when the ions involved have higher ionic charge.

Ionic Bonds and Material Properties Ionic solids generally have high melting temperatures. It is observed in Table 2.5 that as the lattice energy of an ionic solid increases, its melting temperature also increases, as evidenced in MgO with the highest lattice energy of 3932 kJ/mol and highest melt temperature of 2800°C . In addition, ionic solids

Table 2.5 The lattice energy and melting point values for various ionic solids

Ionic Solid	Lattice Energy*		Melting Point (°C)
	kJ/mol	kcal/mol	
LiCl	829	198	613
NaCl	766	183	801
KCl	686	164	776
RbCl	670	160	715
CsCl	649	155	646
MgO	3932	940	2800
CaO	3583	846	2580
SrO	3311	791	2430
BaO	3127	747	1923

*All values are negative for bond formation (energy is released).

**Figure 2.19**

The fracture mechanism of ionic solids. The blow will force like ions to face each other and produce large repulsive forces. The large repulsive forces can fracture the material.

(©McGraw-Hill Education/Stephen Frisch, photographer)

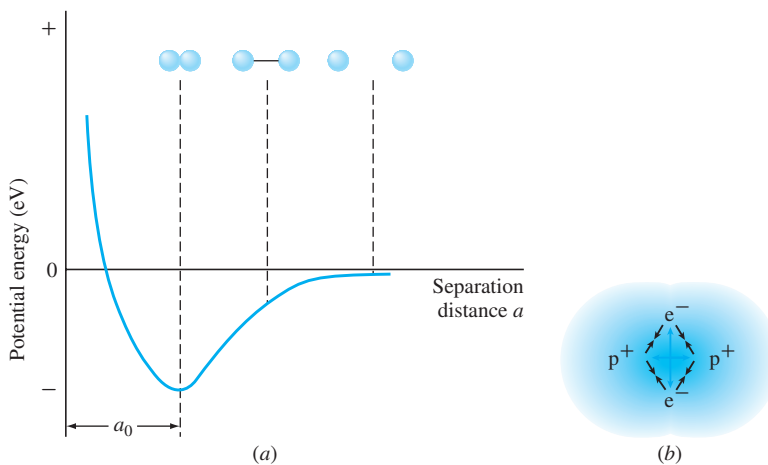
are generally hard (do not dent), rigid (do not bend or do not have any springiness), strong (hard to break), and brittle (deform little before fracture). These properties of ionic solids are due to the strong electrostatic forces that hold the ions together. Note in Figures 2.18 and 2.19 that anions and cations alternate in their positioning. If large forces are applied to ionic solids, they could force a shift in the positioning that would put like ions against each other. This would create a large repulsive force that would fracture the solid (Fig. 2.19).

Finally, generally speaking, ionic solids do not conduct electricity well and are therefore excellent insulators. The reason for this is that electrons are tightly held inside the bond and cannot participate in the conduction process. However, when melted or dissolved in water, ionic materials can conduct electricity through ionic diffusion (movement of ions). This is also evidence that ions are in fact present in the solid state.

2.5.2 Covalent Bonds

Shared Electron Pairs and Bond Order **Covalent bonding** is typically observed between atoms with small differences in their electronegativities and mostly between nonmetals. Nonmetal atoms bond through localized sharing of electrons and covalent bonding. Covalent bonding is the most common form of bonding in nature ranging from diatomic hydrogen to biological materials to synthetic macromolecules. This type of bond can also form as a percentage of total bonds in ionic as well as metallic materials. Similar to ionic bonds, covalent bonds are also very strong.

Consider the covalent bond between two hydrogen atoms. At first, the nucleus of one H atom attracts the electron cloud of the other; the atoms get closer to each other. As they get close, the two electron clouds interact, and both atoms start to take ownership of both electrons (share electrons). The atoms keep getting closer until they reach the equilibrium point in which the two H atoms will form a bond by sharing their electrons, both completing their outer electronic structure, and reaching the lowest state of energy, as shown in Figure 2.20a. In this position, the attraction forces are balanced against repulsion forces, Figure 2.20b. In this figure, the electrons are shown in the

**Figure 2.20**

Covalent bonding between hydrogen atoms. (a) The potential energy diagram and (b) schematic showing the H_2 molecule and the intramolecular forces. Note that the electrons can exist at any location within the diagram; however we have chosen to show them in these locations for ease of force analysis.

given positions for clarity of explanation. In reality, the electrons can be located at any point within the shaded area.

The covalent bonding between atoms is crudely represented by the *Lewis electron dot representation*. The electron dot representation for the covalent bonds in F_2 , O_2 , and N_2 is presented in Figure 2.21. In this figure, the pair of electrons in the formed bond, called the **shared pair** or **bonding pair**, is represented either by a pair of dots or a line. It is important to note that the atoms will form as many shared pairs as needed to complete their outer electronic structure (8 electrons total). Therefore, F atoms ($2s^22p^5$) will form one shared pair resulting in a **bond order** of one, O atoms ($2s^22p^4$) will form two shared pairs (bond order of two), and N ($2s^22p^3$) atoms will form three shared pairs (bond order of three). The strength of a covalent bond depends on

**Figure 2.21**

The Lewis electron dot representation for (a) F_2 , bond order of 1, (b) O_2 , bond order of 2, and (c) N_2 , bond order of 3.

the magnitude of the attraction force between the nuclei and the number of shared pairs of electrons. The energy required to overcome this attraction force is called the **bond energy**. Bond energy will depend on the bonded atoms, electron configurations, nuclear charges, and the atomic radii. Therefore each type of bond has its own bond energy.

It is also important to note that unlike the Lewis dot representation of the covalent molecule, the bonding electrons do not stay in fixed positions between atoms. However, there is a higher probability of finding them in the area between the bonded atoms (Fig. 2.20b). Unlike ionic bonds, covalent bonds are *directional*, and the shape of the molecule is not necessarily conveyed by the dot representation; a majority of these molecules possess complex three-dimensional shapes with nonorthogonal bond angles. Finally, the number of neighbors (or packing efficiency) around an atom will depend on the bond order.

Bond Length, Bond Order, and Bond Energy A covalent bond has a **bond length** that is the distance between the nuclei of two bonded atoms at the point of minimum energy. There exists a close relationship among bond order, bond length, and bond energy: for a given pair of atoms, with higher bond order, the bond length will decrease, and as bond length decreases, bond energy will increase. This is because the attraction force is strong between the nuclei and the multiple shared pairs. The bond energies and length between selected atoms with different bond orders are given in Table 2.6.

Table 2.6 The bond energy and bond lengths for various covalent bonds

Bond	Bond Energy*		Bond Length (nm)
	kcal/mol	kJ/mol	
C—C	88	370	0.154
C=C	162	680	0.13
C≡C	213	890	0.12
C—H	104	435	0.11
C—N	73	305	0.15
C—O	86	360	0.14
C=O	128	535	0.12
C—F	108	450	0.14
C—Cl	81	340	0.18
O—H	119	500	0.10
O—O	52	220	0.15
O—Si	90	375	0.16
N—O	60	250	0.12
N—H	103	430	0.10
F—F	38	160	0.14
H—H	104	435	0.074

*Approximate values since environment changes energy. All values are negative for bond formation (energy is released).

(Source: L.H. Van Vlack, *Elements of Materials Science*, 4th ed., Addison-Wesley, 1980.)

The relationship between bond length and bond energy can be extended by considering situations where one atom in the bond remains constant and the other varies. For instance, the bond length of C–I is greater than C–Br is greater than C–Cl. Note that bond length increases as the diameter of the atom bonding with C increases (diameter of I > Br > Cl). Thus, the bond energy will be greatest in C–Cl, lower in C–Br, and lowest in C–I.

Nonpolar and Polar Covalent Bonds Depending on the differences in electronegativities between the bonding atoms, a covalent bond could be either polar or nonpolar (to various degrees). Examples of a nonpolar covalent bond are H₂, F₂, N₂, and other covalent bonds between atoms of similar electronegativities. In these bonds, the sharing of the bonding electrons is equal between the atoms, and the bonds are therefore *nonpolar*. On the other hand, as the difference in electronegativities between the covalently bonding atoms increases, for instance in HF, the sharing of the bonding electrons is unequal (the bonding electrons displace toward the more electronegative atom). This produces a *polar covalent bond*. As the difference in electronegativity increases, the polarity of the bond increases, and if the difference becomes large enough, the bond becomes ionic. For instance, F₂, HBr, HF, and NaF will have, respectively, nonpolar covalent, polar covalent, highly polar covalent, and ionic types of bonds.

Covalent Bonding in Carbon-Containing Molecules In the study of engineering materials, carbon is very important since it is the basic element in most polymeric materials. The carbon atom in the ground state has the electron configuration 1s²2s²2p². This electron arrangement indicates that carbon should form *two covalent bonds* with its two half-filled 2p orbitals. However, in many cases, carbon forms *four covalent bonds* of equal strength. The explanation for the four carbon covalent bonds is provided by the concept of *hybridization* whereby upon bonding, one of the 2s electrons is promoted to a 2p orbital so that *four equivalent sp³ hybrid orbitals* are produced, as indicated in the orbital diagrams of Figure 2.22. Even though energy is required to promote the 2s electron to the 2p state in the hybridization process, the energy necessary for the promotion is more than compensated for by the decrease in energy accompanying the bonding process.

Carbon in the form of diamond exhibits sp³ tetrahedral covalent bonding. The four sp³ hybrid orbitals are directed symmetrically toward the corners of a regular

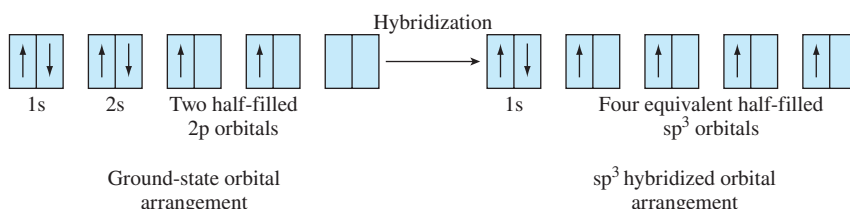
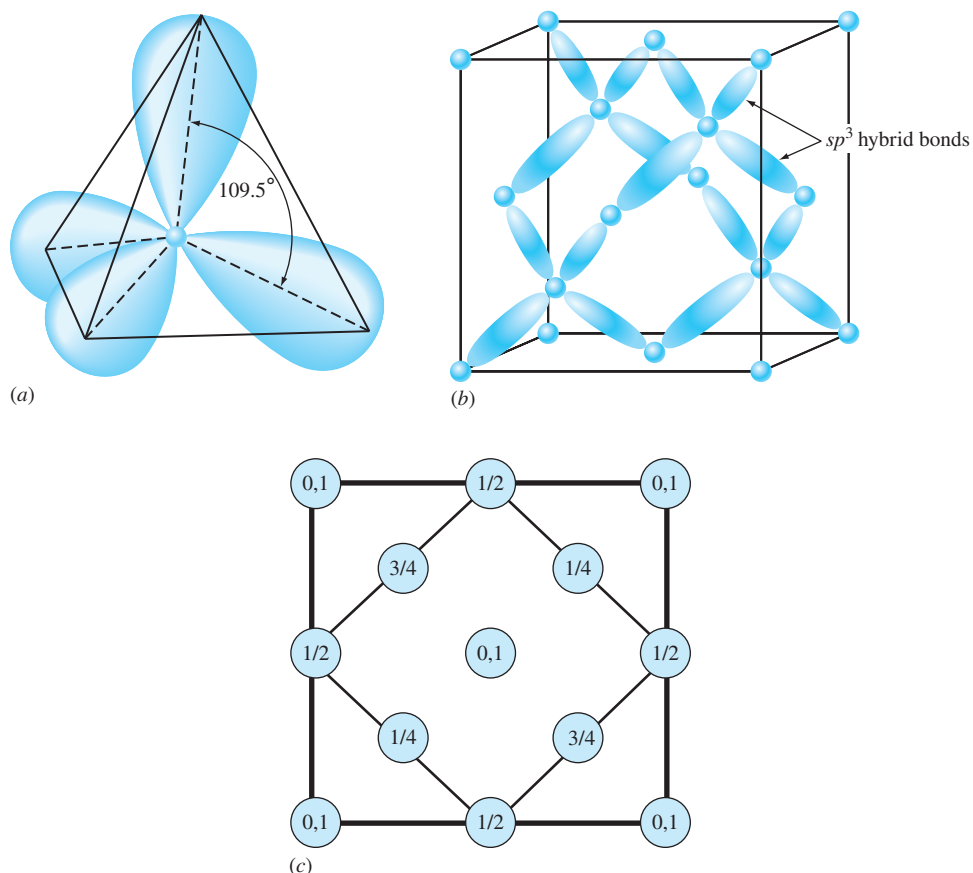


Figure 2.22

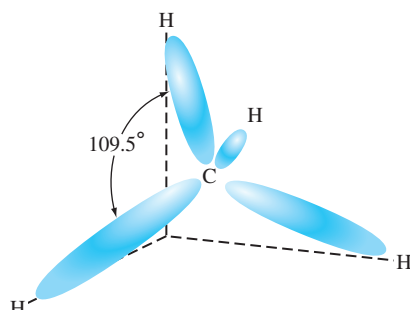
The hybridization of carbon orbitals for the formation of single bonds.

**Figure 2.23**

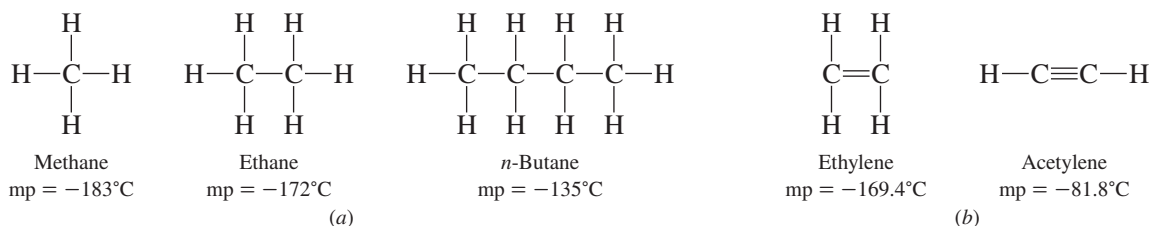
(a) The angle between the symmetric hybridized sp^3 orbitals in a carbon atom.
 (b) Tetrahedral sp^3 covalent bonds in diamond called the diamond cubic structure. Each shaded region represents a shared pair of electrons. (c) The z location of each carbon atom is shown in the basal plane. The notation “0, 1” means there is one atom at $z = 0$, and one atom at $z = 1$.

tetrahedron, as shown in Figure 2.23. The structure of diamond consists of a massive network with sp^3 tetrahedral covalent bonding, as shown in Figure 2.23. This structure accounts for the extremely high hardness of diamond and its high bond strength and melting temperature. Diamond has a bond energy of 711 kJ/mol (170 kcal/mol) and a melting temperature of 3550°C.

Covalent Bonding in Hydrocarbons Covalently bonded molecules containing only carbon and hydrogen are called *hydrocarbons*. The simplest hydrocarbon is methane, in which carbon forms four sp^3 tetrahedral covalent bonds with hydrogen atoms, as

**Figure 2.24**

The methane molecule with four tetrahedral sp^3 bonds.

**Figure 2.25**

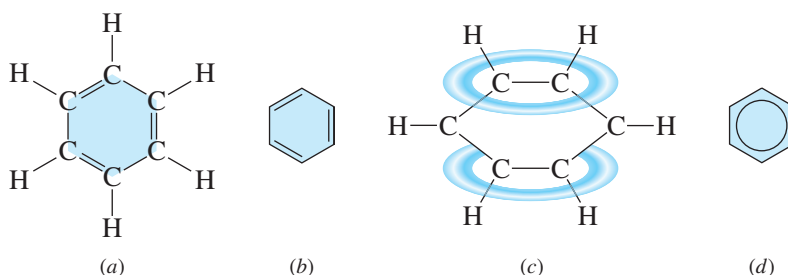
Structural formulas for (a) hydrocarbons with single bonds and (b) hydrocarbons with multiple bonds.

shown in Figure 2.24. The intramolecular bonding energy of methane is relatively high at 1650 kJ/mol (396 kcal/mol), but the intermolecular bond energy is very low at about 8 kJ/mol (2 kcal/mol). Thus, the methane molecules are very weakly bonded together, resulting in a low melting point of -183°C .

Figure 2.25a shows structural formulas for methane, ethane, and normal (*n*-) butane, which are single covalently bonded, volatile hydrocarbons. As the molecular mass of the molecule increases, so does its stability and melting point.

Carbon can also bond itself to form double and triple bonds in molecules as indicated in the structural formulas for ethylene and acetylene shown in Figure 2.25b. Double and triple carbon–carbon bonds are chemically more reactive than single carbon–carbon bonds. Multiple carbon–carbon bonds in carbon-containing molecules are referred to as *unsaturated bonds*.

An important molecular structure for some polymeric materials is the benzene structure. The benzene molecule has the chemical composition C_6H_6 with the carbon atoms forming a hexagonal-shaped ring referred to sometimes as the *benzene ring* (Fig. 2.26). The six hydrogen atoms of benzene are covalently bonded with single bonds to the six carbon atoms of the ring. However, the bonding arrangement between the carbon atoms in the ring is complex. The simplest way of satisfying the requirement that each

**Figure 2.26**

Structural formulas for benzene (a) using straight-line bonding notation and (b) simplified notation of (a). (c) Bonding arrangement showing the delocalization of the carbon–carbon electrons within the ring, and (d) simplified notation of (c).

carbon atom have four covalent bonds is to assign alternating single and double bonds to the carbon atoms in the ring itself (Fig. 2.26a). This structure can be represented more simply by omitting the external hydrogen atoms (Fig. 2.26b). This structural formula for benzene will be used in this book since it more clearly indicates the bonding arrangement in benzene.

However, experimental evidence indicates that a normal reactive double carbon–carbon bond does not exist in benzene and that the bonding electrons within the benzene ring are delocalized, forming an overall bonding structure intermediate in chemical reactivity to that between single and double carbon–carbon bonds (Fig. 2.26c). Thus, most chemistry books are written using a circle inside a hexagon to represent the structure of benzene (Fig. 2.26d).

Covalent Bonds and Material Properties Materials that consist of covalent bonds are numerous: most gas molecules, liquid molecules, and low-melting solid molecules are formed through covalent bonds. Also, what is common among these materials is that they are molecular (the bond between molecules is weak). The covalent bonds between the atoms are very strong and are difficult to break; however, the bond between molecules is weak and breaks easily. Therefore, such materials boil or melt very easily. We will cover the nature of these bonds in future sections.

In contrast to the above molecular materials, in some materials called **network covalent solids** (no molecules), all the bonds are covalent. In such materials, the number of neighbors for an atom depends on the number of covalent bonds available as per the bond order. Two examples of such covalent solids are quartz and diamond. The properties of quartz reflect the strength of the covalent bonds in it. Quartz is made up of Si and O atoms (SiO_2) continuously connected to each other through covalent bonds in a 3-D network. There are no molecules in this material. Similar to diamond, quartz is very hard and melts at a high temperature of 1550°C . The high melting point of network covalent solids is a reflection of the high bonding energies and the true strength of covalent bonds. Covalent materials are poor

conductors of electricity not only in a network solid form but also in a liquid or molten form. This is because electrons are tightly bonded in the shared pairs, and no ions are available for charge transport.

2.5.3 Metallic Bonds

Although two isolated metal atoms may form strong covalent bonds between atoms (Na_2), the resulting material will be gaseous, that is, the bond between Na_2 molecules will be weak. The question is then, “What type of bond holds the atoms of solid sodium (or any other solid metal) together?” It is observed that during solidification, from a molten state, the atoms of a metal pack tightly together, in an organized and repeating manner, to lower their energy and achieve a more stable state in the form of a solid, thus creating **metallic bonds**. For instance in copper, each copper atom will have 12 neighbors packed around it in an orderly fashion (Fig. 2.27a). In the process, all the atoms contribute their valence electrons to a “sea of electrons” or the “electron charge cloud” (Fig. 2.27b). These valence electrons are delocalized, move freely in the sea of electrons, and do not belong to any specific atoms. For this reason, they are also called *free electrons*. The nuclei and the remaining core electrons of tightly packed atoms form a cationic or a positive core (because they have lost their valence electrons). What keeps the atoms together in solid metals is the attraction force between the positive ionic core (metal cations) and the negative electron cloud. This is referred to as *metallic bonding*.

The metallic bond is three-dimensional and nondirectional, similar to the ionic bond. However, since there are no anions involved, there are no electrical neutrality restrictions. Also, the metallic cations are not held in place as rigidly as they are in ionic solids. In contrast to the directional covalent bonds, there are no shared localized electron pairs between atoms; metallic bonds are therefore weaker than covalent bonds.

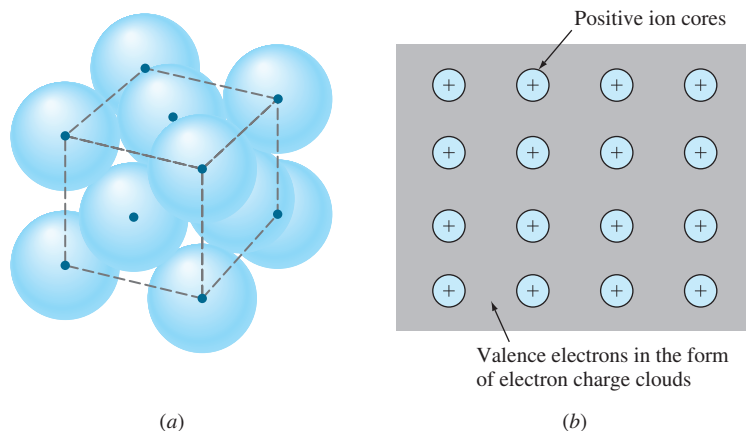


Figure 2.27

(a) The ordered, efficiently packed structure of copper atoms in a metallic solid. (b) The positive ion core and the surrounding sea of electrons model for metallic bonding.

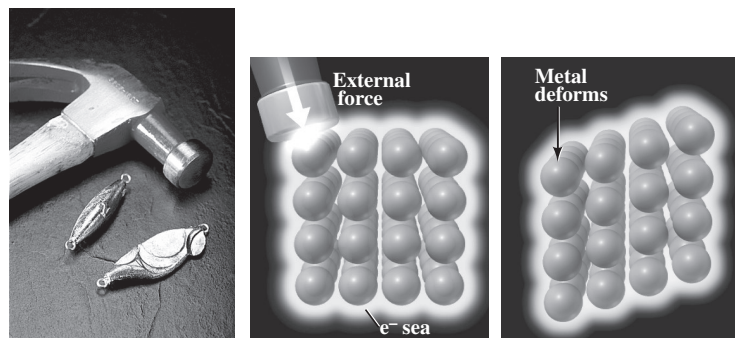
Metallic Bonds and Material Properties The melting points of pure metals are only moderately high because, for melting, it is not required to break the bond between the ionic core and the electron cloud. Thus, on average, ionic materials and covalent networks have higher melting temperatures because they both require breakage of the bonds for melting. The bond energies and the melting point of metals vary greatly, depending on the number of valence electrons and the percent metallic bonding. In general, group 1A elements (alkali metals) have only one valence electron and possess almost exclusively metallic bonds. As a result, these metals have lower melt temperatures than group 2A elements that have two valence electrons and a higher percentage of covalent bonding.

The elements in the fourth period, including the transition metals, their outer electronic configurations, bond energies, and melt temperatures, are presented in Table 2.7. In metals, as the number of valence electrons increases, the attraction force between the positive core and the electron cloud also increases; K ($4s^1$) with one valence electron has a melt temperature of 63.5°C compared to a considerably higher 851°C for Ca ($4s^2$) with two valence electrons (Table 2.7). With the introduction of 3d electrons in the transition metals, the number of valence electrons increases, as does the melt temperature with a maximum of 1903°C for Cr ($3d^54s^1$). This increase in bonding energy and melt temperature in transition metals is attributed to an increase in the percentage of covalent bonding. As the 3d and 4s orbitals become full, the melt temperature again starts to drop among transition metals, with the lowest being 1083°C for copper ($3d^{10}4s^1$). After Cu, there is an even more significant drop in melt temperature for Zn ($4s^2$) to 419°C .

The mechanical properties of metals are significantly different than those of ionically and covalently networked materials. Pure metals are much more malleable (soft

Table 2.7 Bonding energies, electron configurations, and melting points of the fourth-period metals of the periodic table

Element	Electron Configuration	Bonding Energy kJ/mol	Bonding Energy kcal/mol	Melting Point (°C)
K	$4s^1$	89.6	21.4	63.5
Ca	$4s^2$	177	42.2	851
Sc	$3d^14s^2$	342	82	1397
Ti	$3d^24s^2$	473	113	1660
V	$3d^34s^2$	515	123	1730
Cr	$3d^54s^1$	398	95	1903
Mn	$3d^54s^2$	279	66.7	1244
Fe	$3d^64s^2$	418	99.8	1535
Co	$3d^74s^2$	383	91.4	1490
Ni	$3d^84s^2$	423	101	1455
Cu	$3d^{10}4s^1$	339	81.1	1083
Zn	$4s^2$	131	31.2	419
Ga	$4s^24p^1$	272	65	29.8
Ge	$4s^24p^2$	377	90	960

**Figure 2.28**

(a) The deformation behavior of metallic solids. (b) The blow will force the cations to slide past each other and thus allow a great deal of malleability.

(©McGraw-Hill Education/Stephen Frisch, photographer)

and deformable) than ionically or covalently networked materials. As a matter of fact, there are few structural applications for pure metals because of their softness. This is because, under the action of an external force, the ions in the metal can slip past each other with relative ease (Fig. 2.28). The bonds between the ions in a metal can be broken at lower energy levels compared to ionic and covalent bonds. Compare this behavior to that presented in Figure 2.19 for ionic materials. In future chapters, we will explain how the strength of a pure metal can be significantly increased through alloying impurities, plastic deformation, grain refinement, and heat treatment.

The main use of pure metals is in electrical and electronic applications. Pure metals are excellent conductors of electricity because of the delocalized nature of the valence electrons. As soon as a metal component is placed in an electrical circuit, each valence electron will rather freely carry a negative charge module toward the positive electrode. This is impossible in ionic or covalent materials because the valence electrons are tightly held in place by the nuclei. Metals are also excellent conductors of heat because of the efficient transfer of thermal atomic vibrations across the metal.

2.5.4 Mixed Bonding

The chemical bonding of atoms or ions can involve more than one type of primary bond and can also involve secondary dipole bonds. For primary bonding there can be the following combinations of mixed-bond types: (1) ionic-covalent, (2) metallic-covalent, (3) metallic-ionic, and (4) ionic-covalent-metallic.

Ionic-Covalent Mixed Bonding Most covalent-bonded molecules have some ionic binding, and vice versa. The partial ionic character of covalent bonds can be interpreted in terms of the electronegativity scale of Figure 2.14. The greater the difference in the electronegativities of the elements involved in a mixed ionic-covalent bond,

the greater the degree of ionic character of the bond. Pauling proposed the following equation to determine the percentage ionic character of bonding in a compound AB:

$$\% \text{ ionic character} = (1 - e^{(-1/4)(X_A - X_B)^2})(100\%) \quad (2.12)$$

where X_A and X_B are the electronegativities of the atoms A and B in the compound, respectively.

Many semiconducting compounds have mixed ionic-covalent bonding. For example, GaAs is a 3–5 compound (Ga is in group 3A and As in group 5A of the periodic table) and ZnSe is a 2–6 compound. The degree of ionic character in the bonding of these compounds increases as the electronegativity between the atoms in the compounds increases. Thus, one would expect a 2–6 compound to have more ionic character than a 3–5 compound because of the greater electronegativity difference in the 2–6 compound. Example Problem 2.9 illustrates this.

**EXAMPLE
PROBLEM 2.9**

Calculate the percentage ionic character of the semiconducting compounds GaAs (3–5) and ZnSe (2–6) by using Pauling's equation

$$\% \text{ ionic character} = (1 - e^{(-1/4)(X_A - X_B)^2})(100\%)$$

- a. For GaAs, electronegativities from Figure 2.14 are $X_{\text{Ga}} = 1.6$ and $X_{\text{As}} = 2.0$. Thus,

$$\begin{aligned} \% \text{ ionic character} &= (1 - e^{(-1/4)(1.6 - 2.0)^2})(100\%) \\ &= (1 - e^{(-1/4)(-0.4)^2})(100\%) \\ &= (1 - 0.96)(100\%) = 4\% \end{aligned}$$

- b. For ZnSe, electronegativities from Figure 2.14 are $X_{\text{Zn}} = 1.6$ and $X_{\text{Se}} = 2.4$. Thus,

$$\begin{aligned} \% \text{ ionic character} &= (1 - e^{(-1/4)(1.6 - 2.4)^2})(100\%) \\ &= (1 - e^{(-1/4)(-0.8)^2})(100\%) \\ &= (1 - 0.85)(100\%) = 15\% \end{aligned}$$

Note that as the electronegativities differ, more for the 2–6 compound, the percentage ionic character increases.

Metallic-Covalent Mixed Bonding Mixed metallic-covalent bonding occurs commonly. For example, the transition metals have mixed metallic-covalent bonding involving dsp bonding orbitals. The high melting points of the transition metals are attributed to mixed metallic-covalent bonding. Also in group 4A of the periodic table, there is a gradual transition from pure covalent bonding in carbon (diamond) to some metallic character in silicon and germanium. Tin and lead are primarily metallically bonded.

Metallic-Ionic Mixed Bonding If there is a significant difference in electronegativity in the elements that form an intermetallic compound, there may be a significant amount of electron transfer (ionic binding) in the compound. Thus, some intermetallic

compounds are good examples for mixed metallic-ionic bonding. Electron transfer is especially important for intermetallic compounds such as NaZn_{13} and less important for compounds Al_9Co_3 and $\text{Fe}_5\text{Zn}_{21}$ since the electronegativity differences for the latter two compounds are much less.

2.6 SECONDARY BONDS

Until now, we have considered only primary bonding between atoms and showed that it depends on the interaction of their valence electrons. The driving force for primary atomic bonding is the lowering of the energy of the bonding electrons. Secondary bonds are relatively weak in contrast to primary bonds and have energies of only about 4 to 42 kJ/mol (1 to 10 kcal/mol). The driving force for secondary bonding is the attraction of the electric dipoles contained in atoms or molecules.

An electric dipole moment is created when two equal and opposite charges are separated, as shown in Figure 2.29a. Electric dipoles are created in atoms or molecules when positive and negative charge centers exist (Fig. 2.29b).

Dipoles in atoms or molecules create dipole moments. A *dipole moment* is defined as the charge value multiplied by the separation distance between positive and negative charges, or

$$\mu = qd \quad (2.13)$$

where μ = dipole moment

q = magnitude of electric charge

d = separation distance between the charge centers

Dipole moments in atoms and molecules are measured in Coulomb-meters ($\text{C} \cdot \text{m}$) or in debye units, where $1 \text{ debye} = 3.34 \times 10^{-30} \text{ C} \cdot \text{m}$.

Electric dipoles interact with each other by electrostatic (Coulombic) forces, and thus atoms or molecules containing dipoles are attracted to each other by these forces. Even though the bonding energies of secondary bonds are weak, they become important when they are the only bonds available to bond atoms or molecules together.

In general, there are two main kinds of secondary bonds between atoms or molecules involving electric dipoles: fluctuating dipoles and permanent dipoles. Collectively, these secondary dipole bonds are sometimes called *van der Waals bonds (forces)*.

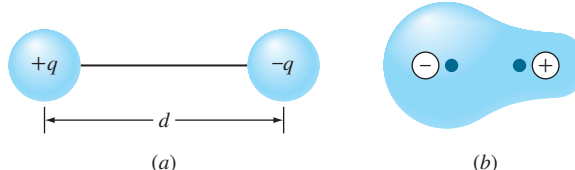


Figure 2.29

(a) An electric dipole. The dipole moment is qd .

(b) An electric dipole moment in a covalently bonded molecule.

Very weak secondary bonding forces can develop between the atoms of noble-gas elements that have complete outer-valence-electron shells (s^2 for helium and s^2p^6 for Ne, Ar, Kr, Xe, and Rn). These bonding forces arise because the asymmetrical distribution of electron charges in these atoms creates electric dipoles. At any instant, there is a high probability that there will be more electron charge on one side of an atom than on the other (Fig. 2.30). Thus, in a particular atom, the electron charge cloud will change with time, creating a “fluctuating dipole.” Fluctuating dipoles of nearby atoms can attract each other, creating weak interatomic nondirectional bonds. The liquefaction and solidification of the noble gases at low temperatures and high pressures are attributed to fluctuating dipole bonds. The melting and boiling points of the noble gases at atmospheric pressure are listed in Table 2.8. Note that as the atomic size of the noble gases increases, the melting and boiling points also increase due to stronger bonding forces since the electrons have more freedom to create stronger dipole moments.

Weak bonding forces among covalently bonded molecules can be created if the molecules contain **permanent dipoles**. For example, the methane molecule, CH_4 ,

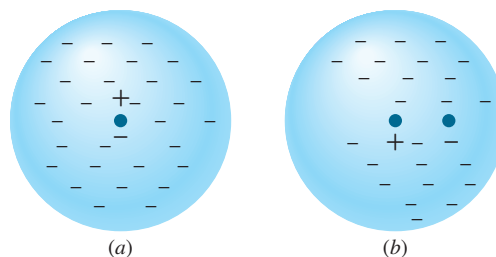


Figure 2.30

Electron charge distribution in a noble gas atom. (a) An idealized symmetric charge distribution in which the negative and positive charge centers are superimposed at the center. (b) The actual asymmetric distribution of electrons causing a temporary dipole.

Table 2.8 The melting and boiling points of various noble gases

Noble Gas	Melting Point (°C)	Boiling Point (°C)
Helium	-272.2	-268.9
Neon	-248.7	-245.9
Argon	-189.2	-185.7
Krypton	-157.0	-152.9
Xenon	-112.0	-107.1
Radon	-71.0	-61.8

with its four C–H bonds arranged in a tetrahedral structure (Fig. 2.24), has a zero dipole moment because of its symmetrical arrangement of four C–H bonds. That is, the vectorial addition of its four dipole moments is zero. The chloromethane molecule, CH_3Cl , in contrast, has an asymmetrical tetrahedral arrangement of three C–H bonds and one C–Cl bond, resulting in a net dipole moment of 2.0 debyes. The replacement of one hydrogen atom in methane with one chlorine atom raises the boiling point from -128°C for methane to -14°C for chloromethane. The much higher boiling point of chloromethane is due to the permanent dipole bonding forces among the chloromethane molecules.

The **hydrogen bond** is a special case of a permanent dipole-dipole interaction between polar molecules. Hydrogen bonding occurs when a polar bond containing the hydrogen atom, O–H or N–H, interacts with the electronegative atoms O, N, F, or Cl. For example, the water molecule, H_2O , has a permanent dipole moment of 1.84 debyes due to its asymmetrical structure with its two hydrogen atoms at an angle of 105° with respect to its oxygen atom (Fig. 2.31a).

The hydrogen atomic regions of the water molecule have positively charged centers, and the opposite end region of the oxygen atom has a negatively charged center (Fig. 2.31a). In hydrogen bonding between water molecules, the negatively charged region of one molecule is attracted by coulombic forces to the positively charged region of another molecule (Fig. 2.31b).

In liquid and solid water, relatively strong intermolecular permanent dipole forces (hydrogen bonding) are formed among the water molecules. The energy associated with the hydrogen bond is about 29 kJ/mol (7 kcal/mol) as compared to about 2 to 8 kJ/mol (0.5 to 2 kcal/mol) for fluctuating dipole forces in the noble gases. The exceptionally high boiling point of water (100°C) for its molecular mass is attributed to the effect of hydrogen bonding. Hydrogen bonding is also very important for strengthening the bonding between molecular chains of some types of polymeric materials.

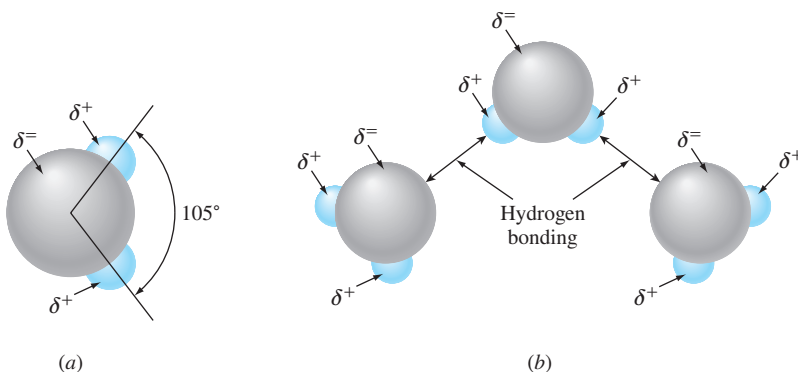


Figure 2.31

(a) Permanent dipole nature of the water molecule. (b) Hydrogen bonding among water molecules due to permanent dipole attraction.

2.7 SUMMARY

Atoms consist mainly of three basic subatomic particles: *protons*, *neutrons*, and *electrons*. The electrons are envisaged as forming a cloud of varying density around a denser atomic nucleus containing almost all the mass of the atom. The outer electrons (high energy electrons) are the valence electrons, and it is mainly their behavior that determines the chemical reactivity of each atom.

Electrons obey the laws of quantum mechanics, and as a result, the energies of electrons are *quantized*. That is, an electron can have only certain allowed values of energies. If an electron changes its energy, it must change to a new allowed energy level. During an energy change, an electron emits or absorbs a photon of energy according to Planck's equation $\Delta E = h\nu$, where ν is the frequency of the radiation. Each electron is associated with four quantum numbers: the principal quantum number n , the subsidiary quantum number l , the magnetic quantum number m_b , and the spin quantum number m_s . According to Pauli's exclusion principle, *no two electrons in the same atom can have all four quantum numbers the same*. Electrons also obey Heisenberg's uncertainty principle, which states that it is impossible to determine the momentum and position of an electron simultaneously. Thus, the location of electrons in atoms must be considered in terms of electron density distributions.

There are two main types of atomic bonds: (1) *strong primary bonds* and (2) *weak secondary bonds*. Primary bonds can be subdivided into (1) *ionic*, (2) *covalent*, and (3) *metallic bonds*, and secondary bonds can be subdivided into (1) *fluctuating dipoles* and (2) *permanent dipoles*.

Ionic bonds are formed by the transfer of one or more electrons from an electropositive atom to an electronegative one. The ions are bonded together in a solid crystal by electrostatic (coulombic) forces and are *nondirectional*. The size of the ions (geometric factor) and electrical neutrality are the two main factors that determine the ion packing arrangement. *Covalent bonds* are formed by the sharing of electrons in pairs by half-filled orbitals. The more the bonding orbitals overlap, the stronger the bond. Covalent bonds are *directional*. *Metallic bonds* are formed by metal atoms by a mutual sharing of valence electrons in the form of delocalized electron charge clouds. In general, the fewer the valence electrons, the more delocalized they are and the more metallic the bonding. *Metallic bonding* only occurs among an aggregate of atoms and is *nondirectional*.

Secondary bonds are formed by the electrostatic attraction of electric dipoles within atoms or molecules. *Fluctuating dipoles* bond atoms together due to an asymmetrical distribution of electron charge within atoms. These bonding forces are important for the liquefaction and solidification of noble gases. *Permanent dipole* bonds are important in the bonding of polar covalently bonded molecules such as water and hydrocarbons.

Mixed bonding commonly occurs between atoms and in molecules. For example, metals such as titanium and iron have mixed metallic-covalent bonds; covalently bonded compounds such as GaAs and ZnSe have a certain amount of ionic character; some intermetallic compounds such as NaZn_{13} have some ionic bonding mixed with metallic bonding. In general, bonding occurs between atoms or molecules because their energies are lowered by the bonding process.

2.8 DEFINITIONS

Sec. 2.1

Law of multiple proportions: when atoms are combined in specific simple fractions, they form different compounds.

Law of mass conservation: a chemical reaction does not lead to the creation or destruction of matter.

Sec. 2.2

Atomic number (Z): the number of protons in the nucleus of an atom.

Atomic mass unit: defined as 1/12 the mass of a carbon atom.

Mass number (A): the sum of protons and neutrons in the nucleus of an atom.

Isotopes: atoms of the same element that have the same number of protons but not the same number of neutrons.

Mole: the amount of substance that contains 6.02×10^{23} elementary entities (atoms or molecules).

Law of chemical periodicity: properties of elements are functions of their atomic number in a periodic manner.

Sec. 2.3

Quanta: discrete (specific) amounts of energy emitted by atoms and molecules.

Electromagnetic radiation: energy released and transmitted in the form of electromagnetic waves.

Photon: quantum of energy emitted or released in the form of electromagnetic radiation with a specific wavelength and frequency.

Ionization energy: the minimum energy required to separate an electron from its nucleus.

Uncertainty principle: it is impossible to simultaneously determine the exact position and the exact momentum of a body (for instance an electron).

Electron density: the probability of finding an electron of a given energy level in a given region of space.

Orbitals: different wave functions that are solutions to the wave equation and can be presented as electron density diagrams.

Boundary surface: an alternative to the electron density diagram showing the area inside which one can find an electron with a probability of 90%.

Principal quantum number: A quantum number representing the energy level of the electron.

Orbital quantum number: the shape of the electron cloud or the boundary space of the orbital is determined by this number.

Magnetic quantum number: represents the orientation of the orbitals within each subshell.

Spin quantum number: represents the spin of the electron.

Pauli's exclusion principle: no two electrons can have the same set of four quantum numbers.

Nucleus charge effect: the higher the charge of the nucleus, the higher is the attraction force on an electron and the lower the energy of the electron.

Shielding effect: when two electrons within the same energy level repel each other and thus counteract the attraction force of the nucleus.

Sec. 2.4

Metallic radius: half the distance between the nuclei of two adjacent atoms in a sample of a metallic element.

Covalent radius: half the distance between the nuclei of the identical atoms within a covalent molecule.

First ionization energy: the energy required for the removal of the outermost electron.

Second ionization energy: the energy required to remove a second outer core electron (after the first one has been removed).

Positive oxidation number: the number of outer electrons that an atom can give up through the ionization process.

Electron affinity: the tendency of an atom to accept one or more electrons and release energy in the process.

Negative oxidation number: the number of electrons that an atom can gain.

Reactive metals: metals with low ionization energies and little or no electron affinity.

Reactive nonmetals: nonmetals with high ionization energies and extensive electron affinity.

Metalloids: elements that can behave either in a metallic or a nonmetallic manner.

Electronegativity: the degree by which atoms attract electrons to themselves.

Hess law: the total heat of formation is equal to the sum of the heat of formation in the five steps of ionic solid formation.

Sec. 2.5

Primary bonds: strong bonds that form between atoms.

Ionic bonding: a primary bond that forms between metals and nonmetals or atoms with large differences in their electronegativities.

Equilibrium interionic distance: the distance between the cation and the anion when the bond is formed (at equilibrium).

Lattice energy: energy associated with the formation of a 3-D solid from gaseous ions through ionic bonding.

Covalent bonding: a type of primary bond typically observed between atoms with small differences in their electronegativities and mostly between nonmetals.

Shared pair (bonding pair): the pair of electrons in the formed covalent bond.

Bond order: the number of shared pairs (covalent bonds) formed between two atoms.

Bond energy: the energy required to overcome the attraction force between the nuclei and the shared pair of electrons in a covalent bond.

Bond length: the distance between the nuclei of two bonded atoms at the point of minimum energy in a covalent bond.

Hybrid orbitals: when two or more atomic orbitals mix to form new orbitals.

Network covalent solids: materials that are made up entirely of covalent bonds.

Metallic bonds: example of a primary bond that forms due to tight packing of atoms in metals during solidification.

Sec. 2.6

Secondary bonds: comparatively weak bonds that form between molecules (and atoms of noble gasses) due to electrostatic attraction electric dipoles.

Fluctuating dipole: a changing dipole created by instantaneous changes in the electron charge clouds.

Permanent dipole: a stable dipole created due to structural asymmetries in the molecule.

Hydrogen bond: a special case of permanent dipole interaction between polar molecules.

2.9 PROBLEMS

Answers to problems marked with an asterisk are given at the end of the book.

Knowledge and Comprehension Problems

- 2.1 Describe the laws of (a) multiple proportions and (b) mass conservation as related to atoms and their chemical properties.
- 2.2 How did scientists find out that atoms themselves are made up of smaller particles?
- 2.3 How was the existence of electrons first verified? Discuss the characteristics of electrons.

- 2.4** How was the existence of protons first verified? Discuss the characteristics of protons.
- 2.5** What are the similarities and differences among protons, neutrons, and electrons? Compare in detail.
- 2.6** One mole of iron atoms has a mass of 55.85 g; without any calculations determine the mass in amu of one iron atom.
- 2.7** One atom of oxygen has a mass of 16.00 amu; without any calculations determine the mass in grams of one mole of oxygen atoms.
- 2.8** Define (a) atomic number, (b) atomic mass, (c) atomic mass unit (amu), (d) mass number, (e) isotopes, (f) mole, (g) relative atomic mass, (h) average relative atomic mass, and (i) Avogadro's number.
- 2.9** Explain the law of chemical periodicity.
- 2.10** What is the nature of visible light? How is the energy released and transmitted in visible light?
- 2.11** (a) Rank the following emissions in increasing magnitude of wavelength: microwave oven emissions, radio waves, sun lamp emissions, X-ray emissions, and gamma ray emissions from the sun. (b) Rank the same emissions in terms of frequency. Which emission has the highest energy?
- 2.12** Describe the Bohr model of the hydrogen atom. What are the shortcomings of the Bohr model?
- 2.13** Describe the uncertainty principle. How does this principle contradict Bohr's model of the atom?
- 2.14** Describe the following terms (give a diagram for each): (a) electron density diagram, (b) orbital, (c) boundary surface representation, and (d) radial probability.
- 2.15** Name and describe all the quantum numbers.
- 2.16** Explain Pauli's exclusion principle.
- 2.17** Describe (a) the nucleus charge effect, and (b) the shielding effect in multielectron atoms.
- 2.18** Describe the terms (a) metallic radius, (b) covalent radius, (c) first ionization energy, (d) second ionization energy, (e) oxidation number, (f) electron affinity, (g) metals, (h) nonmetals, (i) metalloids, and (j) electronegativity.
- 2.19** Compare and contrast the three primary bonds in detail (draw a schematic for each). Explain the driving force in the formation of such bonds, or in other words, why do atoms want to bond at all?
- 2.20** Describe the factors that control packing efficiency (number of neighbors) in ionic and covalent solids. Give an example of each type of solid.
- 2.21** Describe the five stages leading to the formation of an ionic solid. Explain which stages require energy and which stages release energy.
- 2.22** Describe (a) the Hess law, (b) lattice energy, and (c) heat of formation.
- 2.23** Describe the terms (a) shared pair, (b) bond order, (c) bond energy, (d) bond length, (e) polar and nonpolar covalent bonds, and (f) network covalent solid.
- 2.24** Explain the hybridization process in carbon. Use orbital diagrams.
- 2.25** Describe the properties (electrical, mechanical, etc.) of materials that are exclusively made up of (a) ionic bonds, (b) covalent bonds, and (c) metallic bonds. Name a material for each type.

- 2.26** What are secondary bonds? What is the driving force for the formation of such bonds? Give examples of materials in which such bonds exist.
- 2.27** Discuss various types of mixed bonding.
- 2.28** Define the following terms: (a) dipole moment, (b) fluctuating dipole, (c) permanent dipole, (d) van der Waals bonds, and (e) hydrogen bond.

Application and Analysis Problems

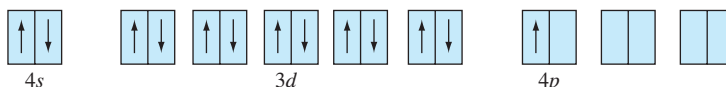
- 2.29** The diameter of a soccer ball is approximately 0.279 m (11 in.). The diameter of the moon is 3.476×10^6 m. Give an “estimate” of how many soccer balls it will take to cover the surface of the moon (assume the moon is a sphere with a flat terrain). Compare this number to Avogadro’s number. What is your conclusion?
- 2.30** Each quarter produced by the U.S. mint is made up of a copper and nickel alloy. In each coin, there is 0.00740 mole of Ni and 0.0886 mole of copper. (a) What is the total mass of a quarter? (b) What percentage of the mass of a quarter is nickel and what percentage is copper?
- 2.31** Sterling silver contains 92.5 wt% silver and 7.5 wt% copper. Copper is added to silver to make the metal stronger and more durable. A small sterling silver spoon has a mass of 100 g. Calculate the number of copper and silver atoms in the spoon.
- 2.32** There are two naturally occurring isotopes for boron with mass numbers 10 (10.0129 amu) and 11 (11.0093 amu); the percentages are 19.91 and 80.09, respectively. (a) Find the average atomic mass and (b) the relative atomic mass (or atomic weight) of boron. (c) Compare your value with that presented in the periodic table.
- 2.33** A monel alloy consists of 70 wt% Ni and 30 wt% Cu. What are the atomic percentages of Ni and Cu in this alloy?
- 2.34** What is the chemical formula of an intermetallic compound that consists of 15.68 wt% Mg and 84.32 wt% Al?
- 2.35** In order to raise the temperature of 100 g of water from room temperature (20°C) to boiling temperature (100°C), an energy input of 33,440.0 J is required. If one uses a microwave oven (λ of radiation of 1.20 cm) to achieve this, how many photons of the microwave radiation is required?
- 2.36** For Prob. 2.35, determine the number of photons to achieve the same increase in temperature if (a) ultraviolet ($\lambda = 1.0 \times 10^{-8}$ m), visible ($\lambda = 5.0 \times 10^{-7}$ m), and infrared ($\lambda = 1.0 \times 10^{-4}$ m) lights were used. What important conclusions can you draw from this exercise?
- 2.37** In order for the human eye to detect visible light, its optic nerves must be exposed to a minimum energy of 2.0×10^{-17} J. (a) Calculate the number of photons of red light needed to achieve this ($\lambda = 700$ nm). (b) Without any additional calculations, determine if you would need more or fewer photons of blue light to excite the optical nerves.
- 2.38** Represent the wavelength of the following rays by comparing each to the length of a physical object [e.g., a ray with a wavelength of 1 m (100 cm) would be approximately the length of a baseball bat]: (a) rays from a dental ray, (b) rays in a microwave oven, (c) rays in a sun lamp, (d) rays in a heat lamp, and (e) an FM radio wave.

- 2.39** For the rays in Prob. 2.38, without any calculations, rank them in increasing order of the energy of the radiation.
- 2.40** In a commercial X-ray generator, a stable metal such as copper (Cu) or tungsten (W) is exposed to an intense beam of high-energy electrons. These electrons cause ionization events in the metal atoms. When the metal atoms regain their ground state they emit X-rays of characteristic energy and wavelength. For example, a “tungsten” atom struck by a high-energy electron may lose one of its K shell electrons. When this happens, another electron, probably from the tungsten L shell, will “fall” into the vacant site in the K shell. If such a $2p \rightarrow 1s$ transition occurs in tungsten, a tungsten K_{α} X-ray is emitted. A tungsten K_{α} X-ray has a wavelength λ of 0.02138 nm. What is its energy? What is its frequency?
- 2.41** A hydrogen atom exists with its electron in the $n = 4$ state. The electron undergoes a transition to the $n = 3$ state. Calculate (a) the energy of the photon emitted, (b) its frequency, and (c) its wavelength in nanometers (nm).
- 2.42** A hydrogen atom exists with its electron in the $n = 6$ state. The electron undergoes a transition to the $n = 2$ state. Calculate (a) the energy of the photon emitted, (b) its frequency, and (c) its wavelength in nanometers.
- 2.43** Use the information given in Example Problems 2.4 and 2.5 to determine the uncertainty associated with the electron’s position if the uncertainty in determining its velocity is 1 percent. Compare the calculated uncertainty in the position with the estimated diameter of the atom. What is your conclusion?
- 2.44** Repeat Prob. 2.43 to determine the uncertainty associated with the electron’s position if the uncertainty in determining its velocity is 2%. Compare the calculated uncertainty in the position with that of Prob. 2.43. What is your conclusion?
- 2.45** For the principal quantum number, n , of value 4, determine all other possible quantum numbers for ℓ and m_{ℓ} .
- 2.46** For each pair of n and ℓ given below, give the sublevel name, possible values of m_{ℓ} , and the corresponding number of orbitals.
- $n = 1, \ell = 0$
 - $n = 2, \ell = 1$
 - $n = 3, \ell = 2$
 - $n = 4, \ell = 3$
- 2.47** Determine if the following combinations of quantum numbers are acceptable.
- $n = 3, \ell = 0, m_{\ell} = +1$
 - $n = 6, \ell = 2, m_{\ell} = -3$
 - $n = 3, \ell = 3, m_{\ell} = -1$
 - $n = 2, \ell = 1, m_{\ell} = +1$
- 2.48** In each row (*a* through *d*) there is only one piece of information that is wrong. Highlight the information that is wrong and explain why.

	n	ℓ	m_{ℓ}	Name
(a)	3	0	1	3s
(b)	2	1	-1	2s
(c)	3	1	+2	3d
(d)	3	3	0	4f

2.49 Determine the four quantum numbers for the third, 15th, and 17th electrons of the Cl atom.

2.50 Determine the electron configuration and group number of the atom in the ground state based on the given partial (valence level) orbital diagram. Identify the element.



2.51 Write the electron configurations of the following elements by using spdf notation:
(a) yttrium, (b) hafnium, (c) samarium, (d) rhenium.

2.52 Write the electron configuration of the following ions using the spdf notation:
(a) Cr²⁺, Cr³⁺, Cr⁶⁺; (b) *Mo³⁺, Mo⁴⁺, Mo⁶⁺; (c) Se⁴⁺, Se⁶⁺, Se²⁻.

2.53 Rank the following atoms by (a) increasing atomic size and (b) decreasing first ionization energy, IE1. Use only the periodic table to answer the questions. Check your answer using Figs. 2.10 and 2.11.

(i) K, Ca, Ga

(ii) Ca, Sr, Ba

(iii) I, Xe, Cs

2.54 Rank the following atoms in (a) increasing atomic size and (b) decreasing first ionization energy, IE1. Use only the periodic table to answer the questions. Check your answer using Figs. 2.10 and 2.11.

(i) Ar, Li, F, O, Cs, C

(ii) Sr, H, Ba, He, Mg, Cs

2.55 The first ionization energies of two atoms with electron configurations (a) 1S²2s²2p⁶ and (b) 1s²2s²2p⁶3s¹ are given to be 2080 kJ/mol and 496 kJ/mol. Determine which IE1 belongs to which electronic structure and justify your answer.

2.56 The first ionization energies of three atoms with electron configurations (a) [He]2s², (b) [Ne]3s¹, (c) [Ar]4s¹, and (d) [He]2s¹ are given to be 496 kJ/mol, 419 kJ/mol, 520 kJ/mol, and 899 kJ/mol. Determine which IE1 belongs to which electronic structure and explain your answer.

2.57 Similar to Fig. 2.15, use (a) orbital diagrams and (b) Lewis symbols to explain the formation of Na⁺ and O²⁻ ions and the corresponding bonding. What is the formula of the compound?

2.58 Calculate the attractive force (●→●←●) between a pair of Ba²⁺ and S²⁻ ions that just touch each other. Assume the ionic radius of the Ba²⁺ ion to be 0.143 nm and that of the S²⁻ ion to be 0.174 nm.

2.59 Calculate the net potential energy for a Ba²⁺ S²⁻ ion pair by using the *b* constant calculated from Prob. 2.58. Assume *n* = 10.5.

2.60 If the attractive force between a pair of Cs⁺ and I⁻ ions is 2.83×10^{-9} N and the ionic radius of the Cs⁺ ion is 0.165 nm, calculate the ionic radius of the I⁻ ion in nanometers.

2.61 For the each pair of bonds presented below, determine which has the higher lattice energy (more negative). Explain your answer. Also, which of the five ionic

compounds do you think has the highest melting temperature and why? Verify your answer.

- (a) LiCl and CsCl
- (b) CsCl and RbCl
- (c) LiF and MgO
- (d) MgO and CaO

2.62 (a) Calculate the lattice energy for the formation of solid NaF if the following information is given. (b) What does the calculated lattice energy tell you about the material?

109 kJ is required to convert solid Na to gaseous Na

243 kJ is required to convert gaseous F₂ to two monatomic F atoms

496 kJ is required to remove the 3s¹ electron of Na (form Na⁺ cation)

−349 kJ of energy (energy is released) to add an electron to the F (form Na[−] anion)

−411 kJ of energy to form gaseous NaF (heat of formation of NaF)

2.63 Calculate the lattice energy for the formation of solid NaCl if the following information is given. What does the calculated lattice energy tell you about the material?

(i) 109 kJ is required to convert solid Na to gaseous Na

(ii) 121 kJ is required to convert gaseous Cl₂ to two monatomic Cl atoms

(iii) 496 kJ is required to remove the 3s¹ electron of Na (form Na⁺ cation)

(iv) −570 kJ of energy (energy is released) to add an electron to the Cl

(v) −610 kJ of energy to form gaseous NaCl (heat of formation of NaCl)

2.64 For each bond in the following series of bonds, determine the bond order, rank bond length, and rank bond strength. Use only the periodic table. Explain your answers.

(a) S–F; S–Br; S–Cl

(b) C–C; C=C; C≡C

2.65 Rank the following covalently bonded atoms according to the degree of polarity: C–N; C–C; C–H; C–Br.

2.66 List the number of atoms bonded to a C atom that exhibits sp³, sp², and sp hybridization. For each, give the geometrical arrangement of the atoms in the molecule.

2.67 Is there a correlation between the electron configurations of the elements scandium ($Z = 21$) through copper ($Z = 29$) and their melting points? (See Table 2.7.)

2.68 Compare the percentage ionic character in the semiconducting compounds CdTe and InP.

Synthesis and Evaluation Problems

2.69 ^{39}K , ^{40}K , and ^{41}K are the three isotopes of potassium. If ^{40}K has the lowest abundance, which other isotope has the highest?

2.70 Most modern *scanning electron microscopes* (SEMs) are equipped with energy-dispersive X-ray detectors for the purpose of chemical analysis of the specimens. This X-ray analysis is a natural extension of the capability of the SEM because the electrons that are used to form the image are also capable of creating characteristic X-rays in the sample. When the electron beam hits the specimen, X-rays specific to the elements in the specimen are created. These can be detected and used to deduce

the composition of the specimen from the well-known wavelengths of the characteristic X-rays of the elements. For example:

Element	Wavelength of K _{α} X-Rays
Cr	0.2291 nm
Mn	0.2103 nm
Fe	0.1937 nm
Co	0.1790 nm
Ni	0.1659 nm
Cu	0.1542 nm
Zn	0.1436 nm

Suppose a metallic alloy is examined in an SEM and three different X-ray energies are detected. If the three energies are 7492, 5426, and 6417 eV, what elements are present in the sample? What would you call such an alloy? (Look ahead to Chap. 9 in the textbook.)

- 2.71 According to Sec. 2.5.1, in order to form monatomic ions from metals and nonmetals, energy must be added. However, we know that primary bonds form because the involved atoms want to lower their energies. Why then do ionic compounds form?
- 2.72 Of the noble gases Ne, Ar, Kr, and Xe, which should be the most chemically reactive?
- 2.73 The melt temperature of Na is 89°C and is higher than the melt temperature of K (63.5°C). Can you explain this in terms of the differences in electronic structure?
- 2.74 The melt temperature of Li (180°C) is significantly lower than the melt temperature of its neighbor Be (1287°C). Can you explain this in terms of the differences in electronic structure?
- 2.75 The melting point of the metal potassium is 63.5°C, while that of titanium is 1660°C. What explanation can be given for this great difference in melting temperatures?
- 2.76 Cartridge brass is an alloy of two metals: 70 wt% copper and 30 wt% zinc. Discuss the nature of the bonds between copper and zinc in this alloy.
- 2.77 After ionization, why is the sodium ion smaller than the sodium atom? After ionization, why is the chloride ion larger than the chlorine atom?
- 2.78 Regardless of the type of primary bond, why does the tendency exist for atoms to bond?
- 2.79 Pure aluminum is a ductile metal with low tensile strength and hardness. Its oxide Al₂O₃ (alumina) is extremely strong, hard, and brittle. Can you explain this difference from an atomic bonding point of view?
- 2.80 Graphite and diamond are both made from carbon atoms. (a) List some of the physical characteristics of each. (b) Give one application for graphite and one for diamond. (c) If both materials are made of carbon, why does such a difference in properties exist?
- 2.81 Silicon is extensively used in the manufacture of integrated circuit devices such as transistors and light-emitting diodes. It is often necessary to develop a thin oxide layer (SiO₂) on silicon wafers. (a) What are the differences in properties between the silicon substrate and the oxide layer? (b) Design a process that produces the oxide layer on a silicon wafer. (c) Design a process that forms the oxide layer only in certain desired areas.

- 2.82** How can the high electrical and thermal conductivities of metals be explained by the “electron gas” model of metallic bonding? Ductility?
- 2.83** Describe fluctuating dipole bonding among the atoms of the noble gas neon. Of a choice between the noble gases krypton and xenon, which noble gas would be expected to have the strongest dipole bonding, and why?
- 2.84** Carbon tetrachloride (CCl_4) has a zero dipole moment. What does this tell us about the C–Cl bonding arrangement in this molecule?
- 2.85** Methane (CH_4) has a much lower boiling temperature than does water (H_2O). Explain why this is true in terms of the bonding between molecules in each of these two substances.
- 2.86** For each of the following compounds, state whether the bonding is essentially metallic, covalent, ionic, van der Waals, or hydrogen: (a) Ni, (b) ZrO_2 , (c) graphite, (d) solid Kr, (e) Si, (f) BN, (g) SiC, (h) Fe_2O_3 , (i) MgO , (j) W, (k) H_2O within the molecules, (l) H_2O between the molecules. If ionic and covalent bonding are involved in the bonding of any of the compounds listed, calculate the percentage ionic character in the compound.
- 2.87** In the manufacturing of a lightbulb, the bulb is evacuated of air and then filled with argon gas. What is the purpose of this?
- 2.88** Stainless steel is a corrosion-resistant metal because it contains large amounts of chromium. How does chromium protect the metal from corrosion? Hint: Chromium reacts with oxygen.
- 2.89** Robots are used in auto industries to weld two components at specific locations. Clearly, the end position of the arm must be determined accurately in order to weld the components at a precise position. (a) In selecting the material for the arms of such robots, what factors must be considered? (b) Select a proper material for this application.
- 2.90** A certain application requires a material that is lightweight, an electrical insulator, and has some flexibility. (a) Which class of materials would you search for this selection? (b) Explain your answer from a bonding point of view.
- 2.91** A certain application requires a material that is electrically nonconductive (insulator), extremely stiff, and lightweight. (a) Which classes of materials would you search for this selection? (b) Explain your answer from a bonding point of view.
- 2.92** Solid potassium and solid calcium have densities 0.862 gr/cm^3 and 1.554 g/cm^3 . Compare the mass of individual potassium and calcium atoms; what is your observation? How do you explain the difference in the solid density between the two elements?

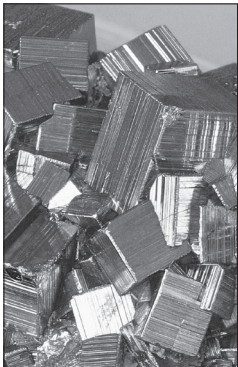
3

CHAPTER

Crystal and Amorphous Structure in Materials



(a)



(b)



(c)



(d)



(e)

((a) © McGraw-Hill Education; (b) © Doug Sherman/Geofile; (c) © Zadiraka Evgenii/Shutterstock; (d) © Getty Images/iStockphoto; (e) Source: James St. John)

Solids may be categorized broadly into crystalline and amorphous solids. Crystalline solids, due to orderly structure of their atoms, molecules, or ions, possess well-defined shapes. Metals are crystalline and are composed of well-defined crystals or grains. The grains are small and are not clearly observable due to the opaque nature of metals. In minerals, mostly translucent to transparent in nature, the well-defined crystalline shapes are clearly observable. The following images show the crystalline nature of minerals such as (a) celestite (SrSO_4) with a sky blue or celestial color, (b) pyrite (FeS_2), also called “fool’s gold” due to its brassy yellow color, (c) amethyst (SiO_2), a purple variety of quartz, and (d) halite (NaCl), better known as rock salt. In contrast, amorphous solids have poor or no long-range order and do not solidify with the symmetry and regularity of crystalline solids. As an example, the amorphous structure of hyalite opal or glass opal is shown in Figure e. Note the lack of symmetry and of sharp and well-defined crystal edges. ■

LEARNING OBJECTIVES

By the end of this chapter, students will be able to

1. Describe what crystalline and noncrystalline (amorphous) materials are.
2. Learn how atoms and ions in solids are arranged in space and identify the basic building blocks of solids.
3. Describe the difference between atomic structure and crystal structure for solid material.
4. Distinguish between crystal structure and crystal system.
5. Explain why plastics cannot be 100 percent crystalline in structure.

6. Explain polymorphism or allotropy in materials.
7. Compute the densities for metals having body-centered and face-centered cubic structures.
8. Describe how to use the X-ray diffraction method for material characterization.
9. Write the designation for atom position, direction indices, and Miller indices for cubic crystals. Specify what are the three densely packed structures for most metals. Determine Miller-Bravais indices for hexagonal close-packed structure. Be able to draw directions and planes in cubic and hexagonal crystals.

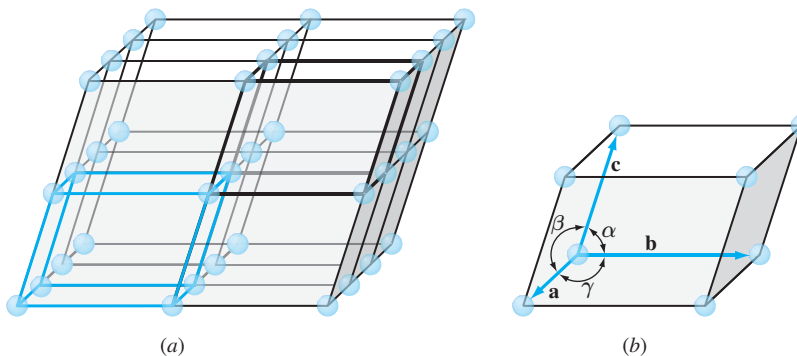
3.1 THE SPACE LATTICE AND UNIT CELLS

The physical structure of solid materials of engineering importance depends mainly on the arrangements of the atoms, ions, or molecules that make up the solid and the bonding forces between them. If the atoms or ions of a solid are arranged in a pattern that repeats itself in three dimensions, they form a solid that has *long-range order* (LRO) and is referred to as a *crystalline solid* or *crystalline material*. Examples of crystalline materials are metals, alloys, and some ceramic materials. In contrast to crystalline materials, there are some materials whose atoms and ions are not arranged in a long-range, periodic, and repeatable manner and possess only *short-range order* (SRO). This means that order exists only in the immediate neighborhood of an atom or a molecule. As an example, liquid water has short-range order in its molecules in which one oxygen atom is covalently bonded to two hydrogen atoms. But this order disappears as each molecule is bonded to other molecules through weak secondary bonds in a random manner. Materials with only short-range order are classified as *amorphous* (without form) or noncrystalline. A more detailed definition and some examples of amorphous materials are given in Section 3.12.

Atomic arrangements in crystalline solids can be described by referring the atoms to the points of intersection of a network of lines in three dimensions. Such a network is called a **space lattice** (Fig. 3.1a), and it can be described as an infinite three-dimensional array of points. Each point in the space lattice has identical surroundings.



Animation
Tutorial

**Figure 3.1**

(a) Space lattice of ideal crystalline solid. (b) Unit cell showing lattice constants.

In an ideal **crystal**, the grouping of **lattice points** about any given point are identical with the grouping about any other lattice point in the crystal lattice. Each space lattice can thus be described by specifying the atom positions in a repeating **unit cell**, such as the one heavily outlined in Figure 3.1a. The unit cell may be considered the smallest subdivision of the lattice that maintains the characteristics of the overall crystal. A group of atoms organized in a certain arrangement relative to each other and associated with lattice points constitutes the **motif** or basis. The crystal structure may then be defined as the collection of lattice and basis. It is important to note that atoms do not necessarily coincide with lattice points. The size and shape of the unit cell can be described by three lattice vectors \mathbf{a} , \mathbf{b} , and \mathbf{c} , originating from one corner of the unit cell (Fig. 3.1b). The axial lengths a , b , and c and the interaxial angles α , β , and γ are the *lattice constants* of the unit cell.

3.2 CRYSTAL SYSTEMS AND BRAVAIS LATTICES

By assigning specific values for axial lengths and interaxial angles, unit cells of different types can be constructed. Crystallographers have shown that only seven different types of unit cells are necessary to create all space lattices. These crystal systems are listed in Table 3.1.



Many of the seven crystal systems have variations of the basic unit cell. A.J. Bravais¹ showed that 14 standard unit cells could describe all possible lattice networks. These Bravais lattices are illustrated in Figure 3.2. There are four basic types of unit cells: (1) simple, (2) body-centered, (3) face-centered, and (4) base-centered.

¹ August Bravais (1811–1863). French crystallographer who derived the 14 possible arrangements of points in space.

Table 3.1 Classification of space lattices by crystal system

Crystal System	Axial Lengths and Interaxial Angles	Space Lattice
Cubic	Three equal axes at right angles $a = b = c, \alpha = \beta = \gamma = 90^\circ$	Simple cubic Body-centered cubic Face-centered cubic
Tetragonal	Three axes at right angles, two equal $a = b \neq c, \alpha = \beta = \gamma = 90^\circ$	Simple tetragonal Body-centered tetragonal
Orthorhombic	Three unequal axes at right angles $a \neq b \neq c, \alpha = \beta = \gamma = 90^\circ$	Simple orthorhombic Body-centered orthorhombic Base-centered orthorhombic Face-centered orthorhombic
Rhombohedral	Three equal axes, equally inclined $a = b = c, \alpha = \beta = \gamma \neq 90^\circ$	Simple rhombohedral
Hexagonal	Two equal axes at 120° , third axis at right angles $a = b \neq c, \alpha = \beta = 90^\circ, \gamma = 120^\circ$	Simple hexagonal
Monoclinic	Three unequal axes, one pair not at right angles $a \neq b \neq c, \alpha = \gamma = 90^\circ \neq b$	Simple monoclinic Base-centered monoclinic
Triclinic	Three unequal axes, unequally inclined and none at right angles $a \neq b \neq c, \alpha \neq \beta \neq \gamma \neq 90^\circ$	Simple triclinic

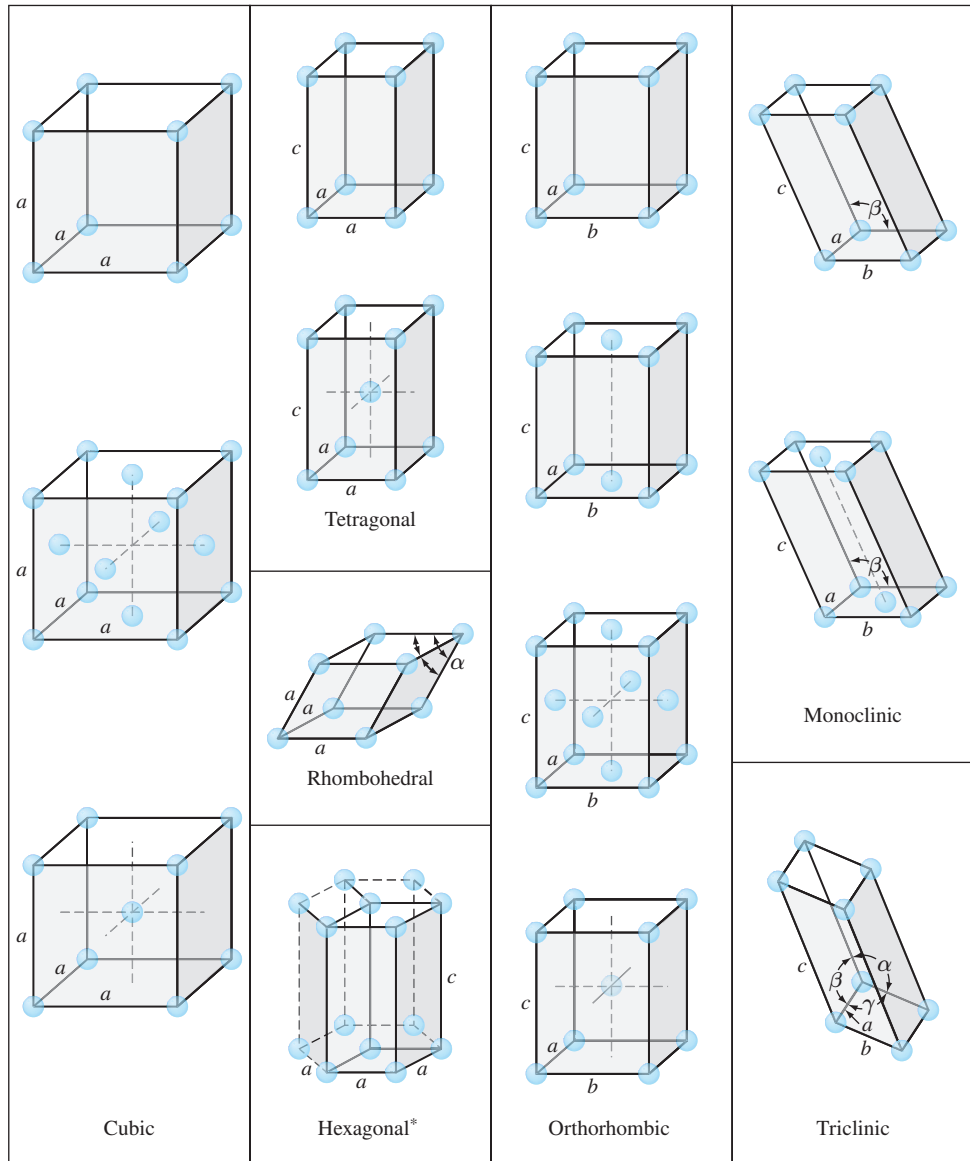
In the cubic system there are three types of unit cells: simple cubic, body-centered cubic, and face-centered cubic. In the orthorhombic system all four types are represented. In the tetragonal system there are only two: simple and body-centered. The face-centered tetragonal unit cell appears to be missing but can be constructed from four body-centered tetragonal unit cells. The monoclinic system has simple and base-centered unit cells, and the rhombohedral, hexagonal, and triclinic systems have only one simple type of unit cell.

3.3 PRINCIPAL METALLIC CRYSTAL STRUCTURES

In this chapter, the principal crystal structures of elemental metals will be discussed in detail. Most ionic and covalent materials also possess a crystal structure which will be discussed in detail in Chapter 11.

Most elemental metals (about 90%) crystallize upon solidification into three densely packed crystal structures: **body-centered cubic (BCC)** (Fig. 3.3a), **face-centered cubic (FCC)** (Fig. 3.3b), and **hexagonal close-packed (HCP)** (Fig. 3.3c). The HCP structure is a denser modification of the simple hexagonal crystal structure shown in Figure 3.2. Most metals crystallize in these dense-packed structures because energy is released as the atoms come closer together and bond more tightly with each other. Thus, the densely packed structures are in lower and more stable energy arrangements.

The extremely small size of the unit cells of crystalline metals that are shown in Figure 3.3 should be emphasized. The cube side of the unit cell of body-centered cubic iron, for

**Figure 3.2**

The 14 Bravais conventional unit cells grouped according to crystal system. The dots indicate lattice points that, when located on faces or at corners, are shared by other identical lattice unit cells.

(Source: W.G. Moffatt, G.W. Pearsall, and J. Wulff, *The Structure and Properties of Materials*, vol. 1: "Structure," Wiley, 1964, p. 47.)

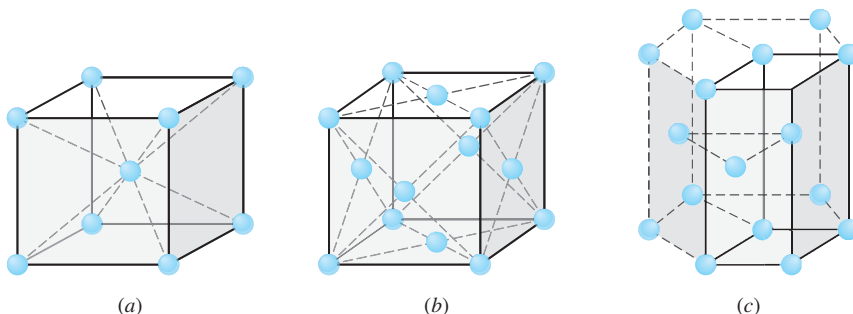


Figure 3.3

Principal metal crystal structure and unit cells: (a) body-centered cubic, (b) face-centered cubic, (c) hexagonal close-packed crystal structure (the unit cell is shown by solid lines).

example, at room temperature is equal to 0.287×10^{-9} m, or 0.287 nanometer (nm).² Therefore, if unit cells of pure iron are lined up side by side, in 1 mm there will be

$$1 \text{ mm} \times \frac{1 \text{ unit cell}}{0.287 \text{ nm} \times 10^{-6} \text{ mm/nm}} = 3.48 \times 10^6 \text{ unit cells!}$$

Let us now examine in detail the arrangement of the atoms in the three principal crystal structure unit cells. Although an approximation, we shall consider atoms in these crystal structures to be hard spheres. The distance between the atoms (interatomic distance) in crystal structures can be determined experimentally by X-ray diffraction analysis.³ For example, the interatomic distance between two neighboring aluminum atoms in a piece of pure aluminum at 20°C is 0.286 nm. The radius of the aluminum atom in the aluminum metal is assumed to be half the interatomic distance, or 0.143 nm. The atomic radii of selected metals are listed in Tables 3.2 to 3.4.

3.3.1 Body-Centered Cubic (BCC) Crystal Structure

First, consider the atomic-site unit cell for the BCC crystal structure shown in Figure 3.4a. In this unit cell, the solid spheres represent the centers where atoms are located and clearly indicate their relative positions. If we represent the atoms in this cell as hard spheres, then the unit cell appears as shown in Figure 3.4b. In this unit cell, we see that the central atom is surrounded by eight nearest neighbors and is said to have a coordination number of 8.



Animation Tutorial

If we isolate a single hard-sphere unit cell, we obtain the model shown in Figure 3.4c. Each of these cells has the equivalent of two atoms per unit cell. One complete atom is located at the center of the unit cell, and an eighth of a sphere (an

² 1 nanometer = 10^{-9} meter.

³ Some of the principles of X-ray diffraction analysis will be studied in Section 3.11.

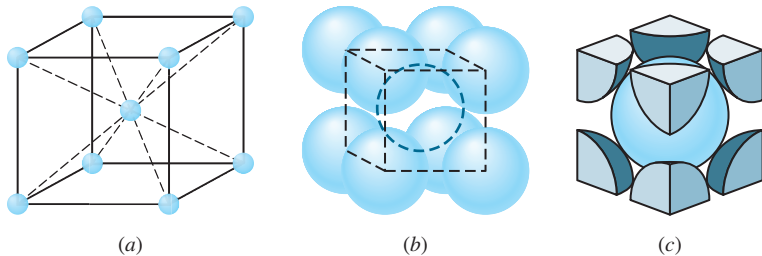


Figure 3.4

BCC unit cells: (a) atomic-site unit cell, (b) hard-sphere unit cell, and (c) isolated unit cell.

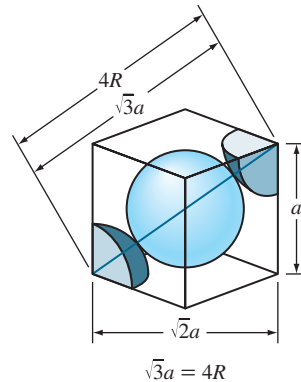


Figure 3.5

BCC unit cell showing relationship between the lattice constant a and the atomic radius R .



Tutorial Animation

octant) is located at each corner of the cell, making the equivalent of another atom. Thus, there is a total of 1 (at the center) + $8 \times \frac{1}{8}$ (at the corners) = 2 atoms per unit cell. The atoms in the BCC unit cell contact each other across the cube diagonal, as indicated in Figure 3.5, so the relationship between the length of the cube side a and the atomic radius R is

$$\sqrt{3}a = 4R \quad \text{or} \quad a = \frac{4R}{\sqrt{3}} \quad (3.1)$$

EXAMPLE PROBLEM 3.1

Iron at 20°C is BCC with atoms of atomic radius 0.124 nm. Calculate the lattice constant a for the cube edge of the iron unit cell.

■ Solution

From Figure 3.5 it is seen that the atoms in the BCC unit cell touch across the cube diagonals. Thus, if a is the length of the cube edge, then

$$\sqrt{3}a = 4R \quad (3.1)$$

where R is the radius of the iron atom. Therefore, considering that three significant digits should be used in all calculations, the answer will be (use three significant digits for $\sqrt{3}$)

$$a = \frac{4R}{\sqrt{3}} = \frac{4(0.124 \text{ nm})}{\sqrt{3}} = 0.287 \text{ nm} \blacktriangleleft$$

use three significant digits

Table 3.2 Selected metals that have the BCC crystal structure at room temperature (20°C) and their lattice constants and atomic radii

Metal	Lattice Constant a (nm)	Atomic Radius R^* (nm)
Chromium	0.289	0.125
Iron	0.287	0.124
Molybdenum	0.315	0.136
Potassium	0.533	0.231
Sodium	0.429	0.186
Tantalum	0.330	0.143
Tungsten	0.316	0.137
Vanadium	0.304	0.132

*Calculated from lattice constants by using Eq. (3.1), $R = \sqrt{3} a/4$.

If the atoms in the BCC unit cell are considered to be spherical, an **atomic packing factor** (APF) can be calculated by using the equation

$$\text{APF} = \frac{\text{volume of atoms in unit cell}}{\text{volume of unit cell}} \quad (3.2)$$

Using this equation, the APF for the BCC unit cell (Fig. 3.4c) is calculated to be 68% (see Example Problem 3.2). That is, 68% of the volume of the BCC unit cell is occupied by atoms and the remaining 32% is empty space. The BCC crystal structure is *not* a close-packed structure since the atoms could be packed closer together. Many metals such as iron, chromium, tungsten, molybdenum, and vanadium have the BCC crystal structure at room temperature. Table 3.2 lists the lattice constants and atomic radii of selected BCC metals.

Calculate the atomic packing factor (APF) for the BCC unit cell, assuming the atoms to be hard spheres.

**EXAMPLE
PROBLEM 3.2**

■ **Solution**

$$\text{APF} = \frac{\text{volume of atoms in BCC unit cell}}{\text{volume of BCC unit cell}} \quad (3.2)$$

Since there are two atoms per BCC unit cell, the volume of atoms in the unit cell of radius R is

$$V_{\text{atoms}} = (2) \left(\frac{4}{3} \pi R^3 \right) = 8.373 R^3$$

The volume of the BCC unit cell is

$$V_{\text{unit cell}} = a^3$$



Tutorial

where a is the lattice constant. The relationship between a and R is obtained from Figure 3.5, which shows that the atoms in the BCC unit cell touch each other across the cubic diagonal. Thus,

$$\sqrt{3}a = 4R \quad \text{or} \quad a = \frac{4R}{\sqrt{3}} \quad (3.1)$$

Thus,

$$V_{\text{unit cell}} = a^3 = 12.32R^3$$

The atomic packing factor for the BCC unit cell is, therefore,

$$\text{APF} = \frac{V_{\text{atoms}}/\text{unit cell}}{V_{\text{unit cell}}} = \frac{8.373R^3}{12.32R^3} = 0.6796 \approx 0.68 \blacktriangleleft$$

3.3.2 Face-Centered Cubic (FCC) Crystal Structure

Consider next the FCC lattice-point unit cell of Figure 3.6a. In this unit cell, there is one lattice point at each corner of the cube and one at the center of each cube face. The hard-sphere model of Figure 3.6b indicates that the atoms in the FCC crystal structure are packed as close together as possible, and are thus called a close-packed structure. The APF for this close-packed structure is 0.74 as compared to 0.68 for the BCC structure, which is not close-packed.

The FCC unit cell as shown in Figure 3.6c has the equivalent of four atoms per unit cell. The eight corner octants account for one atom ($8 \times \frac{1}{8} = 1$), and the six half-atoms on the cube faces contribute another three atoms, making a total of four atoms per unit cell. The atoms in the FCC unit cell contact each other across the cubic face diagonal, as indicated in Figure 3.7, so the relationship between the length of the cube side a and the atomic radius R is

$$\sqrt{2}a = 4R \quad \text{or} \quad a = \frac{4R}{\sqrt{2}} \quad (3.3)$$

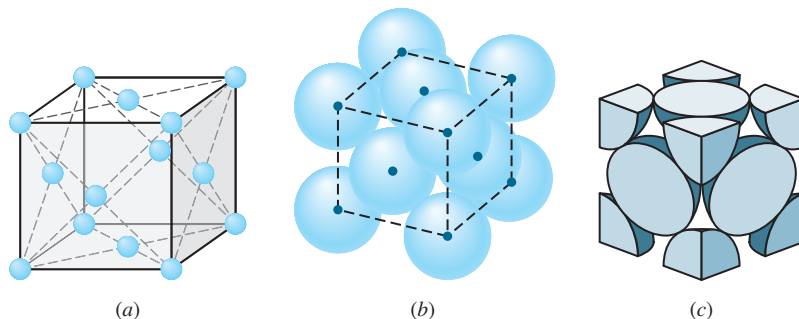
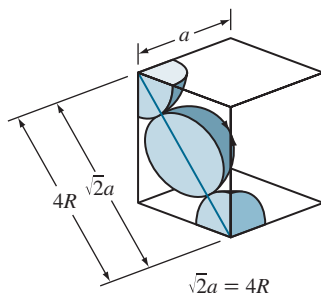


Figure 3.6

FCC unit cells: (a) atomic-site unit cell, (b) hard-sphere unit cell, and (c) isolated unit cell.

**Figure 3.7**

FCC unit cell showing relationship between the lattice constant a and atomic radius R . Since the atoms touch across the face diagonals, $\sqrt{2}a = 4R$.



[Tutorial
Animation](#)

The APF for the FCC crystal structure is 0.74, which is greater than the 0.68 factor for the BCC structure. The APF of 0.74 is for the closest packing possible of “spherical atoms.” Many metals such as aluminum, copper, lead, nickel, and iron at elevated temperatures (912°C to 1394°C) crystallize with the FCC crystal structure. Table 3.3 lists the lattice constants and atomic radii for some selected FCC metals.

3.3.3 Hexagonal Close-Packed (HCP) Crystal Structure

The third common metallic crystal structure is the hexagonal close-packed (HCP) structure shown in Figures 3.8a and b. Metals do not crystallize into the simple hexagonal crystal structure shown in Figure 3.2 because the APF is too low. The atoms can attain a lower energy and a more stable condition by forming the HCP structure of Figure 3.8b. The APF of the HCP crystal structure is 0.74, the same as that for the FCC crystal structure since in both structures the atoms are packed as tightly as

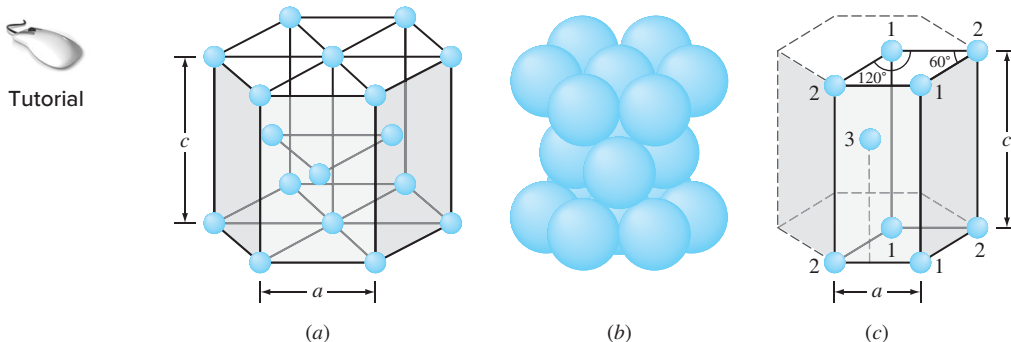
Table 3.3 Selected metals that have the FCC crystal structure at room temperature (20°C) and their lattice constants and atomic radii

Metal	Lattice Constant a (nm)	Atomic Radius R^* (nm)
Aluminum	0.405	0.143
Copper	0.3615	0.128
Gold	0.408	0.144
Lead	0.495	0.175
Nickel	0.352	0.125
Platinum	0.393	0.139
Silver	0.409	0.144



[Tutorial](#)

*Calculated from lattice constants by using Eq. 3.3, $R = \sqrt{2}a/4$.

**Figure 3.8**

HCP crystal structure: (a) schematic of the crystal structure, (b) hard-sphere model, and (c) isolated unit cell schematic.

(Source: F.M. Miller *Chemistry: Structure and Dynamics*, McGraw-Hill, 1984, p. 296.)

possible. In both the HCP and FCC crystal structures, each atom is surrounded by 12 other atoms, and thus both structures have a coordination number of 12. The differences in the atomic packing in FCC and HCP crystal structures will be discussed in Section 3.8.

The isolated HCP unit cell, also called the *primitive cell*, is shown in Figure 3.8c. The atoms at locations marked “1” on Figure 3.8c contribute $\frac{1}{6}$ of an atom to the unit cell. The atoms at locations marked “2” contribute $\frac{1}{12}$ of an atom to the unit cell.

Thus, the atoms at the eight corners of the unit cell collectively contribute one atom $(4 \cdot \frac{1}{6}) + 4(\frac{1}{12}) = 1$. The atom at location “3” is centered inside the unit cell but extends slightly beyond the boundary of the cell. The total number of atoms inside an HCP unit cell is therefore two (one at corners and one at center). In some textbooks the HCP unit cell is represented by Figure 3.8a and is called the “larger cell.” In such a case, one finds six atoms per unit cell. This is mostly for convenience, and the true unit cell is presented in Figure 3.8c by the solid lines. When presenting the topics of crystal directions and planes we will also use the larger cell for convenience, in addition to the primitive cell.

The ratio of the height c of the hexagonal prism of the HCP crystal structure to its basal side a is called the *c/a ratio* (Fig. 3.8a). The *c/a ratio* for an ideal HCP crystal structure consisting of uniform spheres packed as tightly together as possible is 1.633. Table 3.4 lists some important HCP metals and their *c/a* ratios. Of the metals listed, cadmium and zinc have *c/a* ratios higher than the ideal ratio, which indicates that the atoms in these structures are slightly elongated along the c axis of the HCP unit cell. The metals magnesium, cobalt, zirconium, titanium, and beryllium have *c/a* ratios less than the ideal ratio. Therefore, in these metals, the atoms are slightly compressed in the direction along the c axis. Thus, for the HCP metals listed in Table 3.4, there is a certain amount of deviation from the ideal hard-sphere model.

Table 3.4 Selected metals that have the HCP crystal structure at room temperature (20°C) and their lattice constants, atomic radii, and c/a ratios

Metal	Lattice Constants (nm)		Atomic Radius R (nm)	c/a Ratio	% Deviation from Ideality
	a	c			
Cadmium	0.2973	0.5618	0.149	1.890	+15.7
Zinc	0.2665	0.4947	0.133	1.856	+13.6
Ideal HCP				1.633	0
Magnesium	0.3209	0.5209	0.160	1.623	-0.66
Cobalt	0.2507	0.4069	0.125	1.623	-0.66
Zirconium	0.3231	0.5148	0.160	1.593	-2.45
Titanium	0.2950	0.4683	0.147	1.587	-2.81
Beryllium	0.2286	0.3584	0.113	1.568	-3.98

- Calculate the volume of the zinc crystal structure unit cell by using the following data: pure zinc has the HCP crystal structure with lattice constants $a = 0.2665$ nm and $c = 0.4947$ nm.
- Find the volume of the larger cell.

■ Solution

The volume of the zinc HCP unit cell can be obtained by determining the area of the base of the unit cell and then multiplying this by its height (Fig. EP3.3).

- The area of the base of the unit cell is area $ABDC$ of Figure EP3.3a and b. This total area consists of the areas of two equilateral triangles of area ABC of Figure EP3.3b. From Figure EP3.3c,

$$\begin{aligned}\text{Area of triangle } ABC &= \frac{1}{2}(\text{base})(\text{height}) \\ &= \frac{1}{2}(a)(a \sin 60^\circ) = \frac{1}{2}a^2 \sin 60^\circ\end{aligned}$$

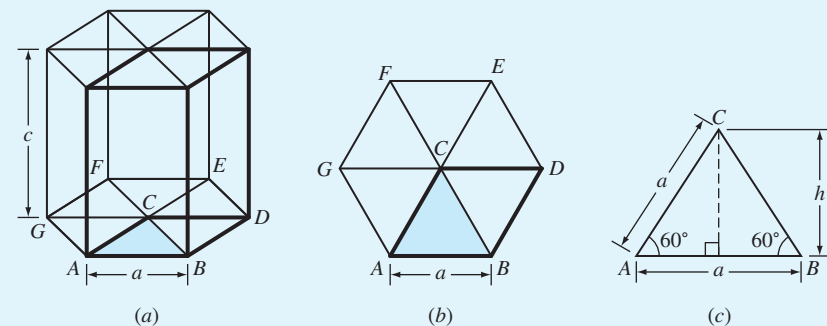
From Figure EP3.3b,

$$\begin{aligned}\text{Total area of HCP base, area } ABDC &= (2)\left(\frac{1}{2}a^2 \sin 60^\circ\right) \\ &= a^2 \sin 60^\circ\end{aligned}$$

From Figure EP3.3a,

$$\begin{aligned}\text{Volume of zinc HCP unit cell} &= (a^2 \sin 60^\circ)(c) \\ &= (0.2665 \text{ nm})^2(0.8660)(0.4947 \text{ nm}) \\ &= 0.03043 \text{ nm}^3 \blacktriangleleft\end{aligned}$$

EXAMPLE PROBLEM 3.3

**Figure EP3.3**

Diagrams for calculating the volume of an HCP unit cell. (a) HCP unit cell.
(b) Base of HCP unit cell. (c) Triangle ABC removed from base of unit cell.

- b. From Figure EP3.3a,

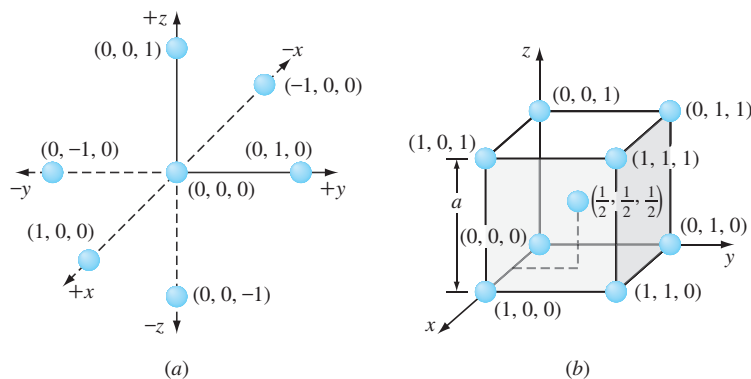
$$\begin{aligned}\text{Volume of "large" zinc HCP cell} &= 3(\text{volume of the unit cell or primitive cell}) \\ &= 3(0.0304) = 0.09130 \text{ nm}^3\end{aligned}$$

3.4 ATOM POSITIONS IN CUBIC UNIT CELLS

To locate atom positions in cubic unit cells, we use rectangular x , y , and z axes. In crystallography, the positive x axis is usually the direction coming out of the paper, the positive y axis is the direction to the right of the paper, and the positive z axis is the direction to the top (Fig. 3.9). Negative directions are opposite to those just described.



Tutorial

**Figure 3.9**

(a) Rectangular x , y , and z axes for locating atom positions in cubic unit cells. (b) Atom positions in a BCC unit cell.

Atom positions in unit cells are located by using unit distances along the x , y , and z axes, as indicated in Fig. 3.9a. For example, the position coordinates for the atoms in the BCC unit cell are shown in Fig. 3.9b. The atom positions for the eight corner atoms of the BCC unit cell are

$$(0, 0, 0) (1, 0, 0) (0, 1, 0) (0, 0, 1) \\ (1, 1, 1) (1, 1, 0) (1, 0, 1) (0, 1, 1)$$

The center atom in the BCC unit cell has the position coordinates $(\frac{1}{2}, \frac{1}{2}, \frac{1}{2})$. For simplicity, sometimes only two atom positions in the BCC unit cell are specified, which are $(0, 0, 0)$ and $(\frac{1}{2}, \frac{1}{2}, \frac{1}{2})$. The remaining atom positions of the BCC unit cell are assumed to be understood. In the same way, the atom positions in the FCC unit cell can be located.

3.5 DIRECTIONS IN CUBIC UNIT CELLS

Often it is necessary to refer to specific directions in crystal lattices. This is especially important for metals and alloys with properties that vary with crystallographic orientation. *For cubic crystals, the crystallographic direction indices are the vector components of the direction resolved along each of the coordinate axes and reduced to the smallest integers.*

To diagrammatically indicate a direction in a cubic unit cell, we draw a direction vector from an origin, which is usually a corner of the cubic cell, until it emerges from the cube surface (Fig. 3.10). The position coordinates of the unit cell where the direction vector emerges from the cube surface after being converted to integers are the direction indices. The direction indices are enclosed by square brackets with no separating commas.

For example, the position coordinates of the direction vector OR in Figure 3.10a where it emerges from the cube surface are $(1, 0, 0)$, and so the direction indices for the direction vector OR are $[100]$. The position coordinates of the direction vector OS (Fig. 3.10a) are $(1, 1, 0)$, and so the direction indices for OS are $[110]$. The position coordinates for the direction vector OT (Fig. 3.10b) are $(1, 1, 1)$, and so the direction indices of OT are $[111]$.

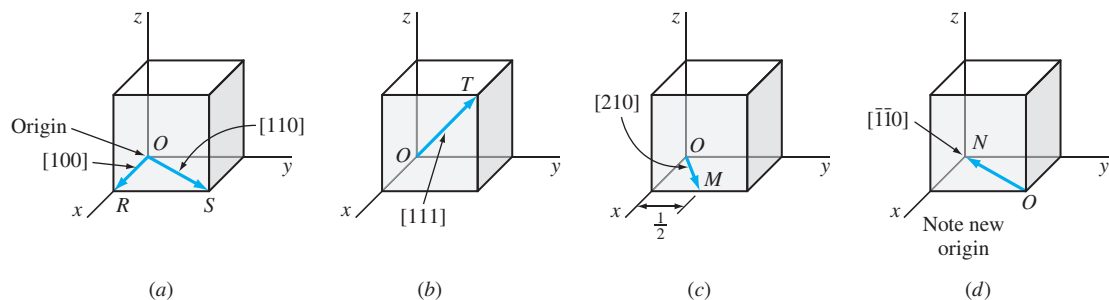


Figure 3.10

Some directions in cubic unit cells.

The position coordinates of the direction vector OM (Fig. 3.10c) are $(1, \frac{1}{2}, 0)$, and since the direction vectors must be integers, these position coordinates must be multiplied by 2 to obtain integers. Thus, the direction indices of OM become $2(1, \frac{1}{2}, 0) = [210]$. The position coordinates of the vector ON (Fig. 3.10d) are $(-1, -1, 0)$. A negative direction index is written with a bar over the index. Thus, the direction indices for the vector ON are $[\bar{1}10]$. Note that to draw the direction ON inside the cube, the origin of the direction vector had to be moved to the front lower-right corner of the unit cube (Fig. 3.10d). Further examples of cubic direction vectors are given in Example Problem 3.4.

Often it is useful to determine the angle between two crystal directions. In addition to geometrical analysis, we can use the definitions of dot product to determine the angles between any two direction vectors. Recall from your knowledge of vectors that

$$\begin{aligned} A \cdot B &= \|A\| \|B\| \cos \theta; A = a_x i + a_y j + a_z k \text{ and } B = b_x i + b_y j + b_z k \\ &\quad \text{also,} \\ A \cdot B &= a_x b_x + a_y b_y + a_z b_z \\ &\quad \text{therefore,} \\ \cos \theta &= \frac{a_x b_x + a_y b_y + a_z b_z}{\|A\| \|B\|} \end{aligned} \tag{3.4}$$

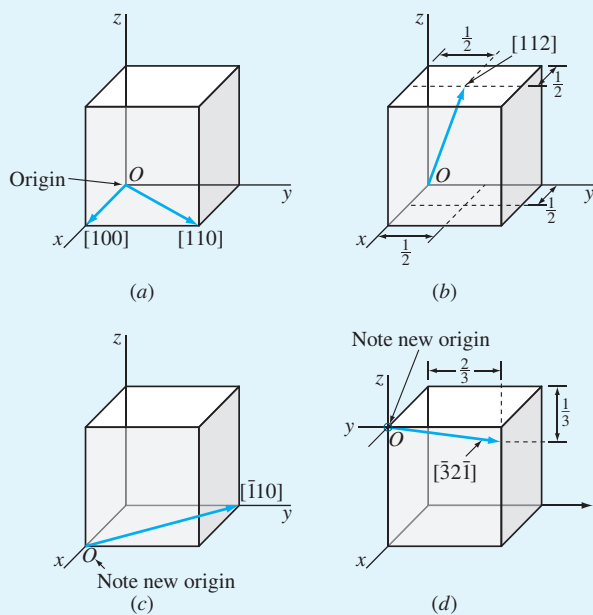
**EXAMPLE
PROBLEM 3.4**

Draw the following direction vectors in cubic unit cells:

- [100] and [110]
- [112]
- [110]
- [321]
- Find the angle between [100] and [110]
- Find the angle between [112] and [110]

■ **Solution**

- The position coordinates for the [100] direction are $(1, 0, 0)$ (Fig. EP3.4a). The position coordinates for the [110] direction are $(1, 1, 0)$ (Fig. EP3.4a).
- The position coordinates for the [112] direction are obtained by dividing the direction indices by 2 so that they will lie within the unit cube. Thus, they are $(\frac{1}{2}, \frac{1}{2}, 1)$ (Fig. EP3.4b).
- The position coordinates for the [110] direction are $(-1, 1, 0)$ (Fig. EP3.4c). Note that the origin for the direction vector must be moved to the lower-left front corner of the cube.
- The position coordinates for the [321] direction are obtained by first dividing all the indices by 3, the largest index. This gives $-1, \frac{2}{3}, -\frac{1}{3}$ for the position coordinates of the exit point of the direction [321], which are shown in Figure EP3.4d.



Tutorial

Figure EP3.4

Direction vectors in cubic unit cells.

- e. The angle between directions [100] and [110] can be determined using Eq. 3.4 as follows:

$$\| \mathbf{A} \| = \sqrt{1^2 + 0^2 + 0^2} = 1$$

$$\| \mathbf{B} \| = \sqrt{1^2 + 1^2 + 0^2} = \sqrt{2}$$

$$\cos \theta = \frac{a_x b_x + a_y b_y + a_z b_z}{\| \mathbf{A} \| \| \mathbf{B} \|} = \frac{(1)(1) + (0)(1) + (0)(0)}{(1)(\sqrt{2})} = \frac{1}{\sqrt{2}}$$

$$\theta = 45^\circ$$

- f. The angle between directions [112] and [110] can be determined using Eq. 3.4 as follows:

$$\| \mathbf{A} \| = \sqrt{1^2 + 1^2 + 2^2} = \sqrt{6}$$

$$\| \mathbf{B} \| = \sqrt{-1^2 + 1^2 + 0^2} = \sqrt{2}$$

$$\cos \theta = \frac{a_x b_x + a_y b_y + a_z b_z}{\| \mathbf{A} \| \| \mathbf{B} \|} = \frac{(1)(-1) + (1)(1) + (2)(0)}{(\sqrt{6})(\sqrt{2})} = \frac{0}{\sqrt{12}}$$

$$\theta = 90^\circ$$

The letters u , v , and w are used in a general sense for the direction indices in the x , y , and z directions, respectively, and are written as $[uvw]$. It is also important to note that *all parallel direction vectors have the same direction indices*.

Directions are said to be *crystallographically equivalent* if the atom spacing along each direction is the same. For example, the following cubic edge directions are crystallographic equivalent directions:

$$[100], [010], [001], [0\bar{1}0], [00\bar{1}], [\bar{1}00] \equiv \langle 100 \rangle$$

Equivalent directions are called *indices of a family or form*. The notation $\langle 100 \rangle$ is used to indicate cubic edge directions collectively. Other directions of a form are the cubic body diagonals $\langle 111 \rangle$ and the cubic face diagonals $\langle 110 \rangle$.

**EXAMPLE
PROBLEM 3.5**


Tutorial

Determine the direction indices of the cubic direction shown in Figure EP3.5a.

Solution

Parallel directions have the same direction indices, and so we move the direction vector in a parallel manner until its tail reaches the nearest corner of the cube, still keeping the vector within the cube. Thus, in this case, the upper-left front corner becomes the new origin for the direction vector (Fig. EP3.5b). We can now determine the position coordinates where the direction vector leaves the unit cube. These are $x = -1$, $y = +1$, and $z = -\frac{1}{6}$. The position coordinates of the direction where it leaves the unit cube are thus $(-1, +1, -\frac{1}{6})$. The direction indices for this direction are, after clearing the fraction $6x$, $(-1, +1, -\frac{1}{6})$, or $[661]$.

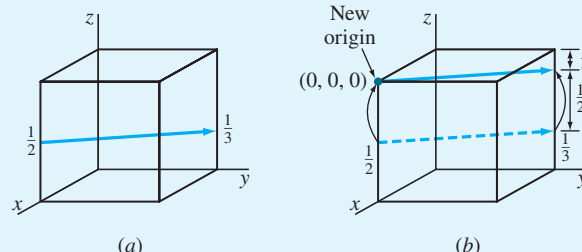


Figure EP3.5

**EXAMPLE
PROBLEM 3.6**

Determine the direction indices of the cubic direction between the position coordinates $(\frac{3}{4}, 0, \frac{1}{4})$ and $(\frac{1}{4}, \frac{1}{2}, \frac{1}{2})$.

Solution

First we locate the origin and termination points of the direction vector in a unit cube, as shown in Figure EP3.6. The fraction vector components for this direction are

$$x = -\left(\frac{3}{4} - \frac{1}{4}\right) = -\frac{1}{2}$$

$$\begin{aligned}y &= \left(\frac{1}{2} - 0\right) = \frac{1}{2} \\&= \left(\frac{1}{2} - \frac{1}{4}\right) = \frac{1}{4}\end{aligned}$$

Thus, the vector direction has fractional vector components of $-\frac{1}{2}, \frac{1}{2}, \frac{1}{4}$. The direction indices will be in the same ratio as their fractional components. By multiplying the fraction vector components by 4, we obtain [221] for the direction indices of this vector direction.

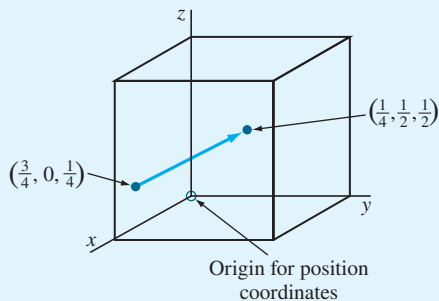


Figure EP3.6

3.6 MILLER INDICES FOR CRYSTALLOGRAPHIC PLANES IN CUBIC UNIT CELLS

Sometimes it is necessary to refer to specific lattice planes of atoms within a crystal structure, or it may be of interest to know the crystallographic orientation of a plane or group of planes in a crystal lattice. To identify crystal planes in cubic crystal structures, the *Miller notation system*⁴ is used. The **Miller indices of a crystal plane** are defined as the *reciprocals of the fractional intercepts (with fractions cleared) that the plane makes with the crystallographic x, y, and z axes of the three nonparallel edges of the cubic unit cell*. The cube edges of the unit cell represent unit lengths, and the intercepts of the lattice planes are measured in terms of these unit lengths.

The procedure for determining the Miller indices for a cubic crystal plane is as follows:

1. Choose a plane that does *not* pass through the origin at (0, 0, 0).
2. Determine the intercepts of the plane in terms of the crystallographic x, y, and z axes for a unit cube. These intercepts may be fractions.



Tutorial

⁴ William Hallowes Miller (1801–1880). English crystallographer who published a “Treatise on Crystallography” in 1839, using crystallographic reference axes that were parallel to the crystal edges and using reciprocal indices.

3. Form the reciprocals of these intercepts.
4. Clear fractions and determine the *smallest* set of whole numbers that are in the same ratio as the intercepts. These whole numbers are the Miller indices of the crystallographic plane and are enclosed in parentheses without the use of commas. The notation (hkl) is used to indicate Miller indices in a general sense, where h , k , and l are the Miller indices of a cubic crystal plane for the x , y , and z axes, respectively.

Figure 3.11 shows three of the most important crystallographic planes of cubic crystal structures. Let us first consider the shaded crystal plane in Figure 3.11a, which has the intercepts $1, \infty, \infty$ for the x , y , and z axes, respectively. We take the reciprocals of these intercepts to obtain the Miller indices, which are therefore $1, 0, 0$. Since these numbers do not involve fractions, the Miller indices for this plane are (100) , which is read as the one-zero-zero plane. Next let us consider the second plane shown in Figure 3.11b. The intercepts of this plane are $1, 1, \infty$. Since the reciprocals of these numbers are $1, 1, 0$, which do not involve fractions, the Miller indices of this plane are (110) . Finally, the third plane (Fig. 3.11c) has the intercepts $1, 1, 1$, which give the Miller indices (111) for this plane.

Consider now the cubic crystal plane shown in Figure 3.12 that has the intercepts $\frac{1}{3}, \frac{2}{3}, 1$. The reciprocals of these intercepts are $3, \frac{3}{2}, 1$. Since fractional intercepts are not allowed, these fractional intercepts must be multiplied by 2 to clear the $\frac{3}{2}$ fraction. Thus, the reciprocal intercepts become $6, 3, 2$, and the Miller indices are (632) . Further examples of cubic crystal planes are shown in Example Problem 3.7.

If the crystal plane being considered passes through the origin so that one or more intercepts are zero, the plane must be moved to an equivalent position in the same unit cell, and the plane must remain parallel to the original plane. This is possible because all equispaced parallel planes are indicated by the same Miller indices.

If sets of equivalent lattice planes are related by the symmetry of the crystal system, they are called *planes of a family or form*, and the indices of one plane of the family are enclosed in braces as $\{hkl\}$ to represent the indices of a family of symmetrical planes. For example, the Miller indices of the cubic surface planes (100) , (010) , and (001) are designated collectively as a family or form by the notation $\{100\}$.

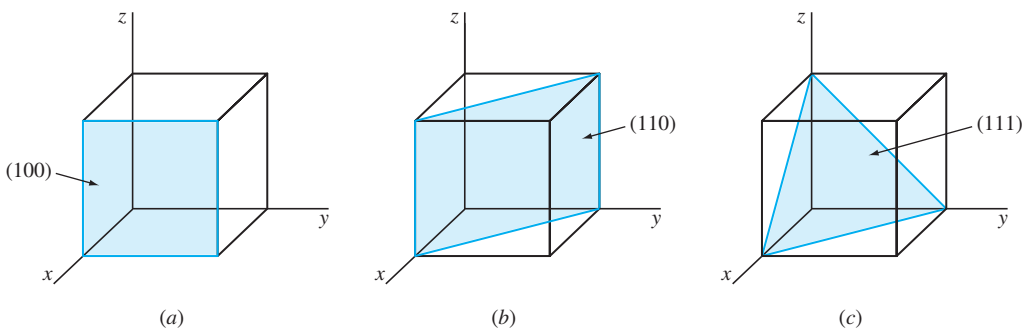


Figure 3.11

Miller indices of some important cubic crystal planes: (a) (100) , (b) (110) , and (c) (111) .



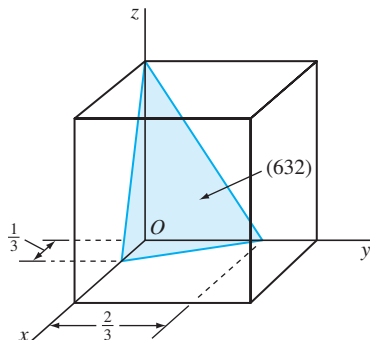


Figure 3.12
Cubic crystal plane (632), which
has fractional intercepts.

Draw the following crystallographic planes in cubic unit cells:

- (101)
- (110)
- (221)
- Draw a (110) plane in a BCC atomic-site unit cell, and list the position coordinates of the atoms whose centers are intersected by this plane.

**EXAMPLE
PROBLEM 3.7**

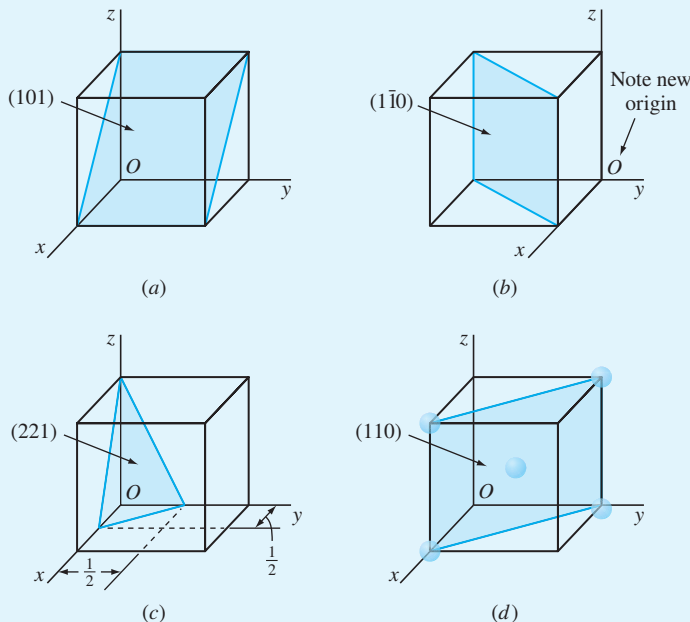


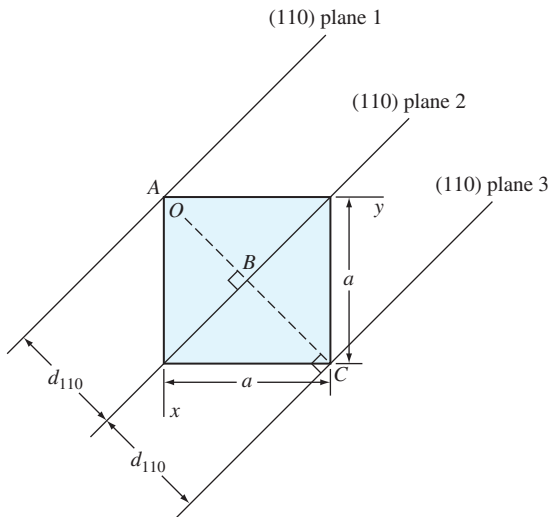
Figure EP3.7
Various important cubic crystal planes.

Solution

- First determine the reciprocals of the Miller indices of the (101) plane. These are 1, ∞ , 1. The (101) plane must pass through a unit cube at intercepts $x = 1$ and $z = 1$ and be parallel to the y axis (Fig. EP3.7a).
- First determine the reciprocals of the Miller indices of the (110) plane. These are 1, -1, ∞ . The (110) plane must pass through a unit cube at intercepts $x = 1$ and $y = -1$ and be parallel to the z axis. Note that the origin of axes must be moved to the lower-right back side of the cube (Fig. EP3.7b).
- First determine the reciprocals of the Miller indices of the (221) plane. These are $\frac{1}{2}, \frac{1}{2}, 1$. The (221) plane must pass through a unit cube at intercepts $x = \frac{1}{2}$, $y = \frac{1}{2}$, and $z = 1$ (Fig. EP3.7c).
- Atom positions whose centers are intersected by the (110) plane are (1, 0, 0), (0, 1, 0), (1, 0, 1), (0, 1, 1), and $(\frac{1}{2}, \frac{1}{2}, \frac{1}{2})$. These positions are indicated by the solid circles (Fig. EP3.7d).

An important relationship for the cubic system, and *only the cubic system*, is that the direction indices of a direction *perpendicular* to a crystal plane are the same as the Miller indices of that plane. For example, the [100] direction is perpendicular to the (100) crystal plane.

In cubic crystal structures, the *interplanar spacing* between two closest parallel planes with the same Miller indices is designated d_{hkl} where h , k , and l are the Miller indices of the planes. This spacing represents the distance from a selected origin containing one plane and another parallel plane with the same indices that is closest to it. For example, the distance between (110) planes 1 and 2, d_{110} , in Figure 3.13 is AB .

**Figure 3.13**

Top view of cubic unit cell showing the distance between (110) crystal planes, d_{110} .

Also, the distance between (110) planes 2 and 3 is d_{110} and is length BC in Figure 3.13. From simple geometry, it can be shown that for cubic crystal structures

$$d_{hkl} = \frac{a}{\sqrt{h^2 + k^2 + l^2}} \quad (3.5)$$

where d_{hkl} = interplanar spacing between parallel closest planes with

Miller indices h , k , and l

a = lattice constant (edge of unit cube)

h , k , l = Miller indices of cubic planes being considered

**EXAMPLE
PROBLEM 3.8**

Determine the Miller indices of the cubic crystallographic plane shown in Figure EP3.8a.

Solution

First, transpose the plane parallel to the z axis $\frac{1}{4}$ unit to the right along the y axis as shown in Figure EP3.8b so that the plane intersects the x axis at a unit distance from the new origin located at the lower-right back corner of the cube. The new intercepts of the transposed plane with the coordinate axes are now $(+1, -\frac{5}{12}, \infty)$. Next, we take the reciprocals of these intercepts to give $(1, -\frac{12}{5}, 0)$. Finally, we clear the $\frac{12}{5}$ fraction to obtain (5120) for the Miller indices of this plane.

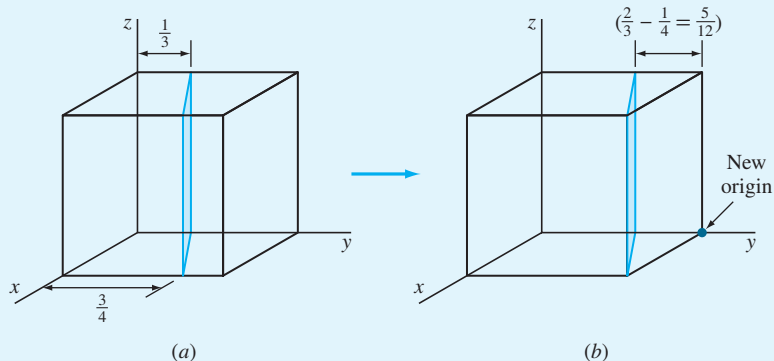


Figure EP3.8

**EXAMPLE
PROBLEM 3.9**

Determine the Miller indices of the cubic crystal plane that intersects the position coordinates $(1, \frac{1}{4}, 0)$, $(1, 1, \frac{1}{2})$, $(\frac{3}{4}, 1, \frac{1}{4})$, and all coordinate axes.

Solution

First, we locate the three position coordinates as indicated in Figure EP3.9 at A , B , and C . Next, we join A and B , extend AB to D , and then join A and C . Finally, we join A to C to complete plane ACD . The origin for this plane in the cube can be chosen at E , which gives

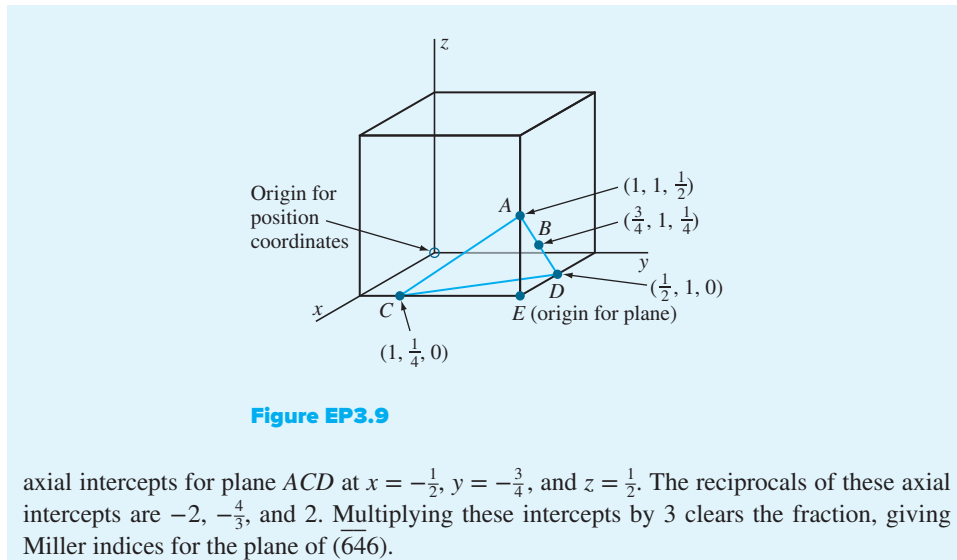


Figure EP3.9

axial intercepts for plane ACD at $x = -\frac{1}{2}$, $y = -\frac{3}{4}$, and $z = \frac{1}{2}$. The reciprocals of these axial intercepts are -2 , $-\frac{4}{3}$, and 2 . Multiplying these intercepts by 3 clears the fraction, giving Miller indices for the plane of (646) .

EXAMPLE**PROBLEM 3.10**

Copper has an FCC crystal structure and a unit cell with a lattice constant of 0.361 nm . What is its interplanar spacing d_{220} ?

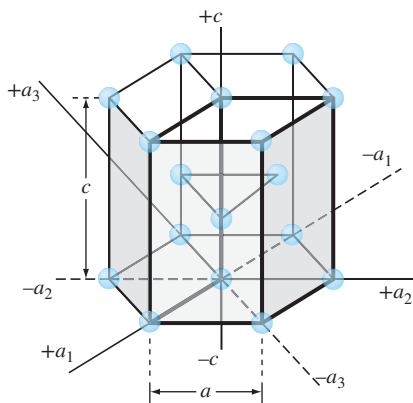
Solution

$$d_{hkl} = \frac{a}{\sqrt{h^2 + k^2 + l^2}} = \frac{0.361\text{ nm}}{\sqrt{(2)^2 + (2)^2 + (0)^2}} = 0.128\text{ nm} \blacktriangleleft$$

3.7 CRYSTALLOGRAPHIC PLANES AND DIRECTIONS IN HEXAGONAL CRYSTAL STRUCTURE

3.7.1 Indices for Crystal Planes in HCP Unit Cells

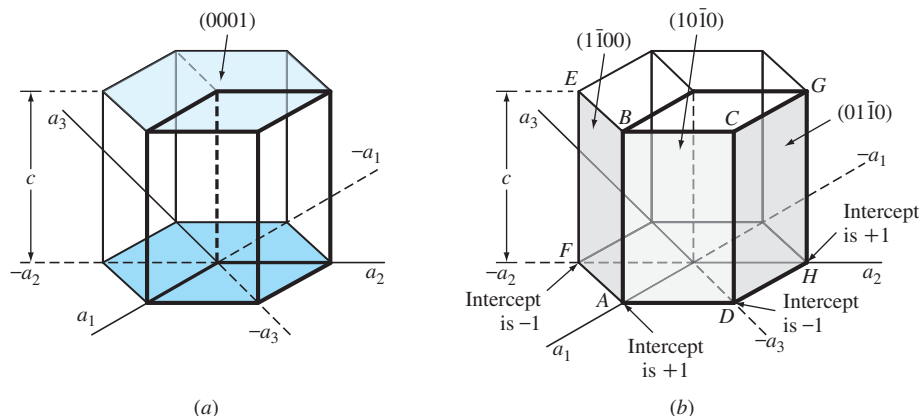
Crystal planes in HCP unit cells are commonly identified by using four indices instead of three. The HCP crystal plane indices, called *Miller-Bravais indices*, are denoted by the letters h , k , i , and l and are enclosed in parentheses as $(hkil)$. These four-digit hexagonal indices are based on a coordinate system with four axes, as shown in Figure 3.14 in an HCP unit cell. There are three basal axes, a_1 , a_2 , and a_3 , which make 120° with each other. The fourth axis or c axis is the vertical axis located at the center of the unit cell. The a unit of measurement along the a_1 , a_2 , and a_3 axes is the distance between the atoms along these axes and is indicated in Figure 3.14. In the discussion of HCP planes and directions, we will use both the “unit cell” and the “larger cell” for the presentation of concepts. The unit of measurement along the c axis is the height of the unit cell. The reciprocals of the intercepts that a crystal plane makes with the a_1 , a_2 ,

**Figure 3.14**

The four coordinate axes (a_1 , a_2 , a_3 , and c) of the HCP crystal structure.

and a_3 axes give the h , k , and i indices, while the reciprocal of the intercept with the c axis gives the l index.

Basal Planes The basal planes of the HCP unit cell are very important planes for this unit cell and are indicated in Figure 3.15a. Since the basal plane on the top of the HCP unit cell in Figure 3.15a is parallel to the a_1 , a_2 , and a_3 axes, the intercepts of this plane with these axes will be at infinity. Thus, $a_{1\text{intercept}} = \infty$, $a_{2\text{intercept}} = \infty$, and $a_{3\text{intercept}} = \infty$. The c axis, however, is unity since the top basal plane intersects the c axis at unit distance, $c_{\text{intercept}} = 1$. Taking the reciprocals of these intercepts gives the Miller-Bravais indices for the HCP basal plane. Thus $h = 0$, $k = 0$, $i = 0$, and $l = 1$. The HCP basal plane is, therefore, a zero-zero-zero-one or (0001) plane.

**Figure 3.15**

Miller-Bravais indices of hexagonal crystal planes: (a) basal planes and (b) prism planes.

Prism Planes Using the same method, the intercepts of the front prism plane ($ABCD$) of Figure 3.15b are $a_{1\text{intercept}} = +1$, $a_{2\text{intercept}} = \infty$, $a_{3\text{intercept}} = -1$, and $c_{\text{intercept}} = \infty$. Taking the reciprocals of these intercepts gives $h = 1$, $k = 0$, $i = -1$, and $l = 0$, or the (1010) plane. Similarly, the $ABEF$ prism plane of Figure 3.15b has the indices (1100) and the $DCGH$ plane the indices (0110) . All HCP prism planes can be identified collectively as the $\{1010\}$ family of planes.

Sometimes HCP planes are identified only by three indices (hkl) since $h + k = -i$. However, the $(hkil)$ indices are used more commonly because they reveal the hexagonal symmetry of the HCP unit cell.

3.7.2 Direction Indices in HCP Unit Cells⁵

Directions in HCP unit cells are also usually indicated by four indices u , v , t , and w enclosed by square brackets as $[uvwxyz]$. The u , v , and t indices are lattice vectors in the a_1 , a_2 , and a_3 directions, respectively (Fig. 3.16), and the w index is a lattice vector in the c direction. To maintain uniformity for both HCP indices for planes and directions, it has been agreed that $u + v = -t$ for directions.

Let us now determine the Miller-Bravais hexagonal indices for the directions a_1 , a_2 , and a_3 , which are the positive basal axes of the hexagonal unit cell. The a_1 direction indices are given in Figure 3.16a, the a_2 direction indices in Figure 3.16b, and the a_3 direction indices in Figure 3.16c. If we need to indicate a c direction also for the a_3 direction, this is shown in Figure 3.16d. Figure 3.16e summarizes the positive and negative directions on the upper basal plane of the simple hexagonal crystal structure.

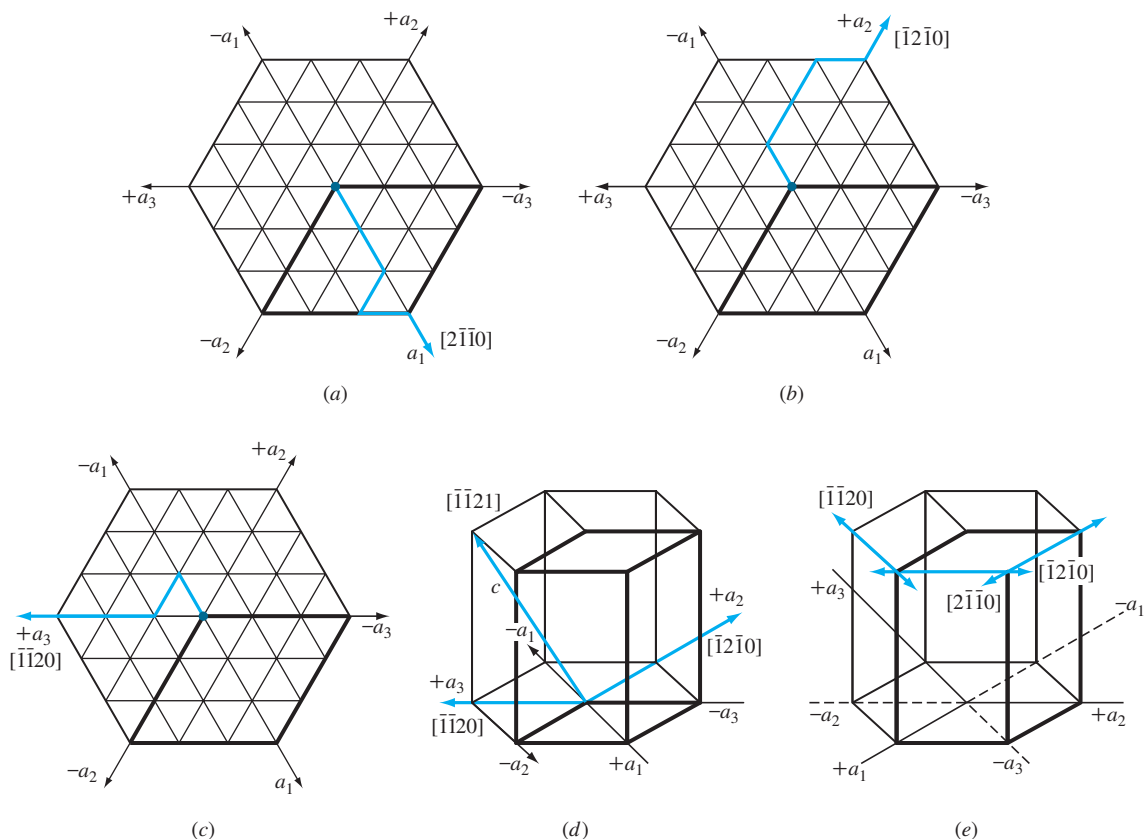
3.8 COMPARISON OF FCC, HCP, AND BCC CRYSTAL STRUCTURES

3.8.1 FCC and HCP Crystal Structures

As previously pointed out, both the HCP and FCC crystal structures are close-packed structures. That is, their atoms, which are considered approximate “spheres,” are packed together as closely as possible so that an atomic packing factor of 0.74 is attained.⁶ The (111) planes of the FCC crystal structure shown in Figure 3.17a have a packing arrangement identical to the (0001) planes of the HCP crystal structure shown in Figure 3.17b. However, the three-dimensional FCC and HCP crystal structures are not identical because there is a difference in the stacking arrangement of their atomic planes, which can best be described by considering the stacking of hard spheres representing atoms. As a useful analogy, one can imagine the stacking of planes of equal-sized marbles on top of each other, minimizing the space between the marbles.

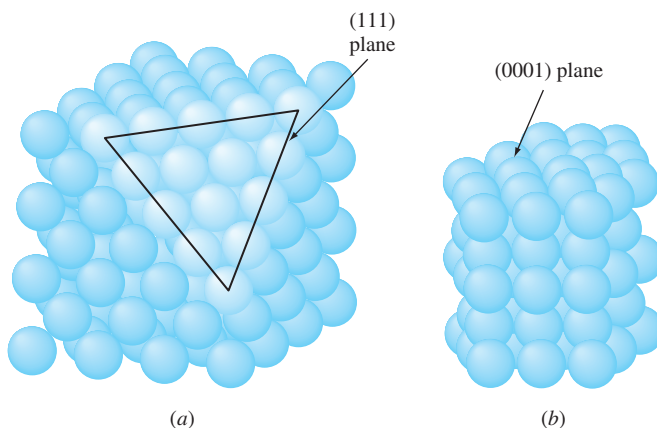
⁵ The topic of direction indices for hexagonal unit cells is not normally presented in an introductory course in materials but is included here for advanced students.

⁶ As pointed out in Section 3.3, the atoms in the HCP structure deviate to varying degrees from ideality. In some HCP metals, the atoms are elongated along the c axis, and in other cases, they are compressed along the c axis (see Table 3.4).

**Figure 3.16**

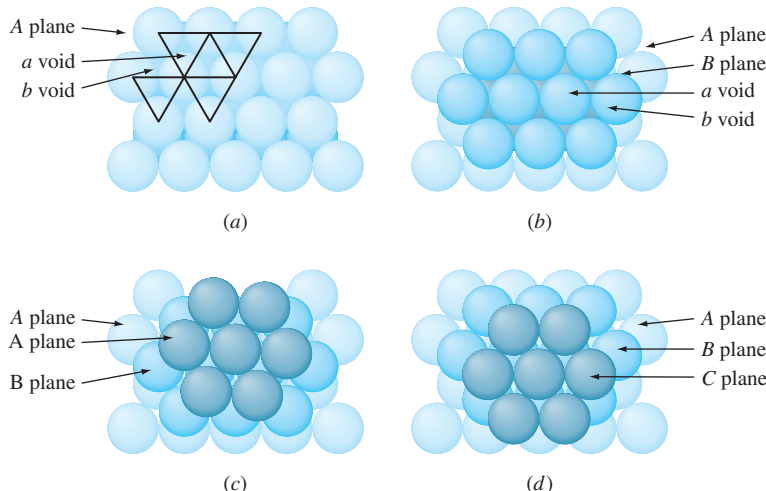
Miller-Bravais hexagonal crystal structure direction indices for principal directions: (a) $+a_1$ axis direction on basal plane, (b) $+a_2$ axis direction on basal plane, (c) $+a_3$ direction axis on basal plane, and (d) $+a_3$ direction axis incorporating c axis. (e) Positive and negative Miller-Bravais directions are indicated in simple hexagonal crystal structure on upper basal plane.

Consider first a plane of close-packed atoms designated the A plane, as shown in Figure 3.18. Note that there are two different types of empty spaces or voids between the atoms. The voids pointing to the top of the page are designated a voids and those pointing to the bottom of the page, b voids. A second plane of atoms can be placed over the a or b voids, and the same three-dimensional structure will be produced. Let us place plane B over the a voids, as shown in Figure 3.18b. Now if a third plane of atoms is placed over plane B to form a closest-packed structure, it is possible to form two different close-packed structures. One possibility is to place the atoms of the third plane in the b voids of the B plane. Then the atoms of this third plane will lie directly over those of the A plane and thus can be designated another A plane (Fig. 3.18c). If subsequent planes of atoms are placed in this same alternating stacking arrangement, then

**Figure 3.17**

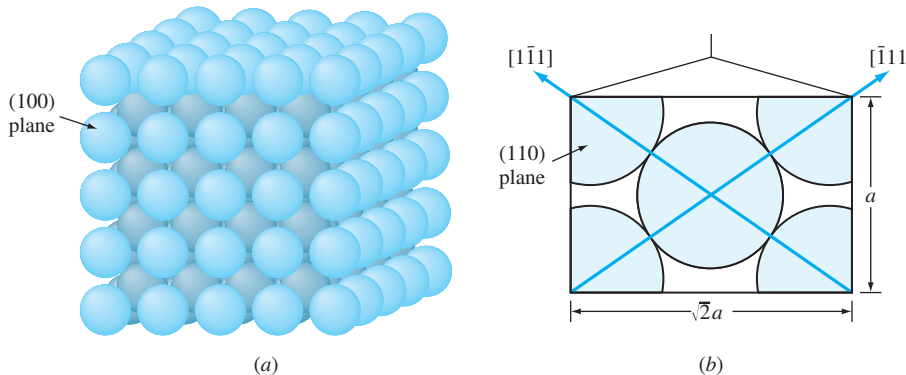
Comparison of the (a) FCC crystal structure showing a close-packed (111) plane and (b) an HCP crystal structure showing the close-packed (0001) plane.

(Source: W.G. Moffatt, G.W. Pearsall, and J. Wulff, *The Structure and Properties of Materials*, vol. 1: "Structure," Wiley, 1964, p. 51.)

**Figure 3.18**

Formation of the HCP and FCC crystal structures by the stacking of atomic planes. (a) A plane showing the *a* and *b* voids. (b) B plane placed in *a* voids of plane A. (c) Third plane placed in *b* voids of B plane, making another A plane and forming the HCP crystal structure. (d) Third plane placed in the *a* voids of B plane, making a new C plane and forming the FCC crystal structure.

(Source: Ander, P.; Sonnessa, A.J., *Principles of Chemistry*, 1st ed.)

**Figure 3.19**

BCC crystal structure showing (a) the (100) plane and (b) a section of the (110) plane. Note that this is not a close-packed structure, but that the diagonals have close-packed directions.

(Source: W.G. Moffatt, G.W. Pearsall and J. Wulff, *The Structure and Properties of Materials*, vol. 1: "Structure," Wiley, 1964, p. 51.)

the stacking sequence of the three-dimensional structure produced can be denoted by $ABABAB\ldots$ Such a stacking sequence leads to the HCP crystal structure (Fig. 3.17b).

The second possibility for forming a simple close-packed structure is to place the third plane in the a voids of plane B (Fig. 3.18d). This third plane is designated the C plane since its atoms do not lie directly above those of the B plane or the A plane. The stacking sequence in this close-packed structure is thus designated $ABCABCABC\ldots$ and leads to the FCC structure shown in Figure 3.17a.

3.8.2 BCC Crystal Structure

The BCC structure is not a close-packed structure and hence does not have close-packed planes like the $\{111\}$ planes in the FCC structure and the $\{0001\}$ planes in the HCP structure. The most densely packed planes in the BCC structure are the $\{110\}$ family of planes, of which the (110) plane is shown in Figure 3.19b. However, the atoms in the BCC structure do have close-packed directions along the cube diagonals, which are the $\langle 111 \rangle$ directions.

3.9 VOLUME, PLANAR, AND LINEAR DENSITY UNIT-CELL CALCULATIONS

3.9.1 Volume Density

Using the hard-sphere atomic model for the crystal structure unit cell of a metal and a value for the atomic radius of the metal obtained from X-ray diffraction analysis, a value for the **volume density** of a metal can be obtained by using the equation

$$\text{Volume density of metal} = \rho_v = \frac{\text{mass/unit cell}}{\text{volume/unit cell}} \quad (3.6)$$

In Example Problem 3.11, a value of 8.933 Mg/m^3 (8.933 g/cm^3) is obtained for the theoretical density of copper. The handbook experimental value for the density of copper is 8.96 Mg/m^3 (8.96 g/cm^3). The slightly different density of the experimental value could be attributed to various defects, mismatch where grains meet (grain boundaries), and human error. These crystalline defects are discussed in Chapter 4. Another cause of the discrepancy could also be due to the atoms not being perfect spheres.

**EXAMPLE
PROBLEM 3.11**

Copper has an FCC crystal structure and an atomic radius of 0.1278 nm . Assuming the atoms to be hard spheres that touch each other along the face diagonals of the FCC unit cell as shown in Figure 3.7, calculate a theoretical value for the density of copper in mega-grams per cubic meter. The atomic mass of copper is 63.54 g/mol .

Solution

For the FCC unit cell, $1\sqrt{2}a = 4R$, where a is the lattice constant of the unit cell, and R is the atomic radius of the copper atom. Thus,

$$a = \frac{4R}{\sqrt{2}} = \frac{(4)(0.1278 \text{ nm})}{\sqrt{2}} = 0.3615 \text{ nm} \quad (3.6)$$

$$\text{Volume density of copper} = \rho_v = \frac{\text{mass/unit cell}}{\text{volume/unit cell}}$$

In the FCC unit cell, there are four atoms/unit cell. Each copper atom has a mass of (63.54 g/mol) ($6.02 \times 10^{23} \text{ atoms/mol}$). Thus, the mass m of Cu atoms in the FCC unit cell is

$$m = \frac{(4 \text{ atoms})(63.54 \text{ g/mol})}{6.02 \times 10^{23} \text{ atoms/mol}} \left(\frac{10^{-6} \text{ Mg}}{\text{g}} \right) = 4.220 \times 10^{-28} \text{ Mg}$$

The volume V of the Cu unit cell is

$$V = a^3 = \left(0.361 \text{ nm} \times \frac{10^{-9} \text{ m}}{\text{nm}} \right)^3 = 4.724 \times 10^{-29} \text{ m}^3$$

Thus, the theoretical density of copper is

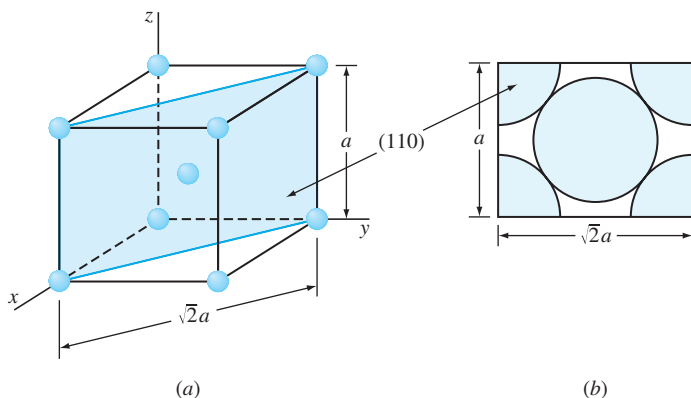
$$\rho_v = \frac{m}{V} = \frac{4.220 \times 10^{-28} \text{ Mg}}{4.724 \times 10^{-29} \text{ m}^3} = 8.933 \text{ Mg/m}^3 (8.933 \text{ g/cm}^3) \blacktriangleleft$$

3.9.2 Planar Atomic Density

Sometimes it is important to determine the atomic densities on various crystal planes. To do this, a quantity called the **planar atomic density** is calculated by using the relationship

$$\text{Planar atomic density} = \rho_p = \frac{\text{equiv. no. of atoms whose centers are intersected by selected area}}{\text{selected area}} \quad (3.8)$$

For convenience, the area of a plane that intersects a unit cell is usually used in these calculations, as shown, for example, in Figure 3.20 for the (110) plane in a BCC unit

**Figure 3.20**

- (a) A BCC atomic-site unit cell showing a shaded (110) plane.
 (b) Areas of atoms in BCC unit cell cut by the (110) plane.

cell. In order for an atom area to be counted in this calculation, the plane of interest must intersect the center of an atom. In Example Problem 3.12, the (110) plane intersects the centers of five atoms, but the equivalent of only two atoms is counted since only one-quarter of each of the four corner atoms is included in the area inside the unit cell.

Calculate the planar atomic density ρ_p on the (110) plane of the α iron BCC lattice in atoms per square millimeter. The lattice constant of α iron is 0.287 nm.

**EXAMPLE
PROBLEM 3.12**
Solution

$$\rho_p = \frac{\text{equiv. no. of atoms whose centers are intersected by selected area}}{\text{selected area}} \quad (3.7)$$

The equivalent number of atoms intersected by the (110) plane in terms of the surface area inside the BCC unit cell is shown in Figure 3.22 and is

$$1 \text{ atom at center} + 4 \times \frac{1}{4} \text{ atoms at four corners of plane} = 2 \text{ atoms}$$

The area intersected by the (110) plane inside the unit cell (selected area) is

$$(\sqrt{2}a)(a) = \sqrt{2}a^2$$

Thus, the planar atomic density is

$$\begin{aligned} \rho_p &= \frac{2 \text{ atoms}}{\sqrt{2}(0.287 \text{ nm})^2} = \frac{17.2 \text{ atoms}}{\text{nm}^2} \\ &= \frac{17.2 \text{ atoms}}{\text{nm}^2} \times \frac{10^{12} \text{ nm}^2}{\text{mm}^2} \\ &= 1.72 \times 10^{13} \text{ atoms/mm}^2 \blacktriangleleft \end{aligned}$$

3.9.3 Linear Atomic Density and Repeat Distance

Sometimes it is important to determine the atomic densities in various directions in crystal structures. To do this, a quantity called the **linear atomic density** is calculated by using the relationship

$$\text{Linear atomic density} = \rho_l = \frac{\text{no. of atomic diam. intersected by selected length of line in direction of interest}}{\text{selected length of line}} \quad (3.8)$$

The distance between two consecutive lattice points along a specific direction is called the **repeat distance**.

Example Problem 3.13 shows how the linear atomic density can be calculated in the [110] direction in a pure copper crystal lattice.

EXAMPLE

PROBLEM 3.13

Calculate the linear atomic density ρ_l in the [110] direction in the copper crystal lattice in atoms per millimeter. Copper is FCC and has a lattice constant of 0.361 nm.

■ Solution

The atoms whose centers the [110] direction intersects are shown in Figure EP3.13. We shall select the length of the line to be the length of the face diagonal of the FCC unit cell, which is $\sqrt{2} a$. The number of atomic diameters intersected by this length of line are $\frac{1}{2} + 1 + \frac{1}{2} = 2$ atoms. Thus using Eq. 3.8, the linear atomic density is

$$\begin{aligned} \rho_l &= \frac{2 \text{ atoms}}{\sqrt{2} a} = \frac{2 \text{ atoms}}{\sqrt{2}(0.361 \text{ nm})} = \frac{3.92 \text{ atoms}}{\text{nm}} \\ &= \frac{3.92 \text{ atoms}}{\text{nm}} \times \frac{10^6 \text{ nm}}{\text{mm}} \\ &= 3.92 \times 10^6 \text{ atoms/mm} \blacktriangleleft \end{aligned}$$

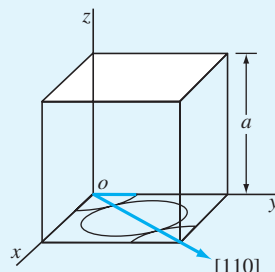


Figure EP3.13

Diagram for calculating the linear atomic density in the [110] direction in an FCC unit cell.

3.10 POLYMORPHISM OR ALLOTROPY

Many elements and compounds exist in more than one crystalline form under different conditions of temperature and pressure. This phenomenon is termed **polymorphism**, or *allotropy*. Many industrially important metals such as iron, titanium, and cobalt undergo allotropic transformations at elevated temperatures at atmospheric pressure. Table 3.5 lists some selected metals that show allotropic transformations and the structure changes that occur.

Iron exists in both BCC and FCC crystal structures over the temperature range from room temperature to its melting point at 1539°C as shown in Figure 3.21. Alpha (α) iron exists from -273°C to 912°C and has the BCC crystal structure. Gamma (γ) iron exists from 912°C to 1394°C and has the FCC crystal structure. Delta (δ) iron exists from 1394°C to 1539°C and has the BCC crystal structure. Liquid iron exists above 1539°C .

Table 3.5 Allotropic crystalline forms of some metals

Metal	Crystal Structure at Room Temperature	At Other Temperatures
Ca	FCC	BCC ($>447^{\circ}\text{C}$)
Co	HCP	FCC ($>427^{\circ}\text{C}$)
Hf	HCP	BCC ($>1742^{\circ}\text{C}$)
Fe	BCC	FCC ($912\text{--}1394^{\circ}\text{C}$) BCC ($>1394^{\circ}\text{C}$)
Li	BCC	HCP ($<-193^{\circ}\text{C}$)
Na	BCC	HCP ($<-233^{\circ}\text{C}$)
Tl	HCP	BCC ($>234^{\circ}\text{C}$)
Ti	HCP	BCC ($>883^{\circ}\text{C}$)
Y	HCP	BCC ($>1481^{\circ}\text{C}$)
Zr	HCP	BCC ($>872^{\circ}\text{C}$)

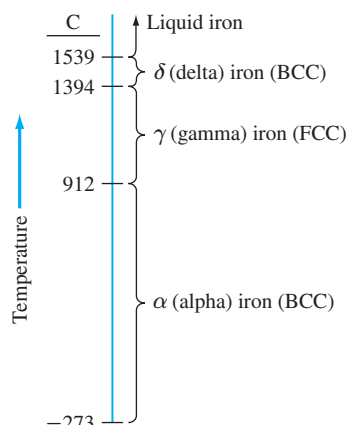


Figure 3.21
Allotropic crystalline forms of iron over temperature ranges at atmospheric pressure.

iron exists from 912°C to 1394°C and has the FCC crystal structure. Delta (δ) iron exists from 1394°C to 1539°C which is the melting point of iron. The crystal structure of δ iron is also BCC but with a larger lattice constant than α iron.

EXAMPLE
PROBLEM 3.14

Calculate the theoretical volume change accompanying a polymorphic transformation in a pure metal from the FCC to BCC crystal structure. Assume the hard-sphere atomic model and that there is no change in atomic volume before and after the transformation.

■ Solution

In the FCC crystal structure unit cell, the atoms are in contact along the face diagonal of the unit cell, as shown in Figure 3.7. Hence,

$$\sqrt{2}a = 4R \quad \text{or} \quad a = \frac{4R}{\sqrt{2}} \quad (3.3)$$

In the BCC crystal structure unit cell, the atoms are in contact along the body diagonal of the unit cell as shown in Figure 3.5. Hence,

$$\sqrt{3}a = 4R \quad \text{or} \quad a = \frac{4R}{\sqrt{3}} \quad (3.1)$$

The volume per atom for the FCC crystal lattice, since it has four atoms per unit cell, is

$$V_{\text{FCC}} = \frac{a^3}{4} = \left(\frac{4R}{\sqrt{2}} \right)^3 \left(\frac{1}{4} \right) = 5.66R^3$$

The volume per atom for the BCC crystal lattice, since it has two atoms per unit cell, is

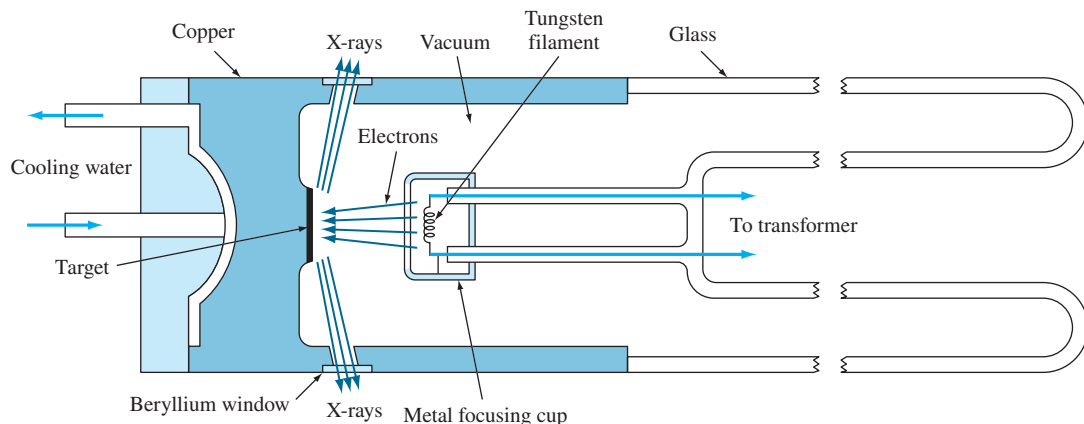
$$V_{\text{BCC}} = \frac{a^3}{2} = \left(\frac{4R}{\sqrt{3}} \right)^3 \left(\frac{1}{2} \right) = 6.16R^3$$

The change in volume associated with the transformation from the FCC to BCC crystal structure, assuming no change in atomic radius, is

$$\begin{aligned} \frac{\Delta V}{V_{\text{FCC}}} &= \frac{V_{\text{BCC}} - V_{\text{FCC}}}{V_{\text{FCC}}} \\ &= \left(\frac{6.16R^3 - 5.66R^3}{5.66R^3} \right) 100\% = +8.83\% \blacktriangleleft \end{aligned}$$

3.11 CRYSTAL STRUCTURE ANALYSIS

Our present knowledge of crystal structures has been obtained mainly by X-ray diffraction techniques that use X-rays whose wavelength are the same as the distance between crystal lattice planes. However, before discussing the manner in

**Figure 3.22**

Schematic diagram of the cross section of a sealed-off filament X-ray tube.

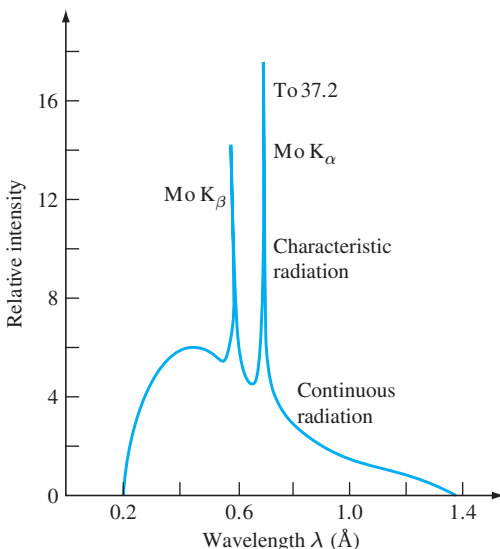
(Source: B. D. Cullity, *Elements of X-Ray Diffraction* 2nd ed., Addison-Wesley, 1978, p. 23.)

which X-rays are diffracted in crystals, let us consider how X-rays are produced for experimental purposes.

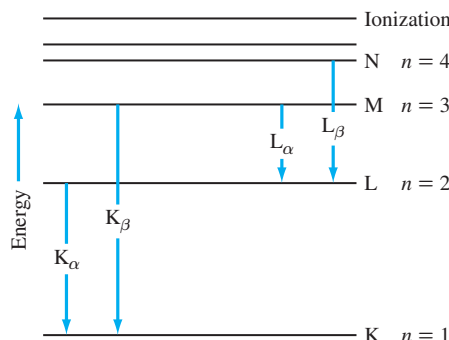
3.11.1 X-Ray Sources

X-rays used for diffraction are electromagnetic waves with wavelengths in the range 0.05 to 0.25 nm (0.5 to 2.5 Å). By comparison, the wavelength of visible light is of the order of 600 nm (6000 Å). In order to produce X-rays for diffraction purposes, a voltage of about 35 kV is necessary and is applied between a cathode and an anode target metal, both of which are contained in a vacuum, as shown in Figure 3.22. When the tungsten filament of the cathode is heated, electrons are released by thermionic emission and accelerated through the vacuum by the large voltage difference between the cathode and anode, thereby gaining kinetic energy. When the electrons strike the target metal (e.g., molybdenum), X-rays are given off. However, most of the kinetic energy (about 98%) is converted into heat, so the target metal must be cooled externally.

The X-ray spectrum emitted at 35 kV using a molybdenum target is shown in Figure 3.23. The spectrum shows continuous X-ray radiation in the wavelength range from about 0.2 to 1.4 Å (0.02 to 0.14 nm) and two spikes of characteristic radiation that are designated the K_{α} and K_{β} lines. The wavelengths of the K_{α} and K_{β} lines are characteristic for an element. For molybdenum, the K_{α} line occurs at a wavelength of about 0.7 Å (0.07 nm). The origin of the characteristic radiation is explained as follows: first, K electrons (electrons in the $n = 1$ shell) are knocked out of the atom by highly energetic electrons bombarding the target, leaving excited atoms. Next, some electrons in higher shells (that is, $n = 2$ or 3) drop down to lower energy levels

**Figure 3.23**

X-ray emission spectrum produced when molybdenum metal is used as the target metal in an X-ray tube operating at 35 kV.

**Figure 3.24**

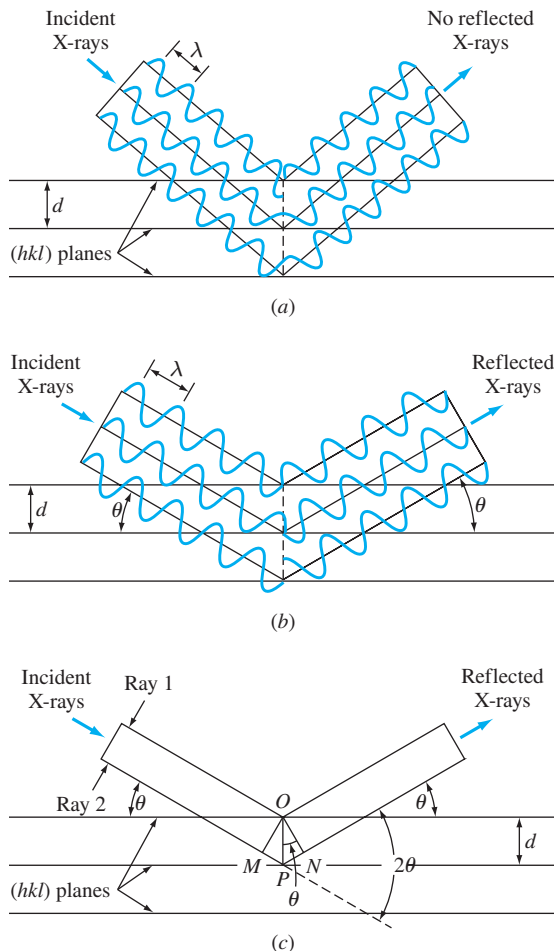
Energy levels of electrons in molybdenum showing the origin of K_{α} and K_{β} radiation.

to replace the lost K electrons, emitting energy of a characteristic wavelength. The transition of electrons from the L ($n = 2$) shell to the K ($n = 1$) shell creates energy of the wavelength of the K_{α} line, as indicated in Figure 3.24.

3.11.2 X-Ray Diffraction

Since the wavelengths of some X-rays are about equal to the distance between planes of atoms in crystalline solids, reinforced diffraction peaks of radiation of varying intensities can be produced when a beam of X-rays strikes a crystalline solid. However, before considering the application of X-ray diffraction techniques to crystal structure analysis, let us examine the geometric conditions necessary to produce diffracted or reinforced beams of reflected X-rays.

Consider a monochromatic (single-wavelength) beam of X-rays to be incident on a crystal, as shown in Figure 3.25. For simplification, let us allow the crystal planes of atomic scattering centers to be replaced by crystal planes that act as mirrors in reflecting the incident X-ray beam. In Figure 3.25, the horizontal lines represent a set of parallel crystal planes with Miller indices (hkl). When an incident beam of monochromatic X-rays of wavelength λ strikes this set of planes at an angle such that the wave patterns of the beam leaving the various planes are *not in phase*, *no reinforced beam will be produced* (Figure 3.25a). Thus, destructive interference occurs. If the reflected wave patterns of the beam leaving the various planes are in phase, then reinforcement of the beam or constructive interference occurs (Fig. 3.25b).

**Figure 3.25**

The reflection of an X-ray beam by the (hkl) planes of a crystal. (a) No reflected beam is produced at an arbitrary angle of incidence. (b) At the Bragg angle θ , the reflected rays are in phase and reinforce one another. (c) Similar to (b) except that the wave representation has been omitted.

(Source: A.G. Guy and J.J. Hren *Elements of Physical Metallurgy* (3rd ed.). Addison-Wesley, 1974, p. 201.)

Let us now consider incident X-rays 1 and 2 as indicated in Figure 3.25c. For these rays to be in phase, the extra distance of travel of ray 2 is equal to $MP + PN$, which must be an integral number of wavelengths λ . Thus,

$$n\lambda = MP + PN \quad (3.9)$$

where $n = 1, 2, 3, \dots$ and is called the *order of the diffraction*. Since both MP and PN equal $d_{hkl} \sin \theta$, where d_{hkl} is the interplanar spacing of the crystal planes of indices (hkl) , the condition for constructive interference (i.e., the production of a diffraction peak of intense radiation) must be

$$n\lambda = 2d_{hkl} \sin \theta \quad (3.10)$$

This equation, known as *Bragg's law*,⁷ gives the relationship among the angular positions of the reinforced diffracted beams in terms of the wavelength λ of the incoming X-ray radiation and of the interplanar spacings d_{hkl} of the crystal planes. In most cases, the first order of diffraction where $n = 1$ is used, and so for this case, Bragg's law takes the form

$$\lambda = 2d_{hkl} \sin \theta \quad (3.11)$$

EXAMPLE
PROBLEM 3.15

A sample of BCC iron was placed in an X-ray diffractometer using incoming X-rays with a wavelength $\lambda = 0.1541$ nm. Diffraction from the $\{110\}$ planes was obtained at $2\theta = 44.70^\circ$. Calculate a value for the lattice constant a of BCC iron. (Assume first-order diffraction with $n = 1$.)

Solution

$$\begin{aligned} 2\theta &= 44.704^\circ \quad \theta = 22.35^\circ \\ \lambda &= 2d_{hkl} \sin \theta \\ d_{110} &= \frac{\lambda}{2 \sin \theta} = \frac{0.1541 \text{ nm}}{2(\sin 22.35^\circ)} \\ &= \frac{0.1541 \text{ nm}}{2(0.3803)} = 0.2026 \text{ nm} \end{aligned} \quad (3.11)$$

Rearranging Eq. 3.5 gives

$$a = d_{hkl} \sqrt{h^2 + k^2 + l^2}$$

Thus,

$$\begin{aligned} a(\text{Fe}) &= d_{110} \sqrt{1^2 + 1^2 + 0^2} \\ &= (0.2026 \text{ nm})(1.414) = 0.2865 \text{ nm} \blacktriangleleft \end{aligned}$$

3.11.3 X-Ray Diffraction Analysis of Crystal Structures

The Powder Method of X-Ray Diffraction Analysis The most commonly used X-ray diffraction technique is the *powder method*. In this technique, a powdered specimen is utilized so that there will be a random orientation of many crystals to ensure that some of the particles will be oriented in the X-ray beam to satisfy the diffraction conditions of

⁷ William Henry Bragg (1862–1942). English physicist who worked on X-ray crystallography.

**Figure 3.26**

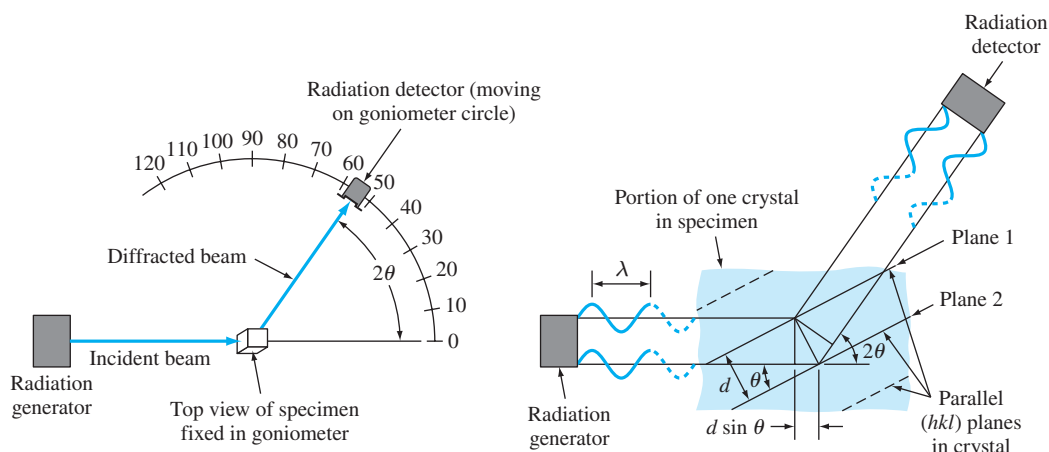
An X-ray diffractometer (with X-radiation shields removed).

(Courtesy of Rigaku)

Bragg's law. Modern X-ray crystal analysis uses an X-ray diffractometer that has a radiation counter to detect the angle and intensity of the diffracted beam (Fig. 3.26). A recorder automatically plots the intensity of the diffracted beam as the counter moves on a goniometer⁸ circle (Fig. 3.27) that is in synchronization with the specimen over a range of 2θ values. Figure 3.28 shows an X-ray diffraction recorder chart for the intensity of the diffracted beam versus the diffraction angles 2θ for a powdered pure-metal specimen. In this way, both the angles of the diffracted beams and their intensities can be recorded at one time. Sometimes a powder camera with an enclosed filmstrip is used instead of the diffractometer, but this method is much slower and in most cases, less convenient.

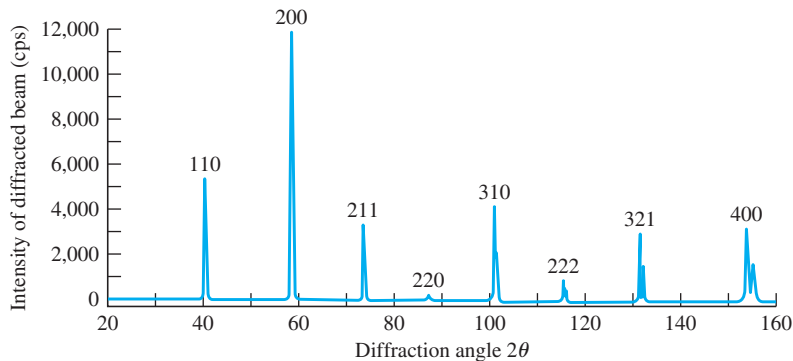
Diffraction Conditions for Cubic Unit Cells X-ray diffraction techniques enable the structures of crystalline solids to be determined. The interpretation of X-ray diffraction data for most crystalline substances is complex and beyond the scope of this

⁸ A goniometer is an instrument for measuring angles.

**Figure 3.27**

Schematic illustration of the diffractometer method of crystal analysis and of the conditions necessary for diffraction.

(Source: A.G. Guy, *Essentials of Materials Science*, McGraw-Hill, 1976.)

**Figure 3.28**

Record of the diffraction angles for a tungsten sample obtained by the use of a diffractometer with copper radiation.

(Source: A.G. Guy and J.J. Hren, *Elements of Physical Metallurgy* 3rd ed., Addison-Wesley, 1974, p. 208.)

book, and so only the simple case of diffraction in pure cubic metals will be considered. The analysis of X-ray diffraction data for cubic unit cells can be simplified by combining Eq. 3.4,

$$d_{hkl} = \frac{a}{\sqrt{h^2 + k^2 + l^2}}$$

with the Bragg equation $\lambda = 2d \sin \theta$, giving

$$\lambda = \frac{2a \sin \theta}{\sqrt{h^2 + k^2 + l^2}} \quad (3.12)$$

This equation can be used along with X-ray diffraction data to determine if a cubic crystal structure is body-centered or face-centered cubic. The rest of this subsection will describe how this is done.

To use Eq. 3.12 for diffraction analysis, we must know which crystal planes are the diffracting planes for each type of crystal structure. For the simple cubic lattice, reflections from all (hkl) planes are possible. However, for the BCC structure, diffraction occurs only on planes whose Miller indices when added together ($h + k + l$) total to an even number (Table 3.6). Thus, for the BCC crystal structure, the principal diffracting planes are $\{110\}$, $\{200\}$, $\{211\}$, etc., which are listed in Table 3.7. In the case of the FCC crystal structure, the principal diffracting planes are those whose Miller indices are either all even or all odd (zero is considered even). Thus, for the FCC crystal structure, the diffracting planes are $\{111\}$, $\{200\}$, $\{220\}$, etc., which are listed in Table 3.7.

Interpreting Experimental X-Ray Diffraction Data for Metals with Cubic Crystal Structures We can use X-ray diffractometer data to determine crystal structures. A simple case to illustrate how this analysis can be used is to distinguish between the

Table 3.6 Rules for determining the diffracting $\{hkl\}$ planes in cubic crystals

Bravais Lattice	Reflections Present	Reflections Absent
BCC	$(h + k + l) = \text{even}$	$(h + k + l) = \text{odd}$
FCC	(h, k, l) all odd or all even	(h, k, l) not all odd or all even

Table 3.7 Miller indices of the diffracting planes for BCC and FCC lattices

Cubic Planes $\{hkl\}$	$h^2 + k^2 + l^2$	Sum $\Sigma[h^2 + k^2 + l^2]$	Cubic Diffracting Planes $\{hkl\}$	
			FCC	BCC
$\{100\}$	$1^2 + 0^2 + 0^2$	1		
$\{110\}$	$1^2 + 1^2 + 0^2$	2	...	110
$\{111\}$	$1^2 + 1^2 + 1^2$	3	111	
$\{200\}$	$2^2 + 0^2 + 0^2$	4	200	200
$\{210\}$	$2^2 + 1^2 + 0^2$	5		
$\{211\}$	$2^2 + 1^2 + 1^2$	6	...	211
...		7		
$\{220\}$	$2^2 + 2^2 + 0^2$	8	220	220
$\{221\}$	$2^2 + 2^2 + 1^2$	9		
$\{310\}$	$3^2 + 1^2 + 0^2$	10	...	310

BCC and FCC crystal structures of a cubic metal. Let us assume that we have a metal with either a BCC or an FCC crystal structure and that we can identify the principal diffracting planes and their corresponding 2θ values, as indicated for the metal tungsten in Figure 3.28.

By squaring both sides of Eq. 3.12 and solving for $\sin^2\theta$, we obtain

$$\sin^2\theta = \frac{\lambda^2(h^2 + k^2 + l^2)}{4a^2} \quad (3.13)$$

From X-ray diffraction data, we can obtain experimental values of 2θ for a series of principal diffracting $\{hkl\}$ planes. Since the wavelength of the incoming radiation and the lattice constant a are both constants, we can eliminate these quantities by forming the ratio of two $\sin^2\theta$ values as

$$\frac{\sin^2\theta_A}{\sin^2\theta_B} = \frac{h_A^2 + k_A^2 + l_A^2}{h_B^2 + k_B^2 + l_B^2} \quad (3.14)$$

where θ_A and θ_B are two diffracting angles associated with the principal diffracting planes $\{h_Ak_Al_A\}$ and $\{h_Bk_Bl_B\}$, respectively.

Using Eq. 3.14 and the Miller indices of the first two sets of principal diffracting planes listed in Table 3.7 for BCC and FCC crystal structures, we can determine values for the $\sin^2\theta$ ratios for both BCC and FCC structures.

For the BCC crystal structure, the first two sets of principal diffracting planes are the $\{110\}$ and $\{200\}$ planes (Table 3.7). Substitution of the Miller $\{hkl\}$ indices of these planes into Eq. 3.14 gives

$$\frac{\sin^2\theta_A}{\sin^2\theta_B} = \frac{1^2 + 1^2 + 0^2}{2^2 + 0^2 + 0^2} = 0.5 \quad (3.15)$$

Thus, if the crystal structure of the unknown cubic metal is BCC, the ratio of the $\sin^2\theta$ values that correspond to the first two principal diffracting planes will be 0.5.

For the FCC crystal structure, the first two sets of principal diffracting planes are the $\{111\}$ and $\{200\}$ planes (Table 3.7). Substitution of the Miller $\{hkl\}$ indices of these planes into Eq. 3.15 gives

$$\frac{\sin^2\theta_A}{\sin^2\theta_B} = \frac{1^2 + 1^2 + 1^2}{2^2 + 0^2 + 0^2} = 0.75 \quad (3.16)$$

Thus, if the crystal structure of the unknown cubic metal is FCC, the ratio of the $\sin^2\theta$ values that correspond to the first two principal diffracting planes will be 0.75.

Example Problem 3.16 uses Eq. 3.14 and experimental X-ray diffraction data for the 2θ values for the principal diffracting planes to determine whether an unknown cubic metal is BCC or FCC. X-ray diffraction analysis is usually much more complicated than Example Problem 3.16, but the principles used are the same. Both experimental and theoretical X-ray diffraction analysis has been and continues to be used for the determination of the crystal structure of materials.

An X-ray diffractometer recorder chart for an element that has either the BCC or the FCC crystal structure shows diffraction peaks at the following 2θ angles: 40, 58, 73, 86.8, 100.4, and 114.7. The wavelength of the incoming X-ray used was 0.154 nm.

EXAMPLE
PROBLEM 3.16

- Determine the cubic structure of the element.
- Determine the lattice constant of the element.
- Identify the element.

Solution

- Determination of the crystal structure of the element.* First, the $\sin^2 \theta$ values are calculated from the 2θ diffraction angles.

$2\theta(\text{deg})$	$\theta(\text{deg})$	$\sin \theta$	$\sin^2 \theta$
40	20	0.3420	0.1170
58	29	0.4848	0.2350
73	36.5	0.5948	0.3538
86.8	43.4	0.6871	0.4721
100.4	50.2	0.7683	0.5903
114.7	57.35	0.8420	0.7090

Next, the ratio of the $\sin^2 \theta$ values of the first and second angles is calculated:

$$\frac{\sin^2 \theta}{\sin^2 \theta} = \frac{0.117}{0.235} = 0.498 \approx 0.5$$

The crystal structure is BCC since this ratio is ≈ 0.5 . If the ratio had been ≈ 0.75 , the structure would have been FCC.

- Determination of the lattice constant.* Rearranging Eq. 3.14 and solving for a^2 gives

$$a^2 = \frac{\lambda^2 h^2 + k^2 + l^2}{4 \sin^2 \theta} \quad (3.17)$$

or

$$a = \frac{\lambda}{2} \sqrt{\frac{h^2 + k^2 + l^2}{\sin^2 \theta}} \quad (3.18)$$

Substituting into Eq. 3.18 $h = 1$, $k = 1$, and $l = 0$ for the h , k , l Miller indices of the first set of principal diffracting planes for the BCC crystal structure, which are the $\{110\}$ planes, the corresponding value for $\sin^2 \theta$, which is 0.117, and 0.154 nm for λ , the incoming radiation, gives

$$a = \frac{0.154 \text{ nm}}{2} \sqrt{\frac{1^2 + 1^2 + 0^2}{0.117}} = 0.318 \text{ nm} \blacktriangleleft$$

- Identification of the element.* The element is tungsten since this element has a lattice constant of 0.316 nm and is BCC.

3.12 AMORPHOUS MATERIALS

As discussed previously, some materials are called amorphous or noncrystalline because they lack long-range order in their atomic structure. It should be noted that, in general, materials have a tendency to achieve a crystalline state because that is the most stable state and it corresponds to the lowest energy level. However, atoms in amorphous materials are bonded in a disordered manner because of factors that inhibit the formation of a periodic arrangement. Atoms in amorphous materials, therefore, occupy random spatial positions as opposed to specific positions in crystalline solids. For clarity, various degrees of order (or disorder) are shown in Figure 3.29.

Most polymers, glasses, and some metals are members of the amorphous class of materials. In polymers, the secondary bonds among molecules do not allow for the formation of parallel and tightly packed chains during solidification. As a result, polymers such as polyvinylchloride consist of long, twisted molecular chains that are entangled to form a solid with amorphous structure, similar to Figure 3.29c. In some polymers such as polyethylene, the molecules are more efficiently and tightly packed in some regions of the material and produce a higher degree of regional long-range order. As a result, these polymers are often classified as *semicrystalline*. A more detailed discussion of semicrystalline polymers will be given in Chapter 10.

Inorganic glass based on glass-forming oxide, silica (SiO_2), is generally characterized as a ceramic material (ceramic glass) and is another example of a material with an amorphous structure. In this type of glass, the fundamental subunit in the molecules is the SiO_4^{4-} tetrahedron. The ideal crystalline structure of this glass is shown in Figure 3.29a. The schematic shows the Si–O tetrahedrons joined corner to corner to form long-range order. In its viscous liquid state, the molecules have limited mobility, and, in general, crystallization occurs slowly. Therefore, a modest cooling rate suppresses the formation of the crystal structure, and instead the tetrahedra join corner to corner to form a network lacking in long-range order (Fig. 3.29b).

In addition to polymers and glasses, some metals also have the ability to form amorphous structures (*metallic glass*) under strict and often difficult-to-achieve conditions. Unlike glasses, metals have very small and mobile building blocks under molten

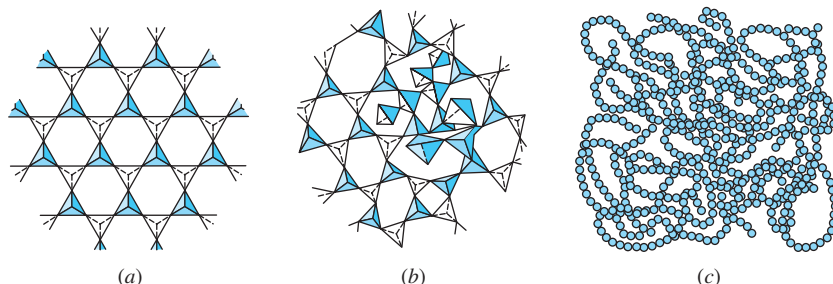


Figure 3.29

A schematic showing various degrees of order in materials: (a) long-range order in crystalline silica, (b) silica glass without long-range order, and (c) amorphous structure in polymers.

conditions. As a result, it is difficult to prevent metals from crystallizing. However, alloys such as 78%Fe–9%Si–13%B that contain a high percentage of semimetals, Si and B, may form metallic glasses through rapid solidification at cooling rates in excess of 10^8 °C/s. At such high cooling rates, the atoms simply do not have enough time to form a crystalline structure and instead form a metal with an amorphous structure, that is, they are highly disordered. In theory, any crystalline material can form a noncrystalline structure if solidified rapidly enough from a molten state.

Amorphous materials, because of their structure, possess properties that are superior. For instance, metallic glasses possess higher strength, better corrosion characteristics, and magnetic properties when compared to their crystalline counterparts. Finally, it is important to note that amorphous materials do not show sharp diffraction patterns when analyzed using X-ray diffraction techniques. This is due to a lack of order and periodicity in the atomic structure. In future chapters, the role of structure of the material on its properties will be explained in detail.

3.13 SUMMARY

Atomic arrangements in crystalline solids can be described by a network of lines called a *space lattice*. Each space lattice can be described by specifying the atom positions in a repeating *unit cell*. The crystal structure consists of space lattice and *motif* or *basis*. Crystalline materials, such as most metals, possess long-range atomic order. But some materials, such as many polymers and glasses, possess only short-range order. Such materials are called semi-crystalline or amorphous. There are seven crystal systems based on the geometry of the axial lengths and interaxial angles of the unit cells. These seven systems have a total of 14 sublattices (unit cells) based on the internal arrangements of atomic sites within the unit cells.

In metals, the most common crystal structure unit cells are: *body-centered cubic* (BCC), *face-centered cubic* (FCC), and *hexagonal close-packed* (HCP) (which is a dense variation of the simple hexagonal structure).

Crystal directions in cubic crystals are the vector components of the directions resolved along each of the component axes and reduced to smallest integers. They are indicated as $[uvw]$. Families of directions are indexed by the direction indices enclosed by pointed brackets as $\langle uvw \rangle$. *Crystal planes* in cubic crystals are indexed by the reciprocals of the axial intercepts of the plane (followed by the elimination of fractions) as (hkl) . Cubic crystal planes of a form (family) are indexed with braces as $\{hkl\}$. Crystal planes in hexagonal crystals are commonly indexed by four indices h, k, i , and l enclosed in parentheses as $(hkil)$. These indices are the reciprocals of the intercepts of the plane on the a_1, a_2, a_3 , and c axes of the hexagonal crystal structure unit cell. Crystal directions in hexagonal crystals are the vector components of the direction resolved along each of the four coordinate axes and reduced to smallest integers as $[uvtw]$.

Using the hard-sphere model for atoms, calculations can be made for the volume, planar, and linear density of atoms in unit cells. Planes in which atoms are packed as tightly as possible are called *close-packed planes*, and directions in which atoms are in closest contact are called *close-packed directions*. Atomic packing factors for different crystal structures can also be determined by assuming the hard-sphere atomic model. Some metals have different crystal structures at different ranges of temperature and pressure, a phenomenon called *polymorphism*.

Crystal structures of crystalline solids can be determined by using X-ray diffraction analysis techniques. X-rays are diffracted in crystals when the *Bragg's law* ($n\lambda = 2d \sin \theta$) conditions are satisfied. By using the X-ray diffractometer and the *powder method*, the crystal structure of many crystalline solids can be determined.

3.14 DEFINITIONS

Sec. 3.1

Amorphous: lacking in long-range atomic order.

Crystal: a solid composed of atoms, ions, or molecules arranged in a pattern that is repeated in three dimensions.

Crystal structure: a regular three-dimensional pattern of atoms or ions in space.

Space lattice: a three-dimensional array of points each of which has identical surroundings.

Lattice point: one point in an array in which all the points have identical surroundings.

Unit cell: a convenient repeating unit of a space lattice. The axial lengths and axial angles are the lattice constants of the unit cell.

Motif (or Basis): a group of atoms that are organized relative to each other and are associated with corresponding lattice points.

Sec. 3.3

Body-centered cubic (BCC) unit cell: a unit cell with an atomic packing arrangement in which one atom is in contact with eight identical atoms located at the corners of an imaginary cube.

Face-centered cubic (FCC) unit cell: a unit cell with an atomic packing arrangement in which 12 atoms surround a central atom. The stacking sequence of layers of close-packed planes in the FCC crystal structure is ABCABC....

Hexagonal close-packed (HCP) unit cell: a unit cell with an atomic packing arrangement in which 12 atoms surround a central identical atom. The stacking sequence of layers of close-packed planes in the HCP crystal structure is ABABAB....

Atomic packing factor (APF): the volume of atoms in a selected unit cell divided by the volume of the unit cell.

Sec. 3.5

Indices of direction in a cubic crystal: a direction in a cubic unit cell is indicated by a vector drawn from the origin at one point in a unit cell through the surface of the unit cell; the position coordinates (x , y , and z) of the vector where it leaves the surface of the unit cell (with fractions cleared) are the indices of direction. These indices, designated u , v , and w , are enclosed in brackets as $[uvw]$. Negative indices are indicated by a bar over the index.

Sec. 3.6

Indices for cubic crystal planes (Miller indices): the reciprocals of the intercepts (with fractions cleared) of a crystal plane with the x , y , and z axes of a unit cube are called the Miller indices of that plane. They are designated h , k , and l for the x , y , and z axes, respectively, and are enclosed in parentheses as (hkl) . Note that the selected crystal plane must *not* pass through the origin of the x , y , and z axes.

Sec. 3.9

Volume density ρ_v : mass per unit volume; this quantity is usually expressed in Mg/m³ or g/cm³.

Planar density ρ_p : the equivalent number of atoms whose centers are intersected by a selected area divided by the selected area.

Linear density ρ_l : the number of atoms whose centers lie on a specific direction on a specific length of line in a unit cube.

Repeat Distance: The distance between two consecutive lattice points along a specific direction.

Sec. 3.10

Polymorphism (as pertains to metals): the ability of a metal to exist in two or more crystal structures. For example, iron can have a BCC or an FCC crystal structure, depending on the temperature.

Sec. 3.12

Semicrystalline: materials with regions of crystalline structure dispersed in the surrounding, amorphous region, for instance, some polymers.

Metallic glass: metals with an amorphous atomic structure.

3.15 PROBLEMS

Answers to problems marked with an asterisk are given at the end of the book.

Knowledge and Comprehension Problems

- 3.1 Define the following terms: (a) crystalline solid, (b) long-range order, (c) short-range order, and (d) amorphous.
- 3.2 Define the following terms: (a) crystal structure, (b) space lattice, (c) lattice point, (d) unit cell, (e) motif, and (f) lattice constants.
- 3.3 What are the 14 Bravais unit cells?
- 3.4 What are the three most common metal crystal structures? List five metals that have each of these crystal structures.
- 3.5 For a BCC unit cell, (a) how many atoms are there inside the unit cell, (b) what is the coordination number for the atoms, (c) what is the relationship between the length of the side a of the BCC unit cell and the radius of its atoms, and (d) what is the atomic packing factor?
- 3.6 For an FCC unit cell, (a) how many atoms are there inside the unit cell, (b) what is the coordination number for the atoms, (c) what is the relationship between the length of the side a of the FCC unit cell and the radius of its atoms, and (d) what is the atomic packing factor?
- 3.7 For an HCP unit cell (consider the primitive cell), (a) how many atoms are there inside the unit cell, (b) what is the coordination number for the atoms, (c) what is the atomic packing factor, (d) what is the ideal c/a ratio for HCP metals, and (e) repeat (a) through (c) considering the “larger” cell.
- 3.8 How are atomic positions located in cubic unit cells?
- 3.9 List the atom positions for the eight corner and six face-centered atoms of the FCC unit cell.
- 3.10 How are the indices for a crystallographic direction in a cubic unit cell determined?

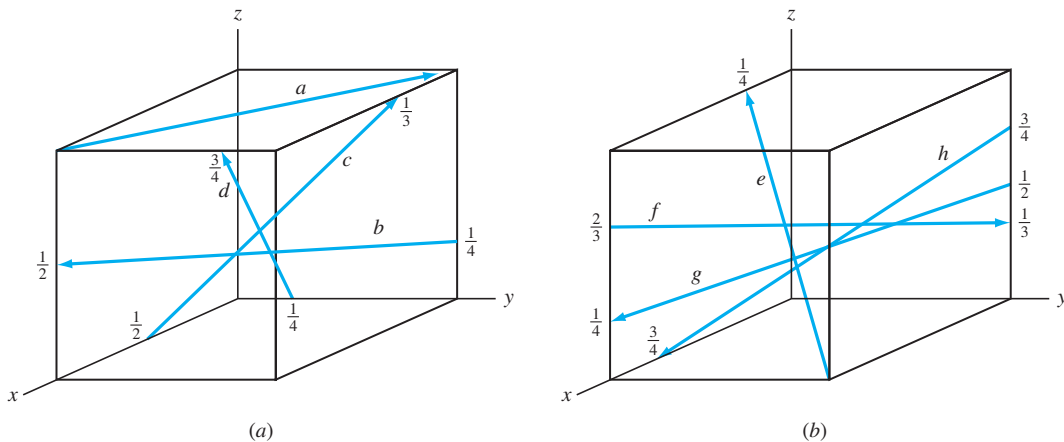
- 3.11 What are the crystallographic directions of a family or form? What generalized notation is used to indicate them?
- 3.12 How are the Miller indices for a crystallographic plane in a cubic unit cell determined? What generalized notation is used to indicate them?
- 3.13 What is the notation used to indicate a family or form of cubic crystallographic planes?
- 3.14 How are crystallographic planes indicated in HCP unit cells?
- 3.15 What notation is used to describe HCP crystal planes?
- 3.16 What is the difference in the stacking arrangement of close-packed planes in (a) the HCP crystal structure and (b) the FCC crystal structure?
- 3.17 What are the closest-packed directions in (a) the BCC structure, (b) the FCC structure, and (c) the HCP structure?
- 3.18 Identify the close-packed planes in (a) the BCC structure, (b) the FCC structure, and (c) the HCP structure.
- 3.19 What is polymorphism with respect to metals?
- 3.20 What are X-rays, and how are they produced?
- 3.21 Draw a schematic diagram of an X-ray tube used for X-ray diffraction, and indicate on it the path of the electrons and X-rays.
- 3.22 What is the characteristic X-ray radiation? What is its origin?
- 3.23 Distinguish between destructive interference and constructive interference of reflected X-ray beams through crystals.



Tutorial

Application and Analysis Problems

- 3.24 Tungsten at 20°C is BCC and has an atomic radius of 0.137 nm. (a) Calculate a value for its lattice constant a in nanometers. (b) Calculate the volume of the unit cell.
- 3.25 Lead is FCC and has an atomic radius of 0.175 nm. (a) Calculate a value for its lattice constant a in nanometers. (b) Calculate the volume of the unit cell in nm³.
- 3.26 Verify that the atomic packing factor for the FCC structure is 0.74.
- 3.27 Calculate the volume in cubic nanometers of the cobalt crystal structure unit cell (use the larger cell). Cobalt is HCP at 20°C with $a = 0.2507$ nm and $c = 0.4069$ nm.
- 3.28 Consider a 0.05-mm-thick, 500 mm² (about three times the area of a dime) piece of aluminum foil. How many unit cells exist in the foil? If the density of aluminum is 2.7 g/cm³, what is the mass of each cell?
- 3.29 Draw the following directions in a BCC unit cell, and list the position coordinates of the atoms whose centers are intersected by the direction vector. Determine the repeat distance in terms of the lattice constant in each direction.
 - (a) [010]
 - (b) [011]
 - (c) [111]
 - (d) Find the angle between directions in (b) and (c).
- 3.30 Draw direction vectors in an FCC unit cell for the following cubic directions, and list the position coordinates of the atoms whose centers are intersected by the direction vector. Determine the repeat distance in terms of the lattice constant in each direction.
 - (a) $\overline{[111]}$
 - (b) $[10\bar{1}]$
 - (c) $[2\bar{1}\bar{1}]$
 - (d) $[\bar{1}3\bar{1}]$
 - (e) Find the angle between directions in (b) and (d).

**Figure P3.32**

- 3.31** Draw direction vectors in unit cells for the following cubic directions:
- [112]
 - [123]
 - [331]
 - [021]
 - [212]
 - [233]
 - [101]
 - [121]
 - [321]
 - [103]
 - [122]
 - [223]
- 3.32** What are the indices of the directions shown in the unit cubes of Figure P3.32?
- 3.33** A direction vector passes through a unit cube from the $(\frac{3}{4}, 0, \frac{1}{4})$ to the $(\frac{1}{2}, 1, 0)$ positions. What are its direction indices?
- 3.34** A direction vector passes through a unit cube from the $(1, 0, \frac{3}{4})$ to the $(\frac{1}{4}, 1, \frac{1}{4})$ positions. What are its direction indices?
- 3.35** What are the directions of the $\langle 10\bar{3} \rangle$ family or form for a unit cube? Draw all directions in a unit cell.
- 3.36** What are the directions of the $\langle 111 \rangle$ family or form for a unit cube? Draw all directions in a BCC unit cell. Can you identify a special quality of these directions?
- 3.37** What $\langle 110 \rangle$ type directions lie on the (111) plane of a cubic unit cell? Draw those directions in an FCC unit cell. Can you identify a special quality of these directions?
- 3.38** What $\langle 111 \rangle$ type directions lie on the (110) plane of a BCC unit cell? Draw those directions in a unit cell. Can you identify a special quality of these directions?
- 3.39** Draw in unit cubes the crystal planes that have the following Miller indices:
- (111)
 - (102)
 - (121)
 - (213)
 - (321)
 - (302)
 - (201)
 - (212)
 - (232)
 - (133)
 - (312)
 - (331)
- 3.40** What are the Miller indices of the cubic crystallographic planes shown in Figure P3.40?
- 3.41** What are the $\{100\}$ family of planes of the cubic system? Draw those planes in a BCC unit cell and show all atoms whose centers are intersected by the planes. What is your conclusion?
- 3.42** Draw the following crystallographic planes in a BCC unit cell, and list the position of the atoms whose centers are intersected by each of the planes:
- (010)
 - (011)
 - (111)

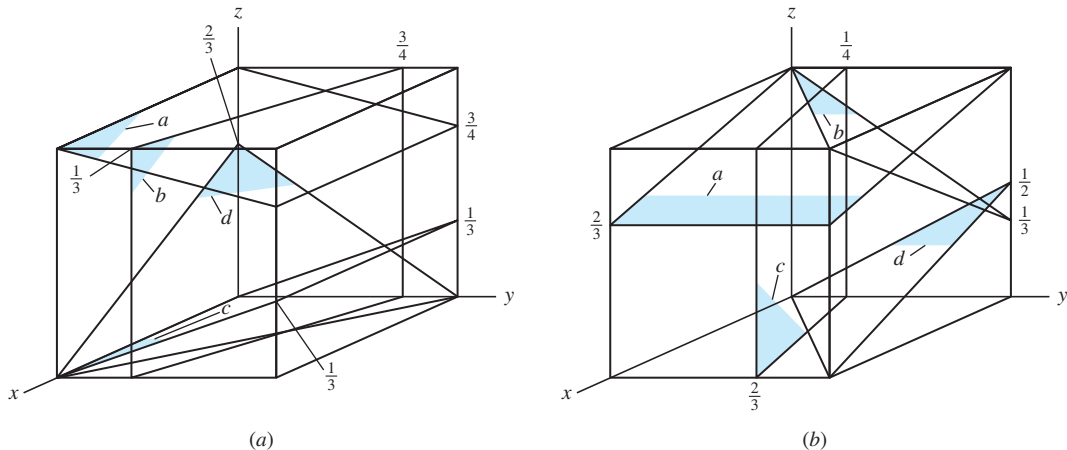
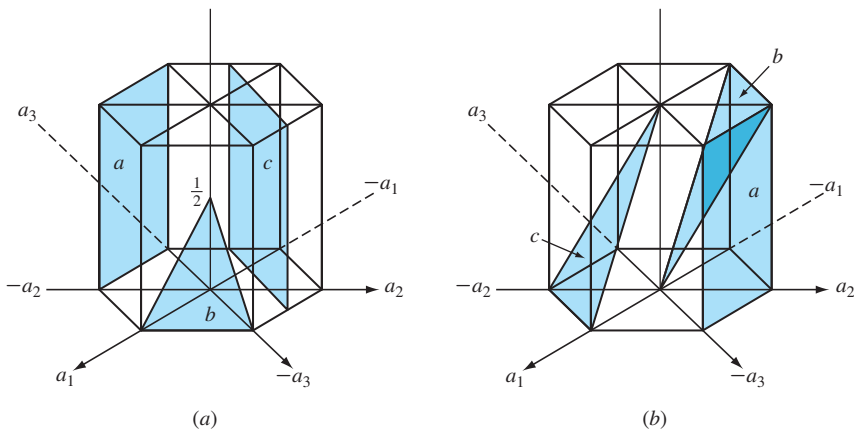


Figure P3.40

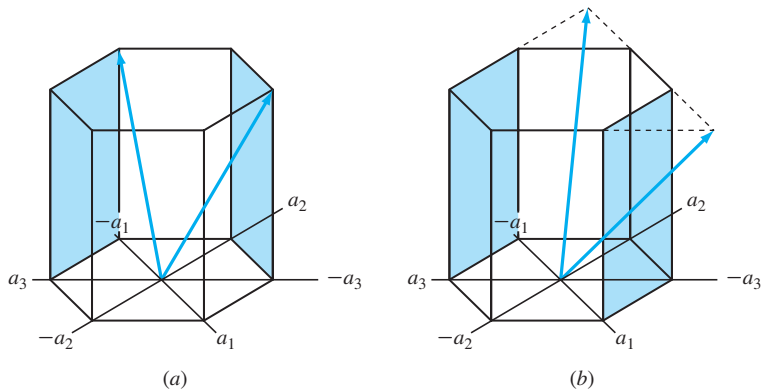


Tutorial

- 3.43** Draw the following crystallographic planes in an FCC unit cell, and list the position coordinates of the atoms whose centers are intersected by each of the planes:
 (a) (010) (b) (011) (c) (111)
- 3.44** A cubic plane has the following axial intercepts: $a = \frac{1}{3}$, $b = -\frac{2}{3}$, $c = \frac{1}{2}$. What are the Miller indices of this plane?
- 3.45** A cubic plane has the following axial intercepts: $a = -\frac{1}{2}$, $b = -\frac{1}{2}$, $c = \frac{2}{3}$. What are the Miller indices of this plane?
- 3.46** Determine the Miller indices of the cubic crystal plane that intersects the following position coordinates: $(1, \frac{1}{2}, 1)$; $(\frac{1}{2}, 0, \frac{3}{4})$; $(1, 0, \frac{1}{2})$.
- 3.47** Determine the Miller indices of the cubic crystal plane that intersects the following position coordinates: $(0, 0, \frac{1}{2})$; $(1, 0, 0)$; $(\frac{1}{2}, \frac{1}{4}, 0)$.
- 3.48** Rodium is FCC and has a lattice constant a of 0.38044 nm. Calculate the following interplanar spacings:
 (a) d_{111} (b) d_{200} (c) d_{220}
- 3.49** Tungsten is BCC and has a lattice constant a of 0.31648 nm. Calculate the following interplanar spacings:
 (a) d_{110} (b) d_{220} (c) d_{310}
- 3.50** The d_{310} interplanar spacing in a BCC element is 0.1587 nm. (a) What is its lattice constant a ? (b) What is the atomic radius of the element? (c) What could this element be?
- 3.51** The d_{422} interplanar spacing in an FCC metal is 0.083397 nm. (a) What is its lattice constant a ? (b) What is the atomic radius of the metal? (c) What could this metal be?
- 3.52** Draw the hexagonal crystal planes whose Miller-Bravais indices are:
 (a) $(\bar{1}0\bar{1})$ (b) $(0\bar{1}1\bar{1})$ (c) $(\bar{1}\bar{2}\bar{1}0)$ (d) $(\bar{1}\bar{2}1\bar{2})$ (e) $(2\bar{1}\bar{1}1)$ (f) $(\bar{1}\bar{1}\bar{0}1)$
 (g) (1212) (h) (2200) (i) (1012) (j) (1100) (k) $(\bar{2}111)$ (l) (1012)
- 3.53** Determine the Miller-Bravais indices of the hexagonal crystal planes in Figure P3.53.

**Figure P3.53**

- 3.54** Determine the Miller-Bravais direction indices of the $-a_1$, $-a_2$, and $-a_3$ directions.
- 3.55** Determine the Miller-Bravais direction indices of the vectors originating at the center of the lower basal plane and ending at the endpoints of the upper basal plane as indicated in Figure 3.16d.
- 3.56** Determine the Miller-Bravais direction indices of the basal plane of the vectors originating at the center of the lower basal plane and exiting at the midpoints between the principal planar axes.
- 3.57** Determine the Miller-Bravais direction indices of the directions indicated in Figure P3.57.
- 3.58** The lattice constant for BCC tantalum at 20°C is 0.33026 nm and its density is 16.6 g/cm³. Calculate a value for its relative atomic mass.
- 3.59** Calculate a value for the density of FCC platinum in grams per cubic centimeter from its lattice constant a of 0.39239 nm and its atomic mass of 195.09 g/mol.

**Figure P3.57**

- 3.60** Calculate the planar atomic density in atoms per square millimeter for the following crystal planes in BCC chromium, which has a lattice constant of 0.28846 nm. Compare the values and draw a conclusion. (a) (100), (b) (110), (c) (111).
- 3.61** Calculate the planar atomic density in atoms per square millimeter for the following crystal planes in FCC gold, which has a lattice constant of 0.40788 nm. Compare the values and draw a conclusion. (a) (100), (b) (110), (c) (111).
- 3.62** Calculate the planar atomic density in atoms per square millimeter for the (0001) plane in HCP beryllium, which has a lattice constant $a = 0.22856$ nm and a c constant of 0.35832 nm. Can you make any observations about this plane?
- 3.63** Calculate the linear atomic density in atoms per millimeter for the following directions in BCC vanadium, which has a lattice constant of 0.3039 nm: (a) [100], (b) [110], (c) [111]. Determine the repeat distance along each direction.
- 3.64** Calculate the linear atomic density in atoms per millimeter for the following directions in FCC iridium, which has a lattice constant of 0.38389 nm: (a) [100], (b) [110], (c) [111]. Determine the repeat distance along each direction.
- 3.65** Titanium goes through a polymorphic change from BCC to HCP crystal structure upon cooling through 332°C. Calculate the percentage change in volume when the crystal structure changes from BCC to HCP. The lattice constant a of the BCC unit cell at 882°C is 0.332 nm, and the HCP unit cell has $a = 0.2950$ nm and $c = 0.4683$ nm.
- 3.66** Pure iron goes through a polymorphic change from BCC to FCC upon heating through 912°C. Calculate the volume change associated with the change in crystal structure from BCC to FCC if at 912°C the BCC unit cell has a lattice constant $a = 0.293$ nm and the FCC unit cell $a = 0.363$ nm.
- 3.67** Derive Bragg's law by using the simple case of incident X-ray beams being diffracted by parallel planes in a crystal.
- 3.68** A sample of BCC metal was placed in an X-ray diffractometer using X-rays with a wavelength of $\lambda = 0.1541$ nm. Diffraction from the {221} planes was obtained at $2\theta = 88.838^\circ$. Calculate a value for the lattice constant a for this BCC elemental metal. (Assume first-order diffraction, $n = 1$.)
- 3.69** X-rays of an unknown wavelength are diffracted by a gold sample. The 2θ angle was 64.582° for the {220} planes. What is the wavelength of the X-rays used? (The lattice constant of gold = 0.40788 nm; assume first-order diffraction, $n = 1$.)
- 3.70** An X-ray diffractometer recorder chart for an element that has either the BCC or the FCC crystal structure showed diffraction peaks at the following 2θ angles: 41.069°, 47.782°, 69.879°, and 84.396°. The wavelength of the incoming radiation was 0.15405 nm. (X-ray diffraction data courtesy of the International Centre for Diffraction Data.)
(a) Determine the crystal structure of the element.
(b) Determine the lattice constant of the element.
(c) Identify the element.
- 3.71** An X-ray diffractometer recorder chart for an element that has either the BCC or the FCC crystal structure showed diffraction peaks at the following 2θ angles: 38.60°, 55.71°, 69.70°, 82.55°, 95.00°, and 107.67°. Wavelength λ of the incoming radiation was 0.15405 nm.
(a) Determine the crystal structure of the element.
(b) Determine the lattice constant of the element.
(c) Identify the element.

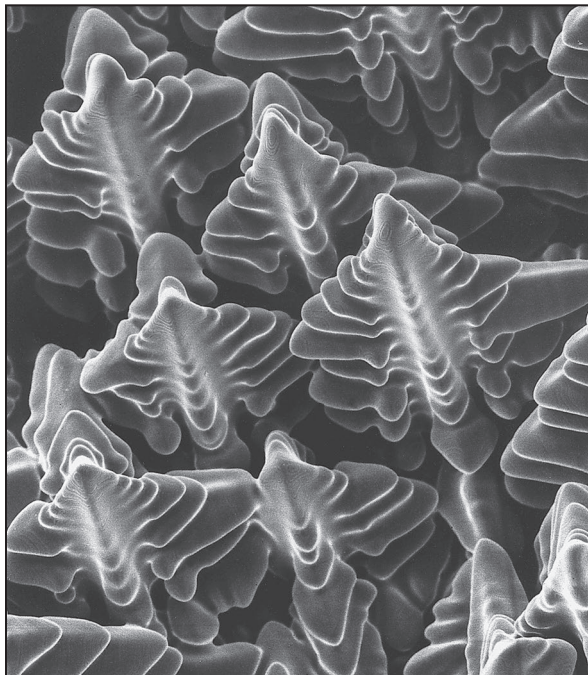
- 3.72** An X-ray diffractometer recorder chart for an element that has either the BCC or the FCC crystal structure showed diffraction peaks at the following 2θ angles: 36.191° , 51.974° , 64.982° , and 76.663° . The wavelength of the incoming radiation was 0.15405 nm.
- Determine the crystal structure of the element.
 - Determine the lattice constant of the element.
 - Identify the element.
- 3.73** An X-ray diffractometer recorder chart for an element that has either the BCC or the FCC crystal structure showed diffraction peaks at the following 2θ angles: 40.663° , 47.314° , 69.144° , and 83.448° . Wavelength λ of the incoming radiation was 0.15405 nm.
- Determine the crystal structure of the element.
 - Determine the lattice constant of the element.
 - Identify the element.

Synthesis and Evaluation Problems

- 3.74** Do you expect iron and silver to have the same (a) atomic packing factor, (b) volume of unit cell, (c) number of atoms per unit cell, and (d) coordination number? How about gold and silver? How about titanium and silver?
- 3.75** In a cubic unit cell, draw the (111) and (011) planes. Highlight the intersection of the two planes. What are the direction indices of the intersection line?
- 3.76** In a cubic unit cell, draw the (011) and (110) planes. Highlight the intersection of the two planes. What are the direction indices of the intersection line?
- 3.77** Show using geometry that the ideal c/a ratio of the hexagonal close-packed unit cell (when atoms are perfect spheres) is 1.633. Hint: Draw the center atom in the top basal plane in contact with the three atoms in the center of the HCP cell; connect the centers of the three atoms inside the HCP cell to each other and to the atom at the center of one of the basal planes.
- 3.78** Assuming that the volume of an HCP metal cell (larger cell) is 0.09130 nm^3 and the c/a ratio is 1.856, determine (a) the values for c and a , and (b) the radius, R , of the atom. (c) If you were told that the metal is zinc, would you be surprised? How do you explain the discrepancy?
- 3.79** Assuming that the volume of an HCP metal cell (larger cell) is 0.01060 nm^3 and the c/a ratio is 1.587, determine (a) the values for c and a , and (b) the radius, R , of the atom. (c) If you were told that the metal is titanium, does the calculated R match that of Ti? How do you explain the discrepancy?
- 3.80** The structure of NaCl (an ionic material) is given in Figure 2.18b. Determine (a) its lattice constant a , and (b) its density. Hint: Since NaCl is ionic, use the ion radius data and note the atomic radii.
- 3.81** The unit cell structure of the ionic solid, CsI, is similar to that in Figure 2.18a. Determine (a) its packing factor, and (b) compare this packing factor with that of BCC metals. Explain the difference, if any.
- 3.82** Iron (below 912°C) and tungsten are both BCC with significantly different atomic radii. However, they have the same atomic packing factor of 0.68. How do you explain this?
- 3.83** Verify that there are eight atoms inside a diamond cubic structure (see Figure 2.23b and c). Draw a 3D schematic of the atoms inside the cell.

- 3.84** The lattice constant for the diamond cubic structure of diamond is 0.357 nm. Diamond is metastable, meaning that it will transform to graphite at elevated temperatures. If this transformation occurs, what percent volume change will occur? (Density of graphite is 2.25 gr/cm³)
- 3.85** Calculate the center-to-center distance between adjacent atoms of gold along the following directions: (a) [100], (b) [101], (c) [111], and (d) [102]. Speculate as to why such information may be important in understanding the behavior of the material.
- 3.86** Calculate the center-to-center distance between adjacent atoms of tungsten along the following directions: (a) [100], (b) [101], (c) [111], and (d) [102]. Speculate as to why such information may be important in understanding the behavior of the material.
- 3.87** A plane in a cubic crystal intersects the x axis at 0.25, the y axis at 2, and is parallel to the z axis. What are the Miller indices for this plane? Draw this plane in a single cube and show all key dimensions.
- 3.88** A plane in a cubic crystal intersects the x axis at 3, the y axis at 1, and the z axis at 1. What are the Miller indices for this plane? Draw this plane in a single cube and show all key dimensions.
- 3.89** A plane in a hexagonal crystal intersects at the a_1 axis at -1 , the a_2 axis at 1, and the c axis at infinity. What are the Miller indices for this plane? Draw this plane in a hexagonal unit cell and show all key dimensions.
- 3.90** A plane in a hexagonal crystal intersects at the a_1 axis at 1, the a_2 axis at 1, and the c axis at 0.5. What are the Miller indices for this plane? Draw this plane in a hexagonal unit cell and show all key dimensions.
- 3.91** Without drawing any of the hexagonal planes given below, determine which of the planes is, in fact, not a plane. (a) (1010), (b) (1010), and (c) (1110).
- 3.92** Name as many carbon allotropes as you can, and discuss their crystal structure.
- 3.93** A thin layer of aluminum nitride is sometimes deposited on silicon wafers at high temperatures (1000°C). The coefficient of thermal expansion and the lattice constant of the silicon crystal is different than that of aluminum nitride. Will this cause a problem? Explain.
- 3.94** An unknown material is being analyzed using X-ray diffraction techniques. However, the diffraction patterns are extremely broad (no clear peaks are visible). (a) What does this tell you about the material? (b) What are some of the tests that you can perform to help identify the material or narrow the possibilities?
- 3.95** Explain, in general terms, why many polymers and some ceramic glasses have an amorphous or semicrystalline structure.
- 3.96** Explain how ultra-rapid cooling of some metal alloys produces metallic glass.

Solidification and Crystalline Imperfections



(Courtesy of Stan David and Lynn Boatner, Oak Ridge National Library)

When molten alloys are cast, solidification starts at the walls of the mold as it is being cooled. The solidification of an alloy (as opposed to a pure metal) takes place not at a specific temperature but over a range of temperatures. While the alloy is in this range, it has a pasty form that consists of solid, treelike structures called *dendrites* (meaning *treelike*), and liquid metal. The size and shape of the dendrite depends on the cooling rate. The liquid metal existing among these three-dimensional dendritic structures eventually solidifies to form a completely solid structure that we refer to as the grain structure. The study of dendrites is important because they influence compositional variations, porosity, and segregation and therefore the properties of the cast metal. The figure shows the three-dimensional structure of dendrites. The figure shows a “forest” of dendrites formed during the solidification of a nickel-based superalloy.¹ ■

¹ <http://mgnews.msfc.nasa.gov/IDGE/IDGE.html>

LEARNING OBJECTIVES

By the end of this chapter, students will be able to

1. Describe the process of the solidification of metals, distinguishing between homogeneous and heterogeneous nucleation.
2. Describe the two energies involved in the solidification process of a pure metal, and write the equation for the total free-energy change associated with the transformation of the liquid state to solid nucleus.
3. Distinguish between equiaxed and columnar grains and the advantage of the former over the latter.
4. Distinguish between single-crystal and polycrystalline materials, and explain why single-crystal and polycrystalline forms of the material have different mechanical properties.
5. Describe various forms of metallic solid solutions, and explain the differences between solid solution and mixture alloys.
6. Classify various types of crystalline imperfections, and explain the role of defects in the mechanical and electrical properties of crystalline materials.
7. Determine the ASTM grain size number and average grain size diameter, and describe the importance of grain size and grain boundary density on the behavior of crystalline materials.
8. Learn how and why optical microscopy, SEM, TEM, HRTEM, AFM, and STM techniques are used to understand more about the internal and surface structures of materials at various magnifications.
9. Explain, in general terms, why alloys are preferred materials over pure metals for structural applications.

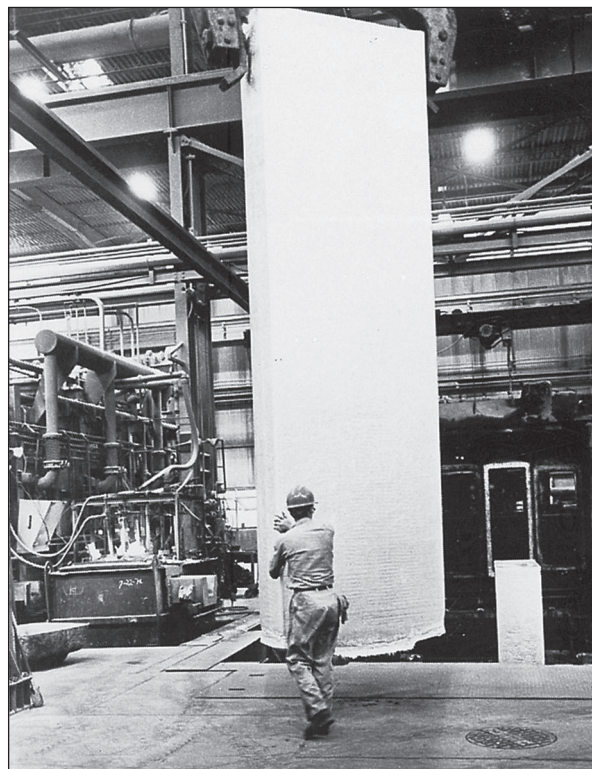
4.1 SOLIDIFICATION OF METALS

The solidification of metals and alloys is an important industrial process since most metals are melted and then cast into a semifinished or finished shape. Figure 4.1 shows a large, semicontinuously² cast aluminum ingot that will be further fabricated into aluminum alloy flat products. It illustrates the large scale on which the casting process (solidification) of metals is sometimes carried out.

In general, the solidification of a metal or alloy can be divided into the following steps:

1. The formation of stable **nuclei** in the melt (nucleation) (Fig. 4.2a)
2. The growth of nuclei into crystals (Fig. 4.2b) and the formation of a grain structure (Fig. 4.2c)

² A semicontinuously cast ingot is produced by solidifying molten metal (e.g., aluminum or copper alloys) in a mold that has a movable bottom block (see Fig. 4.8) that is slowly lowered as the metal is solidified. The prefix *semi-* is used since the maximum length of the ingot produced is determined by the depth of the pit into which the bottom block is lowered.

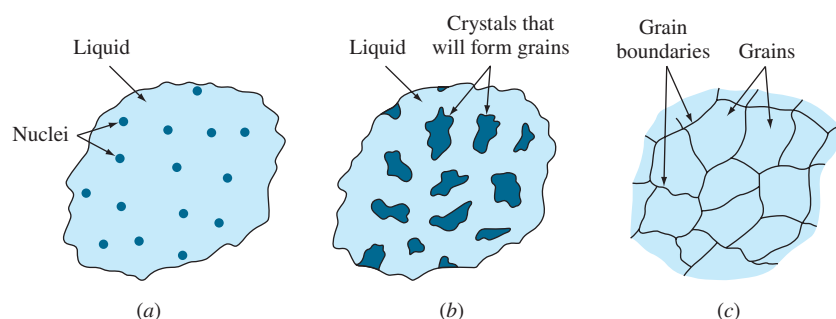
**Figure 4.1**

Large, semicontinuously cast aluminum alloy ingot being removed from casting pit. Ingots of this type are subsequently hot- and cold-rolled into plate or sheet.

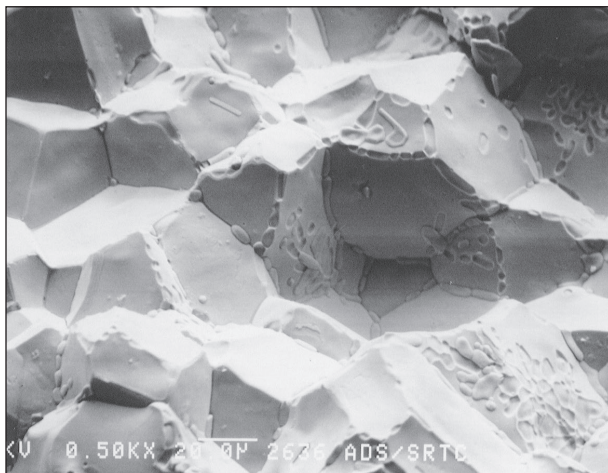
(Courtesy of Reynolds Metals Co.)



Animation

**Figure 4.2**

Schematic illustration showing the several stages in the solidification of metals: (a) formation of nuclei, (b) growth of nuclei into crystals, and (c) joining together of crystals to form grains and associated grain boundaries. Note that the grains are randomly oriented.

**Figure 4.3**

An image showing the equiaxed grains of a nickel–molybdenum alloy at a magnification of 50,000.

(Source: U.S. Department of Energy)

The shapes of some real grains formed by the solidification of a nickel–molybdenum alloy are shown in Figure 4.3. The shape that each grain acquires after solidification of the metal depends on many factors, of which thermal gradients are important. The grains shown in Figure 4.3 are *equiaxed* since their growth is about equal in all directions.

4.1.1 The Formation of Stable Nuclei in Liquid Metals

The two main mechanisms by which the nucleation of solid particles in liquid metal occurs are homogeneous nucleation and heterogeneous nucleation.

Homogeneous Nucleation Homogeneous nucleation is considered first since it is the simplest case of nucleation. **Homogeneous nucleation** in a liquid melt occurs when the metal itself provides the atoms needed to form nuclei. Let us consider the case of a pure metal solidifying. When a pure liquid metal is cooled below its equilibrium freezing temperature to a sufficient degree, many homogeneous nuclei are created by slow-moving atoms bonding together. Homogeneous nucleation usually requires a considerable amount of undercooling, which may be as much as several hundred degrees Celsius for some metals (see Table 4.1). For a nucleus to be stable so that it can grow into a crystal, it must reach a *critical size*. A cluster of atoms bonded together that is less than the critical size is called an **embryo**, and one that is larger than the critical size is called a **nucleus**. Because of their instability, embryos are continuously being formed and redissolved in the molten metal due to the agitation of the atoms.

Energies Involved in Homogeneous Nucleation In the homogeneous nucleation of a solidifying pure metal, two kinds of energy changes must be considered: (1) the *volume (or bulk) free energy* released by the liquid-to-solid transformation and (2) the *surface energy* required to form the new solid surfaces of the solidified particles.

Table 4.1 Values for the freezing temperature, heat of fusion, surface energy, and maximum undercooling for selected metals

Metal	Freezing Temp.		Heat of Fusion (J/cm ³)	Surface Energy (J/cm ²)	Maximum Undercooling, Observed (ΔT[°C])
	°C	K			
Pb	327	600	280	33.3 × 10 ⁻⁷	80
Al	660	933	1066	93 × 10 ⁻⁷	130
Ag	962	1235	1097	126 × 10 ⁻⁷	227
Cu	1083	1356	1826	177 × 10 ⁻⁷	236
Ni	1453	1726	2660	255 × 10 ⁻⁷	319
Fe	1535	1808	2098	204 × 10 ⁻⁷	295
Pt	1772	2045	2160	240 × 10 ⁻⁷	332

(Source: B. Chalmers, *Solidification of Metals*, Wiley, 1964.)

When a pure liquid metal such as lead is cooled below its equilibrium freezing temperature, the driving energy for the liquid-to-solid transformation is the difference in the volume (bulk) free energy ΔG_v of the liquid and that of the solid. If ΔG_v is the change in free energy between the liquid and solid per unit volume of metal, then the free-energy change for a *spherical nucleus* of radius r is $\frac{4}{3}\pi r^3 \Delta G_v$ since the volume of a sphere is $\frac{4}{3}\pi r^3$. The change in volume free energy versus radius of an embryo or nucleus is shown schematically in Figure 4.4 as the lower curve and is a negative quantity since energy is released by the liquid-to-solid transformation.

However, there is an energy opposing the formation of embryos and nuclei, the energy required to form the surface of these particles. The energy needed to create a surface for these spherical particles, ΔG_s , is equal to the specific surface free energy of the particle, γ , times the area of the surface of the sphere, or $4\pi r^2 \gamma$, where $4\pi r^2$ is the surface area of a sphere. This retarding energy ΔG_s for the formation of the solid particles is shown graphically in Figure 4.4 by an upward curve in the positive upper half of the figure. The total free energy associated with the formation of an embryo or nucleus, which is the sum of the volume free-energy and surface free-energy changes, is shown in Figure 4.4 as the middle curve. In equation form, the total free-energy change for the formation of a spherical embryo or nucleus of radius r formed in a freezing pure metal is

$$\Delta G_T = \frac{4}{3}\pi r^3 \Delta G_v + 4\pi r^2 \gamma \quad (4.1)$$

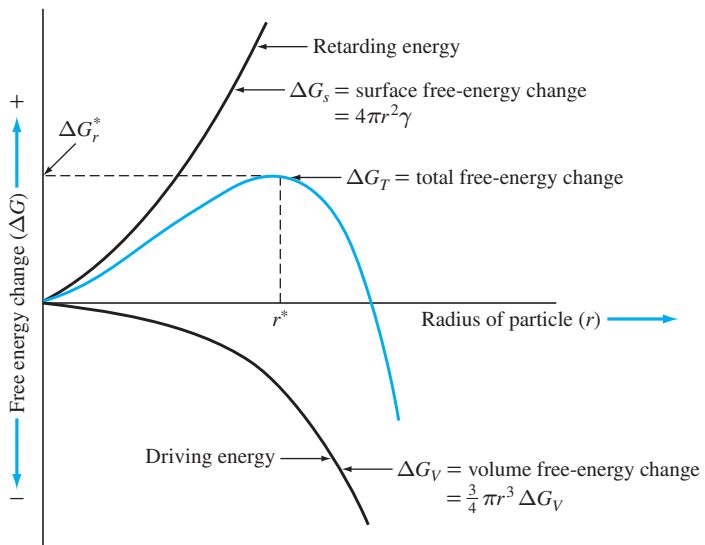
where ΔG_T = total free-energy change

r = radius of embryo or nucleus

ΔG_v = volume free energy

γ = specific surface free energy

In nature, a system can change spontaneously from a higher- to a lower-energy state. In the case of the freezing of a pure metal, if the solid particles formed upon freezing have radii less than the **critical radius** r^* , the energy of the system will be

**Figure 4.4**

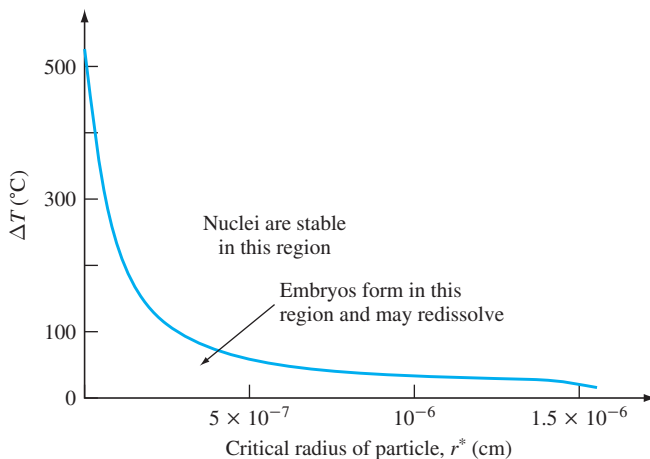
Free-energy change ΔG versus radius of embryo or nucleus created by the solidifying of a pure metal. If the radius of the particle is greater than r^* , a stable nucleus will continue to grow.

lowered if they redissolve. These small embryos can, therefore, redissolve in the liquid metal. However, if the solid particles have radii greater than r^* , the energy of the system will be lowered when these particles (nuclei) grow into larger particles or crystals (Fig. 4.2b). When r reaches the critical radius r^* , ΔG_T has its maximum value of ΔG^* (Fig. 4.4).

A relationship among the size of the critical nucleus, surface free energy, and volume free energy for the solidification of a pure metal can be obtained by differentiating Eq. 4.1. The differential of the total free energy ΔG_T with respect to r is zero when $r = r^*$ since the total free energy versus radius of the embryo or nucleus plot is then at a maximum and the slope $d(\Delta G_T)/dr = 0$. Thus,

$$\begin{aligned} \frac{d(\Delta G_T)}{dr} &= \frac{d}{dr} \left(\frac{4}{3} \pi r^3 \Delta G_V + 4\pi r^2 \gamma \right) \\ \frac{12}{3} \pi r^{*2} \Delta G_V + 8\pi r^* \gamma &= 0 \quad (4.1a) \\ r^* &= -\frac{2\gamma}{\Delta G_V}. \end{aligned}$$

Critical Radius versus Undercooling The greater the degree of undercooling ΔT below the equilibrium melting temperature of the metal, the greater the change in

**Figure 4.5**

Critical radius of copper nuclei versus degree of undercooling ΔT .

(Source: B. Chalmers, *Principles of Solidification*, Wiley, 1964.)

volume free energy ΔG_V . However, the change in free energy due to the surface energy ΔG_s does not change much with temperature. Thus, the critical nucleus size is determined mainly by ΔG_V . Near the freezing temperature, the critical nucleus size must be infinite since ΔT approaches zero. As the amount of undercooling increases, the critical nucleus size decreases. Figure 4.5 shows the variation in critical nucleus size for copper as a function of undercooling. The maximum amount of undercooling for homogeneous nucleation in the pure metals listed in Table 4.1 is from 327°C to 1772°C. The critical-sized nucleus is related to the amount of undercooling by the relation

$$r^* = \frac{2\gamma T_m}{\Delta H_f \Delta T} \quad (4.2)$$

where r^* = critical radius of nucleus

γ = surface free energy

ΔH_f = latent heat of fusion

ΔT = amount of undercooling at which nucleus is formed

Example Problem 4.1 shows how a value for the number of atoms in a critical nucleus can be calculated from experimental data.

EXAMPLE PROBLEM 4.1

- Calculate the critical radius (in centimeters) of a homogeneous nucleus that forms when pure liquid copper solidifies. Assume ΔT (undercooling) = $0.2T_m$. Use data from Table 4.1.
- Calculate the number of atoms in the critical-sized nucleus at this undercooling.

Solution

- a. Calculation of critical radius of nucleus:

$$r^* = \frac{2\gamma T_m}{\Delta H_f \Delta T} \quad (4.2)$$

$$\Delta T = 0.2T_m = 0.2(1083^\circ\text{C} + 273) = (0.2 \times 1356 \text{ K}) = 271 \text{ K}$$

$$\gamma = 177 \times 10^{-7} \text{ J/cm}^2 \quad \Delta H_f = 1826 \text{ J/cm}^3 \quad T_m = 1083^\circ\text{C} = 1356 \text{ K}$$

$$r^* = \frac{2(177 \times 10^{-7} \text{ J/cm}^2)(1356 \text{ K})}{(1826 \text{ J/cm}^3)(271 \text{ K})} = 9.70 \times 10^{-8} \text{ cm} \blacktriangleleft$$

- b. Calculation of number of atoms in critical-sized nucleus:

$$\begin{aligned} \text{Vol. of critical-sized nucleus} &= \frac{4}{3}\pi r^{*3} = \frac{4}{3}\pi(9.70 \times 10^{-8} \text{ cm})^3 \\ &= 3.82 \times 10^{-21} \text{ cm}^3 \end{aligned}$$

$$\begin{aligned} \text{Vol. of unit cell of Cu } (a = 0.361 \text{ nm}) &= a^3 = (3.61 \times 10^{-8} \text{ cm})^3 \\ &= 4.70 \times 10^{-23} \text{ cm}^3 \end{aligned}$$

Since there are four atoms per FCC unit cell,

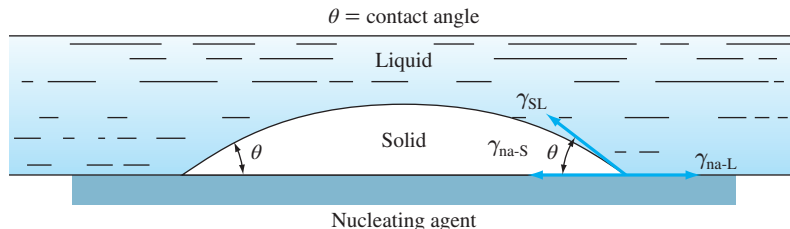
$$\text{Volume/atom} = \frac{4.70 \times 10^{-23} \text{ cm}^3}{4} = 1.175 \times 10^{-23} \text{ cm}^3$$

Thus, the number of atoms per homogeneous critical nucleus is

$$\frac{\text{Volume of nucleus}}{\text{Volume/atom}} = \frac{3.82 \times 10^{-21} \text{ cm}^3}{1.175 \times 10^{-23} \text{ cm}^3} = 325 \text{ atoms} \blacktriangleleft$$

Heterogeneous Nucleation **Heterogeneous nucleation** is nucleation that occurs in a liquid on the surfaces of its container, insoluble impurities, and other structural material that lowers the critical free energy required to form a stable nucleus. Since large amounts of undercooling do not occur during industrial casting operations and usually range between 0.1°C and 10°C , the nucleation must be heterogeneous and not homogeneous.

For heterogeneous nucleation to take place, the solid nucleating agent (impurity solid or container) must be wetted by the liquid metal. Also the liquid should solidify easily on the nucleating agent. Figure 4.6 shows a nucleating agent (substrate) that is wetted by the solidifying liquid, creating a low contact angle θ between the solid metal and the nucleating agent. Heterogeneous nucleation takes place on the nucleating agent because the surface energy to form a stable nucleus is lower on this material than in the pure liquid itself (homogeneous nucleation). Since the surface energy is lower for heterogeneous nucleation, the total free-energy change for the formation of a stable nucleus will be lower, and the critical size of the nucleus will be smaller. Thus, a much smaller amount of undercooling is required to form a stable nucleus produced by heterogeneous nucleation.

**Figure 4.6**

Heterogeneous nucleation of a solid on a nucleating agent. na = nucleating agent, SL = solid-liquid, S = solid, L = liquid; θ = contact angle.

(Source: J.H. Brophy, R.M. Rose and J. Wulff, *The Structure and Properties of Materials*, vol. II: "Thermodynamics of Structure," Wiley, 1964, p. 105.)

4.1.2 Growth of Crystals in Liquid Metal and Formation of a Grain Structure

After stable nuclei have been formed in a solidifying metal, these nuclei grow into crystals, as shown in Figure 4.2b. In each solidifying crystal, the atoms are arranged in an essentially regular pattern, but the orientation of each crystal varies (Fig. 4.2b). When solidification of the metal is finally completed, the crystals join together in different orientations and form crystal boundaries at which changes in orientation take place over a distance of a few atoms (Fig. 4.2c). Solidified metal containing many crystals is said to be *polycrystalline*. The crystals in the solidified metal are called **grains**, and the surfaces between them, *grain boundaries*.

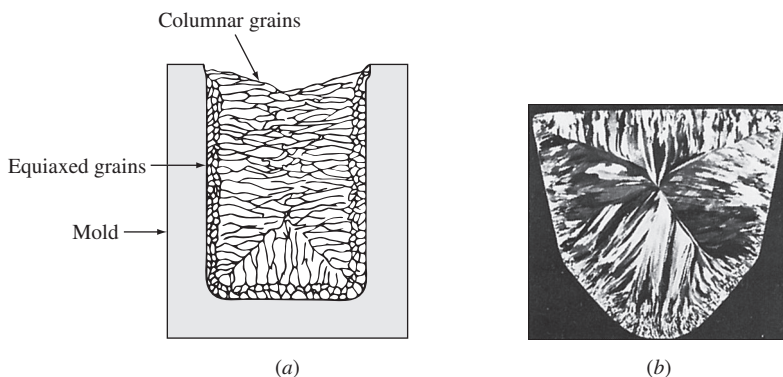
The number of nucleation sites available to the freezing metal will affect the grain structure of the solid metal produced. If relatively few nucleation sites are available during solidification, a coarse, or large-grain, structure will be produced. If many nucleation sites are available during solidification, a fine-grain structure will result. Almost all engineering metals and alloys are cast with a fine-grain structure since this is the most desirable type for strength and uniformity of finished metal products.

When a relatively pure metal is cast into a stationary mold without the use of *grain refiners*,³ two major types of grain structures are usually produced:

1. Equiaxed grains
2. Columnar grains

If the nucleation and growth conditions in the liquid metal during solidification are such that the crystals can grow about equally in all directions, **equiaxed grains** will be produced. Equiaxed grains are commonly found adjacent to a cold mold wall, as shown in Figure 4.7. Large amounts of undercooling near the wall create a relatively high concentration of nuclei during solidification, a condition necessary to produce the equiaxed grain structure.

³ A grain refiner is a material added to a molten metal to attain finer grains in the final grain structure.

**Figure 4.7**

(a) Schematic drawing of a solidified metal grain structure produced by using a cold mold. (b) Transverse section through an ingot of aluminum alloy 1100 (99.0% Al) cast by the Properzi method (a wheel and belt method). Note the consistency with which columnar grains have grown perpendicular to each mold face.

(b: ©ASM International)

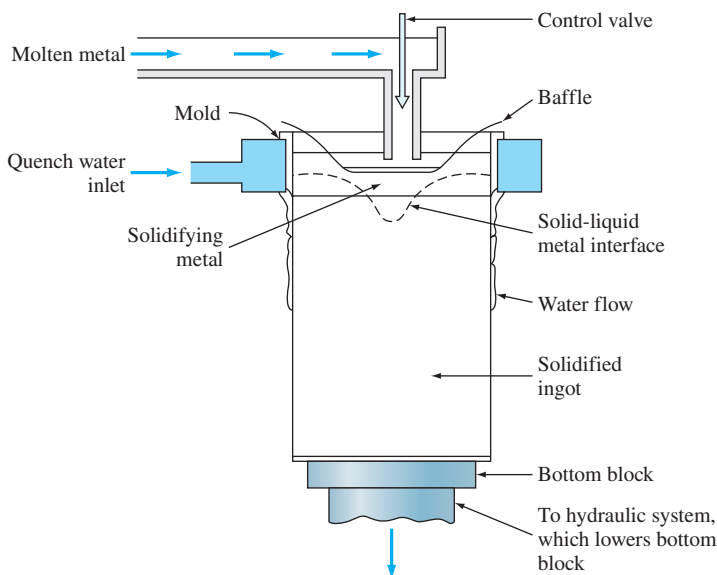
Columnar grains are long, thin, coarse grains created when a metal solidifies rather slowly in the presence of a steep temperature gradient. Relatively few nuclei are available when columnar grains are produced. Equiaxed and columnar grains are shown in Figure 4.7a. Note that in Figure 4.7b the columnar grains have grown perpendicular to the mold faces since large thermal gradients were present in those directions.

4.1.3 Grain Structure of Industrial Castings

In industry, metals and alloys are cast into various shapes. If the metal is to be further fabricated after casting, large castings of simple shapes are produced first and then fabricated further into semifinished products. For example, in the aluminum industry, common shapes for further fabrication are sheet ingots (Fig. 4.1), which have rectangular cross sections, and extrusion⁴ ingots, which have circular cross sections. For some applications, the molten metal is cast into essentially its final shape as, for example, specialized tools (see Fig. 6.3).

The large aluminum alloy sheet ingot in Figure 4.1 was cast by a direct-chill semi-continuous casting process. In this casting method, the molten metal is cast into a mold with a movable bottom block that is slowly lowered after the mold is filled (Fig. 4.8).

⁴ Extrusion is the process of converting a metal ingot into lengths of uniform cross section by forcing solid plastic metal through a die or orifice of the desired cross-sectional outline.

**Figure 4.8**

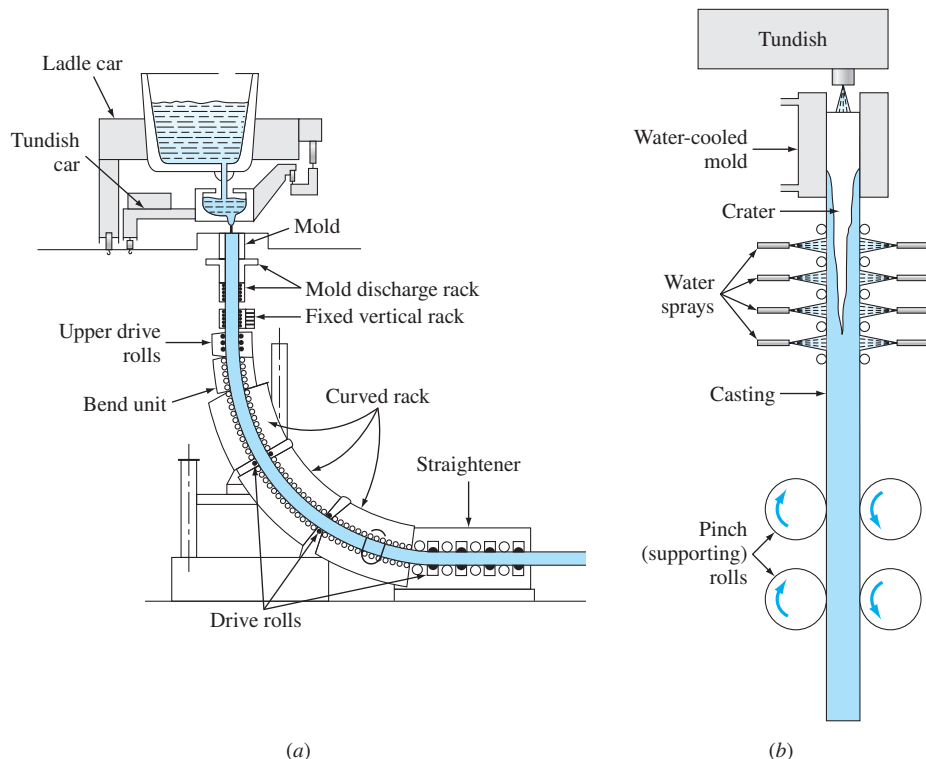
Schematic of an aluminum alloy ingot being cast in a direct-chill semicontinuous casting unit.

The mold is water-cooled by a water box, and water is also sprayed down the sides of the solidified surface of the ingot. In this way, large ingots about 15 ft long can be cast continuously, as shown in Figure 4.1. In the steel industry, about 60% of the metal is cast into stationary molds, with the remaining 40% being continuously cast, as shown in Figure 4.9.

To produce cast ingots with a fine grain size, grain refiners are usually added to the liquid metal before casting. For aluminum alloys, small amounts of grain-refining elements such as titanium, boron, or zirconium are included in the liquid metal just before the casting operation so that a fine dispersion of heterogeneous nuclei will be available during solidification. Figure 4.10 shows the effect of using a grain refiner while casting 6-in.-diameter aluminum extrusion ingots. The ingot section cast without the grain refiner has large columnar grains (Fig. 4.10a), and the section cast with the grain refiner has a fine, equiaxed grain structure (Fig. 4.10b).

4.2 SOLIDIFICATION OF SINGLE CRYSTALS

Almost all engineering crystalline materials are composed of many crystals and are therefore **polycrystalline**. However, there are a few that consist of only one crystal and are therefore *single crystals*. For example, high-temperature creep-resistant gas turbine

**Figure 4.9**

Continuous casting of steel ingots. (a) General setup and (b) close-up of the mold arrangement.

(Source: *Making, Shaping and Treating of Steel*, 10th ed., Association of Iron and Steel Engineers, 1985.)

blades. Single-crystal turbine blades are more creep resistant at high temperatures than the same blades made with an equiaxed grain structure or a columnar grain structure because at high temperatures above about half the absolute melting temperature of a metal, the grain boundaries become weaker than the grain bodies.

In growing single crystals, solidification must take place around a single nucleus so that no other crystals are nucleated and grow. To accomplish this, the interface temperature between the solid and liquid must be slightly lower than the melting point of the solid, and the liquid temperature must increase beyond the interface. To achieve this temperature gradient, the latent heat of solidification⁵ must be conducted through

⁵ The latent heat of solidification is the thermal energy released when a metal solidifies.

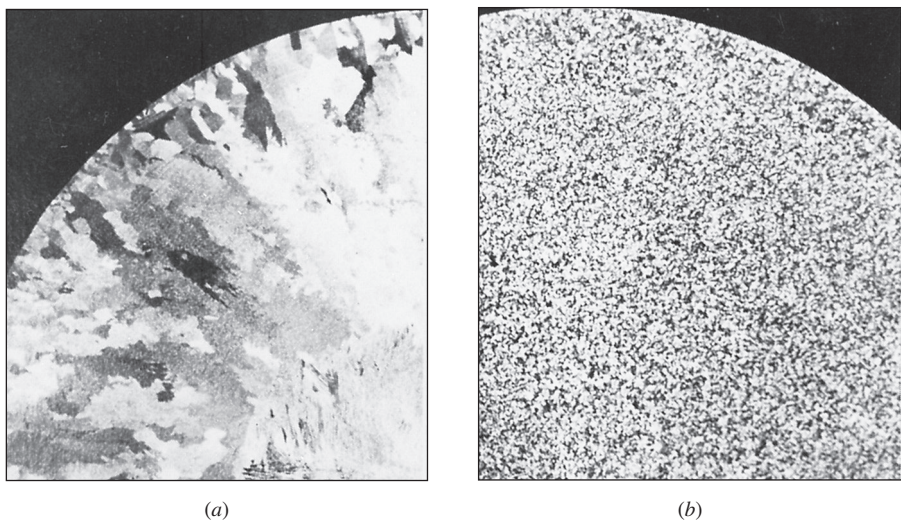


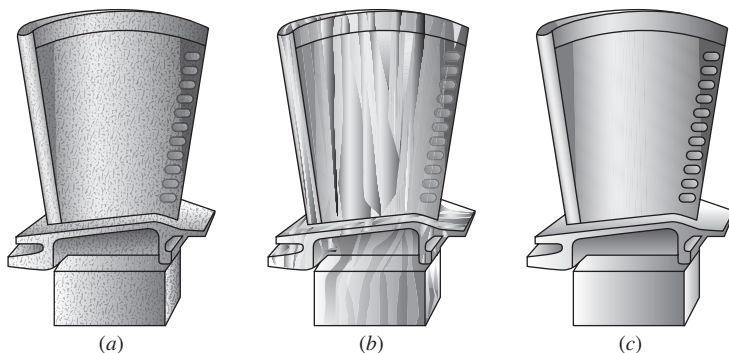
Figure 4.10

Parts of transverse sections through two 6-in.-diameter ingots of alloy 6063 (Al-0.7% Mg-0.4% Si) that were direct-chill semicontinuous cast. (a) Ingot section was cast without the addition of a grain refiner; note columnar grains and colonies of feather-like crystals near the center of the section. (b) Ingot section was cast with the addition of a grain refiner and shows a fine, equiaxed grain structure. (Tucker's reagent; actual size.)

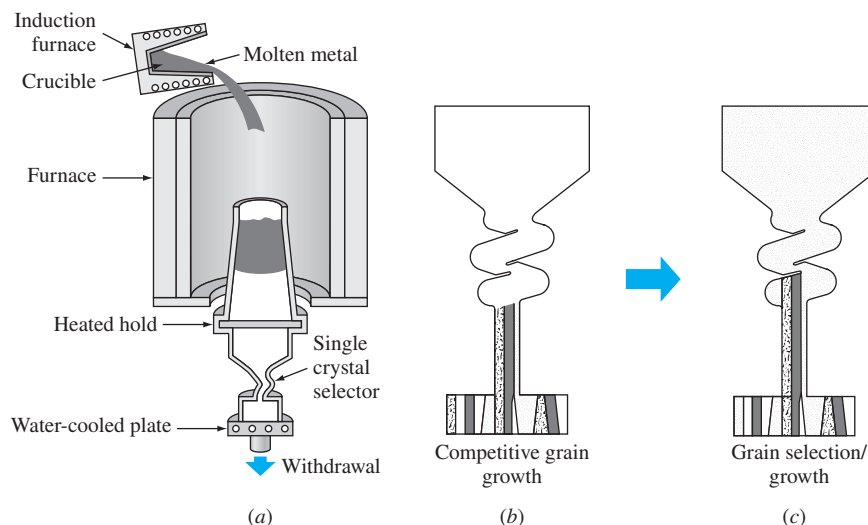
(a-b: ©ASM International)

the solidifying solid crystal. The growth rate of the crystal must be slow so that the temperature at the liquid–solid interface is slightly below the melting point of the solidifying solid. Figure 4.12a illustrates how single-crystal turbine blades can be cast, and Figure 4.12b and c show how competitive grain growth is reduced to a single grain by using a “pigtail” selector.

Another example of an industrial use of single crystals is the silicon single crystals that are sliced into wafers for solid-state electronic integrated circuit chips (see Fig. 14.1). Single crystals are necessary for this application since grain boundaries would disrupt the flow of electrons in devices made from semiconductor silicon. In industry, single crystals of silicon 8 to 12 in. (20 to 25 cm) in diameter have been grown for semiconducting device applications. One of the commonly used techniques to produce high-quality (minimization of defects) silicon single crystals is the Czochralski method. In this process, high-purity polycrystalline silicon is first melted in a nonreactive crucible and held at a temperature just above the melting point. A high-quality seed crystal of silicon of the desired orientation is lowered into the melt while it is rotated. Part of the surface of the seed crystal is melted in the liquid to

**Figure 4.11**

Different grain structures of gas turbine airfoil blades: (a) Polycrystal equiaxed, (b) polycrystal columnar, and (c) single crystal.

**Figure 4.12**

- (a) A process schematic for producing a single-crystal gas turbine airfoil.
- (b) Starter section of casting for producing a single-crystal airfoil showing competitive growth during solidification below the single-crystal selector ("pigtail").
- (c) Same as (b) but showing the survival of only one grain during solidification through the single-crystal selector.

(Source: Pratt and Whitney Co.)

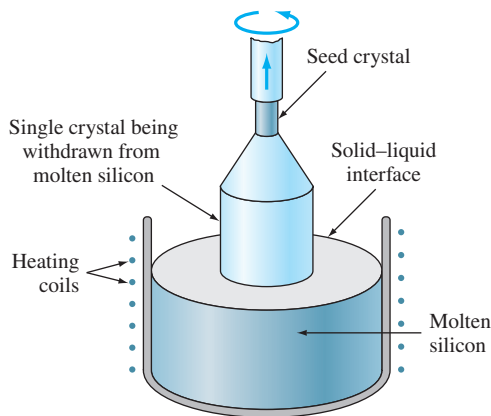


Figure 4.13
Formation of single crystal of silicon by the Czochralski process.

remove the outer strained region and to produce a surface for the liquid to solidify on. The seed crystal continues to rotate and is slowly raised from the melt. As it is raised from the melt, silicon from the liquid in the crucible adheres and grows on the seed crystal, producing a much larger diameter single crystal of silicon (Fig. 4.13). With this process, large single-crystal silicon ingots up to about 12 in. ($\cong 30$ cm) in diameter can and have been made.

4.3 METALLIC SOLID SOLUTIONS

Although very few metals are used in the pure or nearly pure state, a few are used in the nearly pure form. For example, high-purity copper of 99.99% purity is used for electronic wires because of its very high electrical conductivity. High-purity aluminum (99.99% Al) (called *super pure aluminum*) is used for decorative purposes because it can be finished with a very bright metallic surface. However, most engineering metals are combined with other metals or nonmetals to provide increased strength, higher corrosion resistance, or other desired properties.

A *metal alloy*, or simply an **alloy**, is a mixture of two or more metals or a metal (metals) and a nonmetal (nonmetals). Alloys can have structures that are relatively simple, such as that of cartridge brass, which is essentially a binary alloy (two metals) of 70 wt% Cu and 30 wt% Zn. On the other hand, alloys can be extremely complex, such as the nickel-base superalloy Inconel 718 used for jet engine parts, which has about 10 elements in its nominal composition.

The simplest type of alloy is that of the solid solution. A **solid solution** is a *solid* that consists of two or more elements atomically dispersed in a single-phase structure. In general there are two types of solid solutions: *substitutional* and *interstitial*.

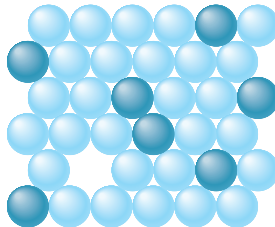


Figure 4.14
Substitutional solid solution. The dark circles represent one type of atom and the light another. The plane of atoms is a (111) plane in an FCC crystal lattice.

4.3.1 Substitutional Solid Solutions

In **substitutional solid solutions** formed by two elements, solute atoms can substitute for parent solvent atoms in a crystal lattice. Figure 4.14 shows a (111) plane in an FCC crystal lattice in which some solute atoms of one element have substituted for solvent atoms of the parent element. The crystal structure of the parent element or solvent is unchanged, but the lattice may be distorted by the presence of the solute atoms, particularly if there is a significant difference in atomic diameters of the solute and solvent atoms.

The fraction of atoms of one element that can dissolve in another can vary from a fraction of an atomic percent to 100%. The following conditions, known as *Hume-Rothery rules*, are favorable for extensive solid solubility of one element in another:

1. The diameters of the atoms of the elements must not differ by more than about 15%.
2. The crystal structures of the two elements must be the same.
3. There should be no appreciable difference in the electronegativities of the two elements so that compounds will not form.
4. The two elements should have the same valence.

If the atomic diameters of the two elements that form a solid solution differ, there will be a distortion of the crystal lattice. Since the atomic lattice can only sustain a limited amount of contraction or expansion, there is a limit in the difference in atomic diameters that atoms can have and still maintain a solid solution with the same kind of crystal structure. When the atomic diameters differ by more than about 15%, the “size factor” becomes unfavorable for extensive solid solubility.

**EXAMPLE
PROBLEM 4.2**

Using the data in the following table, predict the relative degree of atomic solid solubility of the following elements in copper:

- a. Zinc d. Nickel
- b. Lead e. Aluminum
- c. Silicon f. Beryllium

Use the scale very high, 70%–100%; high, 30%–70%; moderate, 10%–30%; low, 1%–10%; and very low, <1%.

Element	Atom Radius (nm)	Crystal Structure	Electro-negativity	Valence
Copper	0.128	FCC	1.8	+2
Zinc	0.133	HCP	1.7	+2
Lead	0.175	FCC	1.6	+2, +4
Silicon	0.117	Diamond cubic	1.8	+4
Nickel	0.125	FCC	1.8	+2
Aluminum	0.143	FCC	1.5	+3
Beryllium	0.114	HCP	1.5	+2

■ Solution

A sample calculation for the atomic radius difference for the Cu–Zn system is

$$\begin{aligned} \text{Atomic radius difference} &= \frac{\text{final radius} - \text{initial radius}}{\text{initial radius}} (100\%) \\ &= \frac{R_{\text{Zn}} - R_{\text{Cu}}}{R_{\text{Cu}}} (100\%) \quad (4.3) \\ &= \frac{0.133 - 0.128}{0.128} (100\%) = +3.91\% \end{aligned}$$

System	Atomic Radius Difference (%)	Electronegativity Difference	Predicted Relative Degree of Solid Solubility	Observed Maximum Solid Solubility (at %)
Cu–Zn	+3.9	0.1	High	38.3
Cu–Pb	+36.7	0.2	Very low	0.1
Cu–Si	-8.6	0	Moderate	11.2
Cu–Ni	-2.3	0	Very high	100
Cu–Al	+11.7	0.3	Moderate	19.6
Cu–Be	-10.9	0.3	Moderate	16.4

The predictions can be made principally on the atomic radius difference. In the case of the Cu–Si system, the difference in the crystal structures is important. There is very little electronegativity difference for all these systems. The valences are all the same except for Al and Si. In the final analysis, the experimental data must be referred to.

If the solute and solvent atoms have the same crystal structure, then extensive solid solubility is favorable. If the two elements are to show complete solid solubility in all proportions, then both elements must have the same crystal structure. Also, there cannot be too great a difference in the electronegativities of the two elements forming solid solutions, or else the highly electropositive element will lose electrons, the highly electronegative element will acquire electrons, and compound formation will result. Finally, if the two solid elements have the same valence, solid solubility will be favored. If there is a shortage of electrons between the atoms, the binding between them will be upset, resulting in conditions unfavorable for solid solubility.

4.3.2 Interstitial Solid Solutions

In interstitial solutions, the solute atoms fit into the spaces between the solvent or parent atoms. These spaces or voids are called *interstices*. The interstices available in a cubic crystal may be classified as a **cubic site** if surrounded by eight neighbors (i.e., coordination number is 8—does not occur in BCC or FCC crystals); **octahedral site** if surrounded by six neighbors (i.e., the coordination number is 6); and **tetrahedral site** if surrounded by four neighbors (i.e., the coordination number is 4). The octahedral sites in a BCC unit cell are located at $(1/2, 1, 1/2)$ or other similar-type positions, while the tetrahedral sites are located at $(1, 1/2, 1/4)$ or other similar positions. Similarly, the octahedral sites in an FCC unit cell are located at $(0, 1/2, 1)$ and $(1/2, 1/2, 1/2)$, while the tetrahedral sites are located at $(1/4, 3/4, 1/4)$ or other similar-type positions.

Interstitial solid solutions can form when the solute atoms position themselves in various interstitial sites. The solute atoms must be and always are larger than the radius of the interstitial void. Since the solute atom is larger than the interstitial void, it creates local distortion in the lattice. Examples of atoms that can form interstitial solid solutions due to their small size are hydrogen, carbon, nitrogen, and oxygen.

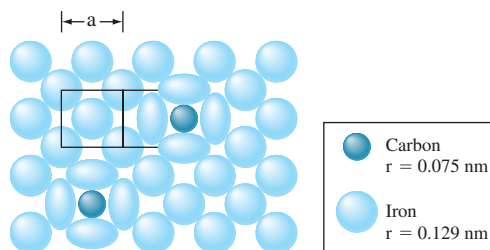


Figure 4.15

Schematic illustration of an interstitial solid solution of carbon in FCC γ iron just above 912°C showing a (100) plane. Note the distortion of the iron atoms (0.129 nm radius) around the carbon atoms (0.075 nm radius), fitting into voids of 0.053 nm radius.

(Source: L. H. Van Vlack, *Elements of Materials Science and Engineering*, 4th ed., p. 113.)

An important example of an interstitial solid solution is that formed by carbon in FCC γ iron that is stable between 912°C and 1394°C. The atomic radius of γ iron is 0.129 nm and that of carbon is 0.075 nm, so there is an atomic radius difference of 42%. However, in spite of this difference, a maximum of 2.08% of the carbon can dissolve interstitially in iron at 1148°C. Figure 4.15 illustrates this schematically by showing distortion around the carbon atoms in the γ iron lattice.

The radius of the largest interstitial hole in FCC γ iron is 0.053 nm (see Example Problem 4.3), and since the atomic radius of the carbon atom is 0.075 nm, it is not surprising that the maximum solid solubility of carbon in γ iron is only 2.08%. The radius of the largest interstitial void in BCC α iron is only 0.036 nm, and as a result, just below 727°C, only 0.025% of the carbon can be dissolved interstitially.

EXAMPLE PROBLEM 4.3

Calculate the radius of the largest interstitial void in the FCC γ iron lattice. The atomic radius of the iron atom is 0.129 nm in the FCC lattice, and the largest interstitial voids occur at the $(\frac{1}{2}, 0, 0)$, $(0, \frac{1}{2}, 0)$, $(0, 0, \frac{1}{2})$, etc., -type positions. Also, identify the classification of the given interstitial sites.

■ Solution

Figure EP4.3 shows a (100) FCC lattice plane on the yz plane. Let the radius of an iron atom be R and that of the interstitial void at the position $(0, \frac{1}{2}, 0)$ be r . Then, from Figure EP4.3,

$$2R + 2r = a \quad (4.4)$$

Also from Figure 4.15b,

$$(2R)^2 = \left(\frac{1}{2}a\right)^2 + \left(\frac{1}{2}a\right)^2 = \frac{1}{2}a^2 \quad (4.5)$$

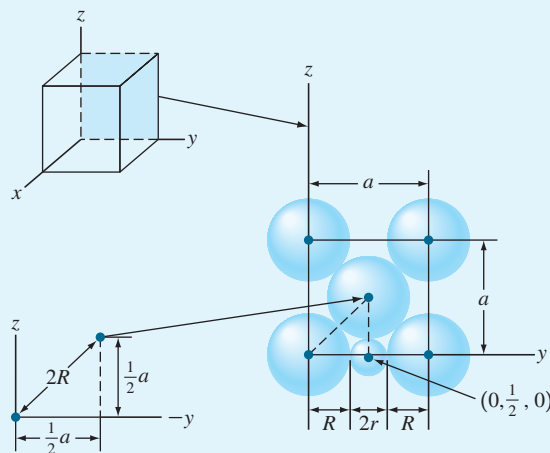
Solving for a gives

$$2R = \frac{1}{\sqrt{2}}a \text{ or } a = 2\sqrt{2}R \quad (4.6)$$

Combining Eqs. 4.4 and 4.6 gives

$$\begin{aligned} 2R + 2r &= 2\sqrt{2}R \\ r &= (\sqrt{2} - 1)R = 0.414R \\ &= (0.414)(0.129 \text{ nm}) = 0.0534 \text{ nm} \blacktriangleleft \end{aligned}$$

The given interstitial voids have four neighbors in the plane shown below, one neighbor directly above, and one neighbor directly below for a total of 6 neighbors or a coordination number of 6. This interstitial void is classified as octahedral.

**Figure EP4.3**

(100) plane of the FCC lattice containing an interstitial atom at the $(0, \frac{1}{2}, 0)$ position coordinate.

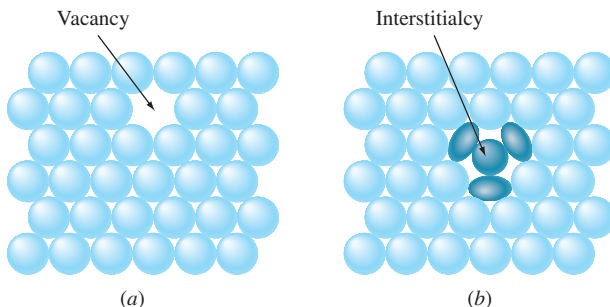
4.4 CRYSTALLINE IMPERFECTIONS

In reality, crystals are never perfect, and they contain various types of imperfections and defects that affect many of their physical and mechanical properties, which in turn affect many important engineering properties of materials such as the cold formability of alloys, the electronic conductivity of semiconductors, the rate of migration of atoms in alloys, and the corrosion of metals.

Crystal lattice imperfections are classified according to their geometry and shape. The three main divisions are (1) zero-dimensional or point defects, (2) one-dimensional or line defects (dislocations), and (3) two-dimensional defects, which include external surfaces, grain boundaries, twins, low-angle boundaries, high-angle boundaries, twists, stacking faults, voids, and precipitates. Three-dimensional macroscopic or bulk defects could also be included. Examples of these defects are pores, cracks, and foreign inclusions.

4.4.1 Point Defects

The simplest point defect is the vacancy, an atom site from which an atom is missing (Fig. 4.16a). **Vacancies** may be produced during solidification as a result of local disturbances during the growth of crystals, or they may be created by atomic rearrangements in an existing crystal due to atomic mobility. In metals, the equilibrium concentration of vacancies rarely exceeds about 1 in 10,000 atoms. Vacancies are equilibrium defects in metals, and their energy of formation is about 1 eV.

**Figure 4.16**

(a) Vacancy point defect. (b) Self-interstitial, or interstitialcy, point defect in a close-packed solid-metal lattice.

Additional vacancies in metals can be introduced by plastic deformation, rapid cooling from higher temperatures to lower ones to entrap the vacancies, and by bombardment with energetic particles such as neutrons. Nonequilibrium vacancies have a tendency to cluster, causing divacancies or trivacancies to form. Vacancies can move by exchanging positions with their neighbors. This process is important in the migration or diffusion of atoms in the solid state, particularly at elevated temperatures where atomic mobility is greater.

Sometimes an atom in a crystal can occupy an interstitial site between surrounding atoms in normal atom sites (Fig. 4.16b). This type of point defect is called a **self-interstitial**, or **interstitialcy**. These defects do not generally occur naturally because of the structural distortion they cause, but they can be introduced into a structure by irradiation.

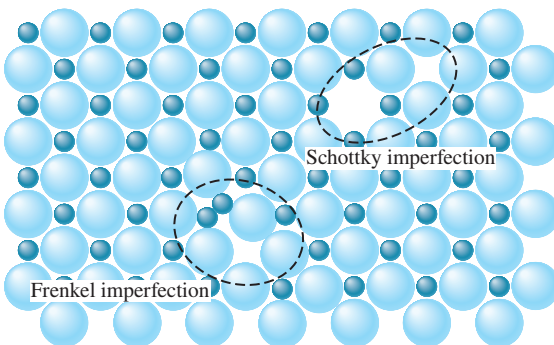
In ionic crystals, point defects are more complex due to the need to maintain electrical neutrality. When two oppositely charged ions are missing from an ionic crystal, a cation-anion divacancy is created that is known as a **Schottky imperfection** (Fig. 4.17). If a positive cation moves into an interstitial site in an ionic crystal, a cation vacancy is created in the normal ion site. This vacancy-interstitialcy pair is called a **Frenkel⁶ imperfection** (Fig. 4.17). The presence of these defects in ionic crystals increases their electrical conductivity.

Impurity atoms of the substitutional or interstitial type are also point defects and may be present in metallic or covalently bonded crystals. For example, very small amounts of substitutional impurity atoms in pure silicon can greatly affect its electrical conductivity for use in electronic devices. Impurity ions are also point defects in ionic crystals.

4.4.2 Line Defects (Dislocations)

Line imperfections, or **dislocations**, in crystalline solids are defects that cause lattice distortion centered around a line. Dislocations are created during the solidification of

⁶ Yakov Ilyich Frenkel (1894–1954). Russian physicist who studied defects in crystals. His name is associated with the vacancy-interstitialcy defect found in some ionic crystals.

**Figure 4.17**

Two-dimensional representation of an ionic crystal illustrating a Schottky defect and a Frenkel defect.

(Source: Wulff et al., *Structure and Properties of Materials*, Vol. I: "Structure," Wiley, 1964, p. 78.)

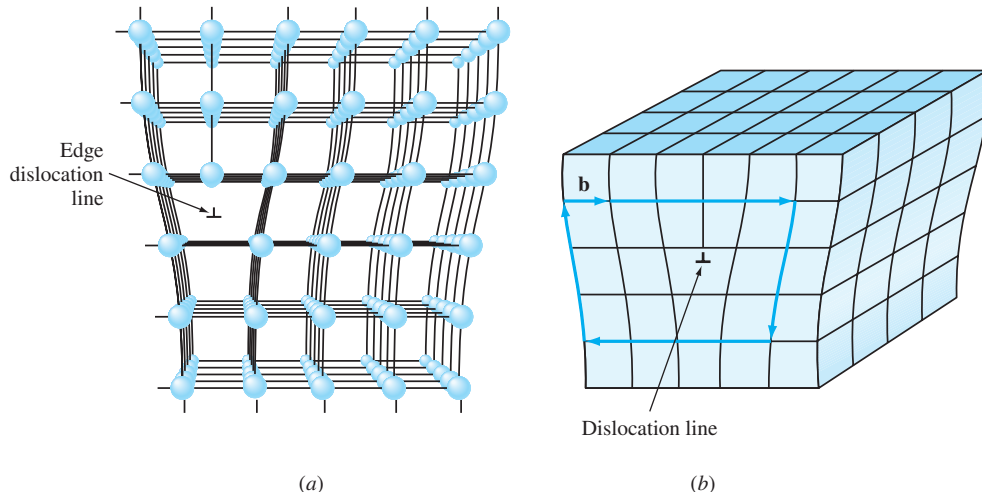
crystalline solids. They are also formed by the permanent or plastic deformation of crystalline solids, vacancy condensation, and atomic mismatch in solid solutions.

The two main types of dislocations are the *edge* and *screw types*. A combination of the two gives *mixed dislocations*, which have edge and screw components. An edge dislocation is created in a crystal by the insertion of an extra half plane of atoms, as shown in Figure 4.18a just above the symbol \perp . The inverted “tee,” \perp , indicates a positive edge dislocation, whereas the upright “tee,” T , indicates a negative edge dislocation.

The displacement distance of the atoms around the dislocation is called the *slip* or *Burgers vector* \mathbf{b} and is *perpendicular* to the edge-dislocation line (Fig. 4.18b). Dislocations are nonequilibrium defects, and they store energy in the distorted region of the crystal lattice around the dislocation. The edge dislocation has a region of compressive strain at the extra half plane and a region of tensile strain below the extra half plane of atoms (Fig. 4.19a).

The screw dislocation can be formed in a perfect crystal by applying upward and downward shear stresses to regions of a perfect crystal that have been separated by a cutting plane, as shown in Figure 4.20a. These shear stresses introduce a region of distorted crystal lattice in the form of a spiral ramp of distorted atoms or screw dislocation (Fig. 4.20b). The region of distorted crystal is not well defined and is at least several atoms in diameter. A region of shear strain is created around the screw dislocation in which energy is stored (Fig. 4.19b). The slip or Burgers vector of the screw dislocation is *parallel* to the dislocation line, as shown in Figure 4.20b.

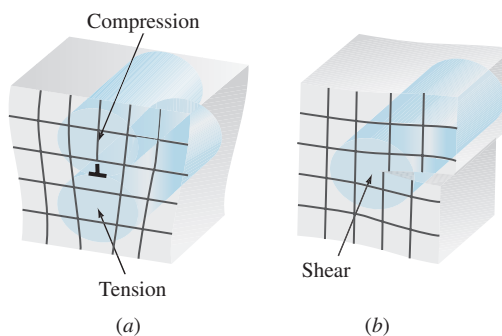
Most dislocations in crystals are of the mixed type, having edge and screw components. In the curved dislocation line AB in Figure 4.21, the dislocation is of the pure screw type at the left where it enters the crystal and of the pure edge type on the right where it leaves the crystal. Within the crystal, the dislocation is of the mixed type, with edge and screw components.

**Figure 4.18**

(a) Positive edge dislocation in a crystalline lattice. A linear defect occurs in the region just above the inverted “tee,” \perp , where an extra half plane of atoms has been wedged in.

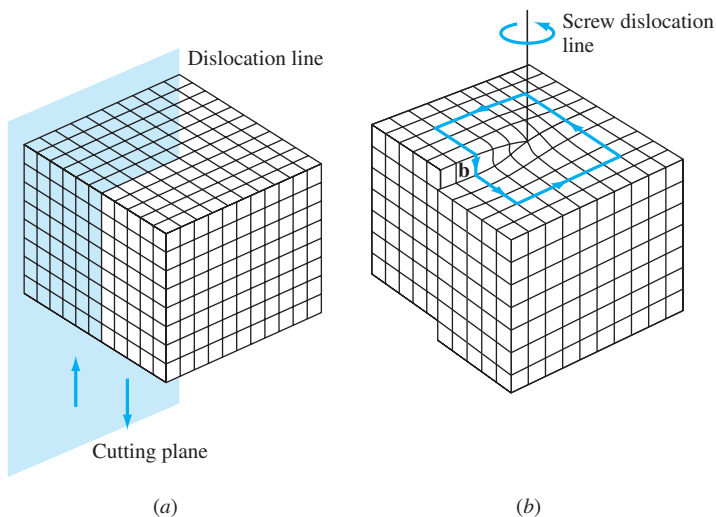
(b) Edge dislocation that indicates the orientation of its Burgers or slip vector \mathbf{b} .

((a) Source: A.G. Guy, *Essentials of Materials Science*, McGraw-Hill, 1976, p. 153.; (b) Source: Eisenstadt, M., *Introduction to Mechanical Properties of Materials: An Ecological Approach*, 1st ed., © 1971.)

**Figure 4.19**

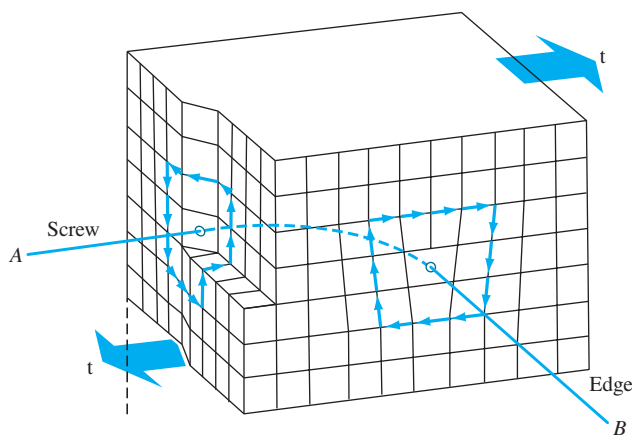
Strain fields surrounding (a) an edge dislocation and (b) a screw dislocation.

(Source: Wulff et al., *Structure and Properties of Materials*, Vol. III, H.W. Hayden, L.G. Moffatt, and J. Wulff, *Mechanical Behavior*, Wiley, 1965, p. 69.)

**Figure 4.20**

Formation of a screw dislocation. (a) A perfect crystal is sliced by a cutting plane, and up and down shear stresses are applied parallel to the cutting plane to form the screw dislocation in (b). (b) A screw dislocation is shown with its slip or Burgers vector \mathbf{b} parallel to the dislocation line.

(Source: Eisenstadt, M., *Introduction to Mechanical Properties of Materials: An Ecological Approach*, 1st ed., © 1971.)

**Figure 4.21**

Mixed dislocation in a crystal. Dislocation line AB is pure screw type where it enters the crystal on the left and pure edge type where it leaves the crystal on the right.

(Source: Wulff et al., *Structure and Properties of Materials*, Vol. III, H.W. Hayden, L.G. Moffatt, and J. Wulff, *Mechanical Properties*, Wiley, 1965, p. 65.)

4.4.3 Planar Defects

Planar defects include external surfaces, **grain boundaries**, **twins**, **low-angle boundaries**, **high-angle boundaries**, **twists**, and **stacking faults**. The free or external surface of any material is the most common type of planar defect. External surfaces are considered defects because the atoms on the surface are bonded to other atoms only on one side. Therefore, the surface atoms have a lower number of neighbors. As a result, these atoms have a higher state of energy when compared to the atoms positioned inside the crystal with an optimal number of neighbors. The higher energy associated with the atoms on the surface of a material makes the surface susceptible to erosion and reaction with elements in the environment. This point further illustrates the importance of defects in the behavior of materials.

Grain boundaries are surface imperfections in polycrystalline materials that separate grains (crystals) of different orientations. In metals, grain boundaries are created during solidification when crystals formed from different nuclei grow simultaneously and meet each other (Fig. 4.2). The shape of the grain boundaries is determined by the restrictions imposed by the growth of neighboring grains. Grain-boundary surfaces of an approximately equiaxed grain structure are shown schematically in Figure 4.22 and in a micrograph in Figure 4.3.

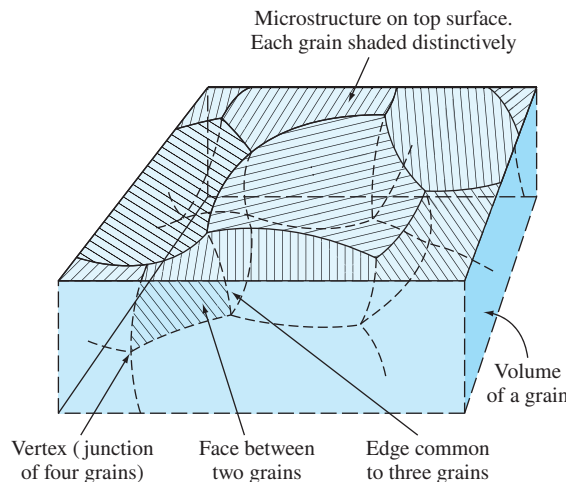


Figure 4.22

Sketch showing the relation of the two-dimensional microstructure of a crystalline material to the underlying three-dimensional network. Only portions of the total volume and total face of any one grain are shown.

(Source: A.G. Guy, *Essentials of Materials Science*, McGraw-Hill, 1976.)

The grain boundary itself is a narrow region between two grains of about two to five atomic diameters in width and is a region of atomic mismatch between adjacent grains. The atomic packing in grain boundaries is lower than within the grains because of the atomic mismatch. Grain boundaries also have some atoms in strained positions that raise the energy of the grain-boundary region.

The higher energy of the grain boundaries and their more open structure make them a more favorable region for the nucleation and growth of precipitates (see Sec. 9.5). The lower atomic packing of the grain boundaries also allows for more rapid diffusion of atoms in the grain boundary region. At ordinary temperatures, grain boundaries also restrict plastic flow by making it difficult for the movement of dislocations in the grain boundary region.

Twins or *twin boundaries* are another example of a two-dimensional defect. A twin is defined as a region in which a mirror image of the structure exists across a plane or a boundary. Twin boundaries form when a material is permanently or plastically deformed (*deformation twin*). They can also appear during the recrystallization process in which atoms reposition themselves in a deformed crystal (*annealing twin*), but this happens only in some FCC alloys. A number of annealing twins formed in the microstructure of brass are shown in Figure 4.23. As the name indicates, twin

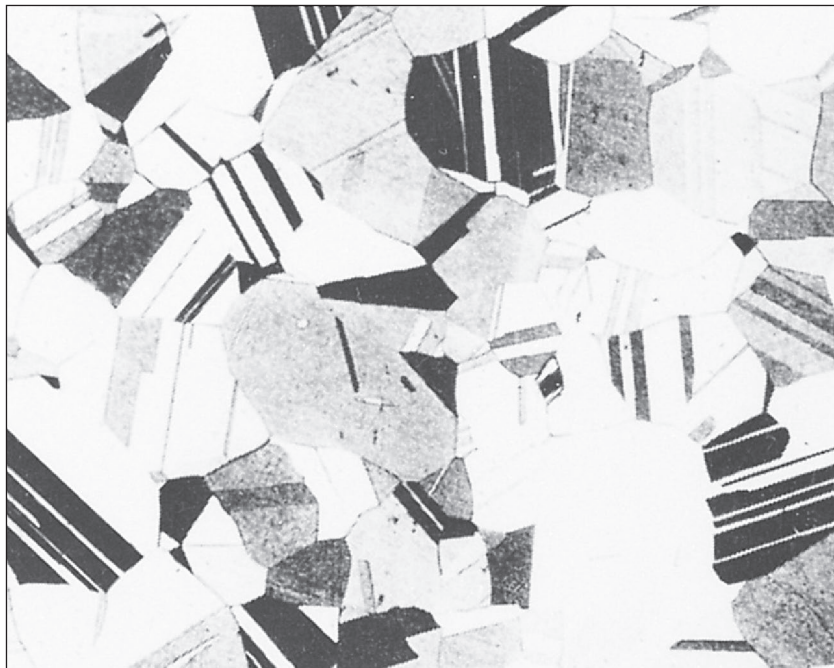
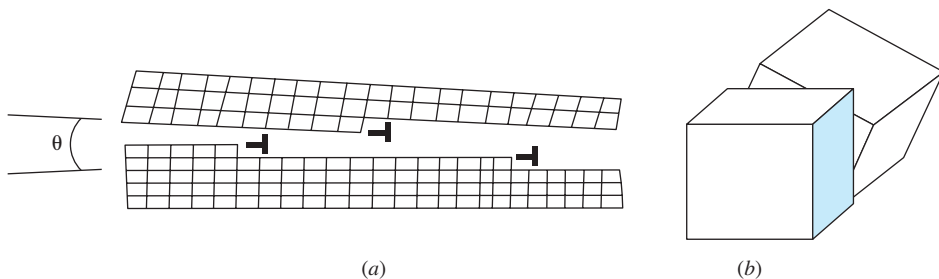


Figure 4.23

Twin boundaries in the grain structure of brass.

(©McGraw-Hill Education)

**Figure 4.24**

(a) Edge dislocations in an array forming a small-angle tilt boundary. (b) Schematic of a small-angle twist boundary.

boundaries form in pairs. Similar to dislocations, twin boundaries tend to strengthen a material. A more detailed explanation of twin boundaries is given in Section 6.5.

When an array of edge dislocations are oriented in a crystal in a manner that seems to misorient or tilt two regions of a crystal (Fig. 4.24a), a two-dimensional defect called a *small-angle tilt boundary* is formed. A similar phenomenon can occur when a network of screw dislocations create a small-angle twist boundary (Fig. 4.24b). The misorientation angle θ for a small-angle boundary is generally less than 10 degrees. As the density of dislocations in small-angle boundaries (tilt or twist) increases, the misorientation angle θ becomes larger. If θ exceeds 20 degrees, the boundary is no longer characterized as a small-angle boundary but is considered a general grain boundary. Similar to dislocations and twins, small-angle boundaries are regions of high energy due to local lattice distortions and tend to strengthen a metal.

In Section 3.8, we discussed the formation of FCC and HCP crystal structures by the stacking of atomic planes. It was noted that the stacking sequence *ABABAB* . . . leads to the formation of an HCP crystal structure while the sequence *ABCABCABC* . . . leads to the FCC structure. Sometimes during the growth of a crystalline material, collapse of a vacancy cluster, or interaction of dislocations, one or more of the stacking planes may be missing, giving rise to another two-dimensional defect called a *stacking fault* or a *piling-up fault*. Stacking faults *ABCABAACBABC* and *ABAABBAB* are typical in FCC and HCP crystals, respectively. The boldfaced planes indicate the faults. Stacking faults also tend to strengthen the material.

It is important to note that, generally speaking, of the two-dimensional defects discussed here, grain boundaries are most effective in strengthening a metal; however, stacking faults, twin boundaries, and small-angle boundaries often also serve a similar purpose. The reason why these defects tend to strengthen a metal will be discussed in more detail in Chapter 6.

4.4.4 Volume Defects

Volume or *three-dimensional* defects form when a cluster of point defects join to form a three-dimensional void or a pore. Conversely, a cluster of impurity atoms may join to form a three-dimensional precipitate. The size of a volume defect may range from a few nanometers to centimeters or sometimes larger. Such defects have a tremendous

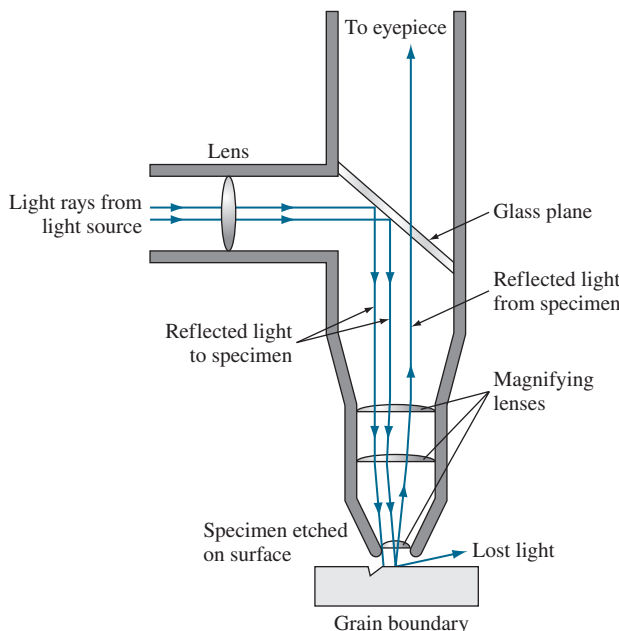
effect or influence on the behavior and performance of the material. Finally, the concept of a three-dimensional or volume defect may be extended to an amorphous region within a polycrystalline material. Such materials were briefly discussed in Chapter 3 and will be more extensively discussed in future chapters.

4.5 EXPERIMENTAL TECHNIQUES FOR IDENTIFICATION OF MICROSTRUCTURE AND DEFECTS

Material scientists and engineers use various instruments to study and understand the behavior of materials based on their microstructures, existing defects, microconstituents, and other features and characteristics specific to the internal structure. The instruments reveal information about the internal makeup and structure of the material at various length scales extending from the micro- to nanorange. In this range, the structure of grains, grain boundaries, various microphases, line defects, surface defects, and their effect on material behavior may be studied by various instruments. In the following sections, we will discuss the use of optical metallography, scanning electron microscopy, transmission electron microscopy, high-resolution transmission electron microscopy, and scanning probe microscopy techniques to learn about the internal and surface features of materials.

4.5.1 Optical Metallography, ASTM Grain Size, and Grain Diameter Determination

Optical metallography techniques are used to study the features and internal makeup of materials at the micrometer level (magnification level of around 2000 \times). Qualitative and quantitative information pertaining to grain size, grain boundary, the existence of various phases, internal damage, and some defects may be extracted using optical metallography techniques. In this technique, the surface of a small sample of a material such as a metal or a ceramic is first prepared through a detailed and rather lengthy procedure. The preparation process includes numerous surface grinding stages (usually four) that remove large scratches and thin plastically deformed layers from the surface of the specimen. The grinding stage is followed by a number of polishing stages (usually four) that remove fine scratches formed during the grinding stage. The quality of the surface is extremely important in the outcome of the process, and generally speaking, a smooth, mirrorlike surface without scratches must be produced at the end of the polishing stage. These steps are necessary to minimize topographic contrast. The polished surface is then exposed to chemical etchants. The choice of the etchant and the etching time (the time interval in which the sample will remain in contact with the etchant) are two critical factors that depend on the specific material under study. The atoms at the grain boundary will be attacked at a much more rapid rate by the etchant than those atoms inside the grain. This is because the atoms at the grain boundary possess a higher state of energy because of the less efficient packing. As a result, the etchant produces tiny grooves along the boundaries of the grains. The prepared sample is then examined using a metallurgical microscope (inverted microscope) based on visible incident light. A schematic representation of the metallurgical microscope is given in Figure 4.25.

**Figure 4.25**

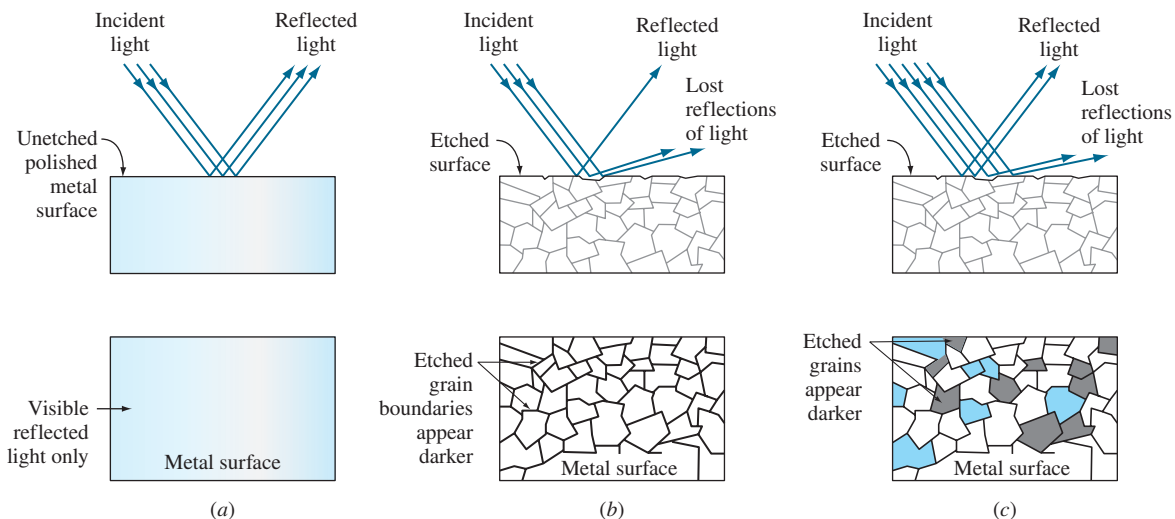
Schematic diagram illustrating how light is reflected from the surface of a polished and etched metal. The irregular surface of the etched-out grain boundary does not reflect light.

(Source: M. Eisenstadt, *Mechanical Properties of Materials*, Macmillan, 1971, p. 126.)

When exposed to incident light in an optical microscope, these grooves do not reflect the light as intensely as the remainder of the grain material (Fig. 4.26). Because of the reduced light reflection, the tiny grooves appear as dark lines to the observer, thus revealing the grain boundaries (Fig. 4.27). Additionally, impurities, other existing phases, and internal defects also react differently to the etchant and reveal themselves in photomicrographs taken from the sample surface. Overall, this technique provides a great deal of qualitative information about the material.

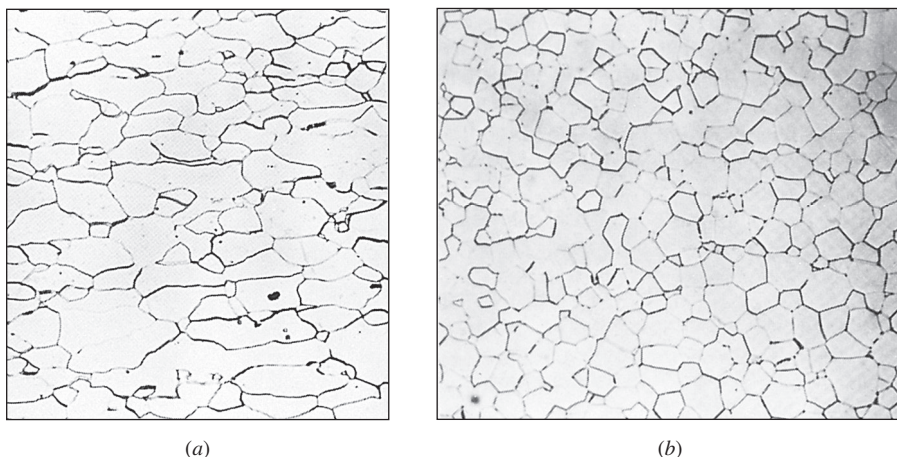
In addition to the qualitative information that is extracted from the photomicrographs, some limited quantitative information may also be extracted. Grain size and average grain diameter of the material may be determined using the photomicrographs obtained by this technique.

The grain size of polycrystalline metals is important since the amount of grain boundary surface has a significant effect on many properties of metals, especially strength. At lower temperatures (less than about one-half of their melting temperature), grain boundaries strengthen metals by restricting dislocation movement under stress. At elevated temperatures, grain boundary sliding may occur, and grain boundaries can become regions of weakness in polycrystalline metals.

**Figure 4.26**

The effect of etching a polished surface of a steel metal sample on the microstructure observed in the optical microscope. (a) In the as-polished condition, no microstructural features are observed. (b) After etching a very low-carbon steel, only grain boundaries are chemically attacked severely, and so they appear as dark lines in the optical microstructure. (c) After etching a medium-carbon steel polished sample, dark (pearlite) and light (ferrite) regions are observed in the microstructure. The darker pearlite regions have been more severely attacked by the etchant and thus do not reflect much light.

(Source: Eisenstadt, M., *Introduction to Mechanical Properties of Materials: An Ecological Approach*, 1st ed., © 1971.)

**Figure 4.27**

Grain boundaries on the surface of polished and etched samples as revealed in the optical microscope. (a) Low-carbon steel (magnification 100x). (b) Magnesium oxide (magnification 225x).

((a) ©ASM International, (b) Courtesy of The American Ceramic Society)

One method of measuring grain size is the *American Society for Testing and Materials* (ASTM) method, in which the **grain-size number** n is defined by

$$N = 2^{n-1} \quad (4.7)$$



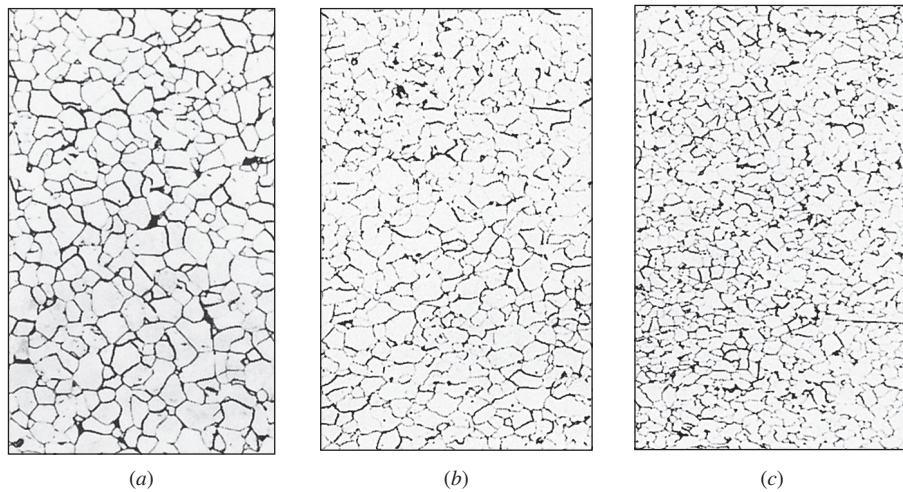
Tutorial

where N is the number of grains per square inch on a polished and etched material surface at a magnification of 100 \times and n is an integer referred to as the *ASTM grain-size number*. Grain-size numbers with the nominal number of grains per square inch at 100 \times and grains per square millimeter at 1 \times are listed in Table 4.2. Figure 4.28 shows some examples of nominal grain sizes for low-carbon sheet steel samples. Generally

Table 4.2 ASTM grain sizes

Grain-Size No.	Nominal Number of Grains	
	Per Sq mm at 1 \times	Per Sq in. at 100 \times
1	15.5	1.0
2	31.0	2.0
3	62.0	4.0
4	124	8.0
5	248	16.0
6	496	32.0
7	992	64.0
8	1980	128
9	3970	256
10	7940	512

(Source: *Metals Handbook*, vol. 7, 8th ed., American Society for Metals, 1972, p. 4.)

**Figure 4.28**

Several nominal ASTM grain sizes of low-carbon sheet steels: (a) no. 7, (b) no. 8, and (c) no. 9. (Etch: nital; magnification 100 \times .)

((a-c): ©ASM International)

speaking, a material may be classified as coarse-grained when $n < 3$; medium-grained, $4 < n < 6$; fine-grained, $7 < n < 9$, and ultrafine-grained, $n > 10$.

A more direct approach of assessing the grain size of a material would be to determine the actual average grain diameter. This offers clear advantages to the ASTM grain-size number that in reality does not offer any direct information about the actual size of the grain. In this approach, once a photomicrograph is prepared at a specific magnification, a random line of known length is drawn on the photomicrograph. The number of grains intersected by this line is then determined, and the ratio of the number of grains to the actual length of the line is determined, n_L . The average grain diameter d is determined using the equation

$$d = C/(n_L M) \quad (4.8)$$

where C is a constant ($C = 1.5$ for typical microstructures) and M is the magnification at which the photomicrograph is taken.

An ASTM grain size determination is being made from a photomicrograph of a metal at a magnification of $100\times$. What is the ASTM grain-size number of the metal if there are 64 grains per square inch?

**EXAMPLE
PROBLEM 4.4**


Tutorial

■ Solution

$$N = 2^{n-1}$$

where N = no. of grains per square inch at $100\times$

n = ASTM grain-size number

Thus,

$$64 \text{ grains/in}^2 = 2^{n-1}$$

$$\log 64 = (n - 1)(\log 2)$$

$$1.806 = (n - 1)(0.301)$$

$$n = 7 \blacktriangleleft$$

If there are 60 grains per square inch on a photomicrograph of a metal at $200\times$, what is the ASTM grain-size number of the metal?

**EXAMPLE
PROBLEM 4.5**
■ Solution

If there are 60 grains per square inch at $200\times$, then at $100\times$ we will have

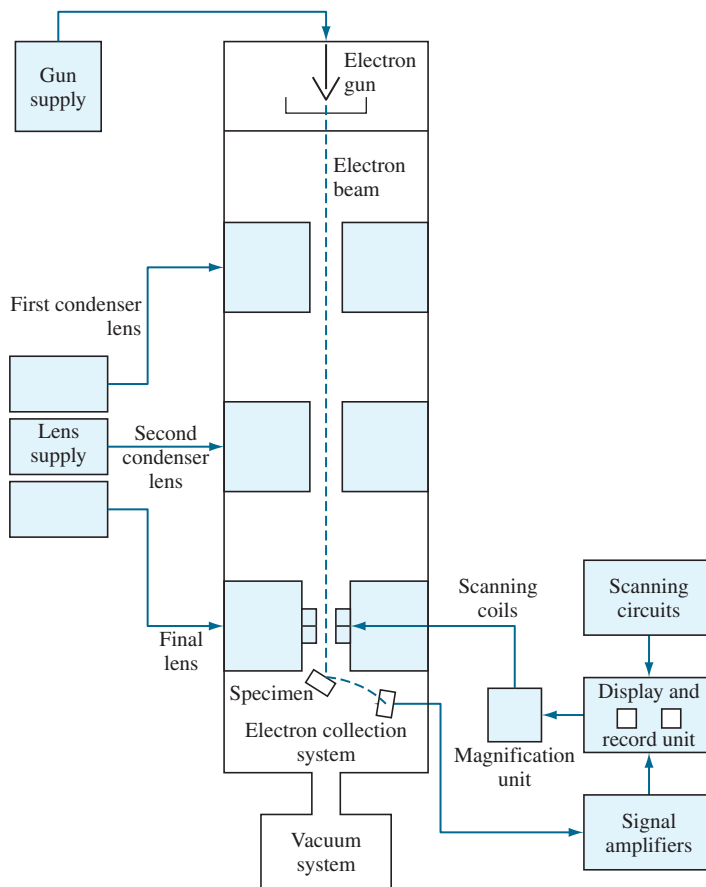
$$N = \left(\frac{200}{100}\right)^2 (60 \text{ grains/in}^2) = 240 = 2^{n-1}$$

$$\log 240 = (n - 1)(\log 2)$$

$$2.380 = (n - 1)(0.301)$$

$$n = 8.91 \blacktriangleleft$$

Note that the ratio of the magnification change must be squared since we are concerned with the number of grains per square inch.

**Figure 4.29**

Schematic diagram of the basic design of a scanning electron microscope.

(Source: V.A. Phillips, *Modern Metallographic Techniques and Their Applications*, Wiley, 1971, p. 425.)

4.5.2 Scanning Electron Microscopy (SEM)

The scanning electron microscope is an important tool in materials science and engineering; it is used for microscopic feature measurement, fracture characterization, microstructure studies, thin coating evaluations, surface contamination examination, and failure analysis of materials. As opposed to optical microscopy, where the sample's surface is exposed to incident visible light, the SEM impinges a beam of electrons in a pinpointed spot on the surface of a target specimen and collects and displays the electronic signals given off by the target material. Figure 4.29 is a schematic illustration of the principles of operation of an SEM. Basically, an electron gun produces an electron beam in an evacuated column that is focused and directed so that it impinges on a small spot on the target. Scanning coils allow the beam to scan a small area of the surface of the sample. Low-angle backscattered electrons interact with the protuberances

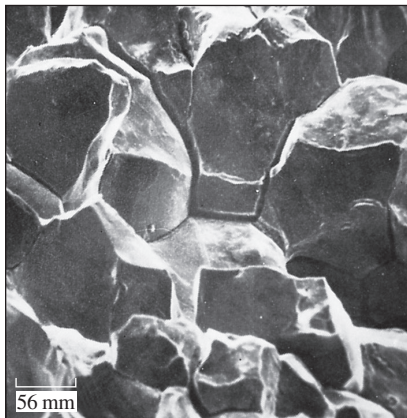


Figure 4.30
Scanning electron fractograph of intergranular corrosion fracture near a circumferential weld in a thick-wall tube made of type 304 stainless steel. (Magnification 180 \times .)

(©ASM International)



Figure 4.31
Man looking into an electron microscope.
(©Steve Allen/Brand X Pictures)

of the surface and generate secondary⁷ backscattered electrons to produce an electronic signal, which in turn produces an image having a depth of field of up to about 300 times that of the optical microscope (about 10 μm at 10,000 diameters magnification). The resolution of many SEM instruments is about 5 nm, with a wide range of magnification (about 15 to 100,000 \times).

The SEM is particularly useful in materials analysis for the examination of fractured surfaces of metals. Figure 4.30 shows an SEM fractograph of an intergranular corrosion fracture. Notice how clearly the metal grain surfaces are delineated and the depth of perception. SEM fractographs are used to determine whether a fractured surface is intergranular (along the grain boundary), transgranular (across the grain), or a mixture of both. The samples to be analyzed using standard SEM are often coated with gold or other heavy metals to achieve better resolution and signal quality. This is especially important if the sample is made of a nonconducting material. Qualitative and quantitative information relating to the makeup of the sample may also be obtained when the SEM is equipped with an X-ray spectrometer.

4.5.3 Transmission Electron Microscopy (TEM)

Transmission electron microscopy (Fig. 4.31) is an important technique for studying defects and precipitates (secondary phases) in materials. Much of what is known about

⁷ Secondary electrons are electrons that are ejected from the target metal atoms after being struck by primary electrons from the electron beam.

defects would be speculative theory and would have never been verified without the use of TEM, which resolves features in the nanometer range.

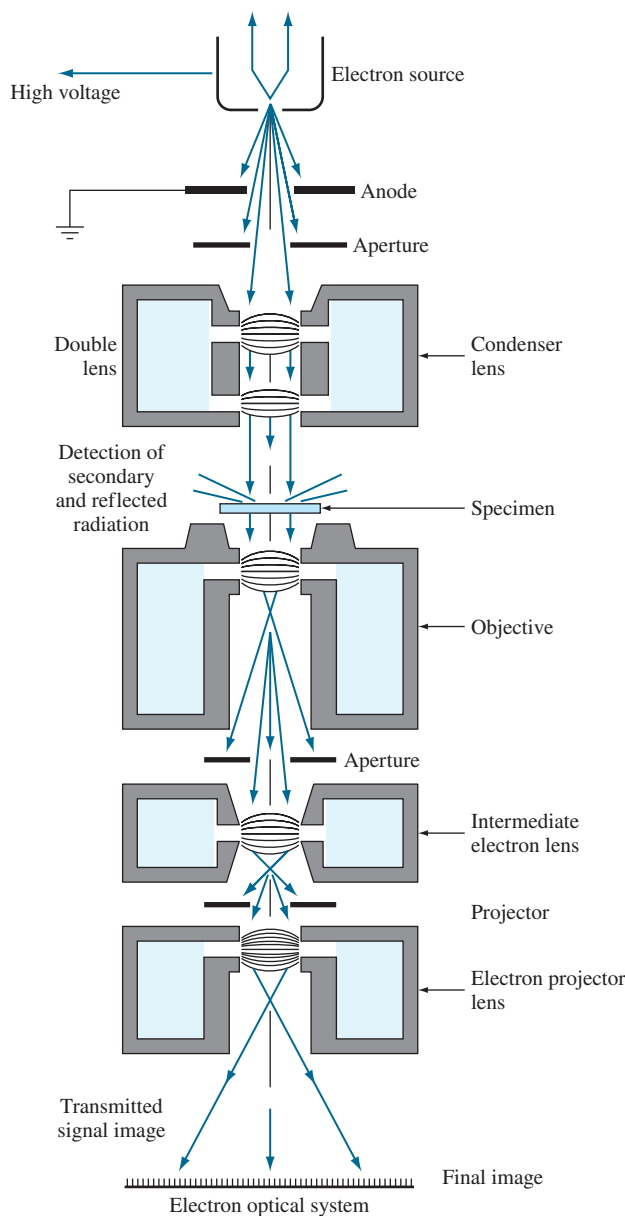
Defects such as dislocations can be observed on the image screen of a TEM. Unlike optical microscopy and SEM techniques where sample preparation is rather basic and easy to achieve, sample preparation for TEM analysis is complex and requires highly specialized instruments. Specimens to be analyzed using a TEM must have a thickness of several hundred nanometers or less, depending on the operating voltage of the instrument. A properly prepared specimen is not only thin but also has flat parallel surfaces. To achieve this, a thin section (3 to 0.5 mm) is cut out of the bulk material using techniques such as electric-discharge machining (used for conducting samples) and a rotating wire saw, among others. The specimen is then reduced to 50 μm thickness while keeping the faces parallel using machine milling or lapping processes with fine abrasives. Other more advanced techniques such as electropolishing and ion-beam thinning are used to thin a sample to its final thickness.

In the TEM, an electron beam is produced by a heated tungsten filament at the top of an evacuated column and is accelerated down the column by high voltage (usually from 100 to 300 kV). Electromagnetic coils are used to condense the electron beam, which is then passed through the thin specimen placed on the specimen stage. As the electrons pass through the specimen, some are absorbed and some are scattered so that they change direction. It is now clear that the sample thickness is critical: a thick sample will not allow the passage of electrons due to excessive absorption and diffraction. Differences in crystal atomic arrangements will cause electron scattering. After the electron beam has passed through the specimen, it is focused with the objective coil (magnetic lens) and then enlarged and projected on a fluorescent screen (Fig. 4.32). An image can be formed by collecting either the direct electrons or the scattered electrons. The choice is made by inserting an aperture into the back focal plane of the objective lens. The aperture is maneuvered so that either the direct electrons or the scattered electrons pass through it. If the direct beam is selected, the resultant image is called a *bright-field image*, and if the scattered electrons are selected, a *dark-field image* is produced.

In a bright-field mode, a region in a metal specimen that tends to scatter electrons to a higher degree will appear dark on the viewing screen. Thus, dislocations that have an irregular linear atomic arrangement will appear as dark lines on the electron microscope screen. A TEM image of the dislocation structure in a thin foil of iron deformed 14% at -195°C is shown in Figure 4.33.

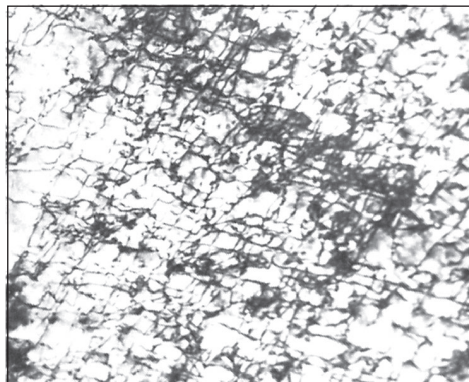
4.5.4 High-Resolution Transmission Electron Microscopy (HRTEM)

Another important tool in the analysis of defects and crystal structure is the high-resolution transmission electron microscope. The instrument has a resolution of about 0.1 nm, which allows viewing of the crystal structure and defects at the atomic level. To grasp what this degree of resolution may reveal about a structure, consider that the lattice constant of the silicon unit cell at approximately 0.543 nm is five times larger than the resolution offered by HRTEM. The basic concepts behind this technique are similar to those of the TEM. However, the sample must be significantly thinner—on

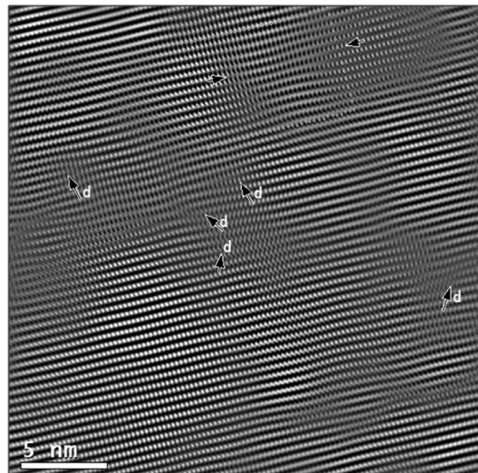
**Figure 4.32**

Schematic arrangement of electron lens system in a transmission electron microscope. All the lenses are enclosed in a column that is evacuated during operation. The path of the electron beam from the electron source to the final projected transmitted image is indicated by arrows. A specimen thin enough to allow an electron beam to be transmitted through it is placed between the condenser and objective lenses as indicated.

(Source: L.E. Murr, *Electron and Ion Microscopy and Microanalysis*, Marcel Decker, 1982, p. 105.)

**Figure 4.33**

Dislocation structure in iron deformed 14% at -195°C . The dislocations appear as dark lines because electrons have been scattered along the linear irregular atomic arrangements of the dislocations. (Thin foil specimen; magnification 40,000x.)
(©ASM International)

**Figure 4.34**

HRTEM image of A_3N atomic structure. The image shows two types of defects: (1) dislocations represented by arrows and the letter "d," and (2) stacking fault represented by two opposing arrows (top of the image).

(Courtesy of Dr. Jharna Chaudhuri)

the order of 10 to 15 nm. In some situations, it is possible to view a two-dimensional projection of a crystal with the accompanying defects. To achieve this, the thin sample is tilted so that a low-index direction in the plane is perpendicular to the direction of the electron beam (atoms are exactly on top of each other relative to the beam). The diffraction pattern is representative of the periodic potential for the electrons in two dimensions. The interference of all the diffracted beams and the primary beam, when brought together again using the objective lens, provides an enlarged picture of the periodic potential. Figure 4.34 shows the HRTEM image of several dislocations (marked by "d") and some stacking faults (marked by arrows) in A_3N thin film. In the figure, the periodic order of the atoms in the undisturbed regions is clearly observed (lower left). Dislocations create a wavy pattern in atomic structure. One can clearly see the disturbance in the atomic structure as a result of defects such as dislocations and stacking faults. It should be noted that due to limitations in the objective lens in HRTEM, accurate quantitative analysis of images is not easy to achieve and must be done with care.

4.5.5 Scanning Probe Microscopes and Atomic Resolution

Scanning tunneling microscopes (STMs) and *atomic force microscopes* (AFMs) are two of many recently developed tools that allow scientists to analyze and image

materials at the atomic level. These instruments and others with similar capabilities are collectively classified as *scanning probe microscopy* (SPM). The SPM systems can magnify the features of a surface to the subnanometer scale, producing an atomic-scale topographic map of the surface. These instruments have important applications in many areas of science, including but not limited to surface sciences, where the arrangement of atoms and their bonding are important; metrology, where surface roughness of materials needs to be analyzed; and nanotechnology, where the position of individual atoms or molecules may be manipulated and new nanoscale phenomena may be investigated. It is appropriate to discuss these systems, how they function, the nature of information they provide, and their applications.

Scanning Tunneling Microscope IBM researchers G. Binnig and H. Rohrer developed the STM technique in the early 1980s and later received the Nobel Prize in Physics in 1986 for their invention. In this technique, an extremely sharp tip (Fig. 4.35), traditionally made of metals such as tungsten, nickel, platinum-iridium, or gold, and more recently out of carbon nanotubes (see Sec. 11.2.12), is used to probe the surface of a sample.

The tip is first positioned a distance in the order of an atom diameter ($\cong 0.1$ to 0.2 nm) from the surface of the sample. At such proximity, the electron clouds of the atoms in the tip of the probe interact with the electron clouds of the atoms on the surface of the sample. If at this point a small voltage is applied across the tip and the surface, the electrons will “tunnel” the gap and, therefore, produce a small current that may be

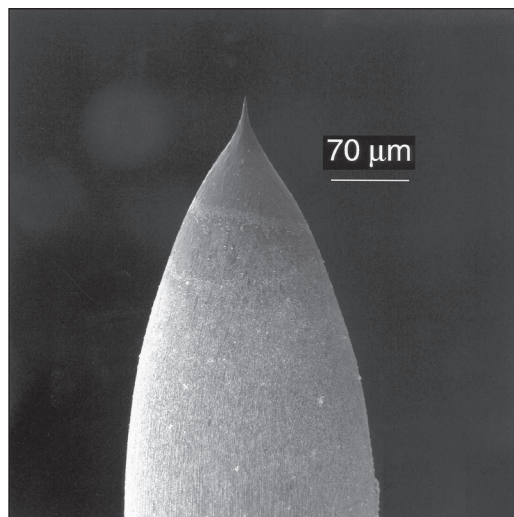


Figure 4.35

STM tip made of Pt-Ir alloy. The tip is sharpened using chemical etching techniques.

(Courtesy of Molecular Imaging Corp)

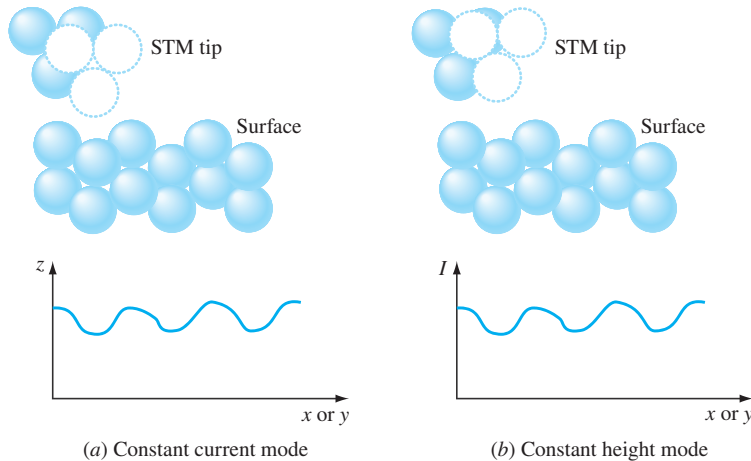


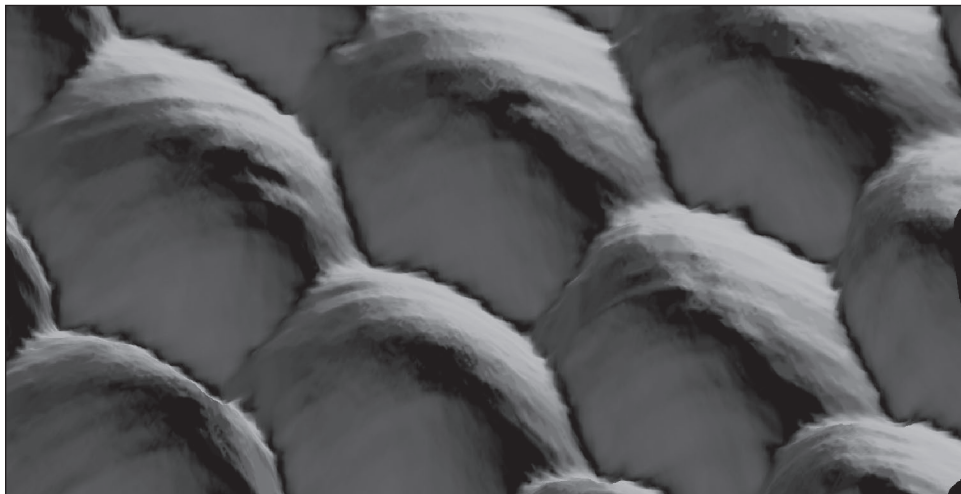
Figure 4.36

Schematics showing the STM modes of operation. (a) Adjust the z coordinate of the tip to maintain constant current (record z adjustments), (b) Adjust the current in the tip to maintain constant height (record current adjustments).

detected and monitored. Generally, the sample is analyzed under ultrahigh vacuum to avoid contamination and oxidation of its surface.

The produced current is extremely sensitive to the gap size between the tip and the surface. Small changes in the gap size produce an exponential increase in the detected current. As a result, small changes (less than 0.1 nm) in the position of the tip relative to the surface may be detected. The magnitude of current is measured when the tip is positioned directly above an atom (its electron cloud). This current is maintained at the same level as the tip moves over the atoms and valleys between the atoms (*constant-current mode*) (Fig. 4.36a). This is accomplished by adjusting the vertical position of the tip. The small movements required to adjust and maintain the current through the tip are then used to map the surface. The surface may also be mapped using a *constant-height mode* in which the relative distance between the tip and the surface is maintained at a constant value and the changes in current are monitored (Fig. 4.36b). The quality of the surface topography achieved by STM is striking as observed in the STM images of the surface of platinum (Fig. 4.37).

Clearly, what is extremely important here is that the diameter of the tip should be on the order of a single atom to maintain atomic-scale resolution. The conventional metal tips can easily be worn and damaged during the scanning process, which results in poor image quality. More recently, carbon nanotubes of about one to tens of nanometers in diameter are being used as nanotips for STM and AFM applications because of their slender structure and strength. The STM is primarily used for topography purposes, and it offers no quantitative insight into the bonding nature and properties of the material. Because the apparatus's function is based on creating and monitoring small amounts of current, only those materials that can conduct electricity may be mapped,

**Figure 4.37**

STM image of the surface of platinum showing outstanding atomic resolution.

(Courtesy of Almaden Research Center)

including metals and semiconductors. However, many materials of high interest to the research community, such as biological materials or polymers, are not conductive and, therefore, cannot be analyzed using this technique. For nonconducting materials, the AFM techniques are applied.

Atomic Force Microscope The AFM uses a similar approach to that of the STM in that it uses a tip to probe the surface. However, in this case, the tip is attached to a small cantilever beam. As the tip interacts with the surface of the sample, the forces (Van der Waals forces) acting on the tip deflect the cantilever beam. The interaction may be a short-range repulsive force (*contact-mode AFM*) or a long-range attractive force (*non-contact-mode AFM*). The deflection of the beam is monitored using a laser and a photodetector set up as shown in Figure 4.38. The deflection is used to calculate the force acting on the tip. During scanning, the force will be maintained at a constant level (similar to the constant-current mode in STM), and the displacement of the tip will be monitored. The surface topography is determined from these small displacements. Unlike STM, the AFM approach does not rely on a current tunneling through the tip, and it can therefore be applied to all materials, even nonconductors. This is the main advantage of AFM over its predecessor, STM. There are currently many other AFM-based techniques available with various imaging modes, including magnetic and acoustic. AFM in various imaging modes is being used in areas such as DNA research, *in situ* monitoring of corrosion in material, *in situ* annealing of polymers, and polymer-coating technology. The fundamental understanding of important issues in these areas has been significantly enhanced because of the application of such techniques.

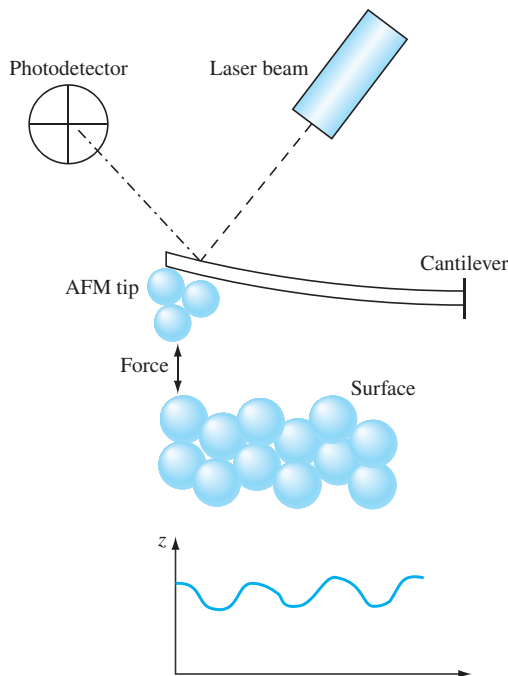


Figure 4.38
A schematic showing the basic AFM technique.

Understanding the behavior of advanced materials at the atomic level drives the state of the art in high-resolution electron microscopy, which in turn provides an opportunity for the development of new materials. Electron and scanning probe microscopy techniques are and will be particularly important in nanotechnology and nanostructured materials.

4.6 SUMMARY

Most metals and alloys are melted and cast into semifinished or finished shapes. During the solidification of a metal into a casting, nuclei are formed that grow into grains, creating solidified cast metal with a polycrystalline grain structure. For most industrial applications, a very small grain size is desirable. The grain size may be indirectly determined by ASTM grain-size number n or directly determined by finding the average grain diameter. Large single crystals are rarely made in industry. However, an exception is the large single crystals of silicon produced for the semiconductor industry. For this material, special solidification conditions must be used, and the silicon must be of very high purity.

Crystal imperfections are present in all real crystalline materials, even at the atomic or ionic size level. Vacancies or empty atomic sites in metals can be explained in terms of the thermal agitation of atoms and are considered equilibrium lattice defects. Dislocations

(line defects) occur in metal crystals and are created in large numbers by the solidification process. Dislocations are not equilibrium defects, and they increase the internal energy of the metal. Images of dislocations can be observed in the transmission electron microscope. Grain boundaries are surface imperfections in metals created by crystals of different orientations meeting each other during solidification. Other important types of defects that affect the properties of materials are twins, low-angle boundaries, high-angle boundaries, twists, stacking faults, and precipitates.

Materials scientists and engineers use high-tech instruments to learn about the internal structure (including defect structure), behavior, and failure of materials. Instruments such as metallographs, SEM, TEM (HRTEM), and SPM allow analysis of materials from macro- to nanorange. Without such instruments, understanding the behavior of materials would be impossible.

4.7 DEFINITIONS

Sec. 4.1

Nuclei: small particles of a new phase formed by a phase change (e.g., solidification) that can grow until the phase change is complete.

Homogeneous nucleation (as pertains to the solidification of metals): the formation of very small regions of a new solid phase (called *nuclei*) in a pure metal that can grow until solidification is complete. The pure homogeneous metal itself provides the atoms that make up the nuclei.

Embryos: small particles of a new phase formed by a phase change (e.g., solidification) that are not of critical size and that can redissolve.

Critical radius r^* of nucleus: the minimum radius that a particle of a new phase formed by nucleation must have to become a stable nucleus.

Heterogeneous nucleation (as pertains to the solidification of metals): the formation of very small regions (called *nuclei*) of a new solid phase at the interfaces of solid impurities.

These impurities lower the critical size at a particular temperature of stable solid nuclei.

Grain: a single crystal in a polycrystalline aggregate.

Equiaxed grains: grains that are approximately equal in all directions and have random crystallographic orientations.

Columnar grains: long, thin grains in a solidified polycrystalline structure. These grains are formed in the interior of solidified metal ingots when heat flow is slow and uniaxial during solidification.

Sec. 4.2

Polycrystalline structure: a crystalline structure that contains many grains.

Sec. 4.3

Alloy: a mixture of two or more metals or a metal (metals) and a nonmetal (nonmetals).

Solid solution: an alloy of two or more metals or a metal(s) and a nonmetal(s) that is a single-phase atomic mixture.

Substitutional solid solution: a solid solution in which solute atoms of one element can replace those of solvent atoms of another element. For example, in a Cu–Ni solid solution, the copper atoms can replace the nickel atoms in the solid-solution crystal lattice.

Interstitial solid solution: a solid solution formed in which the solute atoms can enter the interstices or holes in the solvent-atom lattice.

Sec. 4.4

Vacancy: a point imperfection in a crystal lattice where an atom is missing from an atomic site.

Interstitialcy (self-interstitial): a point imperfection in a crystal lattice where an atom of the same kind as those of the matrix lattice is positioned in an interstitial site between the matrix atoms.

Frenkel imperfection: a point imperfection in an ionic crystal in which a cation vacancy is associated with an interstitial cation.

Schottky imperfection: a point imperfection in an ionic crystal in which a cation vacancy is associated with an anion vacancy.

Dislocation: a crystalline imperfection in which a lattice distortion is centered around a line. The displacement distance of the atoms around the dislocation is called the *slip* or *Burgers vector **b***. For an *edge dislocation*, the slip vector is perpendicular to the dislocation line, while for a *screw dislocation*, the slip vector is parallel to the dislocation line. A *mixed dislocation* has both edge and screw components.

Grain boundary: a surface imperfection that separates crystals (grains) of different orientations in a polycrystalline aggregate.

Twin boundary: a mirror image misorientation of the crystal structure which is considered a surface defect.

Small-angle boundary (tilt): an array of dislocations forming angular mismatch inside a crystal.

Twist boundary: an array of screw dislocations creating mismatch inside a crystal.

Stacking fault: a surface defect formed due to improper (out of place) stacking of atomic planes.

Sec. 4.5

Grain-size number: a nominal (average) number of grains per unit area at a particular magnification.

Scanning electron microscope (SEM): an instrument used to examine the surface of a material at very high magnifications by impinging electrons.

Transmission electron microscope (TEM): an instrument used to study the internal defect structures based on passage of electrons through a thin film of materials.

High-resolution transmission electron microscope (HRTEM): a technique based on TEM but with significantly higher resolution by using significantly thinner samples.

Scanning probe microscopy (SPM): microscopy techniques such as STM and AFM that allow mapping of the surface of a material at the atomic level.

4.8 PROBLEMS

Answers to problems marked with an asterisk are given at the end of the book.

Knowledge and Comprehension Problems

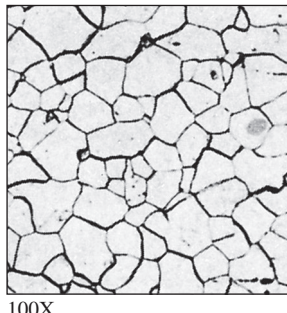
- 4.1 Describe and illustrate the solidification process of a pure metal in terms of the nucleation and growth of crystals.
- 4.2 Define the homogeneous nucleation process for the solidification of a pure metal.
- 4.3 In the solidification of a pure metal, what are the two energies involved in the transformation? Write the equation for the total free-energy change involved in the transformation of liquid to produce a strain-free solid nucleus by homogeneous nucleation. Also, illustrate graphically the energy changes associated with the formation of a nucleus during solidification.

- 4.4 In the solidification of a metal, what is the difference between an embryo and a nucleus? What is the critical radius of a solidifying particle?
- 4.5 During solidification, how does the degree of undercooling affect the critical nucleus size? Assume homogeneous nucleation.
- 4.6 Distinguish between homogeneous and heterogeneous nucleation for the solidification of a pure metal.
- 4.7 Describe the grain structure of a metal ingot that was produced by slow-cooling the metal in a stationary open mold.
- 4.8 Distinguish between equiaxed and columnar grains in a solidified metal structure.
- 4.9 How can the grain size of a cast ingot be refined? How is grain refining accomplished industrially for aluminum alloy ingots?
- 4.10 What special techniques must be used to produce single crystals? Discuss as many differences as you can in appearances at the micro/nanoscale as well as properties between a single crystal and polycrystalline structures of a material.
- 4.11 How are large silicon single crystals for the semiconductor industry produced?
- 4.12 What is a metal alloy? What is a solid solution?
- 4.13 Distinguish between a substitutional solid solution and an interstitial solid solution.
- 4.14 What are the conditions that are favorable for extensive solid solubility of one element in another (Hume-Rothery rules)?
- 4.15 Describe an interstitial site, and name various classifications in cubic cells and the respective coordination numbers.
- 4.16 Describe and illustrate the following types of point imperfections that can be present in metal lattices: (a) vacancy, (b) divacancy, and (c) interstitialcy.
- 4.17 Describe and illustrate the following imperfections that can exist in crystal lattices: (a) Frenkel imperfection and (b) Schottky imperfection.
- 4.18 Describe and illustrate the edge- and screw-type dislocations. What types of strain fields surround both types of dislocations?
- 4.19 Describe the structure of a grain boundary. Why are grain boundaries favorable sites for the nucleation and growth of precipitates?
- 4.20 Describe and illustrate the following planar defects: (a) twins, (b) low-angle tilt boundaries, (c) small-angle twist boundaries, (d) external surfaces, and (e) stacking faults. For each defect, express the impact on the properties of the material.
- 4.21 Describe the concept of volume or three-dimensional defects.
- 4.22 Describe the optical metallography technique. What qualitative and quantitative information can this technique provide? What levels of magnification can be achieved by this technique?
- 4.23 Why are grain boundaries easily observed in the optical microscope?
- 4.24 How is the grain size of polycrystalline materials measured by the ASTM method?
- 4.25 Describe various ranges of grain size. What do these ranges tell you about a metal?
- 4.26 Explain how one can measure the average grain size of a metal using a micrograph at a known magnification.
- 4.27 What is a scanning electron microscope (SEM)? What magnifications can it achieve? How does it work (draw a schematic)? What information can it provide?

- 4.28** What is a transmission electron microscope (TEM)? How does it work (draw a schematic)? What is the dimensional resolution that it can achieve? What information can it provide?
- 4.29** What is a high-resolution transmission electron microscope (HRTEM)? What is the dimensional resolution that it can achieve? What information can it provide?
- 4.30** Describe the scanning tunneling microscope (STM). What are its modes of operation (draw a schematic)? What is the dimensional resolution that it can achieve? What information can it provide?
- 4.31** Describe the atomic force microscope (AFM). What are the modes of operation (draw a schematic)? What is the dimensional resolution that it can achieve? What information can it provide?

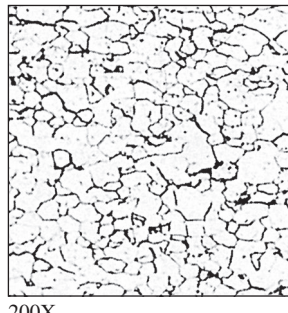
Application and Analysis Problems

- 4.32** Calculate the size (radius) of the critically sized nucleus for pure platinum when homogeneous nucleation takes place.
- 4.33** Calculate the number of atoms in a critically sized nucleus for the homogeneous nucleation of pure platinum.
- 4.34** Calculate the size (radius) of the critical nucleus for pure iron when nucleation takes place homogeneously.
- 4.35** Calculate the number of atoms in a critically sized nucleus for the homogeneous nucleation of pure iron.
- 4.36** (a) The alloy used for the gold medal awarded to the first place winner in the Salt Lake City Olympics had a composition of 92.0 at% silver, 7.5 at% copper, and 0.5 at% gold (the medal is gold-plated). Determine the absolute mass of each metal in a 253-gram medal. Repeat the same calculation for (b) the silver medal: 92.5 at% silver and 7.5 at% copper, and (c) the bronze medal: 90 at% copper and 10 at% tin.
- 4.37** Assume that Figure 4.14 shows a representative image of the overall atomic composition of a substitutional solid solution of an alloy of nickel (dark spheres) and copper (light spheres) and estimate (a) the at% of each element in overall crystal, (b) the defect density in at%, and (c) the wt% of each metal?
- 4.38** (a) Calculate the radius of the largest interstitial void in the BCC α iron lattice. The atomic radius of the iron atom in this lattice is 0.124 nm, and the largest interstitial voids occur at the $(\frac{1}{4}, \frac{1}{2}, 0)$; $(\frac{1}{2}, \frac{3}{4}, 0)$; $(\frac{3}{4}, \frac{1}{2}, 0)$; $(\frac{1}{2}, \frac{1}{4}, 0)$, etc., -type positions. (b) If an iron atom occupies this interstitial void, how many iron atom neighbors will it have, or in other words, what will its coordination number be?
- 4.39** In Example Problem 4.3, if a carbon atom occupies the interstitial void, how many iron neighbors will it have, or in other words, what will its coordination number be?
- 4.40** Consider an aluminum lattice with an excessive average of one vacancy in every 100 unit cells. What will be its density? Compare this to the theoretical density of aluminum (must calculate this using a perfect model of the unit cell). What is your conclusion?
- 4.41** If there are 300 grains per square inch on a photomicrograph of a metal at 100 \times , what is its ASTM grain-size number?
- 4.42** If there are 250 grains per square inch on a photomicrograph of a ceramic material at 200 \times , what is the ASTM grain-size number of the material?



100X

Figure P4.43
(©ASM International)



200X

Figure P4.44
(Courtesy of The American
Ceramic Society)

- 4.43** Determine, by counting, the ASTM grain-size number of the low-carbon sheet steel shown in Figure P4.43. This micrograph is at 100 \times . Classify the grain size according to the value of n , that is, coarse, medium, fine, or ultrafine grain size. Measure the area of the image for your calculations.
- 4.44** Determine the ASTM grain-size number of the type 430 stainless steel micrograph shown in Fig. P4.44. This micrograph is at 200 \times . Classify the grain size according to the value of n , that is, coarse, medium, fine, or ultrafine grain size. Measure the area of the image for your calculations.
- 4.45** For the grain structure in Problem 4.43, estimate the average grain diameter.
- 4.46** For the grain structure in Problem 4.44, estimate the average grain diameter.

Synthesis and Evaluation Problems

- 4.47** It is easier for the iron lattice to house carbon atoms at temperatures slightly higher than 912°C than at slightly lower temperatures. Use the results in Example Problem 4.3 and Problem 4.38 (solve this problem first if you have not already done so) to explain why.
- 4.48** The γ iron and silver both possess FCC crystal structures. The location for interstitial voids will be the same for both. Will the size of the interstitial voids be different? If yes, what will be the interstitial void size for silver? Hint: Example Problem 4.3.
- 4.49** The chemical formula for an intermetallics compound of Cu and Al is Cu₂Al. According to the formula, the atom percent of Al should be exactly 33.33% (one out of three atoms should be aluminum). However, in practice, one can find a range of 31% to 37% for Al. How do you explain this discrepancy?
- 4.50** Iron oxide, FeO, is an ionic compound made up of Fe²⁺ cations and O²⁻ anions. However, when available, a small number of Fe³⁺ cations may replace Fe²⁺ cations. How will this substitution affect the atomic structure of the compound, if at all? (Consult Sec. 2.5.1 related to packing of ionic compounds.)
- 4.51** In Chapter 3 (Example Problem 3.11), we calculated the theoretical density of copper to be 8.933 g/cm³. Determine the experimentally measured density of copper by referring to Appendix II. To what do you attribute this difference?

- 4.52** The following pairs of elements can form solid solution alloys. Predict which ones will form substitutional and which ones interstitial alloys. Justify your answers.

- Copper and tin (bronze)
- Aluminum and silicon
- Iron and nitrogen
- Titanium and hydrogen

- 4.53** Using the data in the following table, predict the relative degree of solid solubility of the following elements in aluminum:

- Copper
- Manganese
- Magnesium
- Zinc
- Silicon

Use the following scale: very high, 70%–100%; high, 30%–70%; moderate, 10%–30%; low, 1%–10%; and very low, <1%.



Tutorial

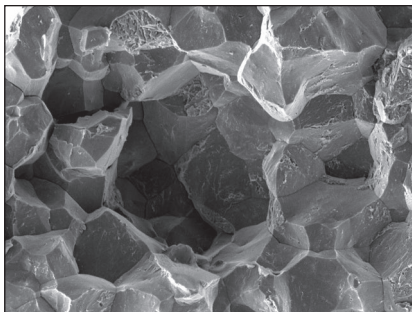
Element	Atom Radius (nm)	Crystal Structure	Electro-negativity	Valence
Aluminum	0.143	FCC	1.5	+3
Copper	0.128	FCC	1.8	+2
Manganese	0.112	Cubic	1.6	+2, +3, +6, +7
Magnesium	0.160	HCP	1.3	+2
Zinc	0.133	HCP	1.7	+2
Silicon	0.117	Diamond cubic	1.8	+4

- 4.54** Using the data in the following table, predict the relative degree of atomic solid solubility of the following elements in iron:

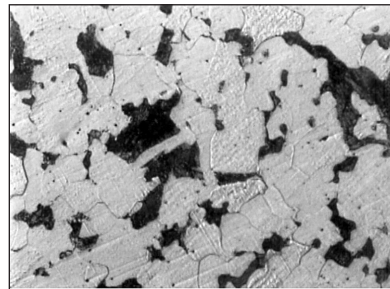
- Nickel
- Chromium
- Molybdenum
- Titanium
- Manganese

Use the following scale: very high, 70%–100%; high, 30%–70%; moderate, 10%–30%; low, 1%–10%; and very low, <1%.

Element	Atom Radius (nm)	Crystal Structure	Electro-negativity	Valence
Iron	0.124	BCC	1.7	+2, +3
Nickel	0.125	FCC	1.8	+2
Chromium	0.125	BCC	1.6	+2, +3, +6
Molybdenum	0.136	BCC	1.3	+3, +4, +6
Titanium	0.147	HCP	1.3	+2, +3, +4
Manganese	0.112	Cubic	1.6	+2, +3, +6, +7

**Figure P4.62**

(Courtesy of Metallurgical Technologies)

**Figure P4.63**

(©Javad Hashemi)

- 4.55** Comment, based on calculations and comparisons, on the extent of solubility of copper in nickel based on the Hume-Rothery rules.
- 4.56** (a) Estimate the density of a 75 wt% copper-25 wt% Ni alloy (use Appendix II for density data). (b) What will be the most probable crystal structure for this alloy? (c) Determine the mass in grams of the atoms inside a unit cell of this alloy. (d) Determine the lattice constant for this alloy.
- 4.57** (a) What is the theoretical atom % of each element in the compound FeO? What is the corresponding wt% of each element in the compound? What is your conclusion?
- 4.58** Sterling silver consists of approximately 93 wt% silver and 7 wt% copper. Discuss all the ways by which the addition of 7 wt% copper is beneficial. What type of a solid solution is this alloy?
- 4.59** What is the significance or impact of Schottky and/or Frenkel imperfection of the properties and behavior of ionic materials?
- 4.60** When the magnification in a metallurgical microscope is increased by a factor of 2, what happens to the size of the area that you are observing (area magnification)? What happens to the number of grains to be counted?
- 4.61** For a given application, you would need to select the metal with larger grain size between copper ($n = 7$) and mild steel ($n = 4$). (a) Which one would you pick? (b) If strength is an important consideration, which alloy would you pick and why? (c) What if the application was at elevated temperatures; would your answer in part b change, and why?
- 4.62** Figure P4.62 is an SEM micrograph (500 \times) and shows the fracture surface of a gear. Describe all the features that you are observing in this micrograph. Can you estimate the average grain diameter (assume $C = 1.5$)?
- 4.63** Figure P4.63 is an optical micrograph of 1018 steel (200 \times) made of mostly iron and a small amount of carbon (only 0.18 wt%). Describe all the features that you observe in this micrograph. What do you think the different colors represent?
- 4.64** Figure P4.64 is a TEM image and shows the structure of a cold-worked aluminum alloy. Describe all the features that you are observing in this micrograph. Speculate as to what happened.

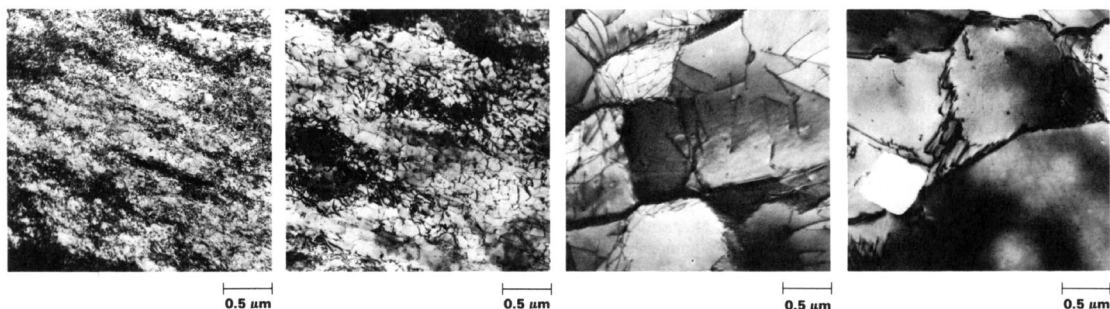


Figure P4.64

(©ASM International)

- 4.65** A low-carbon steel bar of circular cross section is cast such that its grain structure is equiaxed. Your application requires that the diameter of the bar be reduced and the grain dimensions be longer along the longitudinal axis of the bar. How would you accomplish this?
- 4.66** In Figure 4.34, the HRTEM image of AlN is presented. In the figure, the dislocations are highlighted with arrows and the letter "d." Can you verify that what the scientist designates as an edge dislocation is in fact an edge dislocation? (Hint: compare Figure 4.34 to Figure 4.18a.) Also, discuss how the scientist knows that a stacking fault exists at the top of the image.

